UNIVERSITY OF WOLLONGONG AUSTRALIA

University of Wollongong - Research Online

Thesis Collection

Title: Methodology for assessment of serviceability of aged transmission line conductors

Author: Gary Francis Brennan

Year: 1989

Repository DOI:

Copyright Warning
You may print or download ONE copy of this document for the purpose of your own research or study. The University does not authorise you to copy, communicate or otherwise make available electronically to any other person any copyright material contained on this site.
You are reminded of the following: This work is copyright. Apart from any use permitted under the Copyright Act 1968, no part of this work may be reproduced by any process, nor may any other exclusive right be exercised, without the permission of the author. Copyright owners are entitled to take legal action against persons who infringe their copyright. A reproduction of material that is protected by copyright may be a copyright infringement. A court may impose penalties and award damages in relation to offences and infringements relating to copyright material.
Higher penalties may apply, and higher damages may be awarded, for offences and infringements involving the conversion of material into digital or electronic form.

Unless otherwise indicated, the views expressed in this thesis are those of the author and do not necessarily represent the views of the University of Wollongong.

Research Online is the open access repository for the University of Wollongong. For further information contact the UOW Library: research-pubs@uow.edu.au

University of Wollongong Thesis Collections

University of Wollongong Thesis Collection

University of Wollongong *Year* 1989

Methodology for assessment of serviceability of aged transmission line conductors

Gary Francis Brennan
University of Wollongong

Brennan, Gary Francis, Methodology for assessment of serviceability of aged transmission line conductors, Master of Engineering (Hons.) thesis, Department of Mechanical Engineering, University of Wollongong, 1989. http://ro.uow.edu.au/theses/2520

This paper is posted at Research Online.

NOTE

This online version of the thesis may have different page formatting and pagination from the paper copy held in the University of Wollongong Library.

UNIVERSITY OF WOLLONGONG

COPYRIGHT WARNING

You may print or download ONE copy of this document for the purpose of your own research or study. The University does not authorise you to copy, communicate or otherwise make available electronically to any other person any copyright material contained on this site. You are reminded of the following:

Copyright owners are entitled to take legal action against persons who infringe their copyright. A reproduction of material that is protected by copyright may be a copyright infringement. A court may impose penalties and award damages in relation to offences and infringements relating to copyright material. Higher penalties may apply, and higher damages may be awarded, for offences and infringements involving the conversion of material into digital or electronic form.

METHODOLOGY FOR ASSESSMENT OF SERVICEABILITY OF AGED TRANSMISSION LINE CONDUCTORS

A thesis submitted in fulfilment of the requirements for the award of the degree

MASTER OF ENGINEERING (HONOURS)

from

THE UNIVERSITY OF WOLLONGONG

by

GARY FRANCIS BRENNAN B.E. (HONS)

UNIVERSITY OF
WOLLONGONG
LIBRARY

DEPARTMENT OF MECHANICAL ENGINEERING

1989

I hereby declare that I have not submitted this material either in whole or in part, for a degree at this or any other institution. Whilst this thesis has been prepared with the proper care, the information, advice, opinion and recommendations contained herein are offered, I accept no responsibility for the use of the information in any particular application.

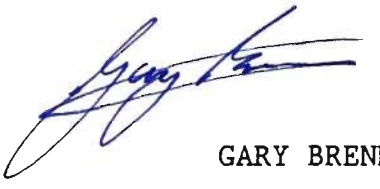

GARY BRENNAN

30 NOVEMBER, 1989

3 0009 02907 6226

ABSTRACT

The degradation of transmission line conductors is attributed to annealing, fatigue, corrosion, creep and in the case of an ACSR construction, stress redistribution in the aluminium and steel wires. A methodology for monitoring and testing for the degradation mechanisms is presented. Simple life expectancy models presented, give confidence in the long term serviceability of conductors.

The methodology and life expectancy models developed are based on examining and testing conductor samples that are representative of various stages of each of the degradation mechanisms. The conductor samples were removed from in service transmission lines that had over twenty years service experience.

ACKNOWLEDGEMENTS

The author wishes to thank the Department of Mechanical Engineering, University of Wollongong, MM Metals and The Electricity Commission of NSW for initially providing the opportunity to research and develop the subject material, creating an environment and atmosphere in which it was a pleasure and privilege to work and the continued support by funding and providing the facilities to carry out the work.

The most sincere thanks are directed to Dr. A. Gouch, Mr. P. Flanagan, Dr. A. Basu, Dr. P. Arnold and Dr. W. Plumbridge for their continuous supervision and interest in the project. Their encouragement, guidance and endless patience during the course of the studies was greatly appreciated.

The author is indebted to Mr F. Van Eimeren for the preparation of all the conductor samples and assistance during the course of the work. An appreciation is extended to Mr J. Maliphant for the scanning election micrographs.

Thanks are also due to my colleagues on the Australian Standards Committee EL/10/1 - Conductors, for their continued interest and encouragement.

I owe a debt of gratitude to Wendy Douglas, Debbie Annetts, Gary Harris and Harry Allen for the cheerful and patient way they carried out the typing and associated drafting for the thesis. A thank you is also extended to David Guille, for his support during the final stages of the preparation of the thesis.

And finally, I would like to take the opportunity to express my deep gratitude to my wife Cheryle, for her support, encouragement and forebearance during the period of these studies. A special thanks also goes to my daughter, Sarah-Ann, for her cheerful smiles during difficult times.

TABLE OF CONTENTS PAGE

LIST OF ABBREVIATIONS

AAAC	-	All Aluminium Alloy Conductor
AAC	-	All Aluminium Conductor
ACAR	-	Aluminium Conductor Aluminium (Alloy) Reinforced
ACSR	-	Aluminium Conductor Steel Reinforced
CBL	-	Calculated Breaking Load
CONCAT	-	Continuous Catenary
CLE	-	Coefficient of Linear Expansion
EDT	-	Every Day Tension
GZ	-	Galvanized Zinc
MWT	-	Maximum Working Tension
MOT	-	Maximum Operating Temperature
NDT	-	Non Destructive Testing
SEM	-	Scanning Electron Microscopy
STESS	-	Sag Tension by Strain Summation
UTS	-	Ultimate Tensile Strength

LIST OF TABLES

LIST OF TABLES (CONT)

LIST OF TABLES (CONT)

LIST OF TABLES (CONT)

LIST OF FIGURES

LIST OF FIGURES (CONT)

LIST OF FIGURES (CONT)

LIST OF FIGURES (CONT)

LIST OF FIGURES (CONT)

LIST OF FIGURES (CONT)

LIST OF PLATES

LIST OF PLATES (CONT)

LIST OF PLATES (CONT)

LIST OF PLATES (CONT)

LIST OF SYMBOLS

The symbols used in this thesis are, as far as possible, the symbols in common use by the electrical industry and published works. In some cases, as a result of the diverse nature of the thesis, the symbols may define more than one parameter. In this regard, to assist the reader, the symbols used, have been categorised into chapters. However in achieving a consistent approach, some duplication in the list of symbols from one chapter to the next will occur.

CHAPTER ONE

E_a - modulus of elasticity of aluminium in Pa

E_s - modulus of elasticity of steel in Pa

m - ratio of cross section area of steel to the total conductor

n - ratio of cross section area of aluminium to the total conductor

z - parameter

ε - parameter

α_a - aluminium CLE in $^{o}C^{-1}$

α_s - steel CLE in $^{o}C^{-1}$

CHAPTER TWO

A - conductor cross sectional area in m^2

A_2 - conductor creep constant

C - constant

c - conductor curve constant

D_a - aluminium thermal strain in $mm.km^{-1}$

D_s - steel thermal strain in $mm.km^{-1}$

LIST OF SYMBOLS (CONT)

E - conductor modulus of elasticity in Pa

H - vertical distance between two adjacent conductor attachment points in m

K_r - conductor radial thermal conductivity coefficient in $W.m^{-1}.C$

L - horizontal span distance in m

l - conductor chord length in m

L_{eff} - effective level span length for a non level span

L_E - equivalent span in m

n_1, n_2 - conductor creep constants

R - d.c. resistance of conductor in $\Omega.m^{-1}$

r_c - radius of conductor in m

r_s - radius of steel core of an ACSR conductor in m

S - conductor sag in m

s - conductor stress in Pa

T - conductor tension in N

T_h - conductor horizontal tension in N

T_{AV} - conductor average tension in a span in N

t - time in hours

t' - conductor tension at any point in the chord length in N

x - conductor weight load in N

ω - conductor weight load in N

α - conductor CLE in $^oC^{-1}$

LIST OF SYMBOLS (CONT)

θ - conductor temperature in ^{o}C

θ_c - conductor core temperature in ^{o}C

θ_s - conductor surface temperature in ^{o}C

θ_a - aluminium temperature in ^{o}C

θ_s' - steel temperature in ^{o}C

$\mu\varepsilon$ - conductor creep in $mm.km^{-1}$

δ - conductor creep constant

γ - an angle in degrees

CHAPTER THREE

A_2 - conductor creep constant

A_a - aluminium cross sectional area in m^2

A_c - conductor cross sectional area in m^2

A_{ci} - wire area constant for the ith layer

A_n - polynominal constant, where n = 1,2,3...etc.

A_s - steel cross sectional area in m^2

B_n - polynominal constant, where n = 1,2,3...etc.

BL_s - steel wire breaking load in N

BL_{ij} - breaking load of the ith wire of material j

C_a - aluminium permanent elongation in $m.m^{-1}$ in a stress strain test

C_s - steel permanent elongation in $m.m^{-1}$ in a stress strain test

E_a - modulus of elasticity of aluminium in Pa

LIST OF SYMBOLS (CONT)

E_{af} - final modulus of elasticity of aluminium in Pa

E_{cf} - final modulus of elasticity of conductor in Pa

E_{ci} - initial modulus of elasticity of conductor in Pa

E_{s} - modulus of elasticity of steel in Pa

E_{sf} - final modulus of elasticity of conductor in Pa

E_{si} - initial modulus of elasticity of conductor in Pa

E_{w} - modulus of elasticity of wire in Pa

E_{x} - wire axial modulus of elasticity in Pa

D - conductor diameter in m

F - conductor axial force in N

i - layer number

j - material type

L - wire length corresponding to one lay length in m

L_{c} - length of the centre wire from the conductor sample in m

LR - lay ratio

Load - instantaneous load in kN during a breaking load test

m - ratio of cross section area of steel to the total conductor

M_{ci} - wire mass constant for the ith layer

M_{c} - mass of conductor sample in $g.m^{-1}$

M_{g} - mass of grease or tar in g

M_{z} - mass of zinc in $g.m^{-1}$

MLR - mean lay ratio

n - ratio of cross section of aluminium to the total conductor

LIST OF SYMBOLS (CONT)

N_n - conductor creep constants where n = 1,2 or 3

N_{ij} - number of wires in i layer of material j

N_i - number of wires in a conductor

R - conductor layer radius in m

R_{ci} - wire resistance constant for the ith layer

S - conductor stress in Pa

S_a - aluminium stress in Pa

S_{ao} - maximum aluminium stress in Pa at initial temperature

S_{av} - conductor average stress in Pa

S_b - conductor birdcaging stress in Pa

S_c - conductor stress in Pa

S_{co} - maximum conductor stress in Pa at initial temperature

S_{kt} - conductor critical stress in Pa

S_s - steel stress in Pa

S_{so} - maximum steel stress in Pa at initial temperature

T - temperature in ^{o}C

t - time in hours

W_i - mass of the ith wire in g after destranding of the conductor sample and removal of all grease or tar from the ith wire

ε - conductor strain in $m.m^{-1}$

ε_L - wire strain in $m.m^{-1}$

$\mu\varepsilon$ - conductor creep in $mm.km^{-1}$

λ - lay length in m

σ - lay angle in degrees

LIST OF SYMBOLS (CONT)

α - CLE in $^{o}C^{-1}$

α_a - aluminium CLE in $^{o}C^{-1}$

α_s - steel CLE in $^{o}C^{-1}$

α' - wire CLE in ^{o}C-1

α_c - conductor temperature in ^{o}C

α_{cmax} - conductor maximum operating temperature in ^{o}C

α_{dp} - grease/tar drop point in ^{o}C

ε_L - wire strain in $m.m^{-1}$

CHAPTER 4

A - defined distance of 89 mm or 3-1/2 inches

A_a - aluminium cross sectional area in m^2

A_c - conductor cross sectional area in m^2

$a_{(i \text{ or } j)}$ - area of the wires in the left hand lay layer (i) or the right hand lay layer (j)

a_c - homogenous conductor area in m

c - distance from the neutral plane to the outermost fibre in m

d_a - aluminium wire diameter in m

d_c - conductor diameter in m

d_s - steel wire diameter in m

d_{ij} - diameter of the wire in the ith layer of material j

d_w - wire diameter in m

E_a - modulus of elasticity of aluminium in Pa

E_j - modulus of elasticity of material j

LIST OF SYMBOLS (CONT)

E_s - modulus of elasticity of steel in Pa

EI - conductor flexural rigidity in $N.m^2$

f - conductor vibration frequency in Hz

L - conductor loop length in m

M - wire torque in N.m

m - conductor mass in g

m_{ij} - number of wires in the ith layer of material j

N_i - number of wires in a conductor

N_n - fatigue life of material at a given stress level in cycles where n = 1,2,3...etc

$N_{(i \text{ or } j)}$ - number of wires in the left hand lay layer i or the right hand lay layer j

n - ratio of cross section of aluminium to the total conductor

n_a - number of alumimiun wires

n_n - proportion of material life at a given stress level in cycles where n = 1,2,3....etc

n_s - number of steel wires

R - bending radius of conductor over suspension point in m

r - conductor layer radius in m

r_{ij} - radius of the ith layer of material j

$r_{(i \text{ or } j)}$ - radius of the left hand layer i of the right hand layer j

S - Stroudal number

T - conductor tension in N

T_4 - conductor force producing rotating torque in N

v - wind velocity in $m.s^{-1}$

Y - conductor peak to peak displacement in mm

Y' - conductor peak displacement in mm

LIST OF SYMBOLS (CONT)

y_a - conductor deflection in m

σ - conductor stress in Pa

σ_a - aluminium wire stringing stress in Pa

σ_b - conductor bending stress in Pa

σ_d' - conductor stress at 89mm from the suspebsion pint in Pa

$\sigma_{(i \text{ or } j)}$ - wire stress in the left hand lay layer i or the right lay layer j

θ - lay angle in degrees

$\theta_{(i \text{ or } j)}$ - lay angle in the left hand lay layer i or the right hand lay layer j

INTRODUCTION

The transmission of power in New South Wales is achieved by over 70,000 km of steel reinforced aluminium conductors of varying size. The major part of these conductors were manufactured and erected between 1955 and 1970 making some of these conductors over 30 years old.

With time, the conductors have experienced a variety of in service conditions that may have varied from emergency operating conditions creating elevated temperatures to long exposures of low velocity winds inducing aeolian vibration. In addition, the pollution levels in the NSW transmission system range from light to very heavy.

The objective of these studies was to ascertain the level of degradation of the conductors, the continued serviceability of the conductors and develop a methodology to test conductors in the future. At the same time, a simple conductor life expectancy model was developed. The methodology presented, is based on actual conductor samples, having been exposed to pollution environments ranging from light to heavy, removed from service for testing. Testing and examinations for degradation of the removed conductor samples cover metallugical examinations, wire tests and full scale conductor tests. The degradation mechanisms discussed include corrosion, fatigue, creep and annealing. Stress distribution changes in an ACSR construction is also discussed.

To assess the level of degradation of an aged conductor, the initial parameters of the conductor need to be established. Much of the discussions are devoted to establishing these initial properties of a conductor. This provides an understanding of the fundamentals of the conductor parameters and gives a greater appreciation as to the effects and consequences of conductor property changes.

In developing the methodology to assess in service conductor creep, a review of the various methods of determining conductor sag and tension was carried out. In addition, to gain a greater understanding of the fatigue mechanism of a conductor, a conductor fatigue tester was designed and constructed. Some S-N fatigue data for a AAC construction is given.

Initially a comprehensive review and appraisal of the available literature on the subject matter is presented.

CHAPTER ONE

REVIEW OF THE LITERATURE

1.1 INTRODUCTION

Fundamental to any research work is a review and appraisal of the currently available literature on the subject matter. It goes without saying that an enormous amount of literature has been published on the subject of the properties of transmission line conductors. Much of the research and development work has culminated in the publication of standard specifications (6, 7, 8 & 22), guides (1 & 3), reports (35, 63 & 64), recommendations (27, 28 & 29) and reference books (2, 36 & 66).

The mechanical properties of transmission line conductors covers a broad range of topics. These topics have been categorised into transmission line conductor tension and sag, mechanical, corrosion resistance and fatigue properties. Accordingly, the literature appraisal has been referenced in these categories. In addition, to allow some historical development to be established the appraisals have been carried out in a chronological order.

1.2 CONDUCTOR TENSION AND SAG PROPERTIES

1.2.1 H.B. Dwight 1926 (32)

Dwight presents a number of formulas given in series form to determine sag, tension and unstretched conductor length for level and non level spans knowing typical conductor parameters and climatic conditions.

Using modern digital computers for transmission line designs it is considered that the ideas presented by Dwight are somewhat dated. However, it is still common practise for some designers to employ approximate parabolic solutions like those given by Dwight. In these cases one of the features of the formulas presented, was that of giving automatically, the percentage errors involved in the use of the parabolic approximations.

In the subsequent discussions, E.V. Parnell points out that sag and tension calculations are presented with a higher degree of accuracy than the known physical properties of the conductors and the accuracy of the results are useless unless the physical properties of the conductors are more soundly established.

Dwight acknowledged that the modulus of elasticity and the temperature coefficient of linear expansion were not known to any degree of accuracy and he suggested further tests to be carried out to determine the average values of these conductor parameters.

It seems quite ironic that as early as 1926 it was recognised that conductor parameters were required to be known with a degree of accuracy and certainity, supported by actual tests. Even today Australian Standards for overhead conductors do not specify the need for type testing. It is to be commended, as part of the research and development policy of some Australian conductor manufactures, type testing to determine actual conductor parameters is being carried out.

1.2.2 D.O. Ehrenburg 1935 (34)

Ehrenburg proposed a method of determining conductor length, sag and tension in terms of a defined parameter, z being directly proportional to the span length and the conductor mass and inversely proportional to the conductor horizontal tension.

Series equations based on the catenary curves are derived using the parameter, z. Equations for conductor length, sag and tension in terms of the parameter, z are presented to enable the construction of tension/temperature charts.

Examples of long and short spans with considerable difference in reduced levels of the conductor attachment points are given to demonstrate the methods.

Ehrenburg includes the derivations, for the effect of insulator sag for low tension spans, point of horizontal tangency, angle of inclination at the conductor attachment point and point of maximum deviation as appendices to the paper.

Like a number of papers presented prior to the availability of computers the methods presented by Ehrenburg lack the accuracy that can be achieved by the use of the exact catenary equiations. Ehrenburg recognised this by the constraint saying that z should always be less than 0.5.

Whilst the author's contributions were valuable at the time, it is considered, that the methods presented are dated and with maybe the exception of the effect of insulator sag, not appropriate for further discussions.

1.2.3 C.O. Boyse and N.G. Simpson 1944 (17)

The Authors presented a paper in two parts. The first part reviews the fundamental relationships of sag, span, load, tension and length of conductor, using parabolic approximations and equivalent span theory. This is the first known published works

which describe in full the "freely supported lines" and the associated equivalent span theory. Boyse and Simpson's contribution with this theory has to be recorded as one of the most valuable design philosphies available to transmission line engineers today. This theory will be reviewed in some detail in Chapter Two.

The second part of the paper discusses in some length the factors of safety in transmission line designs and suggests a new approach to design procedures. This part of the paper warrents further investigations since the Overhead Construction and Maintenance Regulations, 1962 remains today, essential unchanged. However, these investigations are considered outside the scope of these studies and will not be discussed further.

1.2.4 M. Landau 1951 (55)

The paper is a further development of Ehrenburg's (31) work published on "Transmission Line Catenary Calculations" and provides analytical methods for calculating conductor sags, tensions and lengths for level and non-level spans for homogenous and non-homogenous conductors using a slide rule.

However, like Ehrenburg's work the methods, employed by Landau lacks the accuracy achievable by the use of exact catenary equations and modern computers and whilst it is appropriate to recognise Landau's work it will not be discussed in detail.

1.2.5 C.A. Jordan 1952 (54)

Jordan provides a complete interpretation of the ACSR stress strain diagrams and illustrates the calculating techniques for determining the initial, final and weighted final modulus of elasticity for the composite conductor, steel core and the aluminium components. Relationships for the coefficient of linear expansion for the steel core and the composite conductor are also given. In addition, Jordan described the temperature variation of the critical tension and stress distribution of the aluminium and the steel components of a composite conductor.

The assumption that $\alpha_a = 2\alpha_s$ was made throughout the paper. Since nominal values of $\alpha_a = 23 \times 10^{-6}$ and $\alpha_s = 11.5 \times 10^{-6}$ it is considered that this was reasonable. The actual values of the coefficient of linear expansion is dependent on the modulus of elasticity, the lay ratios of the various layers and the cross sectional areas of the component materials of the composite conductor and in general will be less than the nominal values.

Of particular interest is the critical tension of an ACSR conductor where loads less than this tension are solely borne by the steel core. In other words, conductor tensions below this critical point will behave as a steel conductor with the appropriate mE_s and nE_a properties. The critical tension transition point is a function of temperature. An increasing temperature, results in a linear increase in critical tension. Intuition would suggest that when aluminium strands suffer permanent elongation over steel after a period of time then the critical tension may move within the regime of every day operating tensions and temperatures. (i.e. the greater the aluminium permanent elongation the greater the critical tension). The critical tensions will be discussed in some detail in Chapter Three.

Another interesting concept of Jordan's, is that of the secant modulus and is defined as the slope of the line on the stress strain diagram from the maximum stress point, after the customary one hour hold period to the intercept of the initial modulus line of the ACSR composite. The secant modulus gives a direct relationship between any combination of stress and length along the final and initial modulus lines.

Finally, Jordan provides a ten step plan to determine design or final sags and tensions.

1.2.6 B.M. Pickens 1959 (69)

The author published details of digital computer program to determine conductor sag and tension. In fact, Pickens has to be recognised as the first engineer to progress from slide rule and or tables as the calculating medium to a computer.

The program designs for both final and initial values for a series of spans and determines the controlling design limit of the conductor. The basis and principles of the program are similar to those used today however the computer program is considered dated and will not be discussed further.

Of more interest is the inclusion in the paper of typical limiting working tensions and the recognition that different constants need to be applied for different topography and climatic conditions. In addition the initial tension at the regional still air conditions is 33 1/3% of calculated breaking load (CBL) compared with 25% of CBL used in this country. This is of particular interest because it recognises that it is possible that conductor static stress can be increased providing dynamic stresses and bending stresses are minimised.

1.2.7 P.F. Winkleman 1960 (80)

The paper describes the methods of computing sag and tension data of conductors and field measurement methods to determine sag. Much of the author's work has been adopted by ANSI for inclusion in the IEEE Guide to the Installation of Overhead Transmission Line Conductors (3).

Winkleman illustrates the method of using new catenary functions superimposed over tension-strain curves plotted for the various temperatures of interest to determine conductor tension and sag for level dead end spans.

The basis of the catenary function curves is the term slack, being the difference between the curve length and the span length expressed as a percentage of the curve length. Like Ehrenburg (34) the catenary functions for slack in terms of tension and sag are derived from the defined paramter, z.

The resultant conductor stringing charts with the exception of the sag curves are not unlike the stringing charts employed by the Electricity Commission of NSW.

For non level spans Winkleman uses a nomograph for determining a level span equivalent of non level span and provides a correction value to be included in the non level span length.

Two methods of sagging of conductors are presented. The first method of the field sagging equation is based on the parabolic approximation. In cases where the sag exceeds 5% of the span this method will result in measurable errors. The second method of the insulator clipping in offsets is based on the fact that the total length of the conductor at sag in the stringing sheaves equals the total length of the conductor at sag in the suspension clamps at a given stringing temperature. Sags and insulator offsets are related since sag corrections required for computing sags are dependant upon offset computations. The insulator offset calculations are described in detail in reference (3).

Winkleman also provides a method of determining insulator sag similar to that provided by Ehrenburg (34). Both these methods are valuable in determining the effect of insulator sag in low tension, short span, higher voltage transmission lines where the insulator length can be a considerable proportion of the length of the total span length.

Finally, Winkleman commented on conductor creep and suggests prestressing the conductors as a means of overcoming long term increases in conductor sag.

1.2.8 J. Barrien 1975 (12)

Barrien has provided a method to solve the well established catenary equations for the continuous multiple span transmission lines. Like Winkelman (80), Barrien was interested in more exacting solutions to transmission line designs. This is demonstrated by the example of the calculations for a transmission line in undulating terrain where there is a common need to straddle ridges with several short spans and either side of these short spans have relatively large spans. In these cases, considerable discrepancies in the equivalent span theory are revealed, particularly in the sag predications.

The tension calculating method employed is based on the restoring forces of the weight and tension of the conductor and the weight of the insulators, at each suspension structure. Put more simply, the suspension insulator string is a moment arm and forces of weight and tension are resolved about the insulator attachment point.

Barrien also discussed the mathematical solutions available to solve the final tensions. The first method using finite elements is discounted as very accurate but very time consuming with little overall gain. The second method using a derived hyperbolic expression which was solved using Newton-Raphson method provided rapid convergence with results having a greater accuracy than the input data.

Other aspects of sag and tension such as the catenary in an inclined plane, line deviation considerations and flexibility in the computer program to solve problems such as broken conductor conditions were also discussed.

Barrien's contribution in providing exacting solutions to determine tension and sag, culminating in the computer program CONCAT has been accepted and become a design tool for all transmission line engineers. Further, more exacting comments regarding Barrien's work will be discussed in detail in Chapter Two.

1.2.9 G.R. Boal 1977 (14)

Boal presented a model of tension and sag of transmission line conductors that includes the effects of creep, uses precise equations for non linear load elongation behaviour and is said to consider thermal loading history of the conductor. The program developed by Boal employs catenary equations, models stress strain data by a polynominal curve and includes the effect of creep.

Boal illustrates the capabilities of the program and the effects of the governing conditions or design limitations of 26/7 ACSR and 37 AASC/6201 conductors.

Boal also postulates a statistical approach for the predication of extreme load conditions likely to occur, to be used as the basis of transmission line designs.

Unfortunately, much of the details of Boal's work was not included in the published paper. However, it is considered that there is a need for a sag tension program that uses catenary equations, models stress strain data as a polynominal curve and includes the long term effect of creep. The errors in the most widely used sag tension equations and the development of sag tension program that includes the non linear behaviour of conductors will be discussed in Chapter Two.

1.2.10 J. Bradbury, G.F. Kuska and D.J. Tarr 1982 (18)

The authors discuss the inaccuracies of the parabolic theories in very mountainous terrain and highlight the presence of towers and conductors having loads in excess of their design limits. In deriving the theory it was recognized that two theories were available the elastic and the non elastic. The authors chose the elastic theory suggesting that it gives a tolerable accuracy.

The authors derive the catenary change of state equation which is presented and discussed in detail in Chapter 2. Furthermore, Bradbury, Kuska and Tarr examine the effects of the suspension

insulator string when the conductor is in the stringing sheaves and "clamped in" and present the theory of offsets previously mentioned.

In addition five methods of measuring sag are presented and the relative merits of each method is discussed.

In conclusion the catenary change of state equation and the theory present in this paper is similar that of Barrien's (12) presented in 1975. The next appropriate development of the catenary change of state equation is the inclusion of the inelastic theory making the determination of sag time dependent.

1.2.11 J.S. Barrett, S. Dutta and O. Nigol 1983 (9)

The author's present the details of a new sag-tension computer program named STESS which is based on the summation of strains. The concept is a simple approach of given conductor stress and time, the total conductor strain is the accumulation of thermal strain, elastic strain, creep strain and two relatively new strain terms, slack and settling.

The program STESS is the first real departure from the traditional sag tension determination methods. In the previous methods the strain was the independent variable for the necessary calculations and the conductor stress was the dependent variable.

In actual practise, the conductor strain is dependent on component stresses, temperatures and creep history.

The STESS method determines tensions for any given future loading conditions and limiting constraints. This is not possible with the traditional sag-tension methods because it involves a complicated shifting of initial and final stress-strain and creep curves.

In addition STESS includes the effects of load distribution changes previously mentioned by Jordan (54). More significantly a compressive loading of the aluminium wires in an ACSR construction is included that contributes to increases in sags at elevated temperatures.

1.2.12 Future Developments

The logical progression to achieve a greater understanding of tension and sag, behaviour is the combination of the sag tension evaluation of strain summation and the continuous catenary theory of Barrien's (12). This will enable the prediction of time dependent sag and tension using exact conductor behaviour theory, modelling all possible loading conditions and provide an accurate span behaviour model achieved by the continuous catenary theory.

1.3 CONDUCTOR MECHANICAL PROPERTIES

1.3.1 G.W. Stickley 1932 (77)

Stickley presents a paper that recognised the stress strain curves of stranded cables differ appreciably to that of single wires. The author published details of conductor testing equipment and test procedures that are still employed today.

Stickley commented on the results of stress strain tests and discussed the "foot" or as it is known today the zero correction factor or slack caused by unavoidable looseness in the wires resulting in uneven stress distribution at small loads in the conductor.

Stickley is the first known author to discuss the aluminium unloading phenomena at low loads that is discussed by other authors and at some length in Chapter Three of these studies.

Of particular interest is the findings that the modulus of elasticity increased after a second stress strain test. This is attributed to the individual wires acting more homogeneously in subsequent tests.

1.3.2 E. Fritz 1960 (42)

The author published a paper on "The Effects of Tighter Conductor Tensions on Transmission Line Costs" covering many aspects of transmission line designs such as foundations, steel tower masses, insulators and line fittings, earthwires and conductors.

With regard to conductors, Fritz highlights the design limitations of higher conductor tensions, like maximum design tensions within the elastic regime of mechanical behaviour, the effects of increased creep and lastly the fatigue limitations.

Fritz emphasises the fact that tighter tensions will increase conductor vibration and suggests:

> "judicious selection of vibration protection hardware at suspension and strain points or fatigue breaks will occur".

Like many other authors Fritz did not recognise that the accumulation of the stresses at the conductor support point is the design limitation of the conductor. For a given dynamic stress, increasing static stress, decreases bending stress with a single a net gain of decreasing sag. This will be discussed in detail in Chapter Four of this study.

1.3.3 J.B. Roche and E. Dziedzic 1968 (73)

Roche and Dziedzic discuss the factors affecting creep and sag in transmission lines covering three main areas of interest, conductor design and manufacturer, creep at elevated temperatures and component stress analysis in composite conductors.

The first area, conductor design and manufacturer, the authors give an account of the possible variables in the manufacture process and the effects that will result in the conductor parameters and performance affected.

The second subject examines conductor creep at elevated temperatures. The authors comment on high temperature creep rates for AAC, ACAR and AAAC constructions being considerably greater than creep rates of most equivalent ACSR conductors. Several comparisons of the use of ACAR and ACSR are given.

The final area of discussion presented by the authors is that of the calculated breaking load (CBL) of the conductor as being a deceptive design parameter. This is illustrated by comparing the CBL of an AAC and that of an equivalent ACSR using the definition of 20% CBL the ACSR aluminium strands have considerable higher stress levels. Roche and Dziedzic also discuss the ramification of wire stress re-distribution and suggest such load shifts may accelerate the creep rates in an ACSR construction.

Roche and Dziedzic join an increasing number of authorative authors who have suggested that the calculated breaking load of a conductor is an ill founded basis for design. This is supported when one considers aeolian vibration induces a dynamic stress into the conductor, the suspension clamp produces a bending stress and creep of conductors is generally determined as a function of the conductor static stress.

1.3.4 J.R. Harvey 1969 (47)

John Harvey is recognised as one of the first authors to publish papers on conductor creep and creep at elevated temperatures. The author gives an account of the room temperature creep test procedures, model equations and the long term predictions.

In addition the author has carried out a significant number of creep tests at elevated temperatures. Test results are published to illustrate the effect of temperature on the creep of various conductors.

Two points are interesting to note regarding the test results for ACSR construction,

1. "These figures also show that not much difference in creep exists between any of the conductors tested at room temperature at a tension of 20% nominal ultimate strength (CBL);" and
2. "that temperature has a much smaller effect on the creep of ACSR than it has on the creep of AAC".

However, regarding the first comment close examination of the test results suggest that:

1. For Arbutus conductor a tenfold increase in creep occurs after 100,000 hours between tests at 20% CBL at 26°C and 15% CBL at 125°C,

2. For Greedey conductor a fivefold increase in creep occurs after 100,000 hours between tests at 20% CBL at 26°C and 15% CBL at 100°C, and

3. For a 1021.4 kcmil ACAR an eightfold increase in creep occurs after 100,000 hours between tests at 20% CBL and 26°C and 100°C.

It is considered that, contrary to Harvey's remarks that these differences are considerable.

Harvey also commented on the high temperature performance of an ACSR and illustrated the effects of the unloading of the aluminium strands in an ACSR construction. This unloading occurred for Drake conductor between 100°C and 125°C.

Using the test results and a statistical loading model of a transmission line developed by Beers, Gilligan and Schamberger (13), Harvey determined the creep in the conductor for the life of the transmission line. The results suggest that,

> "Operating at these temperatures for the calculated times will not increase the creep of ACSR over that predicted from room temperature operation, but these operations would produce more creep in all-aluminium conductors than that predicted from room temperature operation".

1.3.5 J.R. Harvey and R.E. Larson 1970 (49)

Harvey and Larson's paper on the "Use of Elevated-Temperature Creep Data in Sag-Tension Calculations" is the natural progression from Harvey's previously published work (47) in 1969.

The authors present the results of conductor creep tests with various combinations of stress and temperature and provide an understanding of how creep is accumulated. Creep accumulation methodology is discussed in detail in reference (27).

One series of tests performed suggested that given a conductor exposed to a high tension for a period of time, subsequently allowing the tension to be reduced that the conductor creep will cease. Similar tests carried out during the coarse of these studies suggest a similar conductor behaviour. Tests of this nature are the first step of providing quantified information about the prestressing of the conductor after initial stringing in an attempt to achieve creep stabilisation.

According to the authors Arbutus conductor has similar creep behaviour at 25°C and 40% of calculated breaking load and 75°C and 15% of calculated breaking load. Such behaviour is not consistant with that predicted by the equations published by Bradbury, Dey, Orawski and Pickup (21).

Finally the authors suggest temperature time cycles to predict long term conductor creep. Similar cycles have been predicted by Beers, Gilligan and Schamberger (13) and Rickard and Sproule (72).

1.3.6 Y. Nakayama and T. Kojima 1970 (61)

The authors published details of field measurements of the creep of overhead line conductors that were compared with simultaneous laboratory measurements of creep.

The field tests consisted of three different stress levels and the duration of the test was 4 1/2 years. Laboratory tests were carried out at two different stress levels for a duration of 1000 hrs with the test results extrapolated to 10^5 hours.

The results of the tests confirmed,

1. Sag increased due to non-elastic elongation, and the sag increase was a function of conductor stress;

2. The difficulty of correlating the dynamically behaviour creep data from a transmission line with that of constant tension creep data from a laboratory; and

3. The temperature correction allowance is an effective method to compensate for conductor elongation.

1.3.7 J.R. Harvey 1972 (48)

Harvey's interest in conductor creep was extended to include the publishing of the paper that describes "The Effects of Elevated Temperature Operation on the Strength of Aluminium Conductors". The work deals with the amount of strength lost by conductors operating at elevated temperatures under tension.

The test results suggest that the loss of strength can be represented by parabolic mathematical model in the form of mt^n where for a given wire diameter alloy, m and n are a function of temperature. Furthermore smaller diameter wires lost more strength than larger diameter wires.

Four loss of strength empirical equations are presented for conductor constructions SAC, ACSR, AAAC and ACAR. Finally a methodology of accumulating loss of strength given temperature and exposure times is given.

Unfortunately loss of strength predictions can only be estimates since the precision of such predications exceeds the precision with which actual operating temperatures of transmission lines are measured. Operating tempertures will also vary along the transmission lines and the uncertainity will be highly dependent on the wind velocity and other climatic factors.

1.3.8 J. Bradbury, P. Dey, G. Orawski and K.H. Pickup 1975 (21)

The authors present a paper that describes the long term creep assessment for conductors. Initially, three forms of the creep equations are presented identical to those given by reference (27). Derivation of the dependency of rate of change of tension with rate of change of creep strain is given.

Creep constants are given for various conductor constructions and the effects of manufacturing variables on creep are discussed.

The authors found reasonable correlation between creep estimation using the predictor equations and experimental results from two separate field tests.

Finally the authors discuss the application of the methods given to transmission line designs and conductor sagging procedure. This discussion includes the methods of creep compensation namely prestressing, temperature, marginal allowance and overtensioning;

and the estimations of the increase in sag over the service life of a conductor. The effects of normal and intermittent high temperature are presented which could contribute 0.200 m additional sag change over a 20 year period.

The authors have made a valuable contribution to the understanding of and the need to compensate for creep of conductors. Methods presented have become the foundation of many generating authorities conductor creep compensation methodology.

1.3.9 V.T. Morgan 1979 (60)

Morgan published a paper titled "The Loss of Tensile Strength of Hard-Drawn Conductors by Annealing in Service". The paper is a valuable contribution to understanding the annealing process yet highlights the more difficult task of establishing the thermal history of a conductor.

The author initially describes the metallurgical annnealing process followed by empirical equations to describe the wire loss of strength as a function time, temperature and reduction area during the drawing process.

Morgan postulates that,

> "annealing is cumulative for intermittent heating of untensioned wires and it is possible to calculate the loss of tensile strength during the lifetime of a conductor from knowledge of its thermal history".

Two methods of calculation of annealing are given by Morgan, the first for loss of strength less than 15% and the empirical equation uses a second order polynominal and the second where the loss of strength is stated as proportional to the rate of recrystallization.

The author provides a method to accumulate annealing caused by intermittent or overload currents. The time duration of the incremental heating and cooling periods is initially determined following by calculation of the maximum temperature.

In closing the author suggests an inexpensive method of determining the thermal history of a conductor to determine annealing. Statistical analysis of known load patterns and meterological conditions during the life of a conductor is also given as a further method of determine annealing.

As a rule of thumb Morgan generally suggests that the maximum design temperature for copper, 1350 and 6201 aluminium should not exceed 98, 141 and 102^{o}C respectively.

1.3.10 O. Nigol and J.S. Barrett 1981 (62)

Nigol and Barrett published a paper titled "Characteristics of an ACSR Conductor at High Temperatures and Stress" which disclosed three significant discoveries,

1. The aluminium wires of an ACSR construction are capable of sustaining a compressive load of the order of 6 to 12 MPa that remain essentially constant and may account for as much as 0.6 m additional sag for a typical 300 m span;

2. Substantial radial thermal gradients reported to be as high as 40°C. This phenomena enhances the compressive load previously mentioned; and

3. Permanent elongation of 0.09% of the steel wires will cause an additional sag in the order of 1.3 m for a typical 300 m span.

To quantify their research, Nigol and Barrett provide a number of empirical equations to determine conductor stress. The main departures from the classical equations are;

1. The aluminium and steel strain equations include an additional term to provide for conductor creep;

2. The high temperature performance of the conductor is predicted by determining the birdcaging stress of the conductor; and

3. The coefficient of linear expansion is given by a quadratic equation. The additional term is intended to compensate the change in modulus of elasticity with change in temperature.

Nigol and Barrett have provided a most valuable definitive paper on the characteristics of ACSR constructions at high temperatures and stress. Many of the theories postulated by the authors are supported by actual test results. As the demand for a more efficient transmission system is required by authorities and transmission line construction is restricted due to environmental constraints, higher conductor operating temperatures will become common practise. Nigol and Barrett's work has filled the gap in the theory of operation of an ACSR construction at high temperature.

1.3.11 J.S. Barrett, P. Ralston and O. Nigol 1982 (10)

The author's initially investigate the behaviour of aluminium and steel wires in an ACSR construction. Comparisons have been made the permanent elongation of wires and conductors and increased plastic deformations in conductors is attributed to geometrical

stranding factors. Similar plastic deformations in the steel wires and steel core were small and this is said to be caused by the small lay angles of the steel wires.

Barrett, Ralston and Nigol discuss the calculated rated tensile strength or more commonly known as the calculated breaking load. Historically the calculated breaking load is based on the conductor achieving 1% elongation. Experience has shown that the calculated breaking load is the sum of the individual wire breaking loads having regard to an appropriate rating factor. However in more recent times manufacturers have reported that conductors often exceed the rated strength at strain values of approximately 0.8% before failure.

The author's also discuss the stress strain tests of conductors and an appropriate method of terminating the conductor to minimise aluminium extrusion into the test length. The termination method is not unlike the method used to terminate all the conductor samples tested as part of these studies.

Of most significance is the author's discussion of excessive conductor sags at high temperatures due to compressive loading in the aluminium which has elongated at a greater rate than the steel, but with both members forced to occupy the same length resulting in a greater elongation of the steel core. Tests

carried out by the author's suggests that compressive stresses reach a limiting value corresponding to 6 to 12 MPa which would result in 0.3 to 0.6 m extra sag in a typical span of 300 m.

Finally the author's describe the details of a new sag-tension computer program named STESS which has previously been discussed.

1.3.12 Future Developments

Further works on the prediction of the mechanical behaviour of conductors consist of:

1. The development of a time dependant tension and sag computer program based on conductor creep predications. Subroutines in fortran included in an existing sag tension program have been developed as part of these studies;

2. The development of a mechanical loading history model based on electrical loading and climatic predications proposed as part of an undergraduate study program;

3. The establishment of an accurate thermal model of a conductor;

4. The establishment of a time dependent wire stress redistribution model for an ACSR construction; and

5. Quantitative studies into the prestressing of conductors to establish a creep resistant conductor behaviour. It is anticipated that this will be the subject of a post graduate research project funded by the Electrical Research Board.

1.4 CONDUCTOR, CORROSION RESISTANCE PROPERTIES

1.4.1 J.S. Forrest and J.M. Ward 1954 (39)

Forrest and Ward are the first known authors to publish works on the "Service Experience of the Effects of Corrosion on Steel Cored Aluminium Overhead Line Construction", which still remains today as the most authorative paper on this subject. The paper summarises the investigation and conclusions reach as a result of service experience extending over a period of 20 years.

The authors initially discuss the methods of measuring corrosion and suggest several alternatives such as mechanical, electrical, weight loss, depth of pitting and loss in cross section. Regarding the mechanical assessment of corrosion it is suggested that after measuring the wire tensile properties that the allowable degree of deterioration is of the order of 12% loss of strength for the complete conductor and if the deterioration is

restricted to the aluminium strands and the steel core is not reduced in strength that 30% loss of strength is acceptable. To put this into perspective for Lemon ACSR/GZ the calculated breaking load would be derated from 90.1 kN to 79.3 kN and 65.7 kN respectively.

Forrest and Ward discount the electrical, weight loss, depth of pitting and loss in cross section area as methods of assessment of corrosion having insufficient sensitivity.

Secondly, the authors present an account of the type of conductors used and the service experience of these conductors from 1934 to 1952 installed throughout Great Britain. The degradation results were presented in the form of linear regression equations that determined deterioration as a function of layer and pollution environment. In general outlayer industrial environment rate of deterioration was greatest, followed by inner and outer layer aluminium coastal environment with slowest deterioration rate being that of inner aluminium industrial environment. This is summarises as a mean deterioration of 0.5% and 0.4% per annum for industrial and coastal environments respectively.

Descriptions of the type of corrosion and the factors affecting corrosion are presented emphasizing the effects of the position of the transmission line with respect to the sources of

pollution. Notwithstanding the avoidance of such areas, Forest & Ward suggest that the only method suitable for protection against corrosion is to prevent the ingress of the corrosive substance. This is achieved by the application of a protective grease and if necessary complete impregnation of the conductor.

1.4.2 R.D. Carter (undated) (25)

Carter published a paper on the "Corrosion Resistance of Aluminium Conductors in Overhead Service" which reviews the types of conductor constructions in common use and surveys experience gained in their resistance to corrosion under varying conditions of use.

Initially the author describes the establishment of the aluminium hydroxide and its protective characteristics. Crevice corrosion mechanism and the possibility of electrolytic action of the conductor and fittings is also discussed.

Finally service experience of several samples of conductors and constructions are discussed which would suggest,

1. For an ACSR 30/7 construction after 28 years exposure in a rural environment, slight corrosion of the outside aluminium strands occurred with the ungreased galvanised steel core unaffected. Tensile tests on the wires were regarded as entirely satisfactory;

2. For an ACSR 6/1 construction after 2 1/2 years exposure in a saline environment, severe corrosion of the aluminium wires had occurred despite the use of the protective grease over the steel core. Several wires broke in service;

3. For an AAC 19 construction after seven years exposure to a severe saline environment, some

> "slight overall corrosion had taken place on the outer layers and little crivice pitting internally but the tensile strength of the wires was satisfactory".

4. For an AAC 37 construction after forty two years exposure to a saline environment, the conductor appeared to be unaffected by corrosion with the exception of general weathering.

Carter also published preliminary results of corrosion tests in severe saline environments, commenced in 1964 in collaboration with the Illawarra County Council. The results are consistent with those reported by other authors and indicate,

1. Slight external pitting generally less than 250 um will occur after three years exposure;

2. No difference in external pitting between 1350 and 6201 aluminium;

3. Severe attack on galvanized wires after three years exposure. For complete removal of the zinc coating in three years a salt fall-out in the order of 160 $g.m^{-2}$ is necessary;

4. Protection of the aluminium wires will occur up to the point that degradation of the zinc coating has occurred;

5. Good corrosion resistance to both internal and external attack by AAAC and AAC constructions; and

6. A delay in the onset of internal corrosion results from the use of a protective grease.

Carter is to be commended as providing a detailed account of service experience of the corrosion resistance of aluminium alloy conductors. From the results presented it is concluded that an AAAC or AAC construction will perform equally as well as a copper construction in a saline environment discounting a long time design myth.

1.4.3 J.R. Booker 1986 (16)

The author presents a study on the "Natural Aging of Non-Energised Aluminium Conductors". Booker reports on the changing nature of the surface of the outer strands of the aluminium stranded conductor from one of having hydrophobic surface properties to that of hydepholic properties.

Much of the authors work related to wet corona inception voltages and corona discharge. However Booker suggest an interesting phenomena of expulsion of water droplets from the conductor. This may result in wire corona corrosion (43) being greater in some localised strands than others.

1.4.4 B.J. Maddock, J.G. Allnutt, J.M. Ferguson, K.G. Lewis, D.A. Swift, P.A. Swift, P.W. Teare and M.J. Tunstall 1986 (57)

The authors published results of "Some Investigation of the Ageing of Overhead Lines", that include corrosion of tower legs, conductor corrosion and the ageing of insulators.

Regarding conductor corrosion the authors present details of, eddy current testing to detect the loss of galvanising zinc on the steel wires, infra-red thermography to detect loss of cross sectional area of the conductor and examination of conductor samples for evidence of fatigue.

Not surprising, the authors advocate a fatigue free design with dynamic strains less than internationally accepted values (nominally 150 $mm.km^{-1}$). This is achieved by a combination of the use of generally two stockbridge vibration dampers per subconductor and every day tensions restricted to approximately 20% of nominal breaking load.

Of particular interest is the development of an optical instrument capable of measuring line vibration from the ground, without any special target attached to the conductor. This would be valuable in conductor sampling to identify the most active vibration spans.

The authors also present detailed discussions on the effects of an corrective action for conductor galloping and subconductor oscillations.

1.4.5 Future Developments

A greater understanding of the corrosion mechanisms of conductors will only be achieved by the circulation of a questionnaire to all Australian supply authorities and the establishment of a data base of information. Such work is viewed to be the responsibility of the Electrical Supply Association of Australian (ESAA). As a result of these studies a recommendation will be submitted to ESAA to form an Ad Hoc Committee to institute the questionnaire and data base and publish the findings.

1.5 CONDUCTOR FATIGUE PROPERTIES

1.5.1 J.C. Little, D.G. MacMillan and J.V. Majercak 1950 (56)

The authors published the only known work on the "Vibration and Fatigue Life of Steel Strand", consisting of a study of wire and strand properties that would determine,

1. The fatigue limit of various materials used in overhead ground strands;

2. The effects of operating temmperature on the fatigue limit;

3. The extent to which the change in elastic modulus caused by temperature changes affects the calculated stresses;

4. The extent to which operating stresses were affected by linear expansion coefficient;

5. The effects of working tension on the vibration fatigue life of clamped extra high strength galvanized strand; and

6. Investigation of the possible measures for improving operating performance.

The results of the experiemental work indicated,

1. The fatigue limit of the wire increases as the tensile strength increases;

2. A small increase in fatigue limit exists at temperatures less than $0^{o}C$, however no evidence existed of a decrease in the fatigue limit with high temperatures;

3. A decrease in elastic modulus of the order of 3% with a temperature increase from $0^{o}C$ to $100^{o}C$;

4. That, as expected, temperature increases results in decreasing wire tension;

5. That, as expected, increasing static stress for a constant dynamic stress the fatigue limit is decreased; and

6. That, as expected, with the application of armour rods a marginal increase in fatigue limit is achieved.

1.5.2 J.S. Tompkins, L.L. Merrill and B.L. Jones 1956 (79)

The authors published a paper on the "Quantitative Relationships in Conductor Vibration Damping" based on electrical - mechanical analogies. Parallels are drawn between circuit impedance

matching and the characteristic matching of vibration dampers to conductor tension, mass and diameter.

With the exception of the vibration frequency and conductor diameter relationship and the conductor tension, mass, frequency and loop length relationship, most of the work by Tompkins, Merill and Jones relates to the power input from the wind to the conductor and the power dissipation by line hardware.

Accordingly, whilst it is appropriate to recognise the authors work it will not be discussed in detail.

1.5.3 R.F. Steidel, Jr. 1959 (76)

The author published methods of evaluating the factors affecting the actual stresses or strains in a vibrating conductor. Equations for conductor deflection, slope, bending moment and shear either side of suspension point are derived. In addition an equation of the motion for a conductor is derived and three boundary conditions solutions for the support point are presented, the pinned-pinned loop, clamped-pinned loop and the realistic model, partially clamped-pinned loop.

Steidel used a design parameter ε as the boundary conditions that is somewhere between the regime of pinned and the fixed end model. The fraction $1-\varepsilon$ represents that portion of the maximum

bending moment for the fixed end. Subsequent experimental work suggests the conductor suspension clamp arrangement approached the ideal pinned-end condition where $\varepsilon = 1$.

The author has developed equations for use in the design of suspension clamps and necessary saddle curvature which will uniformly distribute the bearing load of the suspension clamp and reduces the mean stress in the individual strands.

1.5.4 M.B. Elton, A.R. Hard and A.N. Shealy 1959 (38)

The authors have published a paper on "Transmission Conductor Vibration Tests" that initially discusses observations from field and laboratory tests. Two fatigue endurance service experiences presented were,

1. Unarmoured, undamped Drake ACSR operating at $15^{o}C$ with tension of 18.9% of the calculated breaking load and vibration at 70% of the time with a total of 2.5 gigacycles over 7.6 years having no evidence of fatigue damage; and

2. Unarmoured, undamped Drake ACSR with similar conditions as above with 1.4 gigacycles of vibration in 4.7 years having fatigue fractures occurring in the outside wires.

Unfortunately in both these cases the dynamic stress levels were not disclosed; accordingly the published results must be said to be inconclusive.

The authors discuss the effects of armour rods and stockbridge dampers suggesting when used, the cyclic stress can be reduced by approximately 50% and 90% respectively.

An extensive study was carried on in-service Chukar ACSR. The results indicate that 200 megacycles occur at the lowest strain levels whereas only 100 cycles exceed the maximum measured 550 $mm.km^{-1}$ strain. Further,

> "less than 1 megacycles would be expected to exceed 400 $mm.km^{-1}$ strain".

Elton, Hard and Shealy attempted to correlate the hourly changes of strain with wind data however,

> "no definite trend was observable between uniformity of the wind and conductor strain level".

1.5.5 J.C. Poffenberger and R.L. Swart 1965 (67)

The authors provide a mathematical solution for the conductor differential displacement caused by wind induced aeolian vibration. The solution suggests the relationship to be dependent on conductor tension, flexural rigidity and conductor physical properties.

The relationship of bending amplitude is linear with the exception of high frequencies when the loop lengths are relatively short compared to the deflection arm integration constant.

Analytic solutions of the equations are in good agreement with experimental data from three laboratories.

1.5.6 W.G. Fricke, Jr and C.B. Rawlins 1968 (41)

The authors published definitive paper that describes the "Importance of Fretting in Vibration Failures of Stranded Conductor". The purpose of the investigation was

> "to evaluate, by metallographic means, the damage done to a conductor by fretting, to estimate in what proportion of vibration fatigue failures fretting is a contributing influence and establish the order of magnitude of its effect upon fatigue strength".

The research program consisted of two parts,

1. The collection and metallographic examination of a number of fatigued wires from ACSR construction; and

2. Fatigue tests of laboratory spans that quantitative describe the effects of fretting.

The findings of Fricke and Rawlins works suggests, all failures in stranded conductors examined whether induced in the laboratory or found in service initiated at frett sites, fretting reduces the fatigue strength by a factor of about 0.5 or 0.6 and the effect of fretting can be reduced by the application of wire surface coatings such as grease.

1.5.7 Claren and Diana 1969 (30)

Claren and Diana published works on the "Dynamic Strain Distribution of Loaded Stranded Cables", illustrating the relationships of dynamic strains occuring in spans and those occurring at rigid clamped supports and how wire movements contribute to the conductor's internal damping.

The authors solve the partial differential equation of the load circular section beam, the boundary condition problem and provided solutions for the maximum strain and maximum antinode

strain. A series of tests were carried out to correlate predicted and experimental results.

Unlike Poffenberger and Swart (67), Claren and Diana assumed the wires in the conductor to act as and form a completely rigid cylinder. In later discussions the authors agree with the loose wire theory suggesting the results could be too high by a factor of 3. This is significant as the flexural rigidity from the rigid model to that of the free model can vary by a factor of 7.

The authors provided a relationship of the outer wire strains and the anitode vibration, wave length, tensile load and the flexural rigidity. The relationship derived are similar to those of Poffenberger and Swart (67) published in 1965.

1.5.8 R.A. Carter and D.G. Quick 1979 (26)

The authors present a paper titled "NDT of High Voltage Transmission Lines", in which gamma and x-ray radiography were used to detect evidence of early fatigue conditions in a transmission line conductor.

Carter and Quick initially decided on X-ray method for field radiography because of the greater sensitivity and considerably shorter exposure times. Two exposures are necessary at right angles to remove the effect of masking causes by the steel core.

Removal of the suspension clamp also increased the sensitivity of the radiography.

With developments gamma radiography was used on future inspections as the equipment was more reliable and exposure times were reduced to that similar to the X-ray method.

Unfortunately radiography of conductor samples will only detect the presence of broken wires and cannot be used as a method of predicting the long term performance of the conductor.

1.5.9 A.S. Richardson, Jr. and F.S. Smith 1981 (71)

The authors published a paper on "Some Effects of Tension on Static Wire Fatigue in New England" in which a review of the various factors affecting fatigue stress in overhead static wires is carried out.

The authors suggest that the bending stresses due to aeolion vibration are a function of the 3/2 power of tension. Case studies of the present practise in New England of setting the initial tension at 12.5% of the calculated breaking load, no ice and $0^{o}F$ are given. According to Richardson and Smith increasing initial tension to limit sag under ice conditions would not return benefits commensurate with the increased risk of fatigue damage.

Richardson and Smith worked lacked adequate information on the wind energy input and the power dissipation by the various mechanisms. To overcome the lack of background data the authors developed a simplified model to which they applied the available data and made several simple assumptions.

1.5.10 W. Philipps, W. Carlshem and W. Buckner - (Prior 1985) (68)

The authors presented this report to CIGRE Study Committee, Working Group 04, titled "The Endurance Capability of Single and Bundle Transmission Line Conductors and its Evaluation" which is the culmination of other published works (38, 46, 51, 58, 67 and 76) and additional experimental work in Europe.

The object of the studies was to establish the capability of a conductor to endure a combination of static and dynamic stresses; carry out full scale outdoor conductor vibration tests and finally to develop a calculating method for the endurance of the conductor.

Findings of the fatigue tests for AAC and AAAC suggest,

1. Alloyed aluminium conductors exhibit the same fatigue strength as unalloyed aluminium conductors;

2. With the influence of armour rods and suspension clamps, the fatigue strength was reduced to 70% of that of the original conductor;

3. With the influence of suspension clamps the fatigue strength was reduced to 50% of that of the original conductor;

4. That 50% of the fatigue fractures initiated at fretting sites and the other fatigue fractures initiated at wire defect sites;

5. Unlike other investigations, all wire fractures occurred in the outside layer of the conductor and the failures were attributed to fretting between the suspension clamp and the wires; and

6. With a mean static stress increase of approximately 60% the conductor fatigue strength is reduced to 25% of that of the original conductor.

It is the opinion of the authors that conductor designs must be arranged that the dynamic stress in excess of 5 $N.mm^{-1}$ should not be reached in service. Furthermore, that dynamic stress measurements should not be carried out in the initial 6-12 months after stringing as the creep of the conductor will influence the results.

A series of S-N curves produced from field studies suggest, that

1. Self damping of a conductor increases as static stress decreases;

2. Only slightly higher dynamic stresses are reached if static stress is increased from 20.5% to 27.1% and 21.4% to 23.5% for 560/50 and 230/30 ACSR construction respectively;

3. Multiple suspension clamps may reduce the dynamic stress by as much as 20%; and an armour grip suspension unit by as much as 60%;

4. Flat terrain compared to hilly terrain may increase the dynamic stress in the order of 400%;

5. Vibration dammpers will reduce dynamic stress by approximately 500%; and

6. Bundling conductors will reduce dynamic stress by approximately 30%.

Philipps, Carlshem and Buckner calculated the effects of bending stress on realistic conductor span combinations. The results indicate that the bending stress is between two and four times that of the static stress. This will result in higher total

stresses at lower static stresses. In other words the bending stress increases with decreasing tensile stress and increasing span length.

The authors conclusions are,

1. The fatigue limit of hard drawn aluminium wires, is between 10 and 20 $N.mm^{-2}$ depending on static prestessing;

2. For a 593 mm^2 AAC at a mean static and bending stress of 110 $N.mm^{-2}$ and 10^7 load cycles, the mean fatigue limit of the conductor, conductor with suspension clamp and armour rod and conductor with suspension clamp is 22 $N.mm^{-2}$, 15 $N.mm^{-2}$ and 11 $N.mm^{-2}$ respectively;

3. For conductors with normal suspension dampers at 10^8 load cycles an ultimate allowable dynamic bending stress of 7 $N.mm^{-2}$ may be assumed; and

4. The terrain effect will have a significant impact on the conductor and hardware design.

1.5.11 T.V. Gopolan 1985 (45)

Gopolan published a paper on "Fatigue damage criterion for ACSR" in which he discusses the damage criteria based on dynamic stress and fretting.

The author, using the dynamic strain equation derived by Claren and Diana (30) and an appropriate value for the flexural rigidity, derives an equation for the double amplitude of vibration in terms of frequency of vibration. A similar but more general equation is given in Chapter 4. The limiting criteria is 300 $mm.km^{-1}$ and 150 $mm.km^{-1}$ for conductor greater 18 mm diameter and for smaller conductors respectively.

1.5.12 W.F. Buckner, R. Helm & K.O. Papailiou 1986 (23)

The authors published a paper titled "The Effect of Ageing of Overhead Line Conductors due to Aeolion Vibration". The discussion commences with a description of the stresses in and fatigue failures of conductors.

S-N curves for aluminium wires and stranded conductors are presented which suggest that stranded conductors are less fatigue resistance and do not have a asymtopic behaviour. In view of these S-N curves and with permissible strain limits in the outer aluminium layer of the conductor of 150 $mm.km^{-1}$ corresponding to as CIGRE (29) recommend a permissible stress limit of 10-15 $N.mm^{-2}$ fatigue failure is still possible.

The authors describe a very interesting method of sampling for evidence of conductor fatigue. Unlike the methods used in these studies which studied terrain and prevailing climate conditions

and sampling was based on the sites most likely to be susceptible to fatigue, Buckner, Helm and Papailiou carried out a quantitive dynamic stress level survey to identify the critically stressed sites. From these studies an estimation of conductor fatigue life is determined using Miners (58) cumulative fatigue hypothesis and known S-N curves.

Finally the author's gave an account of the effects of different line hardware and terrain on the life estimation of a conductor.

1.5.13 Future Developments

Further works on the predication of the Fatigue Properties of conductors consist of,

1. The establishment a test line with several identical conductors strung at differing tensions, having tailored vibration reducing hardware attached to each span and measuring and comparing the resultant dynamic strains as a function of wind velocity. This program would enable an assessment of the effect of increased static stress, decreased bending stress and constant designed dynamic stress to be achieved simultaneously.

2. The establishment of S-N curves for Australian manufactured conductors and enable an understanding of the effects of alloying aluminium on the fatigue limit. As part of these studies a conductor fatigue tester was constructed and commissioned to achieve the S-N curve test results. This is discussed in detail in Chapter 4.

3. The investigation of the effect of conductor fittings on the S-N curves.

CHAPTER TWO

CONDUCTOR TENSION AND SAG

2.1 INTRODUCTION

The basic theory of transmission line conductor tension and sag has been well established over many years and has become time honoured by transmission line engineers.

Commencing as early as the 1920's history has shown that much work and research has been published to provide definitive methods for determining tension and sag. In those early days the basic calculating tools were mathematical tables, slide rules and in some cases mechanical calculating machines. Consequently to simplify the theoretical catenary equations, most of the early works employed the parabolic approximations of the catenary sag curve.

With the common use of computers by engineers in the 1960's more exacting solutions of the parabolic equations were demanded to provide a more comprehensive understanding of the basic theory and more importantly to minimise the capital costs of transmission line construction. To put this into perspective a modern structure spotting computer program employing catenary equations has been said to save up to three percent of the total capital construction costs.

Even as recent as 1983, Barnett, Dutta and Nigol (9) published the details of a strain summation method for calculating tension and sags of an ACSR conductor,

> "based on a conductor model which is more realistic and conceptually simpler".

The most accepted and widely used method of determining tension and sag is the classical equivalent span theory given by Boyse and Simpson (17). In more recent times Barrien (12) provided the continuous catenary method for determining tension and sag which revealed in particular circumstances, significant discrepancies in the classical equivalent span theory. The most current development in determining tension and sag is that of the strain summation using the computer program STESS (Sag Tension by Strain Summation) published by Nigol and Barrett (9, 63, 64).

It is now appropriate to review the methods available to determine conductor tension and sag. The objectives of these studies is as follows.

1. Determine the benefits of the alternative tension and sag calculating methods;

2. Examine the approximations employed in the various calculating methods;

3. Develop methods to measure conductor tension and sag of in service transmission lines.

4. Correlate the results of survey measurements to determine existing transmission line conductor tension and sag with design parameters.

5. Ascertain the amount of conductor inelastic stretch and loss of strength in aged transmission line conductors by survey measurements.

6. Review the current allowances for conductor inelastic stretch.

2.2 FUNDAMENTAL THEORY

The problem of determining tension and sag designs for transmission line and distribution conductors is generally restricted to determining the conductor mechanical loading conditions within the bounds of the following constraints.

1. Everyday Tension (EDT) or the still air constraint. This constraint determines a suitable level of conductor stress to limit the likelihood of long term conductor fatigue caused by aeolian vibration.

2. Maximum Working Tension (MWT). The maximum working tension usually occurs at the maximum design wind and an everyday ambient temperature. In short spans the maximum working tension can be at low ambient temperatures. For elevations greater than 1200 m a combination of maximum design wind and maximum design ice mass will produce a maximum working tension. The maximum working tension ensures adquate safety factors for all line equipment, structures and foundations.

3. Maximum Operating Temperature (MOT). This constraint ensures that at a maximum operating temperature, the required minimum ground clearance is maintained and the loss of ultimate tensile strength of the conductor due to annealing is minimised.

4. Stringing Constraint. This involves any allowances in sag for the inelastic stretch in the conductor before final termination or the prestressing of the conductor to stabilise the inelastic stretch prior to final termination.

5. Maintenance Constraint. This constraint allows for the compliance of statutory safety factors during maintenance operations.

Further to these mechanical design considerations are the electrical constraints of providing structure earthing, lightning protection, electrical insulation and clearances at supporting structures and electrical clearance at midspan. The latter requires a knowledge of the motion of a conductor under varying prevailing climatic conditions. At higher voltages, corona power loss and in particular its interference with communication systems will have a major influence on conductor diameter, the need to bundle conductors and conductor spacing.

From the abovementioned constraints it is easily concluded that the fundamental requirements for the mechanical design of transmission lines may be restricted to the need to determine conductor vertical sag, conductor tension, long term conductor creep behaviour and the loss of ultimate tensile strength due to annealing. The later two design criteria will be discussed in Chapter Three.

2.2.1 Vertical Conductor Sag

The statutory requirements in NSW (37) for conductor clearance is a function of the operating voltage, the maximum operating temperature and the services that the transmission line will cross. Higher voltage transmission lines require more ground clearance as does the spanning of roads, other aerial services and areas likely to be frequented by motor vehicles. On the other hand, after allowance for the inelastic stretch of the conductor, ground clearance provided in excess of the statutory requirements implies an over design and uneconomical capital expenditure. With these boundary constraints, conductor sag and conductor sag change with time must be determined with a reasonable degree of accuracy.

The allowance for inelastic stretch of the conductor normally consists of a margin on the statutory requirement (37) of clearance. For the Electricity Commission of NSW this marginal allowance varies depending on voltage but may be the same for differing conductors constructions. Table 2.1 lists the adopted clearance policy, the statutory clearances requirement for open country not frequented by motor vehicles and the marginal allowances for inelastic stretch. Included in these marginal allowances is allowances for structure settlement and survey discrepancies.

The methods of calculating and compensating for conductor inelastic stretch will be discussed in detail in Chapter 3.

Voltage	Statutory Requirement (m)	ECNSW Policy (m)	Marginal Allowance (m)
500 kV	9.0	11	2.0
330 kV	8.0	9.0	1.0
220 kV	7.5	8.0	0.5
132 kV	6.7	7.5	0.8
66 kV	6.7	7.5	0.8

TABLE 2.1 - CONDUCTOR GROUND CLEARANCE FOR OPEN COUNTRY

The classical sag catenary and equivalent approximate parabolic equations of a supported flexible conductor for level and non level spans are given in Figures 2.1 and 2.2 respectively. The parabolic equations are the first order approximations of the Talyor series expansion of the hyperbolic functions of cosh and sinh.

In all cases the predicted sag from the parabolic equations will be less than that predicted by the catenary equations. In fact, for small curve constants such as the case of low stringing tensions in long effective spans, the difference between the catenary and parabolic sag can be appreciable. This is illustrated in Figure 2.3 where the percentage error for the

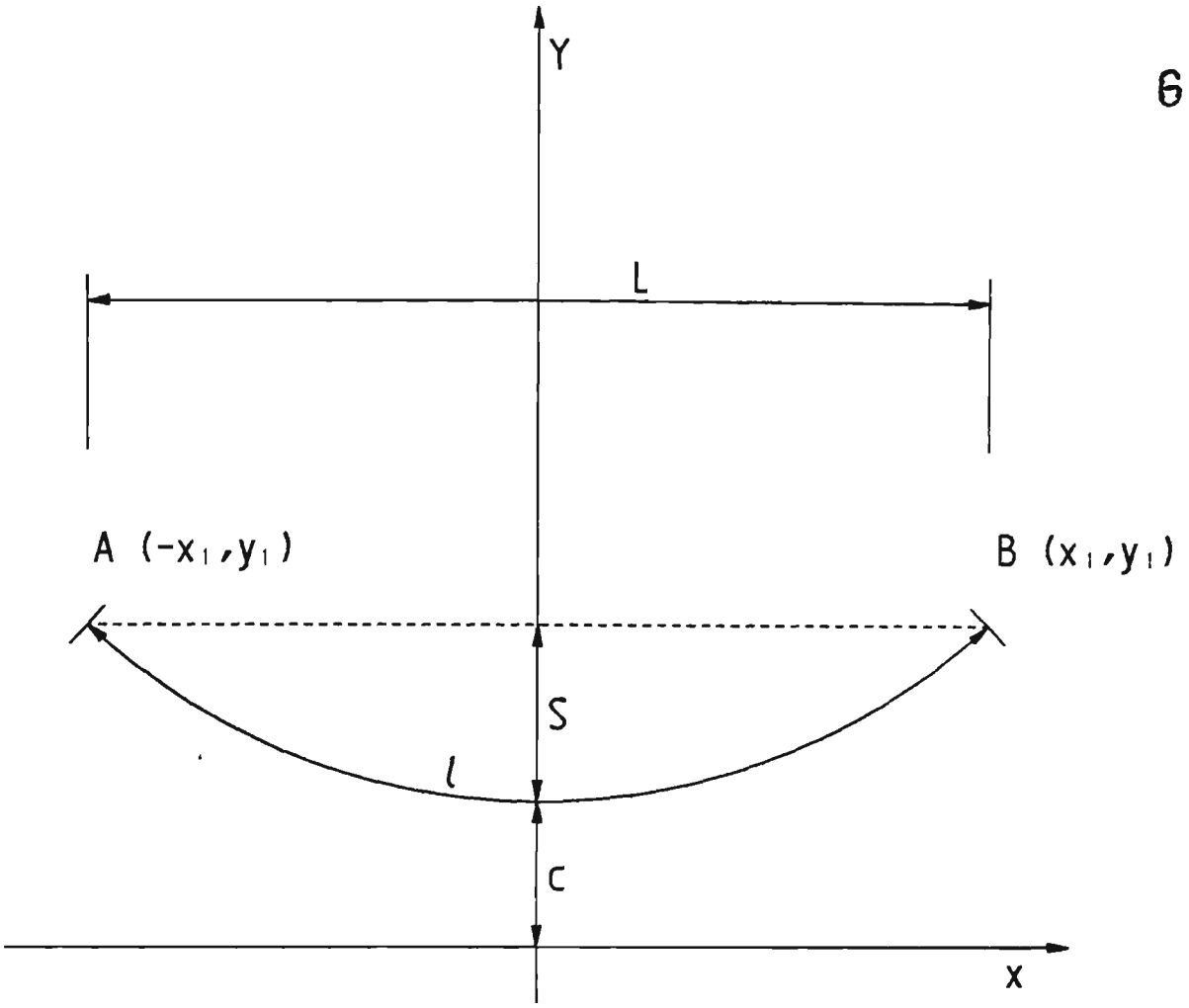

PARAMETER	CATENARY	PARABOLIC
CURVE CONSTANT, c	$\frac{T}{\omega}$	$\frac{T}{\omega}$
SAG AT ANY POINT, x	$c\left[\cosh\left[\frac{x}{c}\right]-1\right]$	$\frac{x^2}{2c}$
MAXIMUM SAG, S	$c\left[\cosh\left[\frac{L}{2c}\right]-1\right]$	$\frac{L^2}{8c}$
CONDUCTOR LENGTH, l	$2c \sinh \frac{L}{2c}$	$L+\frac{L^3}{24c^2}$

FIGURE 2.1 CATENARY AND PARABOLIC SAG EQUATIONS

LEVEL SPANS

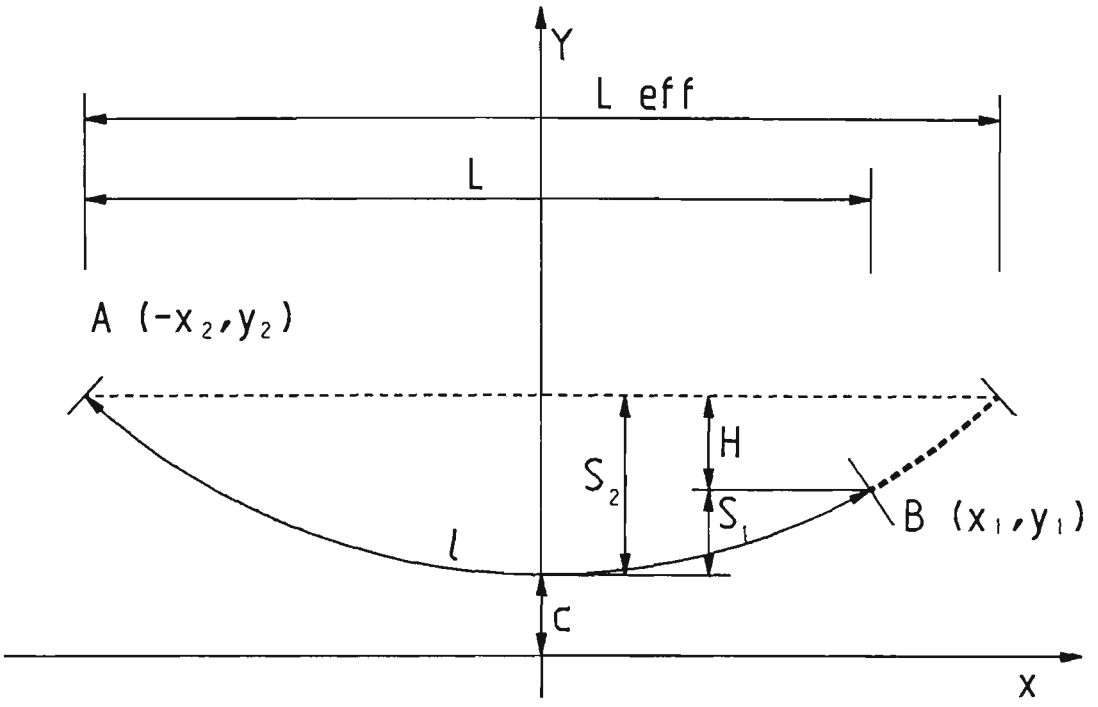

PARAMETER	CATENARY	PARABOLIC
CURVE CONSTANT, c	$\frac{T}{\omega}$	$\frac{T}{\omega}$
SAG AT ANY POINT, x	$c\left[\cosh\left[\frac{x}{c}\right]-1\right]$	$\frac{x^2}{2c}$
MAXIMUM SAG, S_1	$c\left[\cosh\left[\frac{x_1}{c}\right]-1\right]$	$\frac{x_1^2}{2c}$
S_2	$c\left[\cosh\left[\frac{x_2}{c}\right]-1\right]$	$\frac{x_2^2}{2c}$
CONDUCTOR LENGTH, L	$c\left[\sinh\frac{x_1}{c}+\sinh\frac{x_2}{c}\right]$	$L+\frac{L^3}{24c^2}+\frac{H^2}{2L}$
DISTANCE, x_1	$\frac{L}{2}-c\sinh^{-1}\frac{H}{K}$	$\frac{L}{2}-c\frac{H}{L}$
x_2	$\frac{L}{2}+c\sinh^{-1}\frac{H}{K}$	$\frac{L}{2}+c\frac{H}{L}$
EFFECTIVE SPAN LENGTH, L eff	$L+2c\sinh^{-1}\frac{H}{K}$	$L+2c\frac{H}{L}$

where $K = 2c\sinh\frac{L}{2c}$

FIGURE 2.2 CATENARY AND PARABOLIC SAG EQUATIONS NON LEVEL SPANS

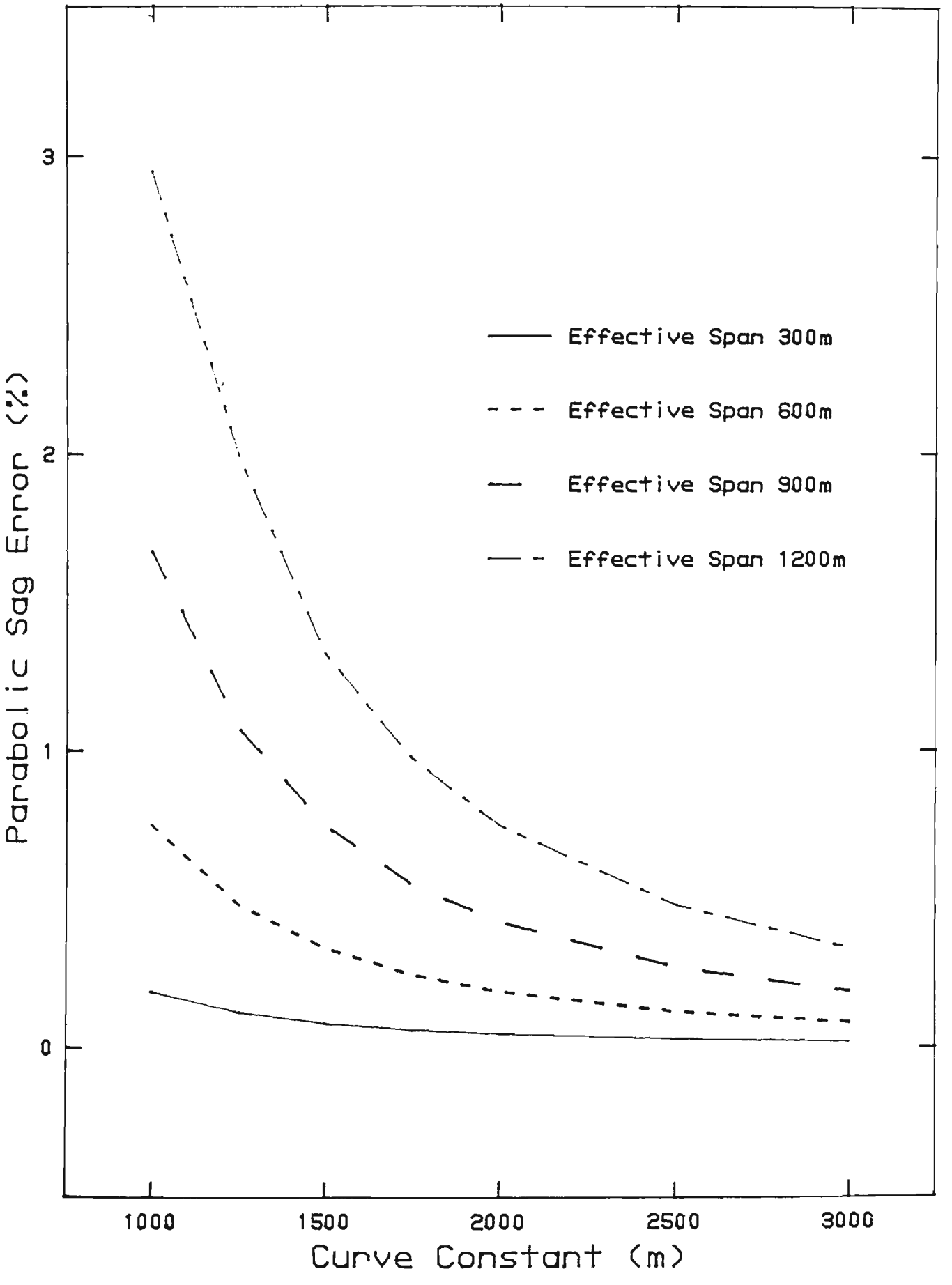

FIG 2.3 PARABOLIC SAG ERROR

predicted sag of a range of effective spans and curve constants for the parabolic sag equation is given. Academically it is also interesting to note as Winkleman (80) commented,

> "that any inflexibility in the conductor will result in sags less than that of the predicted catenary sag.

The predicted conductor length from the parabolic equation will also be less than that predicted by the catenary equation. For small curve constants the difference between the catenary and parabolic lengths can be considerable. This difference is illustrated in Figure 2.4 where the percentage error for the predicted conductor length of a range of effective spans and curve constants for the parabolic conductor length equation is given.

It should be noted that although the conductor length is generally not a design parameter it is the basis of determining conductor tension and inelastic stretch allowances.

2.2.2 Conductor Tension

The statutory requirements in NSW (37) for conductor tension designs after making an allowance for inelastic stretch is based on the following three conditions.

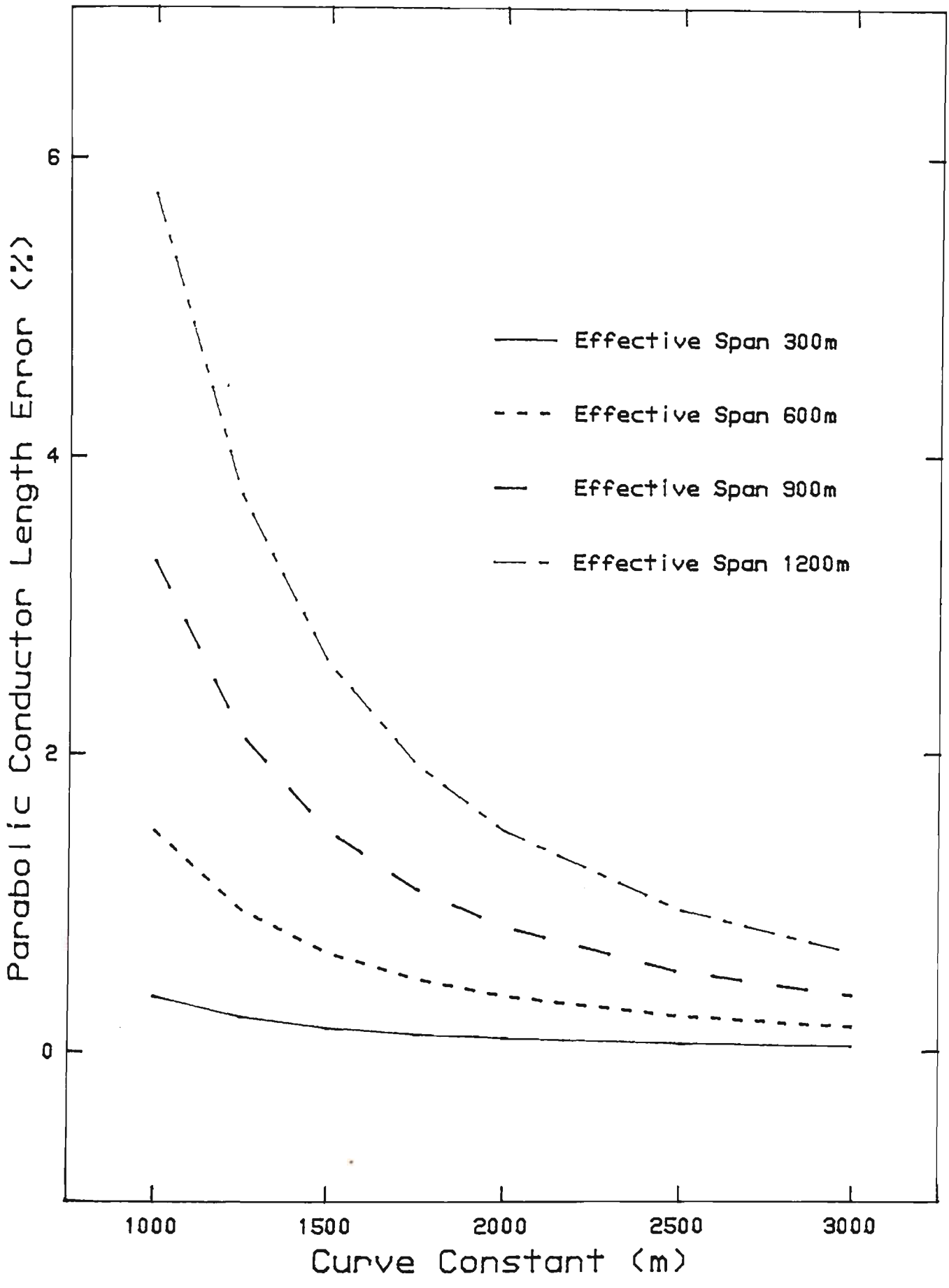

FIG 2.4 PARABOLIC CONDUCTOR LENGTH ERROR

1. At an ambient temperature of 15^{o}C and a horizontal wind pressure of 500 Pa applied orthoginal to the projected area of the conductor, the tension must not exceed 50% of the ultimate tensile strength.

2. At an ambient temperature of 5^{o}C and no wind for ACSR, AAC and AAAC fitted with conductor vibration dampers, the conductor tension must not exceed 25% of the ultimate tensile strength. For ACSR, AAC and AAAC not fitted with vibration dampers the tension is reduced to 18% of the ultimate tensile strength.

3. After making provisions for additional loads on conductors caused by the accumulation of ice and snow the tension must not exceed 50% of the ultimate tensile strength. Plate 2.1 illustrates the accumulation of ice and snow on a transmission line conductor under laboratory conditions.

It is clear from these requirements that the conductor tension needs to be determined for a variety of climatic conditions. A reference design conductor tension or bench mark tension is assumed for all span lengths and is generally taken at a conductor temperature of 5^{o}C and no wind. This assumption satisfies the penultimate abovementioned statutory condition.

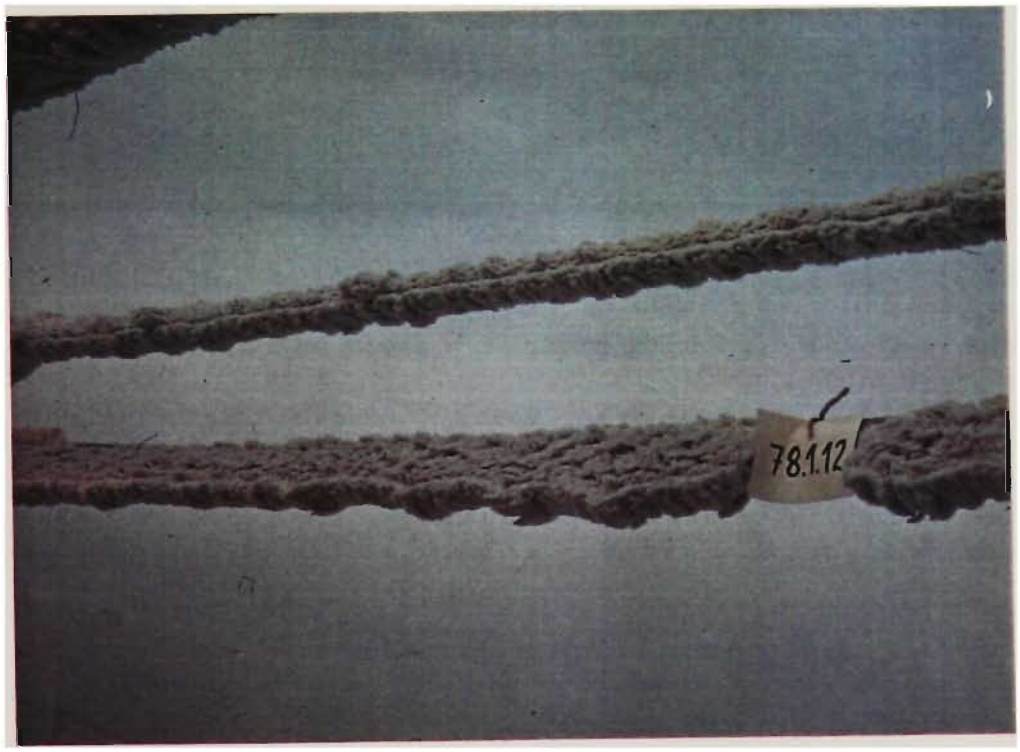

PLATE 2.1 - ACCUMULATION OF ICE AND SNOW ON TRANSMISSION LINE CONDUCTORS

This is the current policy for the Electricity Commission of NSW standard conductor stringing charts and it is also understood that many other Statutory Authorities and Councils adopt a similar basis for design tensions.

Using the bench mark tension, the elastic conductor tension at some other prevailing climatic condition may be determined by examining the change in conductor length and mass. The change in conductor length is described by the initial conductor length less the final conductor length for a given span, equals the change in conductor length due to changes in conductor temperature, weight load and tension. The conductor weight load change is caused by any accumulation of ice and snow on the conductor as previously illustrated in Plate 2.1.

Mathematically this change in conductor length is given as,

$$dl = \frac{\partial l}{\partial \theta} d\theta + \frac{\partial l}{\partial T} dT \qquad (2.1)$$

In particular the classical catenary and equivalent approximate parabolic time independent change of state equations for a supported flexible elastic conductor are derived in Figure 2.5 and 2.6 respectively. The catenary equation describes the very simple case of the level span.

Several comments are necessary to explain the approximations in each of the equations.

initial conductor length	+	change in length due to temperature change	+	change in length due to tension change	=	final conductor length

$$\frac{2T_{h1}}{\omega_1}\sinh\frac{L\omega_1}{2T_{h1}} + \alpha l(\theta_2 - \theta_1) + \frac{1}{AE}(T_2 - T_1) = \frac{2T_{h2}}{\omega_2}\sinh\frac{L\omega_2}{2T_{h2}}$$

Assuming that L=l and T_h=T then,

$$\frac{2C_1T_1}{\omega_1 L}\sinh\frac{L\omega_1}{2T_1} - T_1 - C_2\theta_1 = \frac{2C_1T_2}{\omega_2 L}\sinh\frac{L\omega_2}{2T_2} - T_2 - C_2\theta_2$$

where $C_1 = EA$
$C_2 = \alpha EA$

The suffixes for ω, T and θ denote initial and final conditions.

FIGURE 2.5 CATENARY CHANGE OF STATE EQUATION

initial conductor length	+	change in length due to temperature change	+	change in length due to tension change	=	final conductor length

$$L + \frac{\omega_1^2 L^3}{24T_{h1}^2} + \alpha l(\theta_2 - \theta_1) + \frac{1}{AE}(T_2 - T_1) = L + \frac{\omega_2^2 L^3}{24T_{h2}^2}$$

Assuming that L=l and T_h=T then,

$$\left[\frac{C_1\omega_1 L}{T_1}\right]^2 - T_1 - C_2\theta_1 = \left[\frac{C_1\omega_2 L}{T_2}\right] - T_2 - C_2\theta_2$$

where $C_1 = EA$
$C_2 = \alpha EA$

The suffixes for ω, T and θ denote initial and final conditions.

FIGURE 2.6 PARABOLIC CHANGE OF STATE EQUATION

2.2.2.1 Conductor Horizontal Tension

Both the catenary and parabolic equations approximate the horizontal conductor tension and the actual conductor tension as equal, that is $T_h = T$. At the low point of the sag curve this is obviously true. As a result of the relatively small vertical component of tension due to the weight load of the conductor at the conductor attachment point $T > T_h$. To compensate for this slight increase in conductor tension a rule of thumb reduction of 10% of the bench mark tension has been adopted that adequately accounts for this approximation. In other words, for ACSR conductors fitted with vibration dampers the percentage of ultimate tensile strength is reduced from 25% to 22.5%.

The actual maximum conductor tension at the supporting structure will be a function of the span length and conductor attachment reduced level or put more simply the weight span of the conductor each side of the supporting structure. The exact catenary equation for the conductor tension at the supporting structure for level spans is given as,

$$T = T_h \cosh \frac{\omega L_n}{2T_h} \qquad (2.2)$$

having the first order Talyor series expansion parabolic approximation of,

$$T = T_h + \frac{\omega_n^2 L^2}{8T_h} + \frac{\omega_n^2 L^4}{24T_h^3} \qquad (2.3)$$

2.2.2.2 Average Conductor Tension

When determining conductor inelastic stretch it must be decided whether the horizontal or actual conductor tension at the attachment point should be used. Whilst the difference between both these tensions is marginal, the use of actual conductor will lead to an over estimation in inelastic stretch. In contrast horizontal conductor tension will lead to an under estimate of in inelastic stretch.

A more appropriate tension for determining inelastic stretch is the average conductor tension. The average conductor tension along the conductor length is given as,

$$T_{av} = \frac{2}{l} \int_0^{l/2} t' dl \qquad (2.4)$$

where t' is the conductor tension at any point in the chord length and is derived by substituting $x = L/2$ into equation (2.2), hence

$$t' = T \cosh \frac{x}{c} \qquad (2.5)$$

From Figure 2.1 the conductor length equation for any horizontal distance x is given as,

$$l = c \sinh \frac{x}{c} \tag{2.6}$$

or

$$dl = \cosh \frac{x}{c}\, dx \tag{2.7}$$

Nigol & Barrett (63) provide the solution of equation (2.4) by the substitution of equations (2.5), (2.6) and (2.7) and with the appropriate transformations, the average tension is given by,

$$T_{av} = \frac{T}{2} \left(\cosh \left(\frac{l}{2c} \right) + \frac{l}{2c} \left(\frac{1}{\sinh \left(\frac{l}{2c} \right)} \right) \right) \tag{2.8}$$

2.2.2.3 Conductor Span Length

The next approximation used in both the catenary and the parabolic equations equates the span length and the conductor length, that is L = l. In this instance, the parabolic equation is more exact since the parabolic sag is less than the catenary sag. The error in the parabolic sag for a typical range of curve constants and fixed effective span lengths does not exceed 0.002%. Even for a curve constant of 1000 and a fixed effective span of 1200 m, that is a very slack span, the error is as little as 0.006%.

In contrast figure 2.7 illustrates the error in the catenary/span length error of a range of effective spans and curve constants.

In addition to the span length approximations already mentioned, in non fixed spans such as that of suspension structures which allow longitudinal movement of the conductor attachment point, the conductor horizontal component of tension in adjacent spans having dissimilar length will be equalised to some extent by longitudinal movements of the insulator string. This movement whilst small, contributes to an error in span length.

Maximum longitudinal insulator movement or maximum longitudinal conductor tension acting on a conductor attachment point will occur at maximum operating temperature.

Unlike Boyce and Simpson (17) who assumed the horizontal component of tension in a transmission line section was constant thus establishing the equivalent span theory, Barrien (12) developed the continuous catenary theory by considering a balance of the weight of the insulator string and the weight of the conductor on each side of the insulator string acting at the insulator/structure attachment point.

This continuous catenary theory accounts for the approximate equalisation of the adjacent span tension and longitudinal movement of the suspension insulator string. As previously mentioned this longitudinal movement of the suspension insulator string is effectively a span length change.

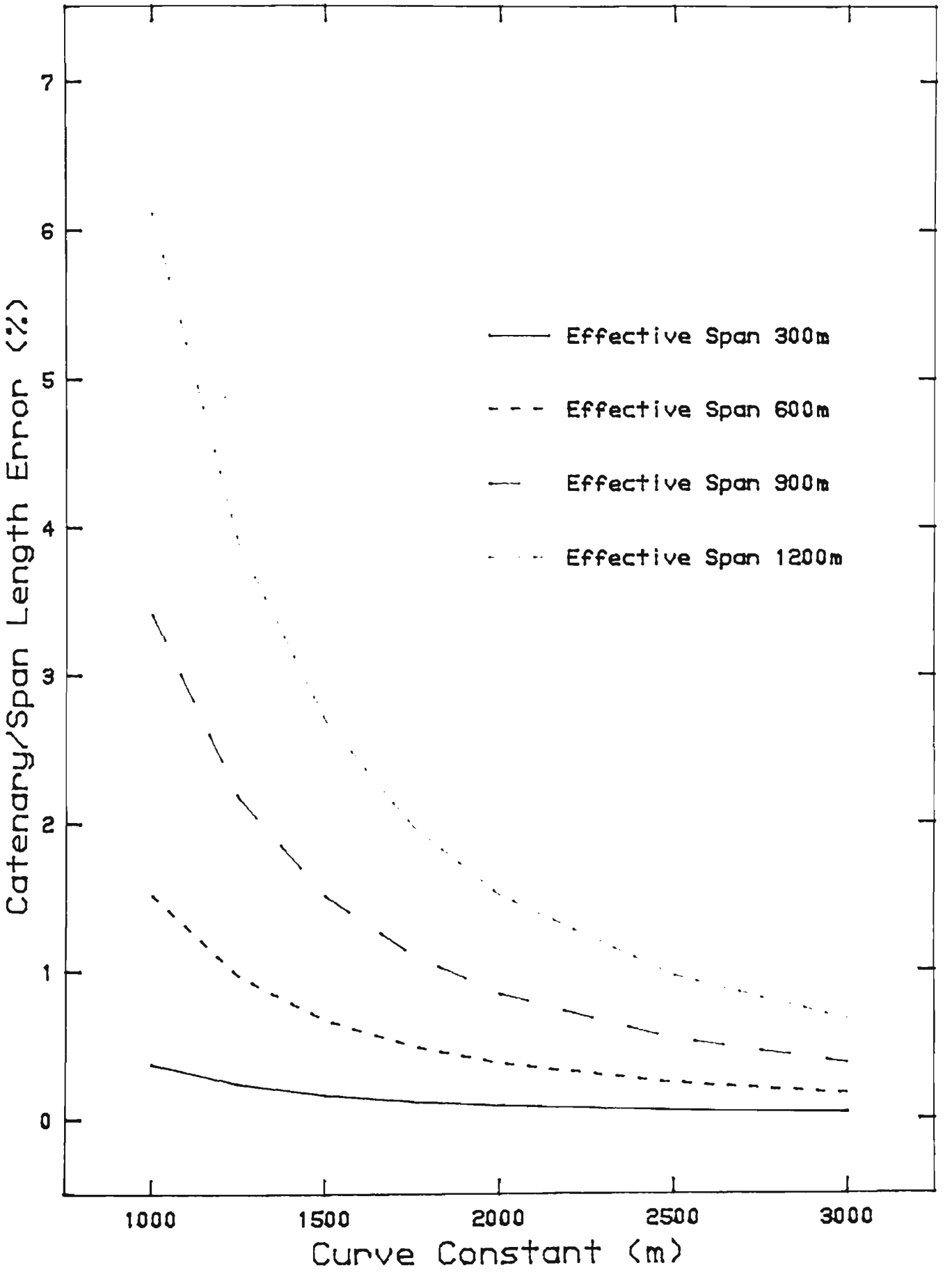

FIG 2.7 CATENARY/SPAN LENGTH ERROR

Typical movements can be of the order of 20 mm for spans of 400 m in gently undulating topography. This represents a differential tension at a suspension structure of the order of 5%.

The next approximation used in the parabolic change of state equations is that of the first order approximation of the parabolic curve length compared with the exact catenary curve length used in the catenary change of state equation. In mathematical terms comparing the catenary curve length equation given as,

$$l = 2c \sinh \frac{L}{2c} \qquad (2.9)$$

with the first order Talyor series expansion parabolic approximation of

$$l = L + \frac{L^3}{24c^2} \qquad (2.10)$$

The error associated with this approximation has already been discussed in section 2.3.1 and illustrated in Figure 2.4.

As previously mentioned Boyce and Simpson (17) established the equivalent span theory by assuming a constant tension in a transmission line section. Any tension variations due to climatic changes will depend on the span length in the section and the whole section of line will behave in a similar way as an "equivalent span".

This is illustrated by assuming a series of freely supported spans l_1, l_2, l_3, l_4 etc. having a total section length of Σl. The total length of conductor under the an initial conditions of T_1 and ω_1 is given by,

$$\Sigma l + \frac{1}{24c_1^2} \Sigma l \qquad (2.11)$$

and at some final condition of T_2 and ω_2 the total conductor length is given by,

$$\Sigma l + \frac{1}{24c_2^2} \Sigma l \qquad (2.12)$$

The change in conductor length is given by,

$$\frac{1}{24}\left(\frac{1}{c_1^2}-\frac{1}{c_2^2}\right)\Sigma l^3 \qquad (2.13)$$

Similarly the total change in length of conductor for n spans each L_E in length would be

$$\frac{1}{24}\left(\frac{1}{c_1^2}-\frac{1}{c_2^2}\right)\Sigma l_E^3 \qquad (2.14)$$

Equating equations (2.13) and (2.14)

$$\Sigma l^3 = nL_E^3 \qquad (2.15)$$

or

$$\Sigma l^3 = \frac{\Sigma l}{L_E} L_E^3 \qquad (2.16)$$

from which,

$$L_E = \sqrt{\frac{\Sigma l^3}{\Sigma l}} \qquad (2.17)$$

In other words equation (2.17) describes the tension variation of a single span of equivalent length, L_E under varying temperature and loading conditions to a similar tension variation in a series of spans, l_1, l_2, l_3, l_4 etc. under the same change of conditions assuming that the tension of the conductor remains the same either side of a suspension string of insulators.

Because of the nature of the equivalent span theory and the assumptions employed, no similar theory is available for the continuous catenary theory.

2.2.2.4 Conductor Physical Parameters

The next approximations used in both change of state equations are attributed to the physical parameters of mass, cross section area, modulus of elasticity, coefficient of linear expansion and the initial conductor horizontal tension. The conductor physical parameters will be discussed in detail in Chapter 3, however it is appropriate to illustrate the changes in sag and tension of a typical conductor with changes in each of the physical parameters.

The mass of the conductor is a function of the density of the material, the number of wires, the lay ratio of the wires, the tolerance on the diameter of the wires and whether the conductor is provided with grease for additional corrosion protection.

Typical conductor mass variations can be of the order of 2.5% and can lead to conductor sag and tension variations as illustrated in Figure 2.8.

The cross sectional area of a conductor is a function of the number of wires, the lay ratio of the wires and the tolerance on the diameter of the wires. Typical conductor cross sectional area variations can be of the order of 2.5% and can lead to conductor sag and tension variations as illustrated in Figure 2.9.

The modulus of elasticity of a conductor is a function of the lay ratios of the wires, the tolerances on the diameter of wires, the conductor construction and the modulus of the individual wires. Typical conductor modulus of elasticity variations from test to calculated values can be of the order of 5% and can lead to conductor sag and tension variations as illustrated in Figure 2.9.

The coefficient of linear expansion of a conductor is a function of the coefficient of thermal expansion, cross sectional area and modulus of elasticity of the component wires. The calculated coefficient of linear expansion and the actual coefficient of linear expansion of a conductor determined by test can vary in the order of 5% and may lead to conductor sag and tension variations as illustrated in Figure 2.10.

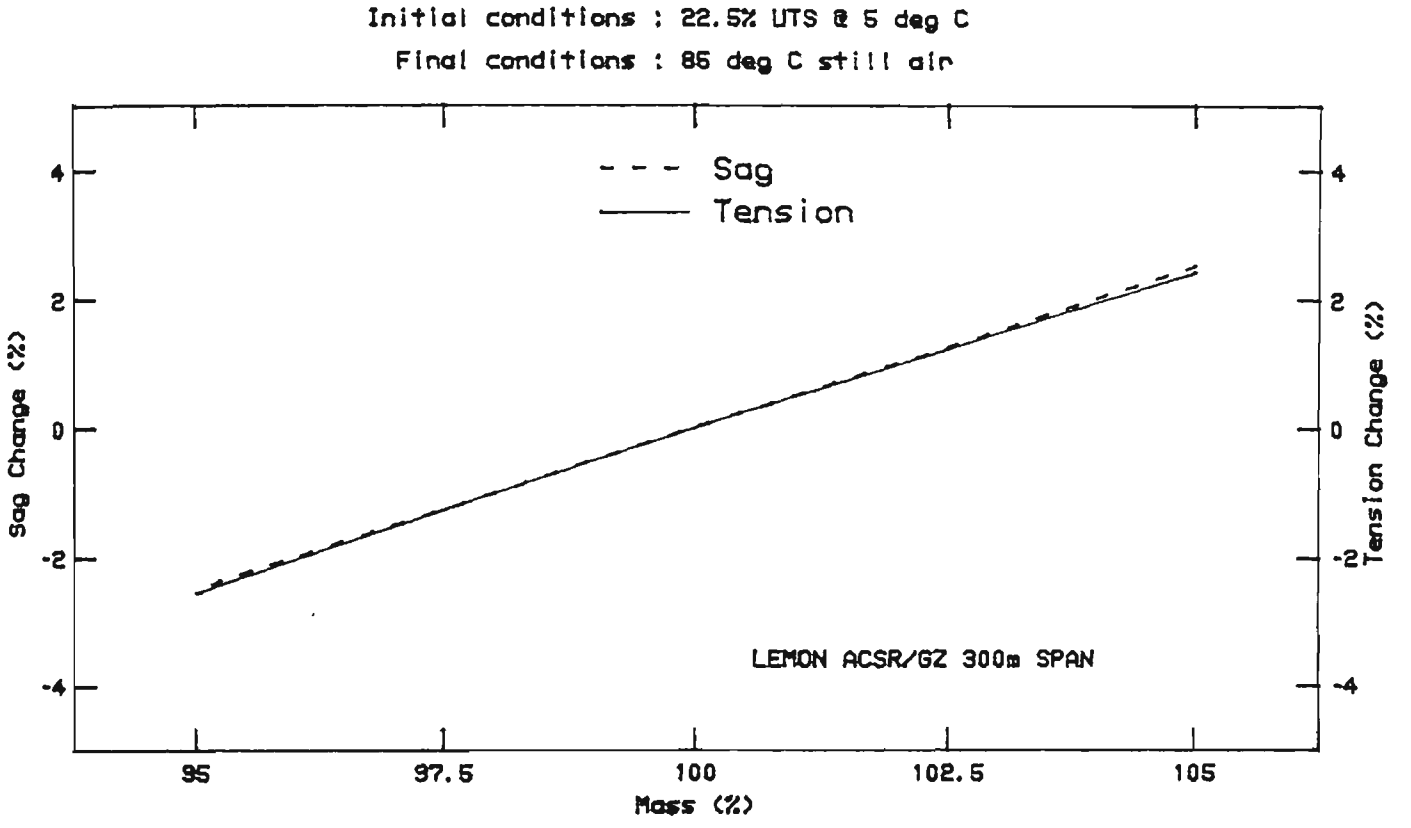

Fig 2.8 Conductor Tension & Sag Change With Change in Mass

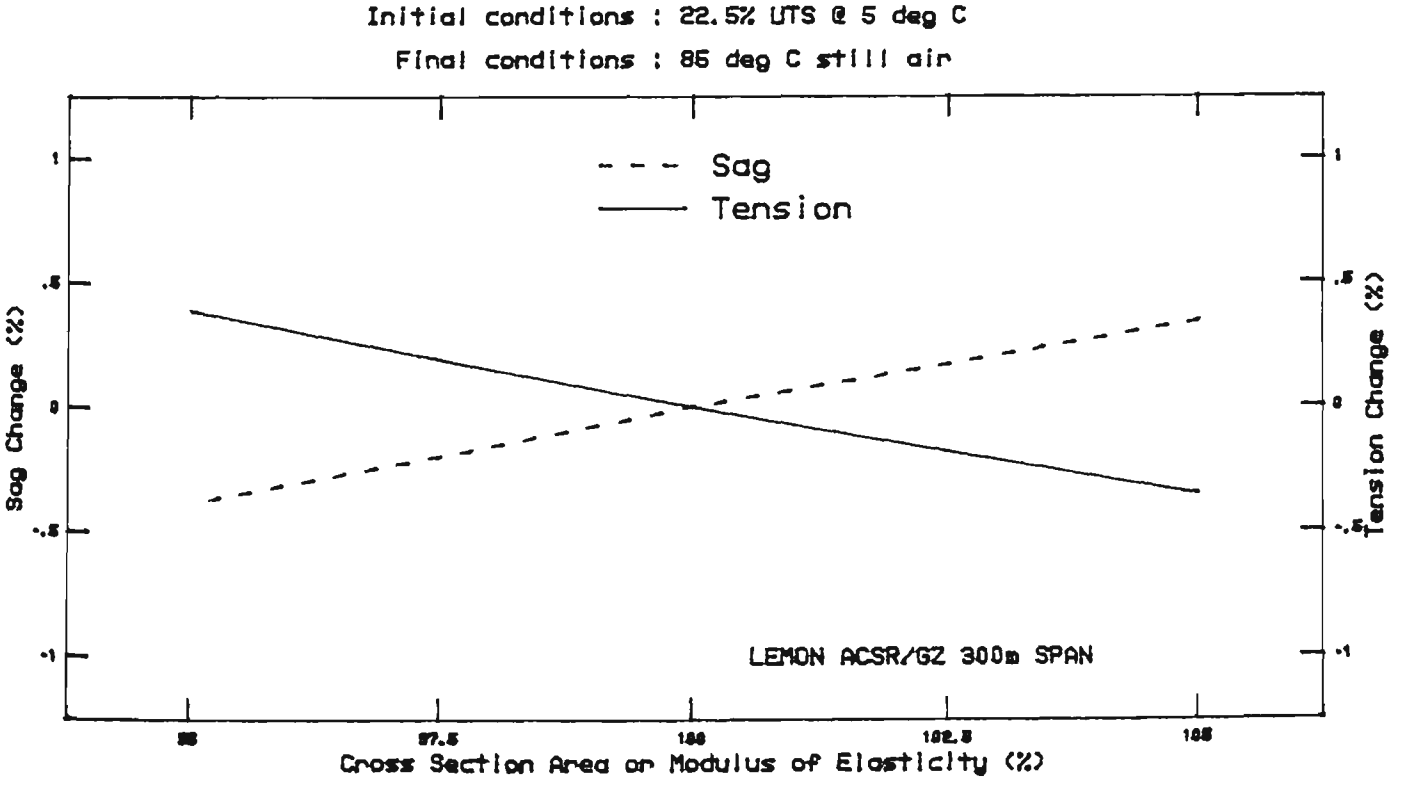

Fig 2.9 Conductor Tension & Sag Change With Change in CSA or Modulus of Elasticity

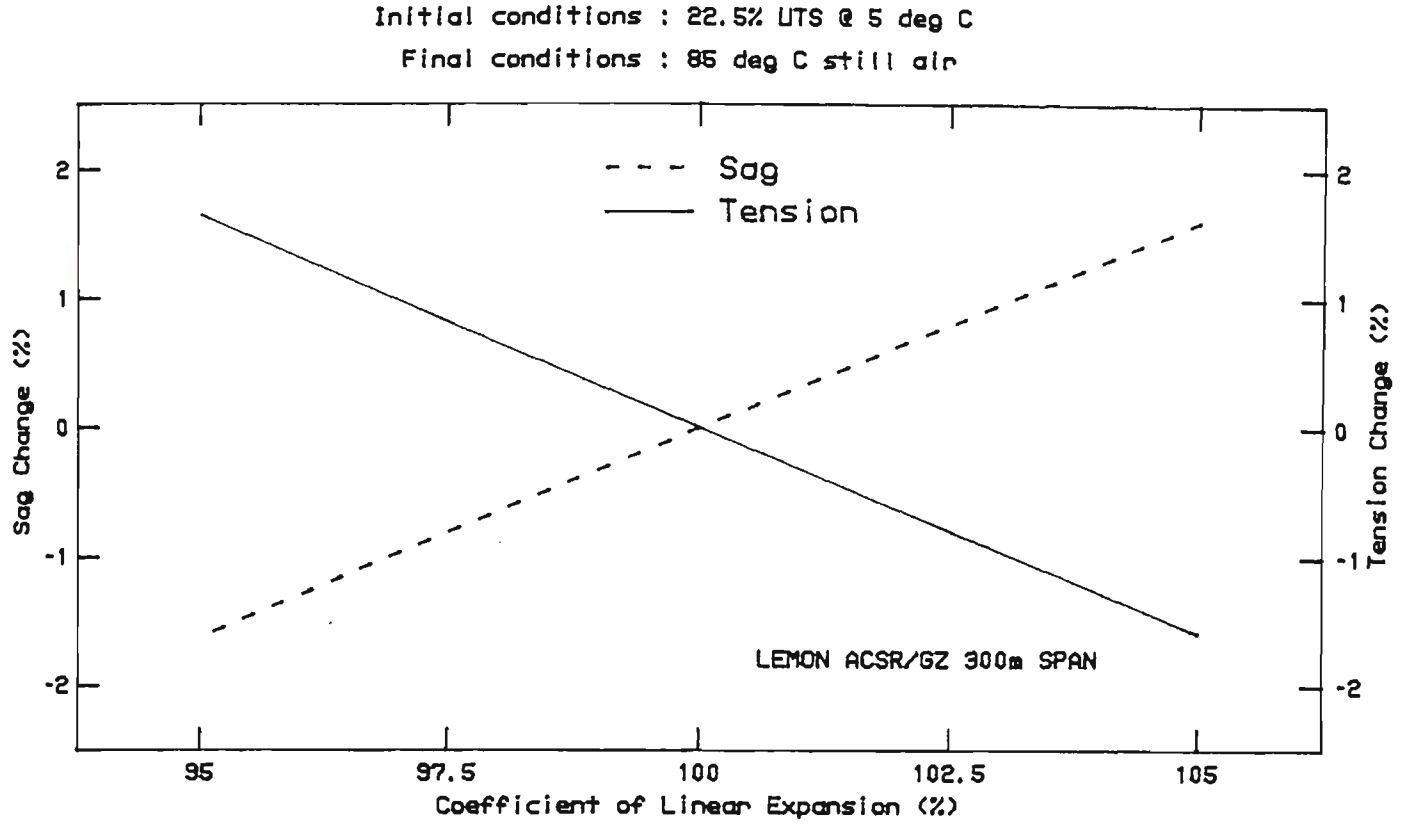

Fig 2.10 Conductor Tension & Sag Change With Change in CLE

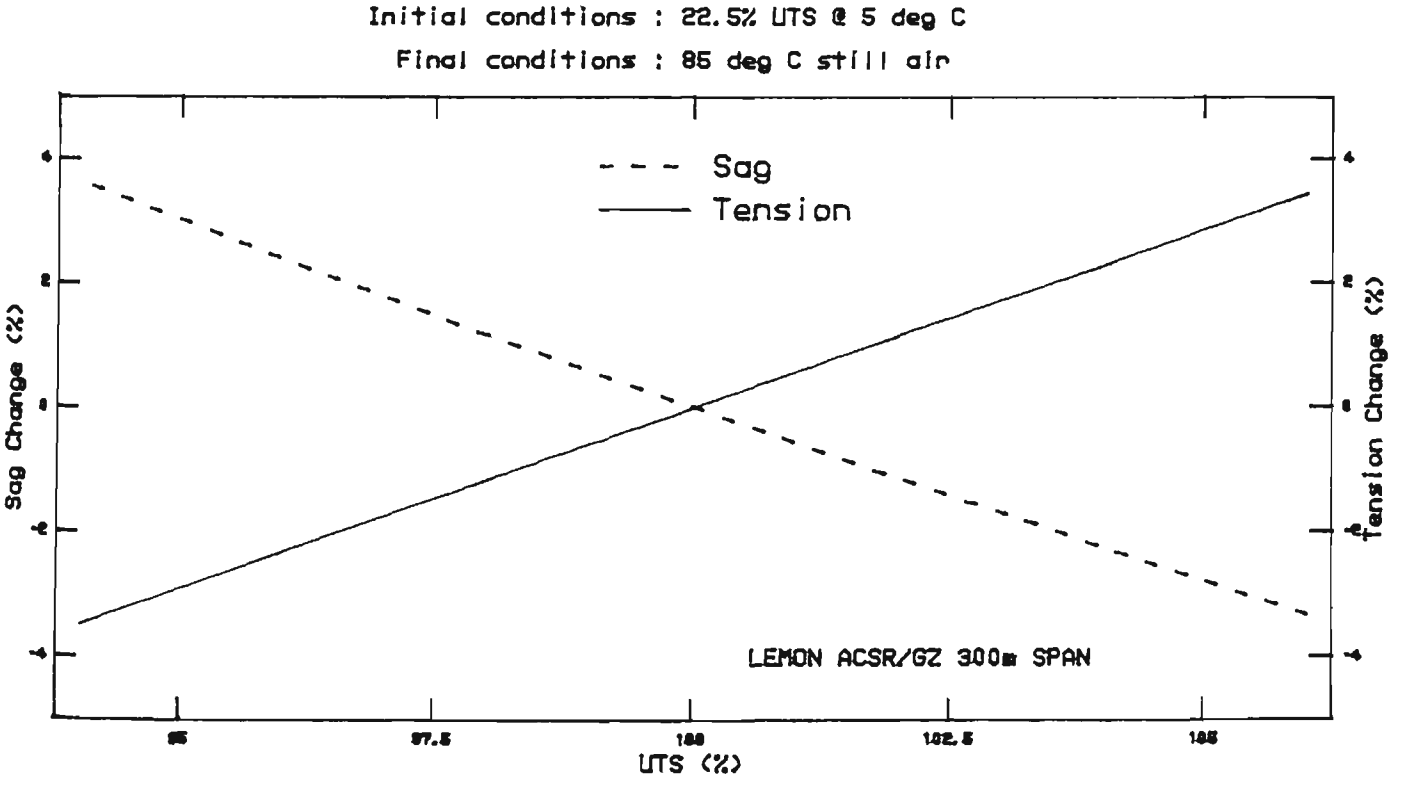

Fig 2.11 Conductor Tension & Sag Change With Change in Ultimate Tensile Strength

The most critical conductor parameter that affects sag and tension is that of the ultimate tensile strength (UTS). The UTS of a conductor is a function of the strength of the component wires and variation between calculated UTS and actual UTS determined by test can be of the under of 5%. The resultant variations to sag and tension of UTS variations is illustrated in Figure 2.11.

2.2.2.5 Conductor Temperature

In some cases where the conductor is operating at or near the maximum operating temperature, the core of the conductor will be at a higher temperature than the outside surface of the conductor. This effect can affect the conductor tension and in particular for an ACSR conductor where the steel core may be carrying most of the mechanical load.

At relatively high conductor temperatures, once elastic elongation of the aluminium of an ACSR has occurred to the extent of the aluminium carrying little mechanical load then the conductor will exhibit the coefficient of linear expansion of the steel core. This load distribution change phenomenon is described in detail by Nigol and Barrett (62) and discussed in Chapter 3.

Douglas (33) provides an empirical equation to determine the temperature variation between the core and surface temperature for an ACSR conductor and is given as,

$$\Delta\theta = \theta_c - \theta_s' = \frac{RI^2}{2K\pi r_c}\left[\frac{1}{2} + \frac{r_c^2}{r_s^2 - r_c^2}\ln\frac{r_c}{r_s}\right] \quad (2.18)$$

A similar equation has also been derived by Morgan (59). From this equation it is concluded that the radial temperature is a function of conductor construction, current, resistance and thermal conductivity. The surface temperature will depend on wind speed and temperature, radiative cooling, solar radiation and emissivity and solar absorption coefficients.

Critical in determining the thermal gradient of the conductor is the value of radial thermal conductivity. Morgan (59) suggests that a value of $2W.m^{-1}.C$ is appropriate even though it is recognised that the thermal conductivity increases with increasing tension.

Foss, Lin & Carberry (40) have published test results to suggest that the temperature thermal gradient of approximately 10% exists. This approximation is also suggested by Douglass (33) and an IEEE working group (74A) on the Dynamic Thermal Line Ratings.

Nigol and Barrett (62) have determined a ratio aluminium temperature rise above ambient to steel core temperature rise above ambient over a full range of currents to be constant in light winds. For standard round wire ACSR and trapezoidul wire compact ACSR this ratio is 0.90 and 0.95 respectively. This support the previous authors approximations.

From this discussion it is concluded that for determining conductor tension at maximum operating temperature the core is likely to be 10% hotter than the surface temperature. Unfortunately the traditional catenary and parabolic tension equations do not allow differing aluminium and steel core temperatures to be used in determining tension.

2.2.3 Sag Tension Evaluation by Strain Summation (STESS)

The STESS computer program details of which have been published by Barrett, Dutta and Nigol (9) is the first real departure of determining conductor tension and sag by the classical equivalent span and continuous catenary theory.

The program evaluates conductor tension by summating the various components of strain including the inelastic strain. Accordingly with the introduction of inelastic strain the conductor tension and sag become not only dependent on prevailing climatic conditions but time dependent with a chronological loading history. The concept of the strain summation is given as follows.

$$\text{Total Strain} = \text{Thermal Strain} + \text{Slack} + \text{Elastic Strain} + \text{Creep Strain} + \text{Settling Strain} \qquad (2.19)$$

2.2.3.1 Thermal Strain

The thermal strain component of equation (2.19) is defined by Nigol and Barrett (7) and is given by the classical linear term and an additional a quadratic term. The quadratic term includes the effect of the change of modulus of elasticity with temperature of 55 $MPa.C^{-1}$. This effect is very small for the aluminium component of an ACSR construction as illustrated in Figure 2.12.

Since STESS summates differing aluminium and steel thermal strains two equations are necessary and are given by,

$$D_s = \left[11.3\,(\theta_s - 20) + 0.008\,(\theta_s^2 - 400)\right] * 10^{-6} \qquad (2.20)$$

and

$$D_a = \left[22.8\,(\theta_a - 20) + 0.009\,(\theta_a^2 - 400)\right] * 10^{-6} \qquad (2.21)$$

These equations do not include the effect of load distribution changes between aluminium and steel components discussed in section 2.2.2.5 and Chapter Three.

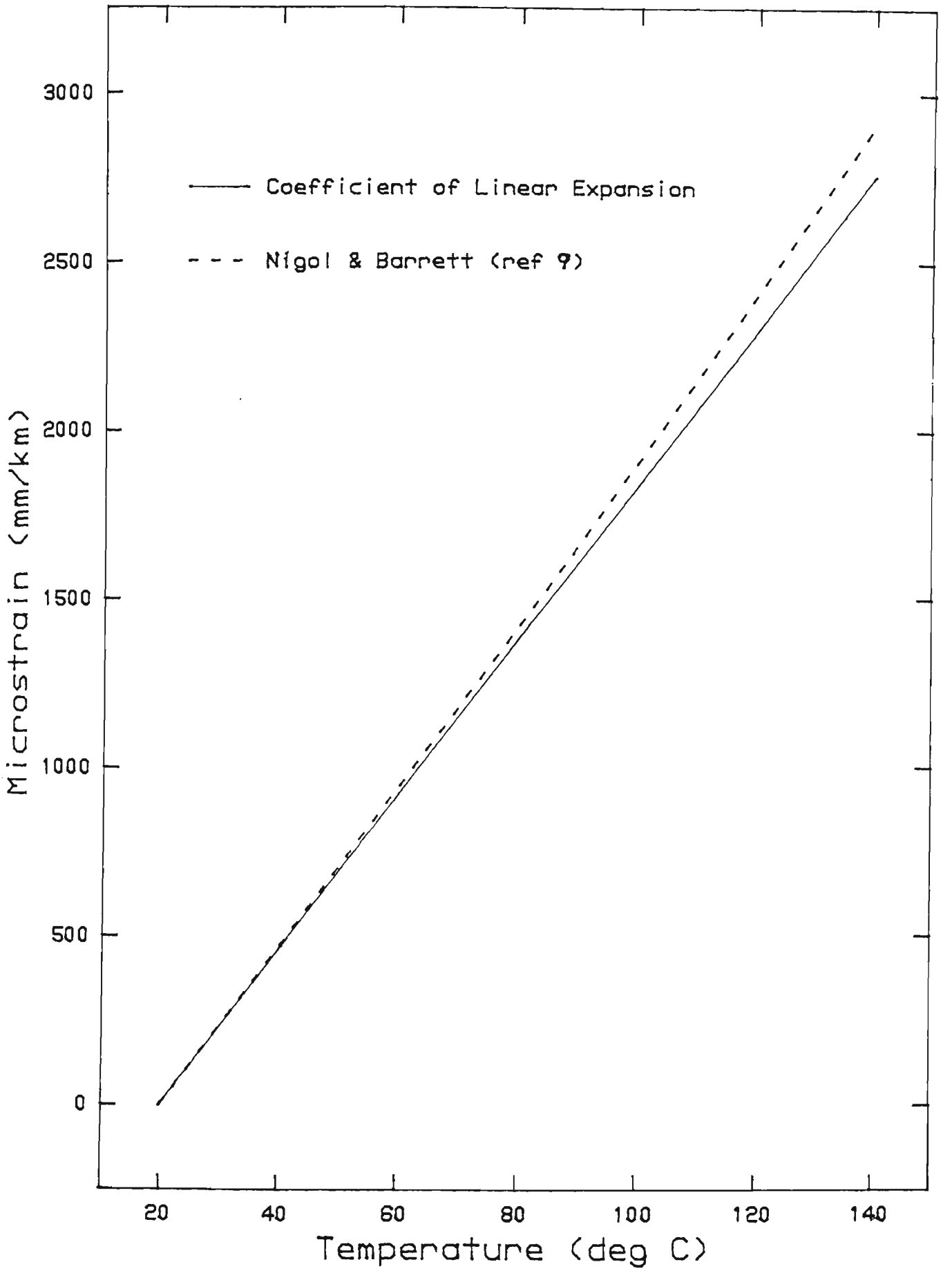

FIG 2.12 EXPANSION OF AL COMP OF ACSR/GZ

2.2.3.2 Slack

The aluminium slack term describes the hysterisis or sometimes termed the zero correction of the initial part of a stress-strain curve on an ACSR conductor. In short test spans the slack component can be up to 150 $mm.km^{-1}$ however over long spans such as those encountered in the field it is considered that the slack would be very small. This is also supported by the practice of removing any slack and some degree of metallurgical creep by prestressing the conductor prior to final termination.

2.2.3.3 Elastic Strain

The elastic strain is determined from the modulus of elasticity of the aluminium and in the case of an ACSR conductor the steel final curves of a stress-strain test.

This is not a departure from current methods and supports the accepted practise of the initial modulus curve to 30% UTS being essentially parallel to the final modulus curve.

2.2.3.4 Creep Strain

Conductor creep strain is non recoverable or inelastic plastic deformation sometimes termed permanent elongation that occurs under tensile load and increases with both temperature and stress. Permanent elongation begins at the instant of applied

tensile load and continues at a decreasing rate as long as the tension and temperature remain constant. This progressive deformation is described in detailed in references (18, 19, 20, 21, 24, 27, 44, 47, 49, 53, 63 and 64).

The equation used by STESS to describe the creep strain behaviour is similar to that found in the abovementioned references and is given by,

$$\mu\varepsilon = A_2 t^{n_1} s^{n_2} e^{\delta(\theta-20)} \qquad (2.22)$$

The four parameters A_2, n_1, n_2 and δ define the creep behaviour of the aluminium and steel components and are determined by test. The details of the creep tests are discussed in Chapter Three.

The procedure adopted by STESS calculates creep and includes a chronological loading history, including all prestressing.

2.2.3.5 Settling Strain

The author's describes settling strain as geometric settling of the wires moving both radically and tangentially during any initial loading.

The settling strain of the steel and aluminium components at any given steel or aluminium stress is defined as,

"the substraction of both the elastic strain
and the one hour room temperature creep strains
from the initial stress strain curve".

This settling is assumed to be independent of temperature and complete in one hour.

2.2.3.6 Other Features of STESS

The main advantage of the program is the ability to determine stringing tensions for any given future loading conditions and limiting constraint. In addition the program can examine the effects of stress relaxation, thermal gradients in the conductor and determine the load distribution of the conductor wire components. This is a more realistic approach if the conductor failure criteria is based on individual wire strengths.

These advantages aside a considerable amount of conductor laboratory testing such as stress strain tests, coefficient of linear expansion tests and creep tests are necessary to be assured of the certainty and accuracy of the tensions and sags.

2.3 CONDUCTOR SAG MEASUREMENTS THEORY

Several techniques have been developed to measure conductor sags. Most techniques have been developed to measure conductor sags. Most techniques are described in references (3) and (80). The methods are used in these studies. The first method is a modified tangent observation

method described by Winkleman (80). Unlike Winkleman's method which is based on a parabola approach employing several approximations, an exact catenary curve is used. The second method used in these studies is the satellite or point distance observation method employing least squares analysis of the observations.

2.3.1 Tangent Observation Technique

Tangent observations of existing conductors are equally as accurate as the common point distance approach and more environmentally acceptable since the method requires little and in most cases no additional clearing of flora other than the necessary routine clearing for the safe operation of the transmission line.

The basic theory of the tangent observation is illustrated in Figure 2.1 where the general equation of the catenary curve applies and is given by,

$$y = c \left[\cosh \left(\frac{x}{c} \right) - 1 \right] \qquad (2.23)$$

It would be an easy task to determine the curve constant if the low point of the curve was easily identified by inspection. As a result of physical constraints, the identification of the low point is not easily achieved. Consequently, it is more convenient to transform the co-ordinate axis to one of the

conductor attachment points and determine the curve constant of a span by a combination of survey measurements and iterative calculations.

The transformed ordinate and abscissa from the origin to the conductor attachment point is obtained from inspection of Figure 2.13 and is given by,

$$X = x + a \tag{2.24}$$

$$Y = y - y' \tag{2.25}$$

where

$$y' = c \left[\cosh \left(\frac{a}{c} \right) - 1 \right] \tag{2.26}$$

The horizontal distance to the low point has been previously defined in Figure 2.2 and is given as,

$$y' = \frac{L}{2} - c \sinh^{-1} \left[\frac{H}{K} \right] \tag{2.27}$$

Substituting equation (2.24) into (2.23)

$$y = c \left[\cosh \left(\frac{x-a}{c} \right) - 1 \right] \tag{2.28}$$

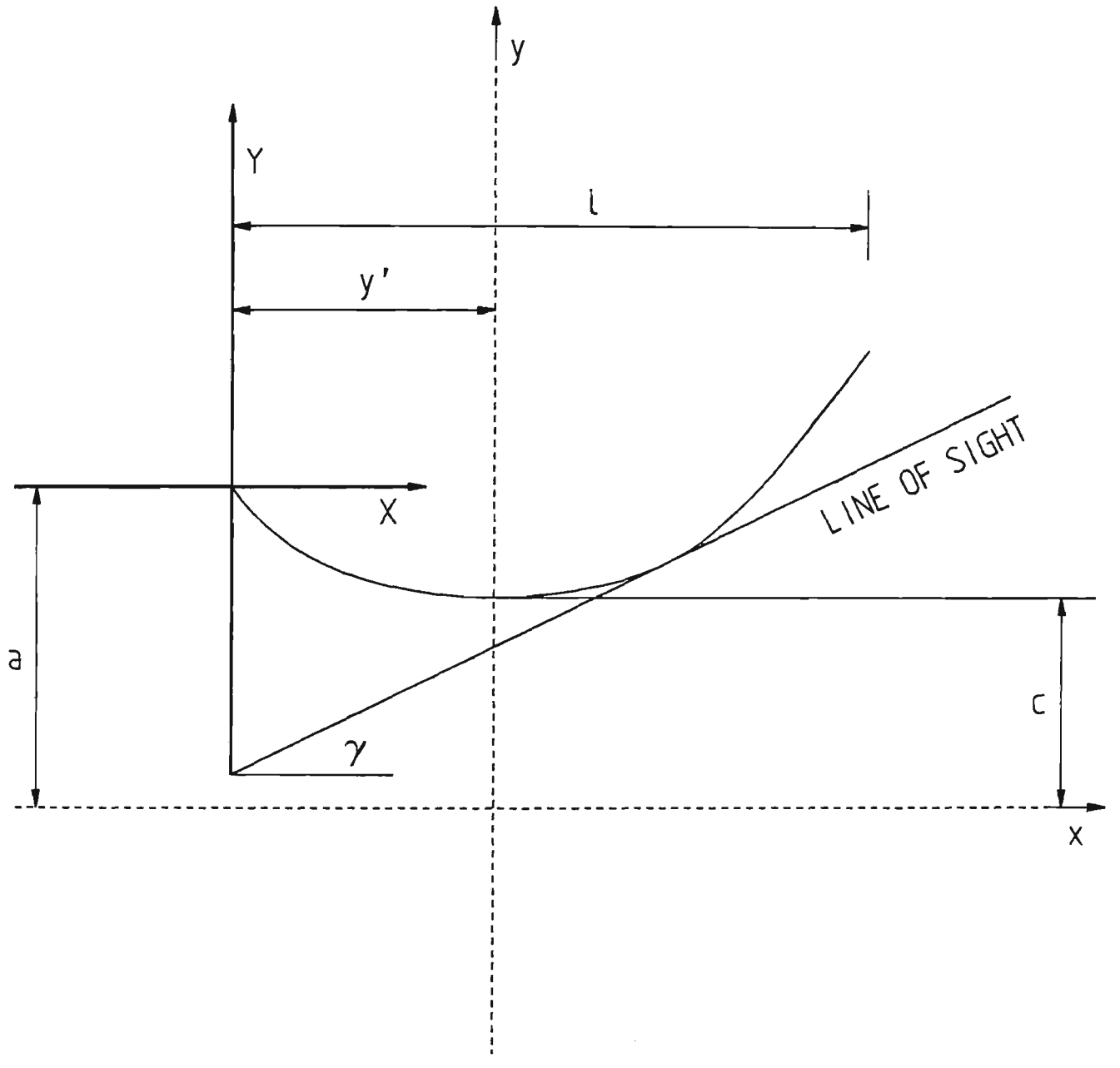

FIGURE 2.13 TRANSFORMED ORDINATE AND ABSCISSA AXIS OF CATENARY CURVE

and substituting equations (2.28) and (2.26) into equation (2.25) the transformed abscissa catenary equation becomes

$$Y = c \left[\cosh \left(\frac{a}{c} \right) - \cosh \left(\frac{x-a}{c} \right) \right] \quad (2.29)$$

The observed line of sight has a slope and an intercept to the abscissa of $\tan \gamma$ and $y_1 - x_1 \tan \gamma$ respectively. The equation of the line of sight is given as,

$$Y = X \tan \gamma + y_1 - x_1 \tan \gamma \quad (2.30)$$

Survey field measurements of conductor attachment reduced levels, conductor span length and tangent angle together with equating equation (2.29) and (2.30) and using computer iterative techniques determines the catenary constant. Backsight and foresight observations are taken to increase the level of confidence in the determined curve constant.

2.3.2 Satellite Observation Technique

In some circumstances it is not practical to make tangent observations of the conductor. An alternative approach using the more traditional point distance method may be employed. To achieve a high level of confidence in these measurements, five points are observed and a least squares method applied to the parabolic survey data.

The basic theory of the least squares analysis is described by reference to Figure 2.14 where the general equation of the parabolic curve applies and for the lowest observed point P_0 as,

$$b_0 = ka_0^2 \tag{2.31}$$

At point P_1,

$$b_0 + b_1 = k\left[a_0 + a_2\right]^2 \tag{2.32}$$

Similarly at points P_2, P_3 and P_4,

$$b_2 + b_1 = k\left[a_0 + a_2 - a_1\right]^2 \tag{2.33}$$

$$b_3 + b_1 = k\left[a_3 - a_0 - a_2\right]^2 \tag{2.34}$$

$$b_4 + b_1 = k\left[a_4 - a_0 - a_2\right]^2 \tag{2.35}$$

By substitution of equation (2.31) into (2.32) to (2.35), thus

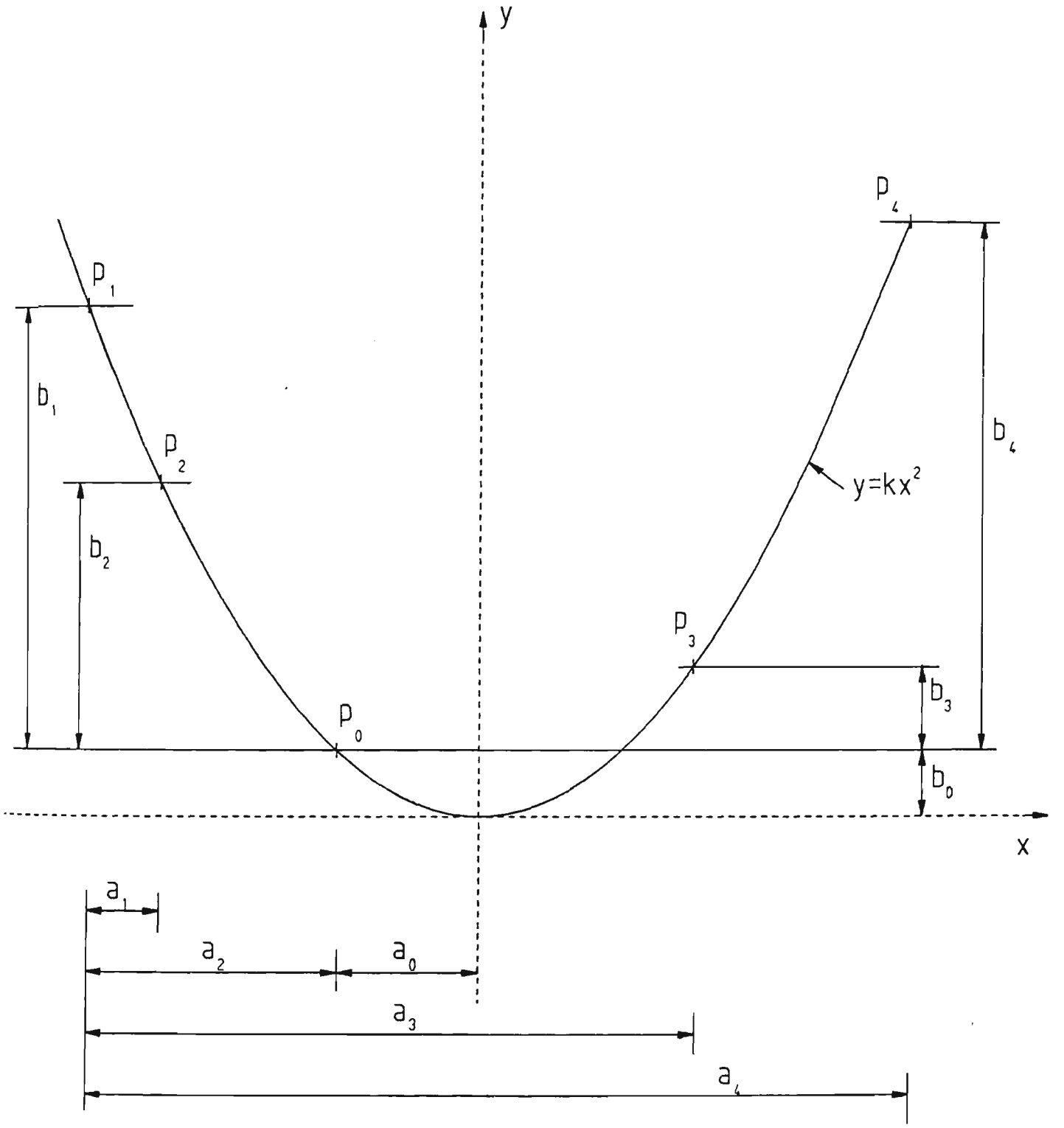

FIGURE 2.14 PARABOLIC SPAN LEAST SQUARES METHOD OF ANALYSIS

$$\left.\begin{aligned} b_1 &= k\left[a_2^2 + 2a_0 a_2\right] \\ b_2 &= k\left[a_5^2 + 2a_0 a_5\right] \\ b_3 &= k\left[a_6^2 - 2a_0 a_6\right] \\ b_4 &= k\left[a_7^2 - 2a_0 a_7\right] \end{aligned}\right\} \qquad (2.36)$$

where

$$a_5 = a_2 - a_1$$

$$a_6 = a_3 - a_2$$

$$a_7 = a_4 - a_2$$

Solution of A and k must satisfy equations (2.31) and (2.36). Solution of B is obtained from equation (2.31). Equation (2.36) the similar form to

$$Y = p_0 + p_1 X + p_2 X^2 \qquad (2.37)$$

where

p_0 = constant

$p_1 = 2kA_N$

$p_2 = k$

The low point horizontal distance to the observed point is given as,

$$A = \frac{p_1}{2p_2} \tag{2.38}$$

and the curve constant is,

$$c = \frac{1}{2k} \tag{2.39}$$

and the solution of p_0, p_1 & p_2 is determined by solution of the least squares parabolic simultaneous equation,

$$\left.\begin{aligned} \Sigma Y &= p_0 N + p_1 \Sigma X + p_2 \Sigma X^2 \\ \Sigma XY &= p_0 \Sigma N + p_1 \Sigma X^2 + p_2 \Sigma X^3 \\ \Sigma X^2 Y &= p_0 \Sigma X^2 + p_1 \Sigma X^3 + p_2 \Sigma X^4 \end{aligned}\right\} \tag{2.40}$$

2.3.3 Conductor Temperature Measurements

Critical to any conductor sag measurements is concurrent conductor temperature measurements. Two methods are available to

measure conductor temperature, remote and direct. The remote method employs infra-red scanning whilst the direct method uses a contact thermocouple with a calibrated indicating instrument.

For the purpose of these studies the conductor temperature measurements were carried out using a commercially available live line conductor temperature measuring instrument illustrated in Plate 2.2.

The instrument was laboratory calibrated before and after all survey measurements to give reassurance of the certainty of conductor temperature measurements. The calibration curve of the instruments is given in Figure 2.15.

The instrument was used strictly in accordance with manufacturer's recommended methods and the application of the instrument to a live conductor via a live line operating rod is illustrated in Plate 2.3.

2.3.4 Systematic Errors

Systematic errors arise from sources which are known and therefore their effects can be either eliminated or compensated.

The tangential and point distance observation techniques have five sources of systematic errors. The first comes from observation error cause by heat haze distorting the surface of the conductor. This problem is generally eliminated by carrying out backsight and foresight measurements on the span under

PLATE 2.2 - DIRECT LIVE LINE CONDUCTOR TEMPERATURE MEASURING INSTRUMENT

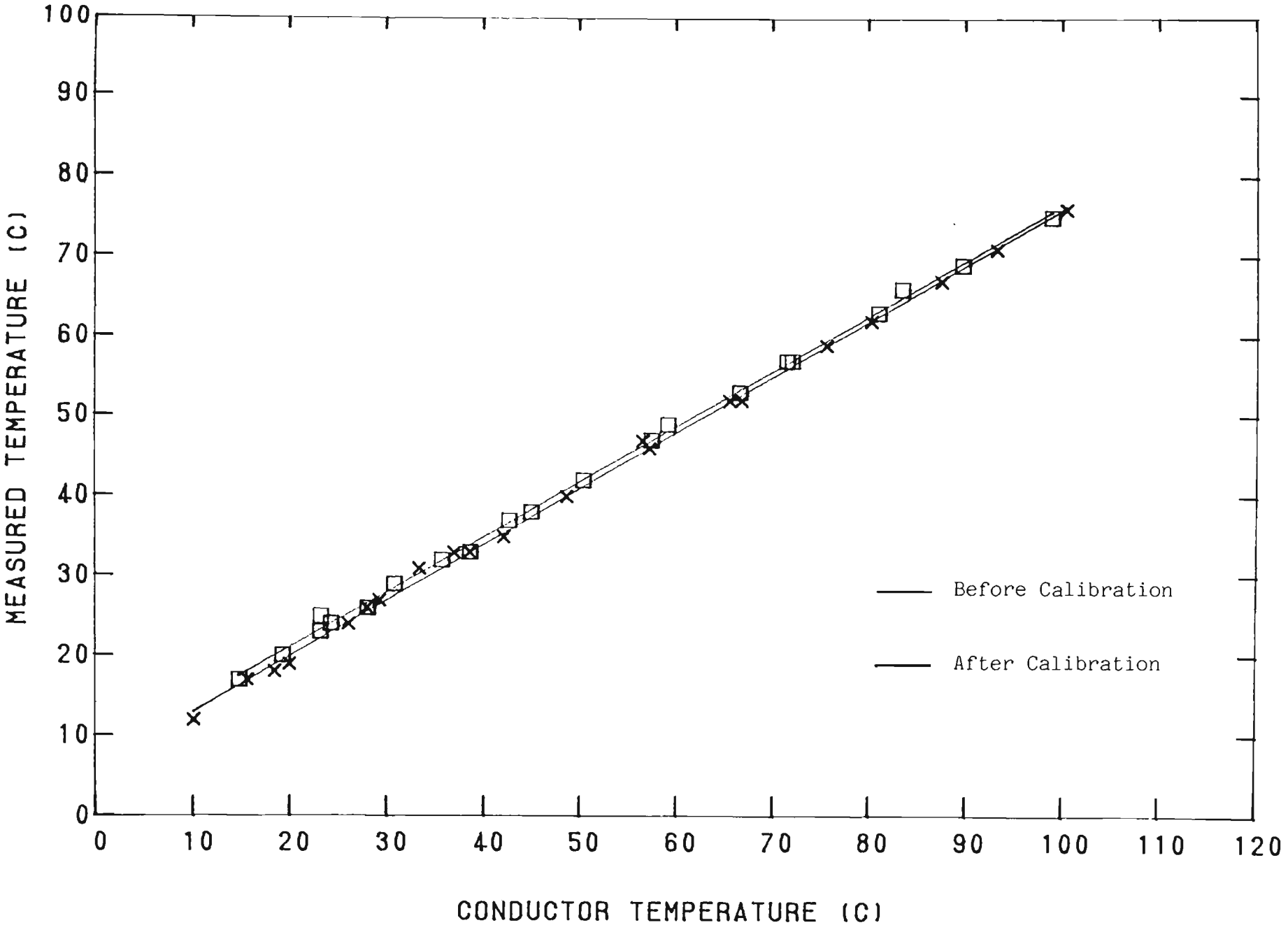

FIGURE 2.15 CALIBRATION CURVE OF LIVE LINE TEMPERATURE MEASURING EQUIPMENT

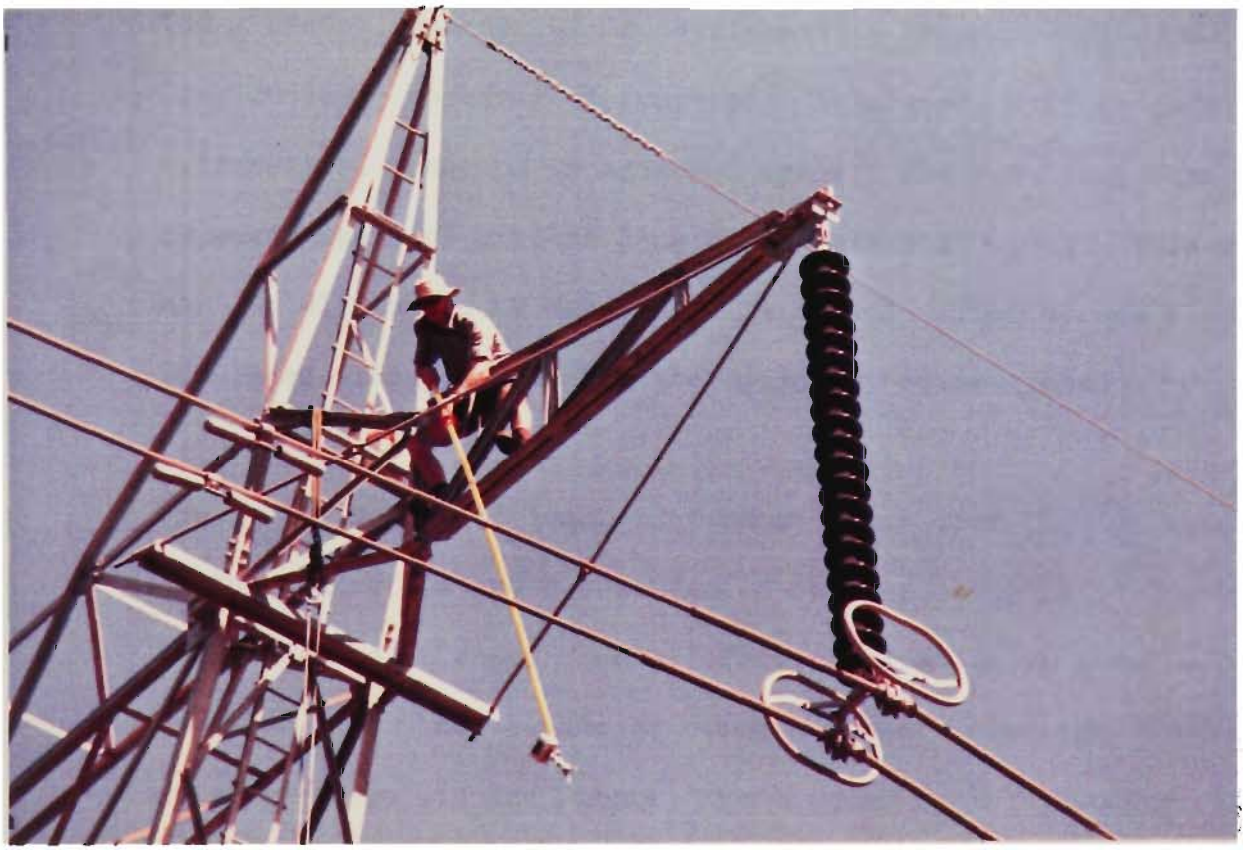

PLATE 2.3 - APPLICATION OF CONDUCTOR TEMPERATURE MEASURING INSTRUMENT

consideration, thus making observations with differing amounts of refracted light. In addition, since the catenary data is determined in the field, a sensitivity analysis of the catenary constant may be carried out to determine the effect of any tangential error.

The second source of a systematic error comes from the longitudinal movement of suspension insulator strings caused by differential tensions in adjacent spans. The resultant error for adjacent spans of similar lengths is generally small. This error may be eliminated by measuring the longitudinal movement of the insulator string and making the necessary corrections.

The third source of inaccuracy comes from wind blowing parallel to the conductors under observation causing a change in the basic shape of the catenary curve. This results in an error of the location of the conductor with respect to the conductor attachment points and hence the tangent angle observed. This problem is partly overcome by carrying out backsight and foresight observations. However a more practical way of eliminating this error source is aborting the sag measurements when the longitudinal component of wind exceeds a velocity of approximately 4 $m.s^{-1}$.

The next source of survey inaccuracy is caused by air movements orthogonal to the line inducing aeolian vibration of the conductor. Observations of the extremes of the conductor

vibration may be taken, thus enabling a more accurate determination of the conductor observed tangent point to be achieved.

The final source of systematic errors is that of the complex dynamics of a transmission line. During the course of any measurements taken the prevailing climatic conditions will change. These changes cause tower movements, suspension insulator string longitudinal movements and lastly, an ever changing catenary constant. Ideally to eliminate these errors it would be possible to carry out all survey mesurements simultaneously. Unfortunately this is not practicable or economical.

Survey errors will not be discussed in these studies apart from mentioning that a controlled network of survey stations was used having a probable error of less than 0.025 m and using a standard field theordolite with a least count of $0^{o}00'10"$.

2.4 TRANSMISSION LINE SAMPLES

The electricity generated in New South Wales is transmitted to load centres by about 12000 route kilometres of 330, 220 and 132 kV transmission lines. In more recent times as a result of major augmentations to the transmission system over 350 route kilometres of 500 kV transmission line has been completed.

The major part of these route kilometres was constructed between the period of 1955 to 1970 making some of these transmission lines between 20 and 30 years old. Further to the degradation of the conductors by the age of the transmission line is the amount of atmospheric pollutants that the conductor has been exposed to, thus any degradation of the conductor due to corrosion causes by the transmission lines geographical location.

Since as part of these studies, conductor samples will be removed from the transmission line and metallurgically examined for evidence of charges in mechanical properties it was considered prudent to identify two transmission lines having similar conductors and age but with differing pollutant environments.

The details of the transmission line samples selected for the study are given in Table 2.3 and are both approximately 24 years old. The transmission lines selected have Moose ACSR conductor with stringing and physical parameters details given in Figure 2.17 and Table 2.4 respectively.

TRANSMISSION LINE FEEDER	TITLE	VOLTAGE	COMMISSIONING DATE	STUDY AREA	POLLUTION LEVEL
37	Avon Kemps Creek	330 kV	5/1964	51 to 54	light
983	Dapto Springhill	132 kV	11/1964	317A to 322A	heavy

TABLE 2.3 TRANSMISSION LINE SAMPLE DATA

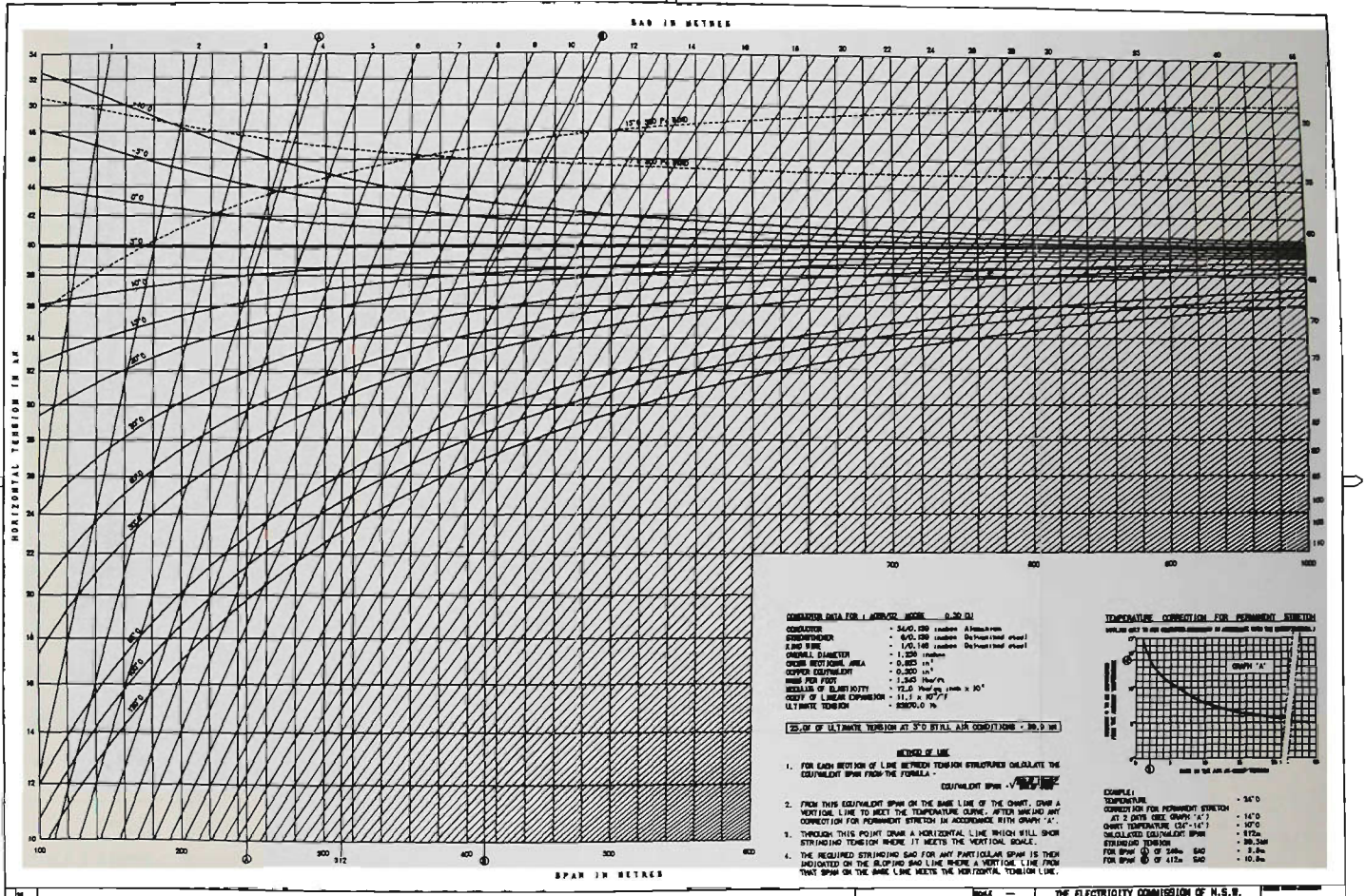

COMPUTER PLOTTED

THE ELECTRICITY COMMISSION OF N.S.W.

TRANSMISSION LINES
ACSR/GZ MOOSE 0.50 OU
25.0% OF ULT. TENSION AT 3°C IN STILL AIR
100-1000 METRE SPAN RANGE
STRINGING CHART

B P PRIDE

2.17

A

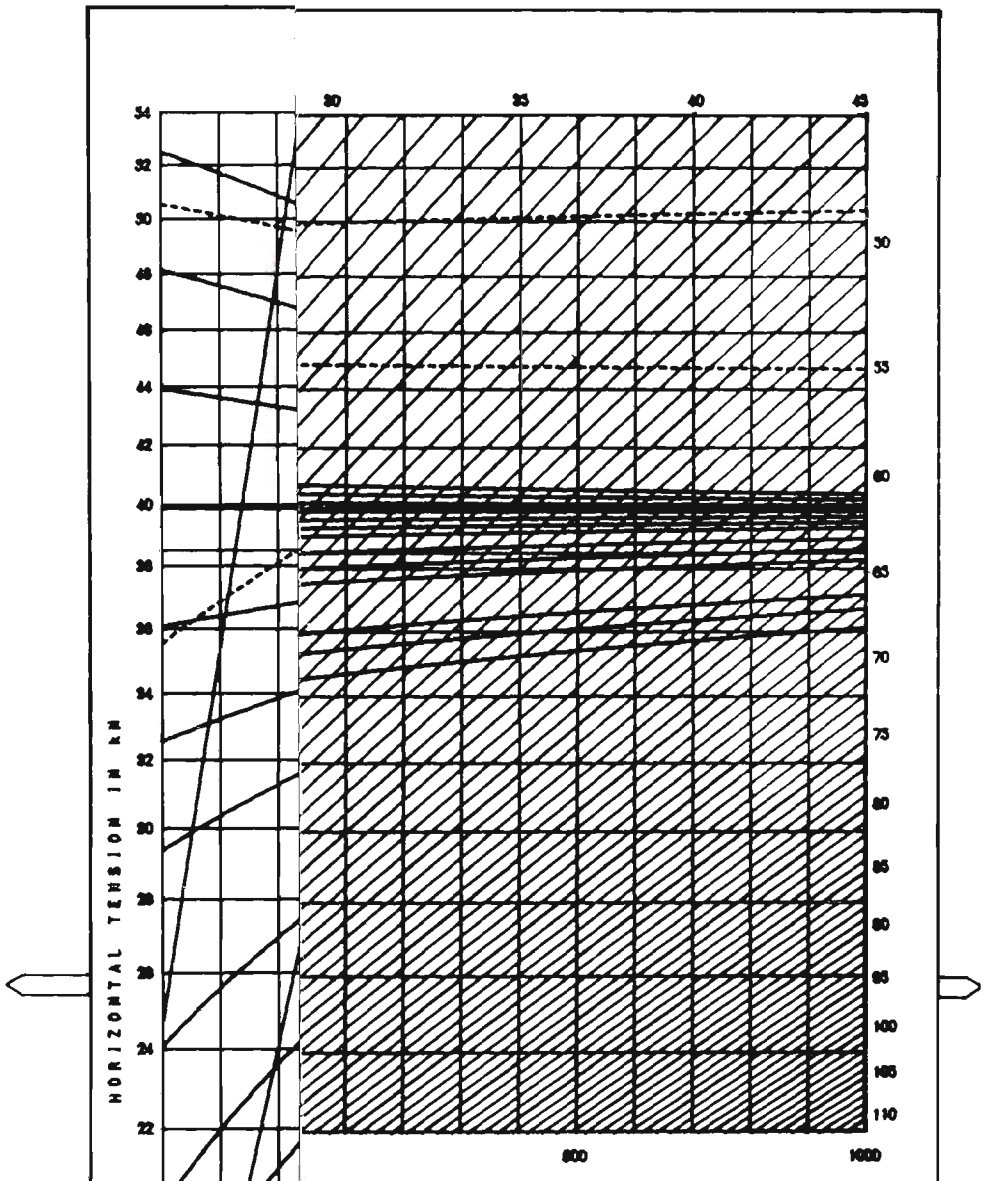
HORIZONTAL TENSION IN kN
54
52
50
48
46
44
42
40
38
36
34
32
30
28
26
24
22
20
18
16
14
12
10
100
800
1000
30
35
40
45
30
55
60
65
70
75
80
85
90
95
100
105
110
TEMPERATURE CORRECTION FOR PERMANENT STRETCH
GRAPH 'A'
EXAMPLE:
TEMPERATURE • 24°C
CORRECTION FOR PERMANENT STRETCH
AT 2 DAYS (SEE GRAPH 'A') • 14°C
CHART TEMPERATURE (24°-14°) • 10°C
CALCULATED EQUIVALENT SPAN • 312m
STRINGING TENSION • 38.3kN
FOR SPAN ① OF 248m SAG • 9.9m
FOR SPAN ② OF 412m SAG • 10.9m
THE ELECTRICITY COMMISSION OF N.S.W.
TRANSMISSION LINES
ACSR/GZ MOOSE 0.50 CU
25.0% OF ULT. TENSION AT 5°C IN STILL AIR
100-1000 METRE SPAN RANGE
STRINGING CHART
W P PRICE per
2.17
A

PARAMETERS	NOMINAL VALUE
MECHANICAL	
Cross Sectional Area	
Aluminium	528.5 mm^2
Steel	69.5 mm^2
Total	598 mm^2
Overall Diameter	31.95 mm^2
Stranding	
Aluminium	
Number	54
Diameter	3.53 mm
Steel Galvanized	
Number	6 1
Diameter	3.53 mm 3.71 mm
Mass	2.002 $kg.m^{-1}$
Ultimate Tensile Strength	159.6 kN
Final Modulus of Elasticity	82.6 GPa
Coefficient of Linear Expansion	19.93 * $10^{-6}.{}^{o}C^{-1}$
ELECTRICAL	
Cross Sectional Area	
Aluminium	515.8 mm^2
Copper Equivalent	324.4 mm^2 (0.5 in^2)
Resistance DC at 20°C	5.48 $m\Omega.km^{-1}$

TABLE 2.4 PHYS ICAL CHARACTERISTICS OF MOOSE CONDUCTOR

2.5 CONDUCTOR SAG TENSION MEASUREMENTS

Employing the fundamental tension and sag theory and the conductor sag measurement theory discussed in sections 2.2 and 2.3 respectively and using the transmission line samples selected in section 2.4 and extensive survey and study of sag and tension was carried.

The detailed results of these studies are given in Appendix Two together with computer plotted profiles of the transmission line spans examined. The profiles illustrate the "AS DESIGNED" conductor curve determined in accordance with the continuous catenary method and the "AS MEASURED" for the tangent and satellite survey methods.

2.5.1 Summary of Results

A summary of the findings of the study is given in Tables 2.5 and Table 2.6 for Avon to Kemps Creek and Dapto to Springhill Transmission Lines, respectively.

Span	"AS DESIGNED" Curve Constants m		"AS MEASURED" Curve Constants $_m$
	Equivalent Span Method	Continuous Catenary Method	
51-52	1815.6	1777.4	1768.9
52-53	1759.2	1717.5	1729.3
53-54	1759.2	1703.6	1702.8

TABLE 2.5 - AVON TO KEMPS CREEK TRANSMISSION LINE
SUMMARY OF SAG & TENSION
MEASUREMENT & CALCULATIONS

Span	"AS DESIGNED" Curve Constants m		"AS MEASURED" Curve Constants $_m$
	Equivalent Span Method	Continuous Catenary Method	
371A-318A	1650.4	1574.0	1606.3
318A-319A	1811.0	1752.3	1667.0
319A-320A	1650.4	1573.2	1580.3
320A-321A	1650.4	1576.5	1592.9
321A-322A	1811.0	1754.6	1683.9

TABLE 2.6 - DAPTO TO SPRINGHILL TRANSMISSION LINE
SUMMARY OF SAG & TENSION
MEASUREMENTS & CALCULATIONS

2.5.2 Conductor Permanent Elongation

As previously discussed in section 2.2.3.4 conductor permanent elongation or creep is non recoverable deformation under tensile load and increases with both temperature and stress.

All transmission line conductors exhibit creep behaviour and the amount of creep in a particular span may be determined by comparing the "AS DESIGNED" conductor length with the "AS MEASURED" conductor length. Several assumptions are necessary before this comparison may be made. The assumptions are as follows,

1. The conductors were originally strung in accordance with design stringing chart, in this case Figure 2.17;

2. Minimal prestressing of the conductor was carried out prior to the cutting and termination; and

3. The conductor temperature during the "AS MEASURED" survey work was measured accurately and reflects the actual conductor temperature of section under examination;

4. No structure settlement has occurred, thus affecting the original span length and conductor attachment reduced level; and

5. No permanent elongation of the conductor due to annealing has occurred.

Employing these assumptions the measured curve constant at some elapsed time should always be less than the designed curve constant. In other words the conductor will sag more at some identical prevailing climatic condition after some elapsed time.

The "AS MEASURED" conductor creep is the difference between "AS MEASURED" and the "AS DESIGNED" conductor length normalised to $mm.km^{-1}$ and $20^{o}C$. These permanent elongation results are compared with those of the predictor equations of CIGRE (27) and the creep test results and equations derived in Chapter Three, calculated for $20^{o}C$ and an every day tension of 20% UTS. These creep results are given in Table 2.7.

Transmission Line	Span	Conductor Creep ($mm.km^{-1}$)		
		"AS MEASURED"	CIGRE Predictor Equations	Creep Predication Equation Derived from Test
Avon-Kemps Creek	51-52	16.8		
	52-53	-38.6	488	274
	53-54	0.5		
Dapto-Springhill	317A-318A	-47.6		
	318A-319A	135.8		
	319A-320A	-6.7	488	185
	320A-321A	-26.7		
	321A-322A	106.0		

TABLE 2.7 CONDUCTOR PERMANENT ELONGATION RESULTS

It is clear from Table 2.7 that the "AS MEASURED" results do not correlate with the predication of the CIGRE predictor equations and those derived in Chapter Three.

The discrepancies of the "AS MEASURED" results may be measurement technique based, a result of unsatisfactory initial assumptions, or an in correct initial assumption used for determining theoretical permanent elongation for the creep predicator equations. The later is the subject of a current undergraduate thesis project.

It needs to be appreciated that the whilst the survey and analysis of transmission line sags is a difficult task, in a controlled network the errors of surveyed reduced levels and chainage are extremely small. That aside, the "AS MEASURED" and

"AS DESIGNED" span length and conductor attachment reduced level are the same. The only variable in the calculations is that of the catenary constant determined by several observations of the tangent angle and point distances.

The remaining measurement required to determine the catenary constant is that of the temperature. To appreciate the effects of temperature variations, an example will illustrate the change in temperature, the effect on curve constant and calculated conductor creep. Using the Avon to Kemps Creek Transmission Line span 52-53 a change of 7.1^{o}C from 34.3^{o}C to 27.2^{o}C represents a change of curve constant of 61.6 m from 1717.5 m to 1779.1 m. This change translated into creep, represents a change from -38.6 mm.km^{-1} to 154.7 mm.km^{-1}. In other words the accuracy of the determination of the conductor creep requires realiable and accurate methods of temperature determination. It is considered that the before and after calibration of the temperature measuring equipment was sufficient to provide the reliability and minimal drift of the instrument.

Accordingly if the measurement technique is assumed to be satisfactory the initial assumptions need to be examined. The likely cause of the marked difference in "AS MEASURED" conductor creep is that of initial prestressing. This is a common practise in the construction of transmission lines and is generally an accepted rule of thumb procedure. The effect of prestressing removes much of the stand setting and metallurgical creep.

Unfortunately, because the history of the initial loading of transmission line conductor was not recorded, the amount of prestressing is indeterminate.

Further to this is the evidence of overtensioning of the conductors revealed by the "AS MEASURED" conductor length being shorter than the "AS DESIGNED", or translated into a negative creep.

However, the postulation of overtensioning should have the net effect of increasing creep, and it can only be concluded that some equilbrium has been reached in these spans.

In a span, conductor creep behaves differently to that of laboratory controlled creep measurements. In a section of transmission line, the tension in a conductor decreases with time because of conductor creep. This means that the amount of conductor creep that occurs during this stress relaxation process is less than the conductor creep in a constant tension span. In an ACSR conductor as the aluminium creeps at a greater rate than the steel, an increasing portion of the total tension is transferred to the steel core. This lower proportion of load on the aluminium contributes further to the stress relaxation in the aluminium.

From the abovementioned discussions it is concluded that the methods employed to measure the conductor sag and to calculate conductor creep are satisfactory. However the history of loading of the conductor or initial survey datum must be established to

determine the initial conditions of a section of transmission line before any future studies can be undertaken.

2.5.3 Conductor Clearance Margins

The marginal allowance given in Table 2.1 for conductor sag provides for inelastic stretch or conductor creep, structure settlement and survey discrepancies.

In view of the sag results obtained, the evidence suggests conductor creep has not occurred on the transmission lines examined to the extent of the original design allowances. As a result of this and the major capital costs of new transmission lines, it considered that a review of the marginal allowances of sag is necessary.

Although additional studies need to be carried out in determine a suitable of marginal allowances, at this stage it is suggested that a reduction of 2% in conductor tension at maximum operating temperature could be used as a basis to determine the sag marginal allowance.

Further to this allowance, it is considered with the use of modern survey measuring equipment and check survey procedures already being used, that any marginal allowance provided for survey discrepancies is unnecessary.

This leaves structure settlement and it is considered that an allowance of approximately 0.1% of the structure height would be more than sufficient.

Accordingly for Lemon ACSR/GZ conductor, 300 m span at maximum operating temperature of 120^{o}C erected on concrete poles with a conductor attachment point of 20 m the suggested marginal allowance would be 0.2 m a reduction 50% on current allowances.

2.6 CONCLUSION

1. Three methods of determining conductor, tension and sag have been examined. Each method requires an increasing understanding and knowledge of conductor behaviour. The advantages of the equivalent span method is that the concepts are easily understood, little knowledge is required of the conductor physical parameter and the ability of being able to produce stringing charts that can be easily interpreted and understood by construction staff. In contrast the continuous catenary method is more complex by its very nature, but does produce very accurate however probably unnecessary results. The continuous catenary method is seen as being a useful aid in mountainous terrain where changes in reduced levels of conductor attachment points may be considerable. The final method examined was the STESS method which like the CONCAT method is complex. It is not agreed that, as the author's describe "conceptually simpler". Any benefits of the STESS method are discounted by the need to undertake an extensive testing programme to determine conductor physical parameters. This is offset against the ability of the STESS to handle

difficult stess relaxation and the thermal gradient behaviour of conductors that may be useful in initial stringing and high temperature operation.

2. The errors in the approximations employed in the traditional methods of calculating conductor tension and sag have been examined in detail. It is considered, with modern computing techniques that no reason is apparent for not using the exact catenary equations. This is reinforced if any marginal allowance for conductor sag is accepted. This aside the errors encountered for average effective spans and curve constants are likely to be less than 1% if the parabolic equations are employed.

3. Correlation of "AS DESIGNED" and "AS MEASURED" conductor sags was achieved and a method is now available to monitor sag changes with time by tangent or satellite survey observations.

4. The difficult task of determining conductor creep after an elapsed time was not achieved. This is primarily due to the lack of original datum available to compare the recent measurements. It is anticipated that as a result of these studies and the methods developed herein, that monitoring of in service transmission lines to determine conductor creep can be achieved in the future.

5. It is considered that a review of the current marginal allowances for conductor inelastic stretch is necessary to minimise transmission line capital costs in the future. Further work is necessary to determine the reduction in marginal allowances however at this stage it is suggested that a 50% reduction on current policies could be achieved.

CHAPTER THREE

MECHANCIAL PROPERTIES OF AGED TRANSMISSION LINE CONDUCTORS

3.1 INTRODUCTION

The development of the electricity transmission system in New South Wales has been characterised by the transmission of power from major generating areas to load centres located throughout the state.

This transmission of power is achieved by over 70,000 km of steel reinforced aluminium conductors of varying size. The conductor size is generally dependent on the required current carrying capacity, thermal limitations imposed by conductor ground clearance, conductor annealing and the need to keep radio interference voltage levels low. In some cases such as long spans the mechanical parameters of the conductor may influence the choose of an appropriate size of conductor.

The major part of these conductors were manufactured and erected in the period between 1955 and 1970 making some of these conductors over 30 years old. The majority of these conductors have been manufactured by the Properzi extrusion method however some of the early conductors manufactured prior to the mid fifties employed the hot rolled process.

With time the conductors have experienced a variety of in service conditions that may vary from emergency operating conditions creating elevated temperatures to long exposures of low velocity winds inducing aeolion vibration, characteristic of conductor fatigue failure.

Some of the geographical features that affect the performance of the conductors are, the excursions of temperature from $-10^{o}C$ in the Snowy Mountains region to $50^{o}C$ in the western plains; gentle breezes to destructive narrow fronted tornado like storms; exposure to salt pollution on the eastern seaboard and the hazards of high temperatures of travelling bushfires.

It is now appropriate to ascertain the level of degradation and the continued serviceability of these conductors. In addition, to carrying out this work it is intended to develop a methodology to test conductors in the future and determine the life expectancy of conductors.

Two categories of testing are available for examining the performance of conductors, non destructive testing and destructive testing.

Non destructive testing will in most cases disclose the occurrence of broken wires and the presence of corrosion products in the case of the aluminium wires of an ACSR. Several methods of non destructive testing are available and are briefly described as follows:

1. Routine visible inspections being by for the most common non destructive testing of conductors. This method will disclose bulging of the conductor caused by bimetallic corrosion (50) and in some cases may reveal fatigue damaged conductor by the presence of outer wire failures;

2. X-ray and gamma ray radiography used with mixed success will reveal non visible wire breakages of fatigue conductors (26);

3. Eddy current testing has been employed and will disclose internal corrosion and it has been reported that aluminium external corrosion of more than 10% reduction in the cross sectional area will be detected (57).

4. Thermovision may be employed to disclose thermal gradients in the conductor and thus possible non visible wire breakages of fatigued conductors.

These diagnostic methods provide valuable information on the short term performance and the need to repair damaged conductors.

Unfortunately, no non destructive test method provides an indication of the long term and component performance of the conductor. On the other hand, destructive testing of samples of conductors, does provide a true measure of the deterioration of the components and the composite of the conductor. An assessment of the test results can determine the long term performance of the aged conductor.

Three categories of test are used to give an overall indication of the level of degradation of the conductor. The test categories are:

1. Metallography examination.
2. Mechanical tests
3. Chemical tests examination.

From these categories it concluded that conductor degradation transgresses several engineering disciplines. The relationship of serviceability of conductors, engineering disciplines, transmission line design parameter and conductor degradation mechanisms is given in Figure 3.1.

The objective of these studies will examine each of the degradation mechanisms and in particular will,

1. Remove sufficient in service aged conductor from the field to allow the following test to be carried out.

2. Carry out metallographic sample analysis of aged wires.

3. Carry out conventional mechanical tests on aged wire and composite conductor.

4. Carry out chemical tests on aged conductor grease.

5. Establish a methodology for testing future aged conductor samples.

6. Determine the life expectancy of aged conductor samples.

3.2 TRANSMISSION LINE CONDUCTOR SAMPLES

As part of the transmission line conductor sag and tension determination, two samples of transmission lines having similiar conductors were selected giving representations of differing pollutant environments. The details of the location and construction of the conductors are given in Tables 2.3 and Table 2.4 respectively.

The criteria for the various pollution environments has been adopted from IEC Recommendation 815, 1986 and is given in Table 3.1. One sample was selected from a heavy pollution environment and one sample from a light pollution environment.

Characteristics of the sites chosen for conductor removal were relatively flat terrain, free from rocky outcrops that may have damaged the conductor, areas of good access and included a section of conductor from a suspension point.

In addition to these two samples of conductor two further samples of conductor from the Tomago to Taree and Bellambi to Heathcote 132kV transmission lines had selected tests carried out during the course of these studies. The Bellambi to Heathcote transmission line sample was removed from a jumper connection not held in tension.

POLLUTION LEVEL	EXAMPLES OF TYPICAL ENVIRONMENTS
I Light	- Areas without industries and low density of houses equipped with heating plants. - Areas with low density of industries or houses but subjected to frequent winds and/or rainfall. - Agricultural areas.# - Mountainous areas. All these areas shall be situated at least 10 km to 20 km from the sea and shall not be exposed to winds directly from the sea.
II Medium	- Areas with industries not producing particularly polluting smoke and/or with average low density of houses equipped with heating plants. - Areas with high density of houses and/or industries subjected to frequent winds and/or rainfall. - Areas exposed to the wind from the sea but not too close to the coast (at least several kilometres distance).*
III Heavy	- Areas with high density of industries and suburbs of large cities with high density of heating plants producing pollution. - Areas close to the sea or in any case exposed to relatively strong winds from the sea.*
IV Very Heavy	- Areas generally of moderate extent, subjected to conductive dusts and to industrial smoke producing thick conductive deposits. - Areas generally of moderate extent, very close to the coast and exposed to sea spray or to very strong polluting winds from the sea. - Desert areas, characterised by no rain for long periods, exposed to strong winds carrying sand and salt, and subjected to regular condensations.

Use of fertilisers by spraying, or the burning of crop residues, can lead to a higher pollution level due to dispersal by wind.

* Distances from the sea coast depend on the topography of the coastal area and the extreme wind conditions.

TABLE 3.1 IEC RECOMMENDATION POLLUTION SEVERITY LEVEL

3.2.1 Conductor Removal

After the attachment of appropriate lowering slings, rigging and winches, the conductor was detached from the insulator string at the suspension structure of interest and the suspension structure either side. The conductor was then lowered at all three structure sites until the required length of conductor rested at ground level.

Prior to the cutting of the conductor, bonding tape and wooden cleats were fitted to the conductor as illustrated in Plates 3.1 and 3.2 to insure that relative wire positions were maintained. Conductor come-along clamps were then fitted to the old conductor and the new replacement conductor and the tension was gradually and simultaneously applied and released to the new replacement conductor and the old conductor section being removed respectively. This was simultaneously repeated at the other end of the length of conductor to be removed. When no apparent tension remained in the old conductor the old conductor was cut and removed.

Midspan joints were applied at the two ends of the new replacement conductor and the new intact section of conductor was raised and reattached to the insulator string.

The removal of the field conductor in this manner was achieved by employing the appropriate resources and the transmission line outage was restricted to approximately 6 hours.

PLATE 3.1 FITTING OF BONDING TAPE TO THE CONDUCTOR SAMPLE

PLATE 3.2 FITTING OF WOODEN CLEATS TO THE CONDUCTOR SAMPLE

The old conductor sample was person handled to rolled onto an oversized conductor drum for subsequent transport to the laboratory. Person handling in this manner insured that no surface damage of the conductor was incurred

3.3 METALLOGRAPHIC EXAMINATION

Metallographic examinations fall into two categories, macro-examination and micro-examinations.

3.3.1 Macro-examination

Macro-examination consists of an inspection and visual examination of the various layers that constitute the conductor and recording the observations. Samples of conductor should be taken from suspension points that are likely to have suffered some degree of degradation due to fatigue.

Observations are likely to reveal, surface pitting, corrosion, foreign particles, closing die depressions, surface abrasion, black and white powders, weeping tars and greases, wire fretting, wire fatigue cracks, broken wires and in the case of steel cores, loss of zinc coating and in some cases rust.

Typical foreign particles found on and within the voids of the various wire layers are white powders, typically sulphates and nitrates used in the manufacturer of fertiliser, sodium chloride cyrstals and dirt particles. In mining and industrial regions foreign particules may be found that are compatible with the

particular activities. The presence of black powder is a product of wire fretting, characteristic of conductor fatigue and is aluminium oxide.

Closing die depressions or elliptical damaged sites are a characteristic of the stranding of the conductor and are generally found on all conductor samples. An example of a closing die depression is given in Plate A3.2 from the 12 wire layer of a 54/6/3.51 + 1/3.71 mm ACSR conductor.

Wire fretting is caused by the movements of one wire in relation to another. Rawlins and Ficke (41) suggest that wire fretting occurs in a series of stages,

> "In the first stage, surface oxide films are disrupted and bare metal rub against bare metal. Minute projections from one metal surface become welded to similar asperities of the other metal surface. When the two metal surfaces move relative to each other, the welded junctions are broken. Because the tips of the asperities had been disturbed before the welds were established, however, they are work-hardened and are somewhat stronger than the bulk material. The welds break, therefore, not at the weld junction itself, but slightly back from the junction. Metal is transferred from one surface to another.
>
> Continued welding and breaking-off of the asperities between mating parts leads to transfer of the material alternately from surface to the other. Gradually a layer is built up on the material surface composed of the remnants of the asperities which have been passed back and forth".

The surface of the wire created by the fretting action will contain many fine cracks. The presence of the cracks are sites of stress concentration which may eventually lead to fatigue cracks. An example of a wire frett site and wire fatigue crack from the 6 wire layer of a 19/3.25 mm AAC conductor is given in Plate 3.3

Broken wires are the result of the continued fretting action and if present will obviously be revealed during a metallographic macro-examination. An example of a broken wire at a suspension site from the 6 wire layer of a 7/4.22 mm AAAC/6201 conductor is illustrated in Plate 3.4.

Evidence of preferential corrosion of one metal in a galvanic cell in the presence of a conducting medium is likely to be the most significant metallographic macro observation made during the examination of a conductor sample.

In a galvanic cell, the metal loss or the amount of current flow depends on the potential difference in the medium, the electrical resistance between the two metals, the conductivity of the electrolyte and the degree of polarisation of the two metals. Severity of attack depends on the anode to cathode contact area or in other words the current density.

In ACSR conductors, Forest and Ward (39) suggested that the electrochemical effects of contact between aluminium and galvanised steel core wire are responsible for corrosion product bulges in conductors in coastal environments. Initially, a cell

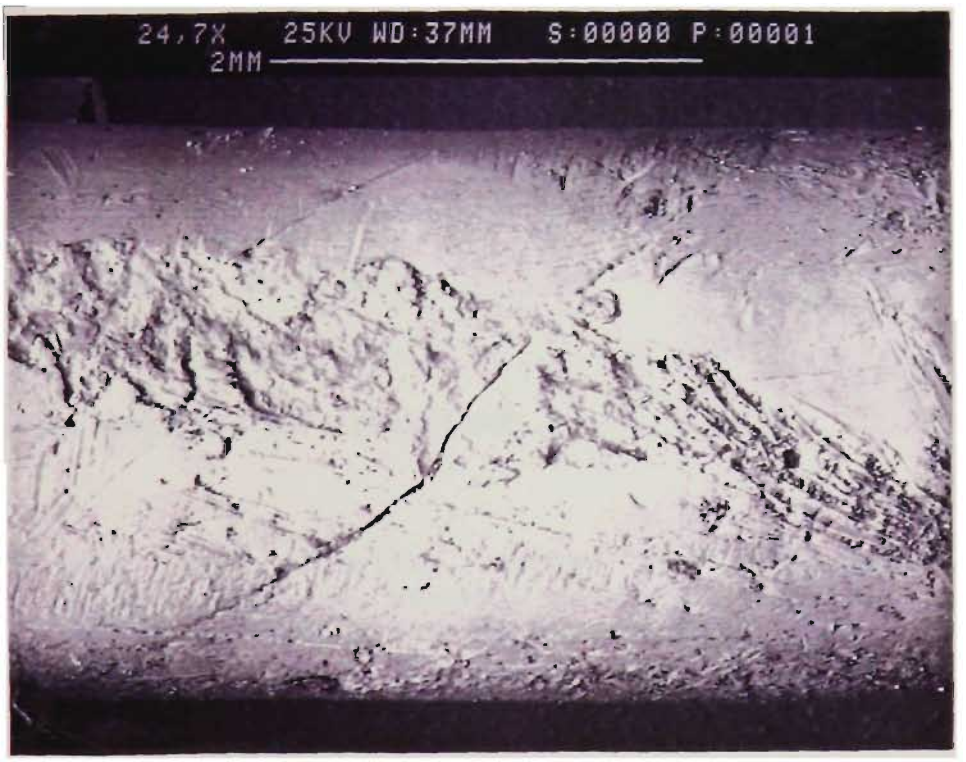

PLATE 3.3 19/3.25 AAC CONDUCTOR
CONDUCTOR FRETTING AND FATIGUE CRACK

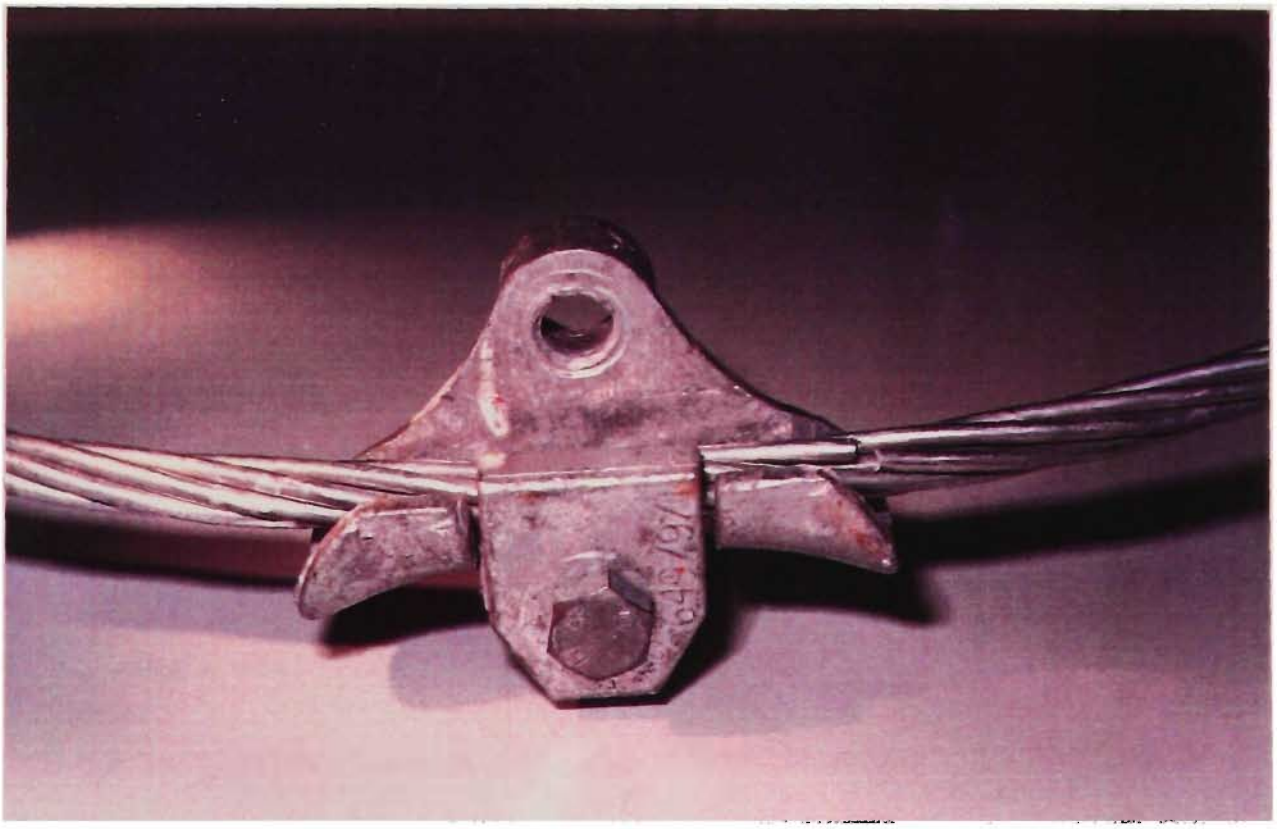

PLATE 3.4 7/4.22 AAAC/6201 CONDUCTOR
BROKEN STRAND ADJACENT SUSPENSION CLAMP

is set up with the zinc anode and the aluminium cathode. The zinc corrodes in the presence of sulphur oxides and the alkaline cathode product might produce some attack on the aluminium. After some of the zinc has been removed, the aluminium will act as an anode and the steel as a cathode and the aluminium will be sacrificial to the steel.

Forrest and Ward (39) described:

> "the most effective method of reducing corrosion is to prevent moisture, sulphur oxides and other corrosive substances from coming into contact with the conductor. This can be done by applying a protective material such as grease, bitumen, paint or a plastic film."

The degree of applying the most convenient protection such as grease or bitumen is described by Haughten and Cole (50) who suggest that the long term corrosion behaviour of a conductor is greatly enhanced if the full advantage of the use of grease to the penultimate layer is employed and

> "that the grease had extended the life of the ACSR by at least a 50 to 60 years".

Other types of corrosion likely to be present in a conductor sample are:

1. Uniform Surface Attack

If the aluminium oxide film, that forms in the presence of either air or water at the instant a new aluminium surface is created, is exposed to an environment containing phosphoric acid or sodium hydroxide, the surface oxide film will dissolve and the parent aluminium will experience a loss of weight or cross section area.

2. Pitting Corrosion

Pitting is the loss of parent material at a localised site on the surface exposed to the environment. Pitting may be caused by corona corrosion as reported by Goldman and Sigmond, (43) or simply by localised electrolytic reaction in which water and oxygen must be present. The pit growth rate is generally very small and an example of 50 μm pit from the 18 wire layer of a 30/7/3.00 mm ACSR/GZ sample is illustrated in Plate 3.5. Surface pitting is generally associated with an exposure to industrial and coastal environments. With time pit corrosion will continue to be initiated and existing shallow pits may widen. Catastrophic localised corrosion is not likely to occur and the overall effect would be the gradual loss of cross sectional area. An example of the widening and growth of a pit is given in

PLATE 3.5 30/7/3.00 MM ACSR/GZ CONDUCTOR
18 WIRE LAYER WIRE SURFACE PITTING
MAGNIFICATION X 200

Plate A3.25 which illustrates a longitudional section from the 18 wire layer of a 30/7/2.99 mm ACSR/GZ conductor. The pit depth is 0.6 mm and the exposure in a coastal marine environment was 27 years.

3. Crevice Corrosion

If an electrolyte such as water is present in the interstitial spaces between the wires, localised corrosion in the form of pits or etch patches may occur. An example of crevice corrosion was reported in 1971 in which voluminous grey to white slightly moist deposits between the penultimate and ultimate aluminium layers was reported. Subsequent investigations revealed that the environment was of particularly high rainfall, frequented by fogs and in close proximity to a railway line. Chemical examination of the white deposits revealed aluminium oxide 66.3%, sulphates 3% and chlorides 0.7%. It was concluded that the corrosion resulted from the intermittent entrapment of moisture within the conductor and the corrosion had been catalysed by the presence of sulphates and chlorides probably emitted from locomotives using the railway line in close proximity to the transmission line.

The detailed macro-examination comments of the conductor samples from the Avon to Kemps Creek and Dapto to Springhill transmission lines are given in Appendix 3. In addition two further samples were examined from the Tomago to Taree and Bellambi to Heathcote transmission lines are given.

Regarding the Avon to Kemps Creek transmission line conductor sample with the exception of the presence of white powder between the armour rods and conductor, the conductor was found to be in a normal and good condition. Chemical tests on the white powder present suggested sulphur and nitrogen elements. The grease appeared to be in good conditions and of adequate quantity to protect the interface between the zinc and the aluminium.

Regarding the Dapto to Springhill transmission line conductor sample, some evidence of wire fretting was present however no traces of aluminium oxide were found. This suggests that some wire movement has occurred but is not of a significant amount to produce the aluminium oxide characteristic of fatigue failure. The conductor was found to be in a normal and good condition consistent with the age and the pollution environment. The grease appeared to be in good condition and of adequate quantity to protect the interface between the zinc and the aluminium.

Regarding the Tomago to Taree transmission line conductor sample, considerable evidence of outer layer pitting existed as illustrated in Plate A3.25. White powder deposits

between the armour rods and the conductor were present and subsequently found to be sulphur and nitrogen elements. The steel core had evidence of corrosion and loss of galvanising on the 6 wire layer. Most sites examined suggested that the loss of galvanising was due to poor galvanising adhesion. The conductor was found to be in an average condition consistent with age and the pollution environment. The bitumen tar was in good condition and of adequate quantity to protect the interface between the zinc and the aluminium. Some future localised areas of corrosion of the steel core is likely which will ultimately lead to the corrosion of the aluminium wires.

Regarding the Bellambi to Heathcote transmission line conductor, the conductor was found to be in a normal and good condition consistent with the age and the pollution environment. The tar was dry on the penultimate layer, however this is probably caused by the ingrest of dirt particles between the loose outer layer wires not held in tension. The remainder of tar appeared to be in good condition and of adequate quantity to protect the interface between the zinc and the aluminium.

3.3.2 Micro-examination

Micro-examination consists of scanning electron microscopy of areas of interest revealed in the micro-examination.

Sites of fretting fatigue in aluminium wires are examined for evidence of crack formation and longitudinal sections of aluminium and steel wires quantify the depth of pit corrosion and the conditions of the galvanising coating.

Typical scanning electron microscopy of aluminium wire fatigued crack surface and longitudinal section showing fatigue crack initiation are illustrated in the Plates 3.6 and 3.7 respectively.

Typically scanning electron microscopy of longitudinal section through a steel wire showing galvanised coating is illustrated in Plate 3.8.

Regarding the Avon to Kemps Creek transmission line conductor sample, no aluminium wire fatigue crack formation was present and no evidence of pitting or loss of the zinc coating of the steel wires existed. Some outer layer aluminium wire pitting corrosion was present and the overall condition of the conductor was consistent with the age and the light pollution environment.

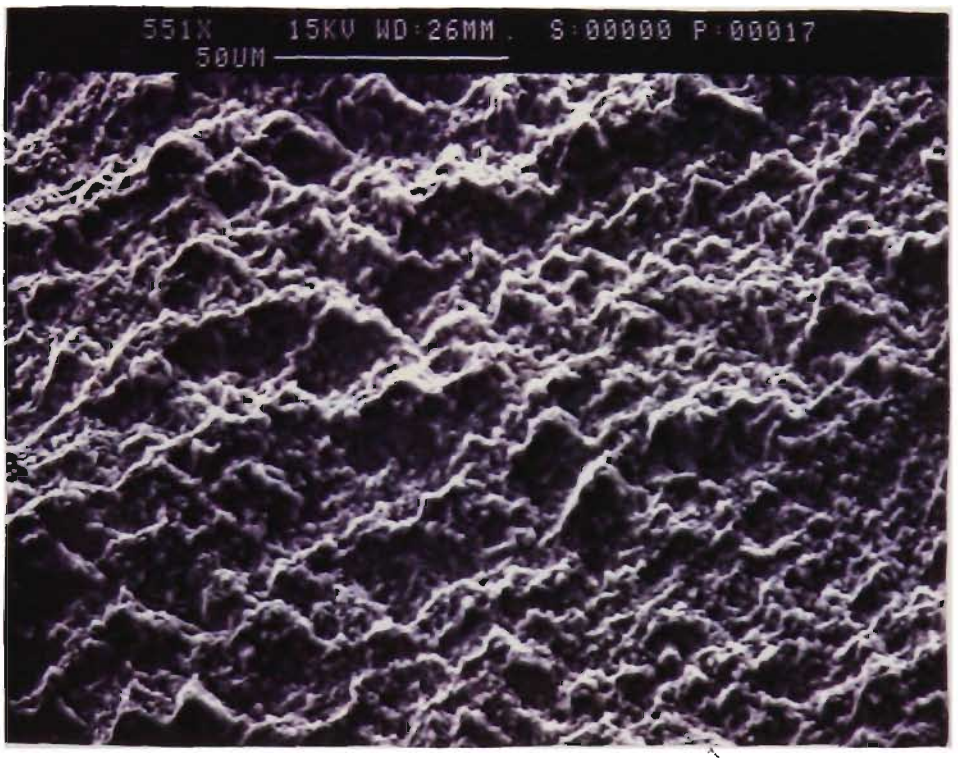

PLATE 3.6 SEM OF 19/3.25 MM AAC
ALUMINIUM WIRE FATIGUE CRACK SURFACE

PLATE 3.7 SEM OF 19/3.25 MM AAC
LONGITUDINAL SECTION OF FATIGUE CRACK

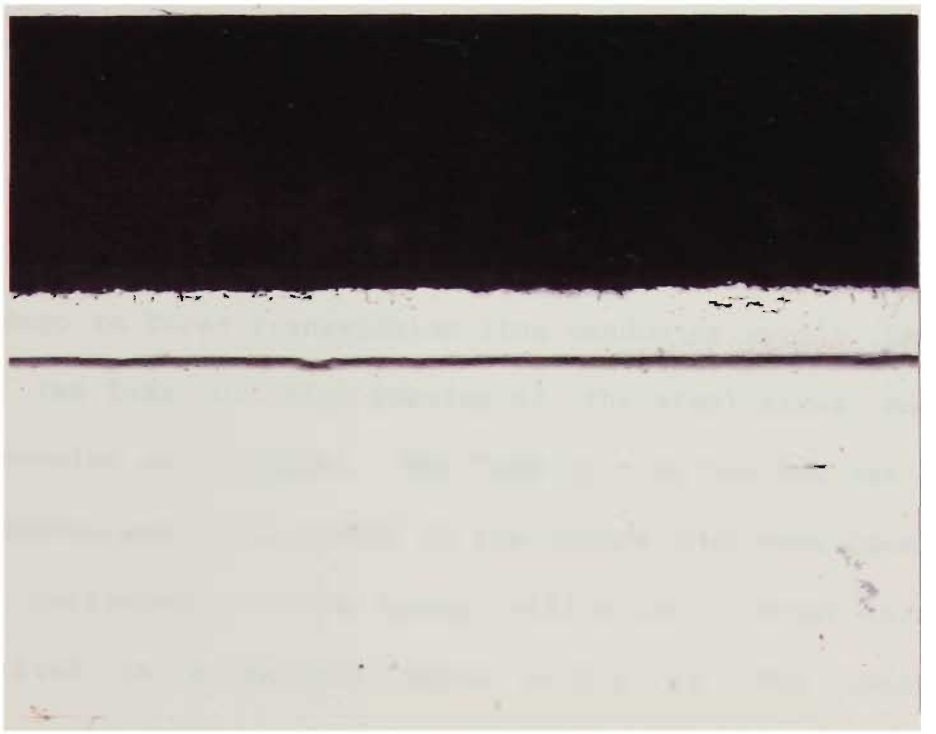

PLATE 3.8 SEM OF 30/7/2.36 MM ACSR/GZ
LONGITUDINAL SECTION OF GALVANIZING COATING
OF STEEL WIRE

Regarding the Dapto to Springhill transmission line conductor sample, no aluminium wire fatigue crack formation was present, however some evidence of excessive closing die force was present on the 12 wire aluminium layer. No evidence of pitting or loss of the zinc coating of the steel wires existed. Similarly to the Avon to Kemps Creek transmission line some outer layer aluminium wire pitting corrosion was present. The condition of the conductor is consistent with the age and the heavy pollution environment.

No aluminium wire fatigue crack formation was present on the Tomago to Taree transmission line conductor sample. Several sites of the loss of zinc coating of the steel wires and initiated corrosion were present. The loss of zinc coating was due to poor adhesion and it is likely in the future that some localised areas of corrosion of the steel will occur. Outer layer pitting existed to a maximum depth of 0.6 mm. The quality of the conductor is consistent with the age and coastal marine environment.

Since the Bellambi to Heathcote transmission line sample was removed from a jumper connection not subjected to stringing tension, examination for aluminium wire fatigue crack formation was not carried out. No evidence of pitting or loss of the zinc coating of the steel wires existed. Some outer layer aluminium wire pitting corrosion was present and the overall condition of the conductor was consistent with the age and the light pollution environment.

3.4 MECHANICAL TESTS

The mechanical tests of conductors fall into two categories, the component or wire tests and the composite or conductor tests.

3.4.1 Wire Tests

At elevated temperature under normal atmospheric conditions for extended times the mechanical and electrical properties of wires can change. In the case of transmission lines having designed thermal ratings of 85°C and in some cases 120°C both the conductivity and tensile strength of the component wires of a conductor will change with time.

Accordingly, wire tests to determine the tensile strength and conductivity are the elementary means of determining the level of degradation in a conductor.

Carrying out the tensile and resistivity tests is a relatively easy task. The difficulty in assessing the level of degradation of the wire commences in the decision to choose the initial wire property acceptance criteria. One could simply take the available initial criteria from the appropriate standard that the wire was manufactured in accordance with and compare the wire property test results. This is one method of measuring the level of degradation of the conductor being assessed.

Unfortunately, this method of assessing the level of degradation does not recognise that it is common practise in any manufacturing process to set the appropriate standard acceptance criteria at approximately minus three standard deviations of typical standard distribution curve.

Typical standard distribution of a manufacturing process for 3 mm diameter, 1350 aluminium wires manufactured in a 12 month period for diameter, ultimate tensile strength and resistivity is illustrated in Figures 3.2 to 3.4 respectively.

These standard distributions illustrate that,

1. the mean diameter is 3.011 mm for a nominal 3.00 mm wire, a marginal tolerance in the manufacturing process of +0.367%;

2. the mean ultimate tensile strength is 0.209 GPa for a nominal 0.169 GPa strength, a marginal tolerance in the manufacturing process of +23.6%; and

3. the mean resistivity is 0.0278 μ.m for a nominal 0.0283 μ.m, a marginal tolerance in the manufacturing process of -1.77%.

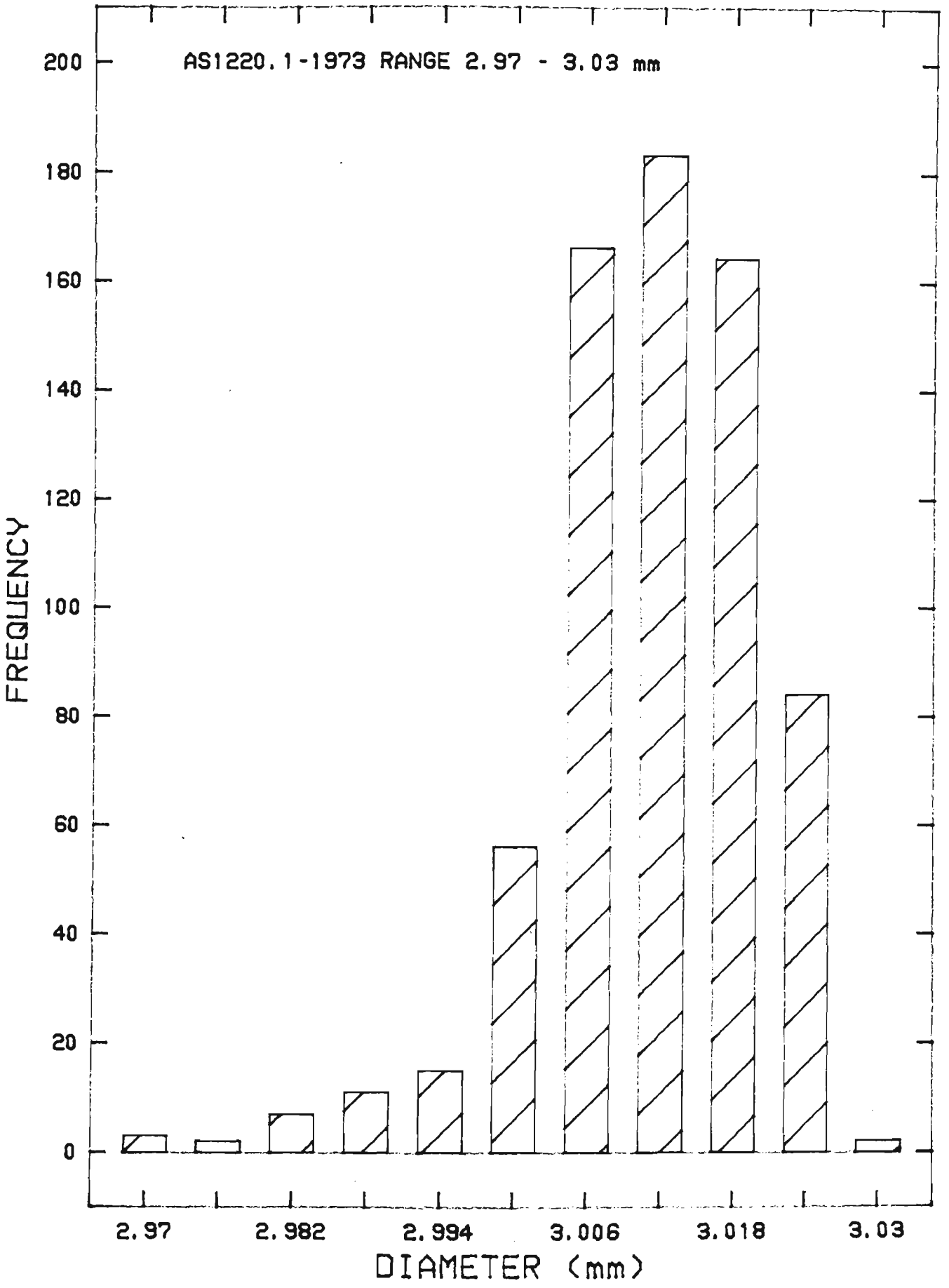

FIGURE 3.2 DISTRUBITION OF DIAMETER OF 3.00MM 1350 WIRE

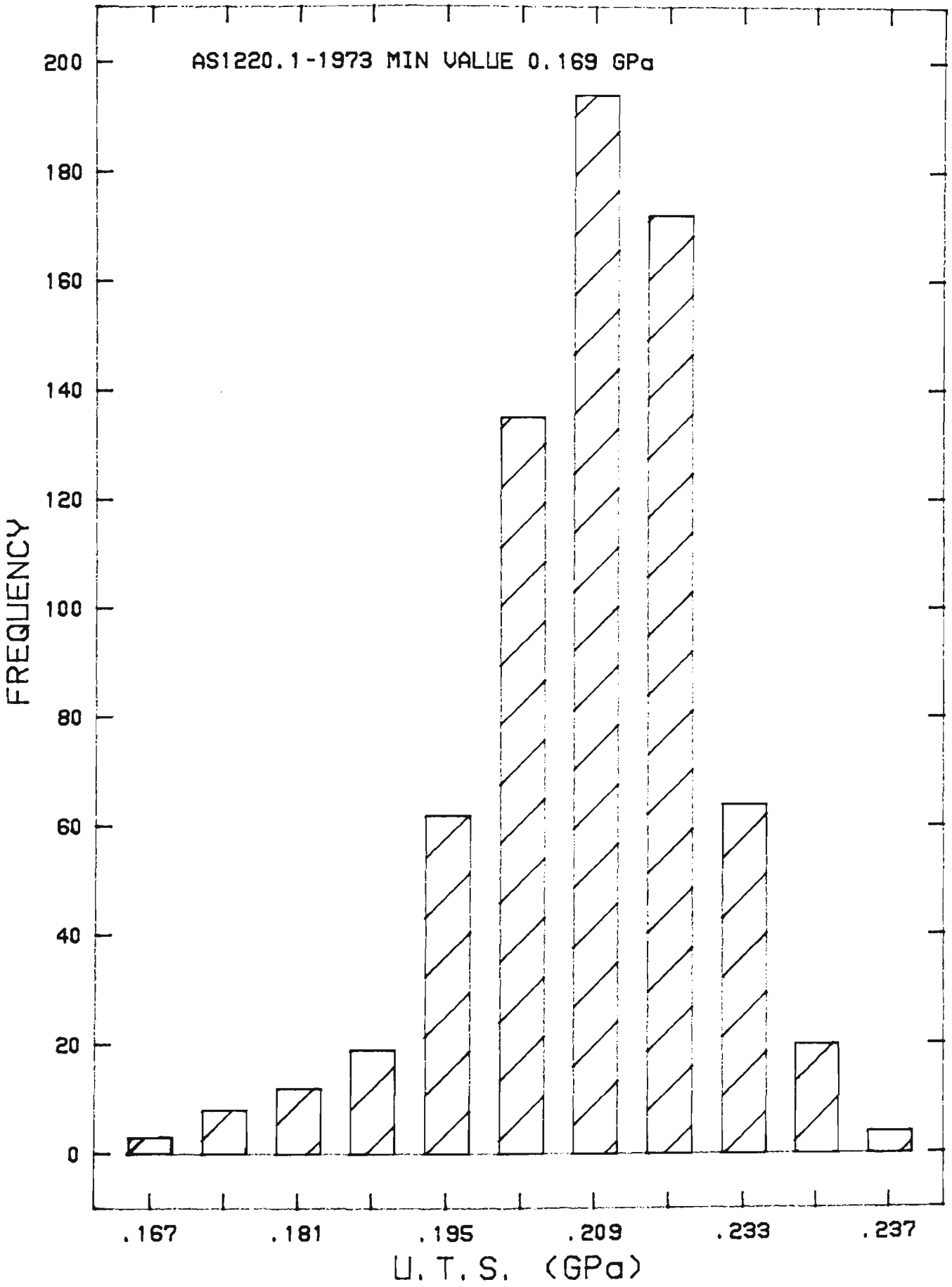

FIGURE 3.3 DISTRUBITION OF UTS OF 3.00MM 1350 WIRE

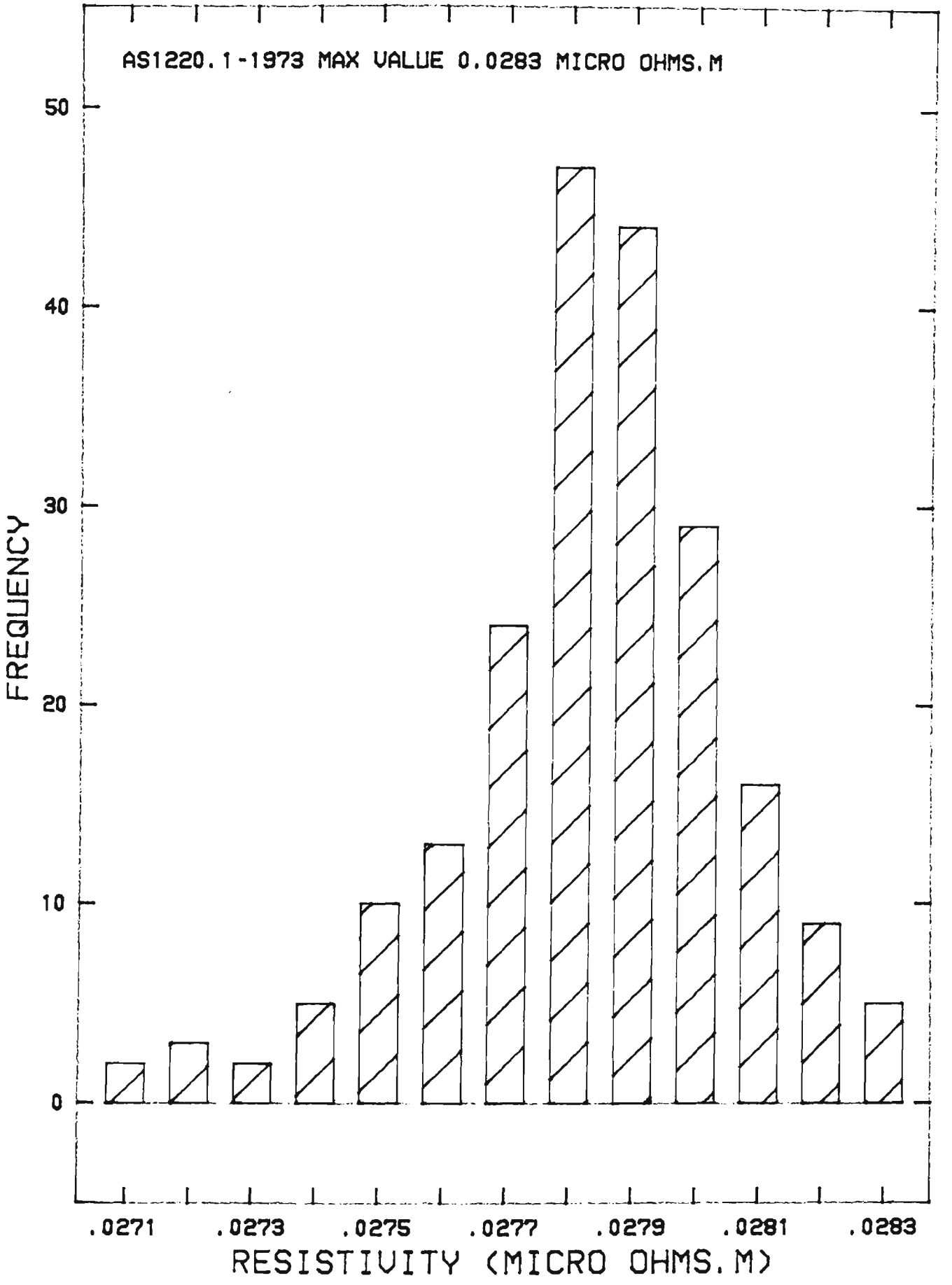

FIGURE 3.4 DISTRUBITION OF RESISTIVITY OF 3.00MM 1350 WIRE

An example of the possible misinterpretation of the level of degradation of a wire is illustrated as follows. After 15 years of service operation, the ultimate tensile strength of a 3.00 mm wire, manufactured during the abovementioned period could be found to be 0.175 GPa. Comparison with the nominal standard value of 0.169 GPa would suggest that no degradation has taken place. In fact, the wire has a strength of 3.55% greater than that of the standard. However, a comparison made with the process capability survey suggests that a degradation of -16.3% has occurred.

Process capability surveys that give manufacturing tolerances are a relatively new concept and arise from quality assurance programs. Conductor manufacturers prior to the early 80's will generally have no standard distribution data available. In the absence of a process capability survey, the wire tests can only be interpretated as complying with the appropriate standard.

As a result of such wire tests it would be concluded that if no degradation has occurred in the period between manufacturer and subsequent assessment than the likelihood of any future degradation under the same operating conditions and future period will be small.

3.4.1.1 Cross Sectional Area

The diameter of a wire is defined as the mean of two measurements taken at right angle at any one section. The cross sectional area is determined from the diameter.

Changes in cross sectional area of a wire may be caused by conductor creep, fatigue fretting and corrosion. For steel wires, loss of galvanising coating is another possible cause of reduction of cross sectional area. The typical cross sectional area reductions caused by fatigue fretting of aluminium wires and loss of galvanising coating of steel wires are illustrated in Plates 3.9 and 3.10 respectively.

The details of the cross sectional area of the wires that constitute the conductor samples from the Avon to Kemps Creek and the Dapto to Springhill transmission lines are given in Appendix 3. In addition two further samples from the Tomago to Taree and Bellambi to Heathcote transmission lines are given.

A summary of the findings of the cross sectional area measurements is given in Tables 3.2 and 3.3 for the aluminium and steel wires, respectively.

Regarding the aluminium wires, with the exception of the Bellambi to Heathcote conductor sample, the mean and minimum cross sectional areas complied with the requirements of Australian Standard C75.1 1963(6). The Bellambi to Heathcote conductor 12 wire layer sample mean and minimum cross sectional areas were

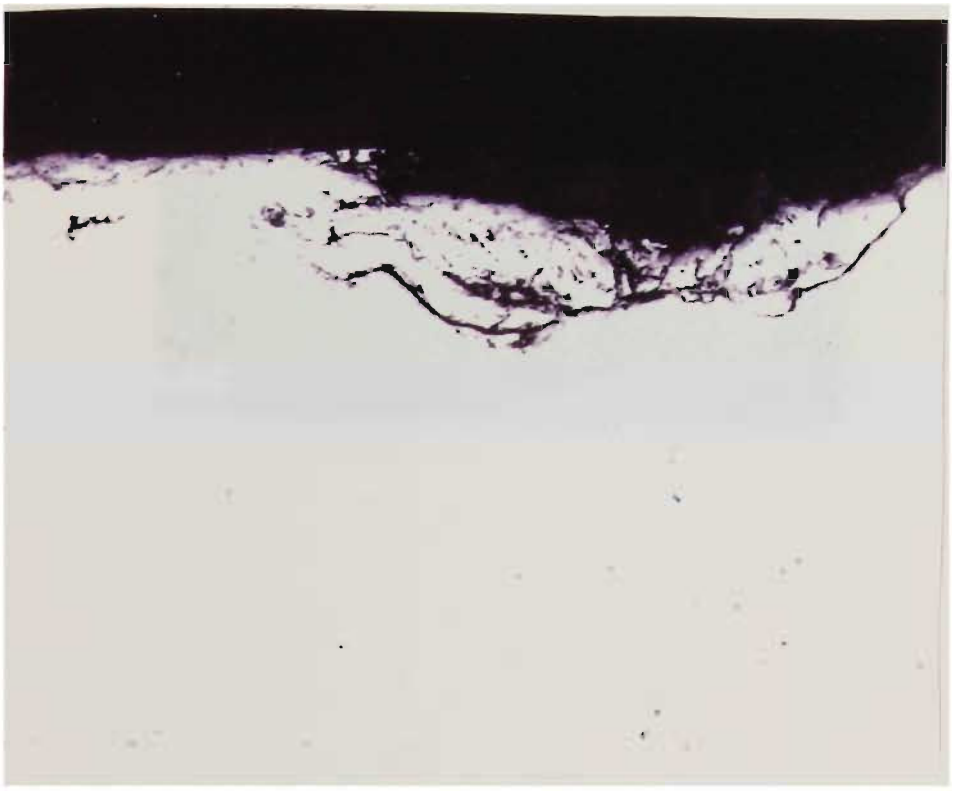

PLATE 3.9 SEM OF 19/3.75 MM AAC
12 WIRE LAYER FATIGUE FRETTING
MAGNIFICATION X 200

PLATE 3.10 SEM OF 30/7/2.997 MM ACSR/G2
6 WIRE LAYER STEEL STRAND
LOSS OF GALVANISING
MAGNIFICATION X 200

Transmission Line	Nominal Wire Diameter	Mean Cross Sectional Area mm^2			Minimum Cross Sectional Area mm^2		
		24 Wire Layer	18 Wire Layer	12 Wire Layer	24 Wire Layer	18 Wire Layer	12 Wire Layer
Avon-Kemps Creek	3.531	9.890	9.797	9.790	9.810	9.631	9.716
Dapto-Springhill	3.531	9.969	9.789	9.801	9.713	9.655	9.620
Tomago-Taree	2.997	-	7.091	7.092	-	7.045	7.012
Bellambi-Heathcote	3.708	-	10.840	10.709	-	10.677	10.527
Australian Standard							
C75.1 1963	3.531		9.790			9.595	
	2.997		7.054			6.914	
	3.708		10.801			10.584	

TABLE 3.2 - SUMMARY OF ALUMINIUM WIRE TEST RESULTS CROSS SECTIONAL AREA

Transmission Line	Nominal Wire Diameter	Mean Cross Sectional Area mm^2		Minimum Cross Sectional Area mm^2
		6 Wire Layer	Core	6 Wire Layer
Avon-Kemps Creek	3.531	9.890	-	9.771
	3.708	-	11.028	-
Dapto-Springhill	3.531	9.918	-	9.802
	3.708	-	10.961	-
Tomago-Taree	2.997	7.087	7.106	7.045
Bellambi-Heathcote	3.708	10.694	10.682	10.636
Australian Standard				
	3.531	9.790	-	9.595
	3.708	-	10.801	10.376
C75.1 1963	2.997	7.054	7.054	6.914
	3.708	10.801	10.801	10.584

TABLE 3.3 - SUMMARY OF STEEL WIRE TEST RESULTS CROSS SECTIONAL AREA

0.9% and 0.5% respectively less than the minimum criteria of the Australian Standard. Even after excluding the wire with the minimum cross sectional area from the mean cross sectional area determination, a 0.7% average reduction in cross sectional area is revealed.

As mentioned in Section 3.3 there was no significant evidence of corrosion or fatigue fretting on all the samples examined.

Regarding the Bellambi to Heathcote conductor sample which was removed from a jumper connection not subjected to stringing tension the reduction of cross sectional area due to creep was discounted. However, since this conductor sample is from one of the oldest transmission lines in the state of NSW and whilst the 18 wire layer mean and minimum cross sectional areas complied with the requirements of the Australian Standard, it is concluded that the quality assurance for the 12 wire layer was unsatisfactory and the wires were probably undersized at manufacturer.

Regarding the steel wires, for all samples, the mean and minimum cross sectional areas complied with the Australian Standard C75.1 1963.

Accordingly, it is concluded that no degradation in cross sectional area of the samples tested has occurred as a result of normal in service use and pollution environments ranging from light to heavy.

3.4.1.2 Mechancial Properties

The mechanical properties of a wire are assessed by determining the breaking load, ultimate tensile strength and elongation.

The breaking load of a wire is defined as the maximum load obtained in a tensile test, the ultimate tensile strength of a wire is defined as the breaking load divided by the cross sectional area of the area, and the elongation of a wire is defined as a measurement of the increase in distance between two gauged marks, after carefully fitting the broken ends of the tensile test wire specimen together.

Changes in a breaking load of a wire may be caused by changes in the cross sectional area or ultimate tensile strength. To eliminate variations in the mechanical properties of the wire caused by variations in cross sectional area and to assess the extent of annealing the ultimate tensile strength of the wire is determined. Annealing of the wires at elevated temperatures can cause appreciable loss of tensile strength as illustrated in Figures 3.5, 3.6 and 3.7 for aluminium 1350 and aluminium alloy 1120 and 6201 respectively (53). Cumulative annealing damage is determined by summating the damage at one temperature and exposure time to an identical damage at a second temperature with an equivalent exposure time. Samples of conductor removed from suspension points may exhibit lower breaking loads caused by an effective reduction in cross sectional area by fatigue initiated microcracks.

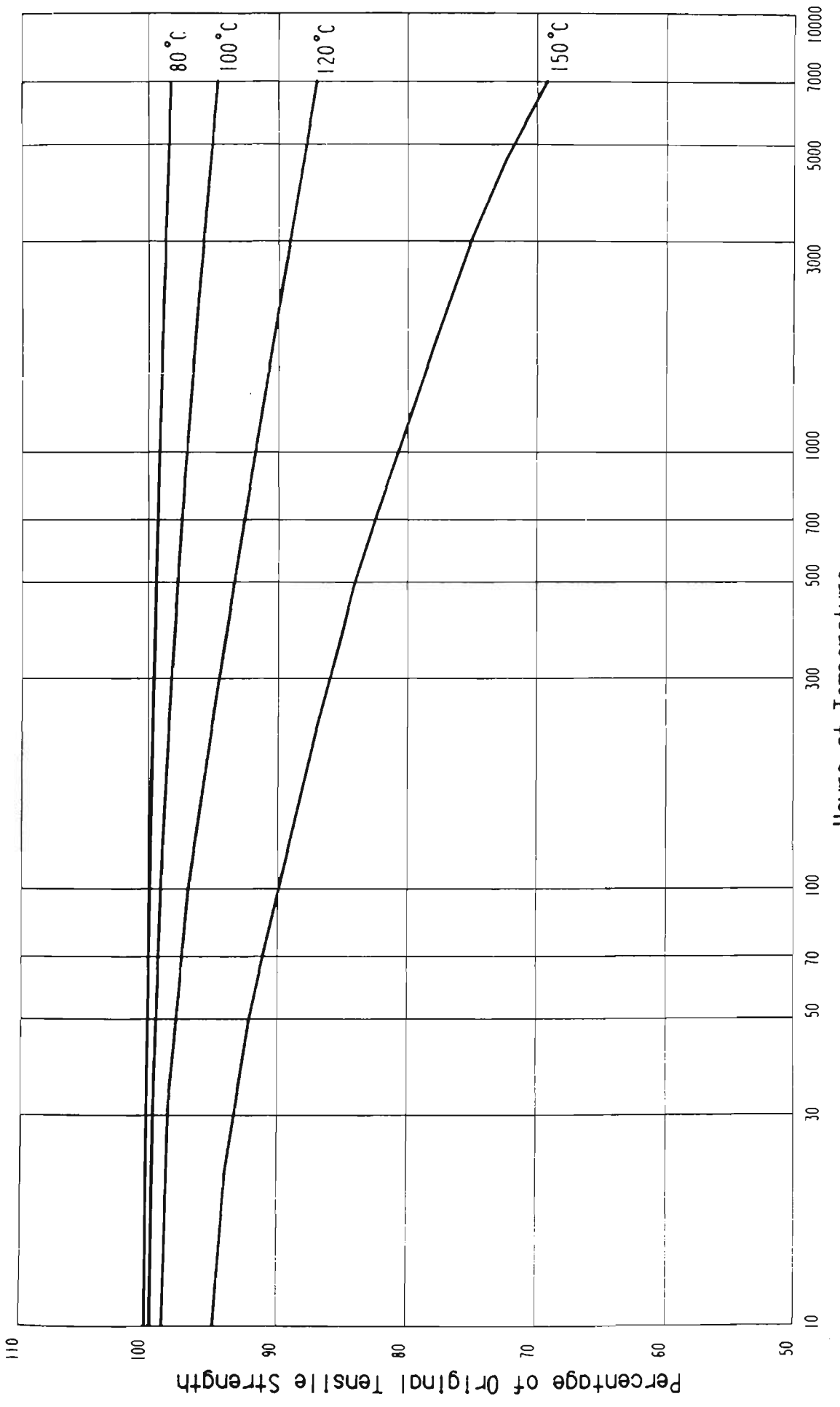

FIGURE 3.5 PERCENTAGE OF ORIGINAL TENSILE STRENGTH FOR ALLOY 1350 vs AGEING TIME

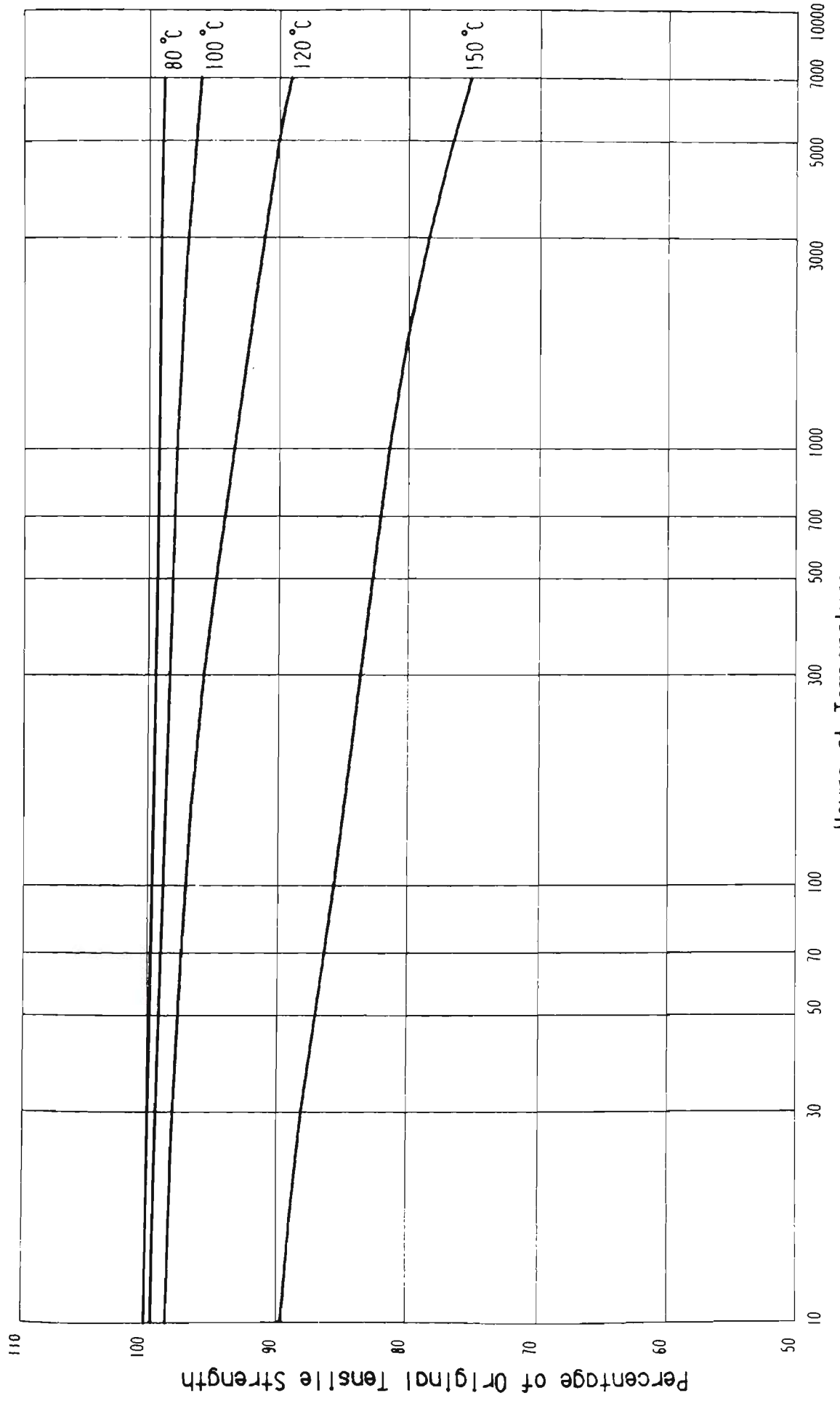

FIGURE 3.6 PERCENTAGE OF ORIGINAL TENSILE STRENGTH FOR ALLOY 1120 vs AGEING TIME

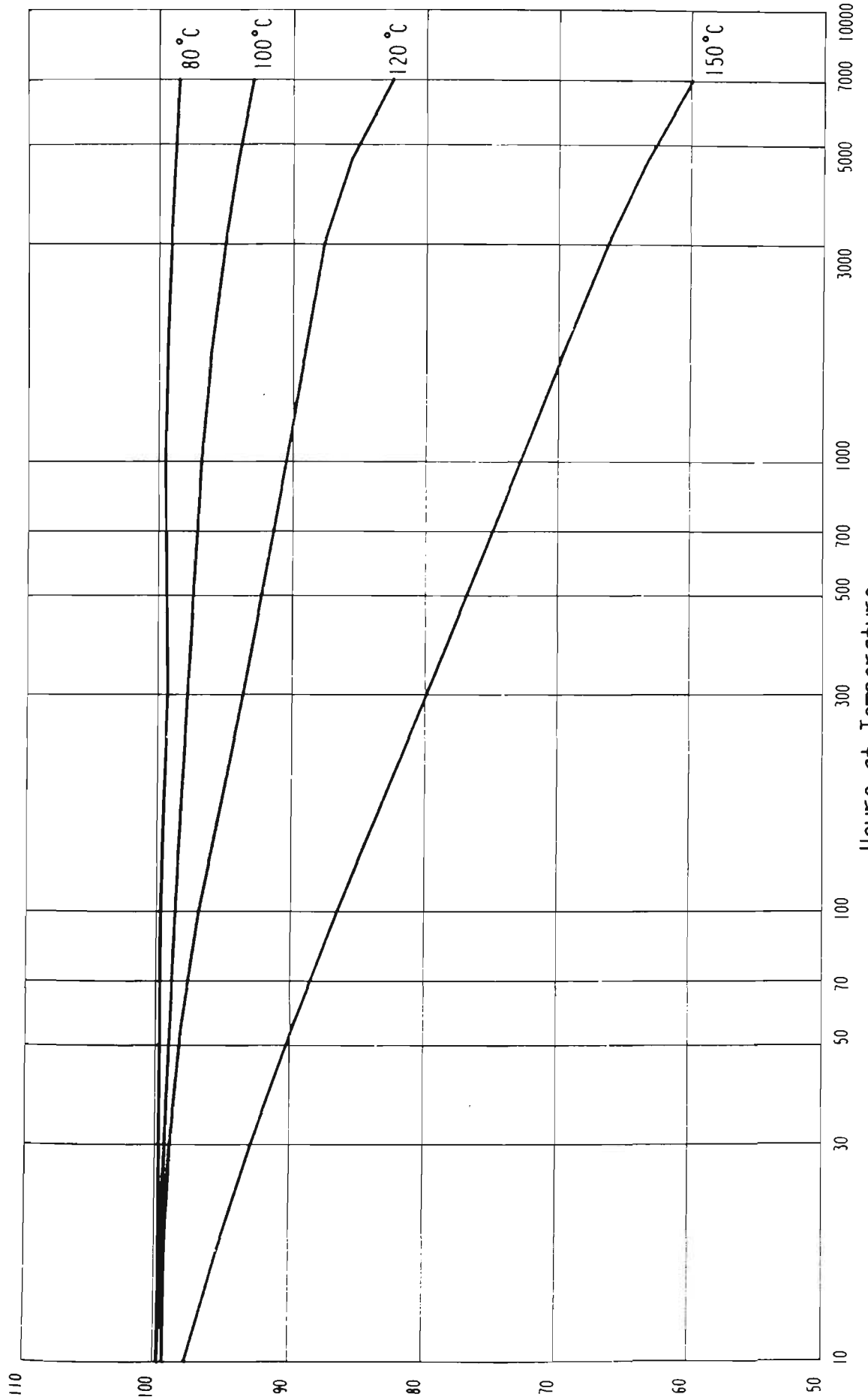

FIGURE 3.7 PERCENTAGE OF ORIGINAL TENSILE STRENGTH FOR ALLOY 6201 vs AGEING TIME

Changes in the elongation of a wire indicate a change in the ductility of the wires.

The details of the breaking loads, ultimate tensile strength and elongation of the wires that constitute the conductor samples from the Avon to Kemps Creek and Dapto to Springhill transmission lines are given in Appendix 3. In addition two further samples from the Tomago to Taree and Bellambi to Heathcote transmission lines are given in Appendix 3.

All samples of the conductor used for the mechanical property tests were taken from areas away from the suspension points. Additional samples from the suspension point were tested after macro and micro-examinations, however no significant difference in the test results were revealed.

A summary of the findings of the wire breaking loads are given in Tables 3.4 and 3.5 for the aluminium and steel strands, respectively. A summary of the findings of the wire ultimate tensile strengths are given in Tables 3.6 and 3.7 for aluminium and steel strands, respectively and finally a summary of the findings of the wire elongations are given in Tables 3.8 and 3.9 for aluminium and steel strands, respectively.

Regarding the aluminium wire breaking loads for the,

1. Avon to Kemps Creek transmission line conductor sample, two wires one from the 18 wire layer and one from the 12 wire layer did not comply with the minimum breaking load criteria

Transmission Line	Nominal Wire Diameter	Mean Cross Sectional Area mm^2			Minimum Cross Sectional Area mm^2		
		24 Wire Layer	18 Wire Layer	12 Wire Layer	24 Wire Layer	18 Wire Layer	12 Wire Layer
Avon-Kemps Creek	3.531	1.731	1.622	1.623	1.6801	1.414	1.563
Dapto-Springhill	3.531	1.746	1.710	1.686	1.686	1.572	1.69
Tomago-Taree	2.997	-	1.17	1.13	-	1.15	1.08
Bellambi-Heathcote	3.708	-	1.64	1.61	-	1.50	1.56
Australian Standard							
C75.1 1963	3.531		-			1.570	
	2.997		-			1.161	
	3.708		-			1.726	

TABLE 3.4 - SUMMARY OF ALUMINIUM WIRE TEST RESULTS BREAKING LOAD

Transmission Line	Nominal Wire Diameter	Mean Cross Sectional Area mm^2		Minimum Cross Sectional Area mm^2
		6 Wire Layer	Core	6 Wire Layer
Avon-Kemps Creek	3.531	14.341	-	13.408
	3.708	-	15.947	-
Dapto-Springhill	3.531	15.115	-	14.551
	3.708	-	15.645	-
Tomago-Taree	2.997	10.057	9.650	9.710
Bellambi-Heathcote	3.708	15.428	15.270	15.11
Australian Standard				
	3.531		-	12.846
C75.1 1963	2.997		-	9.261
	3.708		-	14.181

TABLE 3.5 - SUMMARY OF STEEL WIRE TEST RESULTS BREAKING LOAD

Transmission Line	Nominal Wire Diameter	Mean Cross Sectional Area mm^2			Minimum Cross Sectional Area mm^2		
		24 Wire Layer	18 Wire Layer	12 Wire Layer	24 Wire Layer	18 Wire Layer	12 Wire Layer
Avon-Kemps Creek	3.531	0.175	0.166	0.166	0.167	0.144	0.161
Dapto-Springhill	3.531	0.172	0.175	0.172	0.162	0.161	0.164
Tomago-Taree	2.997	-	0.166	0.159	-	0.162	0.153
Bellambi-Heathcote	3.708	-	0.151	0.151	-	0.140	0.136
Australian Standard							
C75.1 1963	3.531		-			0.162	
	2.997		-			0.165	
	3.708		-			0.160	

TABLE 3.6 - SUMMARY OF ALUMINIUM WIRE TEST RESULTS
ULTIMATE TENSILE STRENGTH

Transmission Line	Nominal Wire Diameter	Mean Cross Sectional Area mm^2		Minimum Cross Sectional Area mm^2
		6 Wire Layer	Core	6 Wire Layer
Avon-Kemps Creek	3.531	1.450	-	1.373
	3.708	-	1.447	-
Dapto-Springhill	3.531	1.525	-	1.472
	3.708	-	1.428	-
Tomago-Taree	2.997	1.419	1.358	1.378
Bellambi-Heathcote	3.708	1.443	1.429	1.415
Australian Standard				
	3.531		-	1.312
	3.708		-	1.312
C75.1 1963	2.997		-	1.312
	3.708	10.801	10.801	10.584

TABLE 3.7 - SUMMARY OF STEEL WIRE TEST RESULTS
ULTIMATE TENSILE STRENGTH

Transmission Line	Nominal Wire Diameter	Mean Cross Sectional Area mm^2			Minimum Cross Sectional Area mm^2		
		24 Wire Layer	18 Wire Layer	12 Wire Layer	24 Wire Layer	18 Wire Layer	12 Wire Layer
Avon-Kemps Creek	3.531	1.85	1.82	1.60	1.6	1.6	1.6
Dapto-Springhill	3.531	1.54	1.56	1.47	1.2	1.4	1.2
Tomago-Taree	2.997	-	1.58	1.63	-	1.6	1.2
Bellambi-Heathcote	3.708		Not		Measured		
Australian Standard							
AS1220 1989	3.531		-			1.2	
	2.997		-			1.0	
	3.708		-			1.2	

TABLE 3.8 - SUMMARY OF ALUMINIUM WIRE TEST RESULTS
ELONGATION

Transmission Line	Nominal Wire Diameter	Mean Cross Sectional Area mm^2		Minimum Cross Sectional Area mm^2
		6 Wire Layer	Core	6 Wire Layer
Avon-Kemps Creek	3.531	5.95	-	5.9
	3.708	-	6.0	-
Dapto-Springhill	3.531	5.97	-	5.6
	3.708	-	5.8	-
Tomago-Taree	2.997	5.63	3.2	5.4
Bellambi-Heathcote	3.708	Not	Measured	
Australian Standard				
	3.531		-	4.0
AS1220 1989	2.997		-	3.5
	3.708		-	4.0

TABLE 3.9 - SUMMARY OF STEEL WIRE TEST RESULTS
ELONGATION

and the mean breaking load was 10.3, 3.3 and 3.4% in excess of the minimum requirement for the 24, 18 and 12 wire layers respectively;

2. Dapto to Springhill transmission line conductor sample, all the wires complied with the minimum breaking load criteria and the mean breaking load was 11.2, 8.9 and 7.4% in excess of the minimum requirement for the 24, 18 and 12 wire layers respectively;

3. Tomago to Taree transmission line conductor sample, one wire from the 18 wire layer and eight wires from the 12 wire layer did not comply with the minimum breaking load criteria and the mean breaking load was 0.78 and -2.60% of the minimum requirements for the 18 and 12 wire layers respectively; and

4. Bellambi to Heathcote transmission line conductor sample, all wires with the exception of two wires from the 18 wire layer did not comply with the minimum breaking load criteria and the mean breaking load was -4.98 and -6.72% of the minimum requirements for the 18 and 12 wire layers respectively.

Regarding the steel wire breaking loads, all the conductor samples complied with the minimum load criteria and for the,

1. Avon to Kemps Creek transmission line conductor sample, the mean breaking load was 11.6 and 7.93% in excess of the minimum requirement for the 6 wire layer and core respectively;

2. Dapto to Springhill transmission line conductor sample, the mean breaking load was 17.7 and 10.3% in excess of the minimum requirements for the 6 wire layer and core respectively;

3. Tomago to Taree transmission line conductor sample, the mean breaking load was 8.60 and 4.2% in excess of the minimum requirements for the 6 wire layer and core respectively; and

4. Bellambi to Heathcote transmission line conductor sample, the mean breaking load was 8.79 and 7.68% in excess of the minimum requirement for the 6 wire layer and core respectively.

Regarding the aluminium wire ultimate tensile strengths for the,

1. Avon to Kemps Creek transmission line conductor sample, two wires, one from the 18 wire layer and one from the 12 wire layer did not comply with the minimum ultimate tensile strength (the same two wires that did not meet the minimum breaking load requirement) and the mean ultimate tensile strength was 8.03, 2.47 and 2.47% in excess of the minimum requirement for the 24, 18 and 12 wire layers respectively;

2. Dapto to Springhill transmission line conductor sample, one wire from the 18 wire layer did not comply with the minimum ultimate tensile strength and the mean ultimate tensile strength was 6.17, 8.02 and 6.17% in excess of the minimum requirements for the 24, 18 and 12 wire layers respectively;

3. Tomago to Taree transmission line conductor sample, fourteen wires, three from the 18 wire layer and eleven from the 12 wire layer did not comply with the minimum ultimate tensile strength (nine of the fourteen wires did not meet the breaking load requirements) and the mean ultimate tensile strength was 0.606 and -3.64% of the minimum requirement for the 18 and 12 wire layers respectively; and

4. Bellambi to Heathcote transmission line conductor sample, twenty six wires, fifteen from the 18 wire layer and eleven wires from the 12 wire layer did not comply with the minimum ultimate tensile strength (all but two wires from the abovementioned twenty six wires did not meet the minimum breaking load requirement) and the mean ultimate tensile strength was -5.63% of the minimum requirement for both the 18 and 12 wire layers.

Regarding the aluminium wire elongations, all the conductor samples complied with the minimum elongations for the,

1. Avon to Kemps Creek transmission line conductor sample, the mean elongation was 54, 52 and 33% in excess of the minimum requirements for the 24, 18 and 12 wires layers respectively;

2. Dapto to Springhill transmission line conductor sample, the mean elongation was 28, 30 and 23% in excess of the minimum requirements for the 24, 18 and 12 wire layers respectively;

3. Tomago to Taree transmission line conductor sample, the mean elongation was 58 and 63% in excess of the minimum requirements for the 18 and 12 wire layers respectively; and

4. Bellambi to Heathcote transmission line conductor sample the elongation were not measured.

Regarding the steel wire elongations, all the conductor samples complied with the minimum elongations with the exception of the core of the Tomago to Taree transmission line conductor sample. For the,

1. Avon to Kemps Creek transmission line conductor sample, the mean elongation was 49 and 50% in excess of the minimum requirements for the 6 wire layer and core respectively;

2. Dapto to Springhill transmission line conductor sample, the mean elongation was 49 and 45% in excess of the minimum requirements for the 6 wire layer and core respectively;

3. Tomago to Taree transmission line conductor sample, the mean elongation was 61 and -9% of the minimum requirements for the 6 wire layer and core respectively; and

4. Bellambi to Heathcote transmission line conductor sample, the elongations were not measured.

3.4.1.3 Electrical Properties

The electrical properties of the aluminium wire are assessed by determining the resistivity. An accepted value for the electrical resistivity of aluminium at 20°C is 0.028034 μm or 61.5% of the International Annealed Copper Standard (IACS). The resistivity of copper at 20°C is 0.017241 μm for 100% conductivity (2). The resistivity is determined by carrying measurements of mass and resistance for a known length.

Changes in the resistivity or conductivity may be caused by changes in the cross sectional area and material microstructure. Annealing of the wires at elevated temperatures can cause an increase of conductivity as illustrated in Figures 3.8, 3.9 and 3.10 for aluminium 1350 and aluminium alloy 1120 and 6201 respectively (53). Samples of conductor removed from suspension points may exhibit a decrease in conductivity caused by an effective reduction in cross sectional area by fatigue initiated cracks.

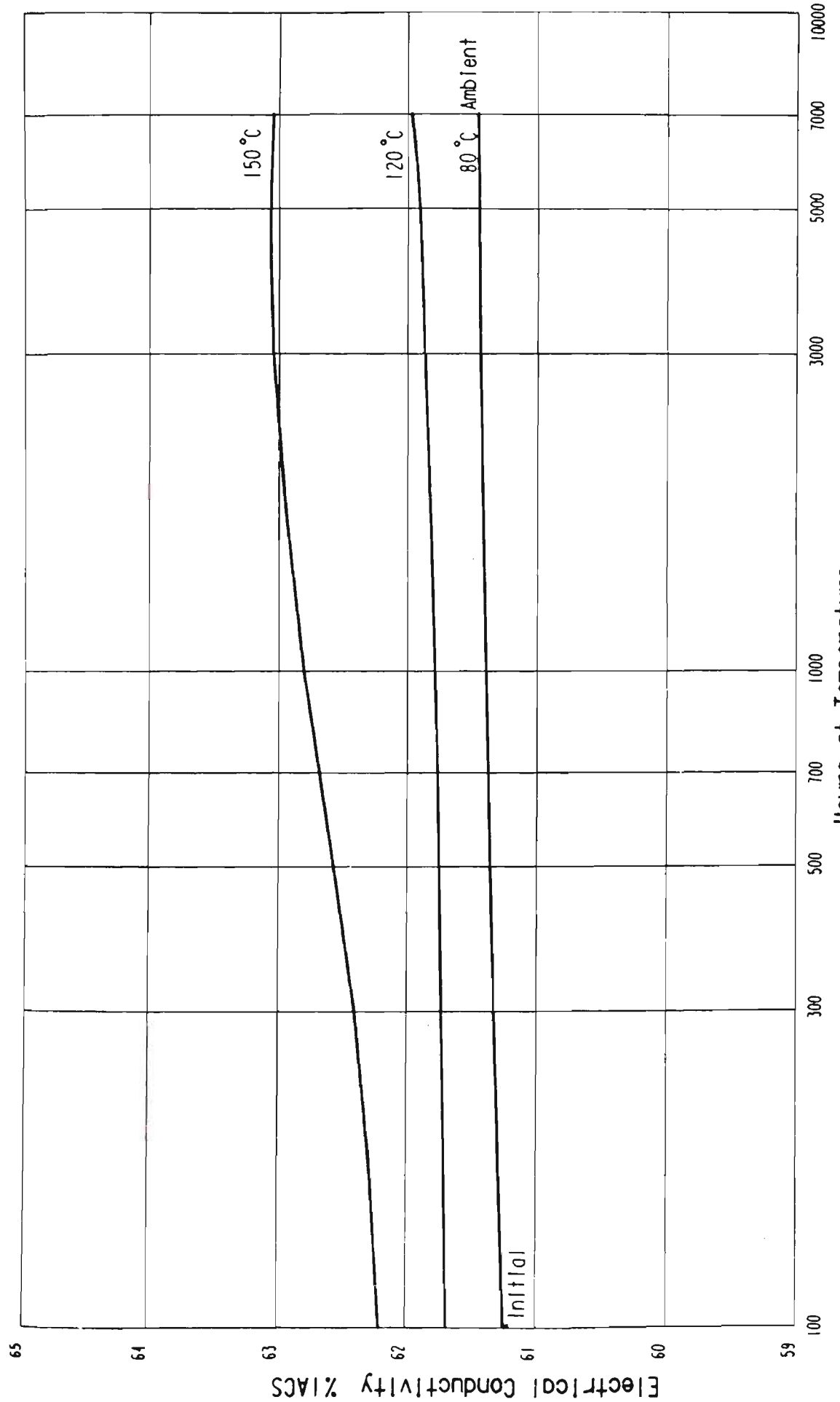

FIGURE 3.8 ELECTRICAL CONDUCTIVITY FOR ALLOY 1350 vs TIME AND TEMPERATURE

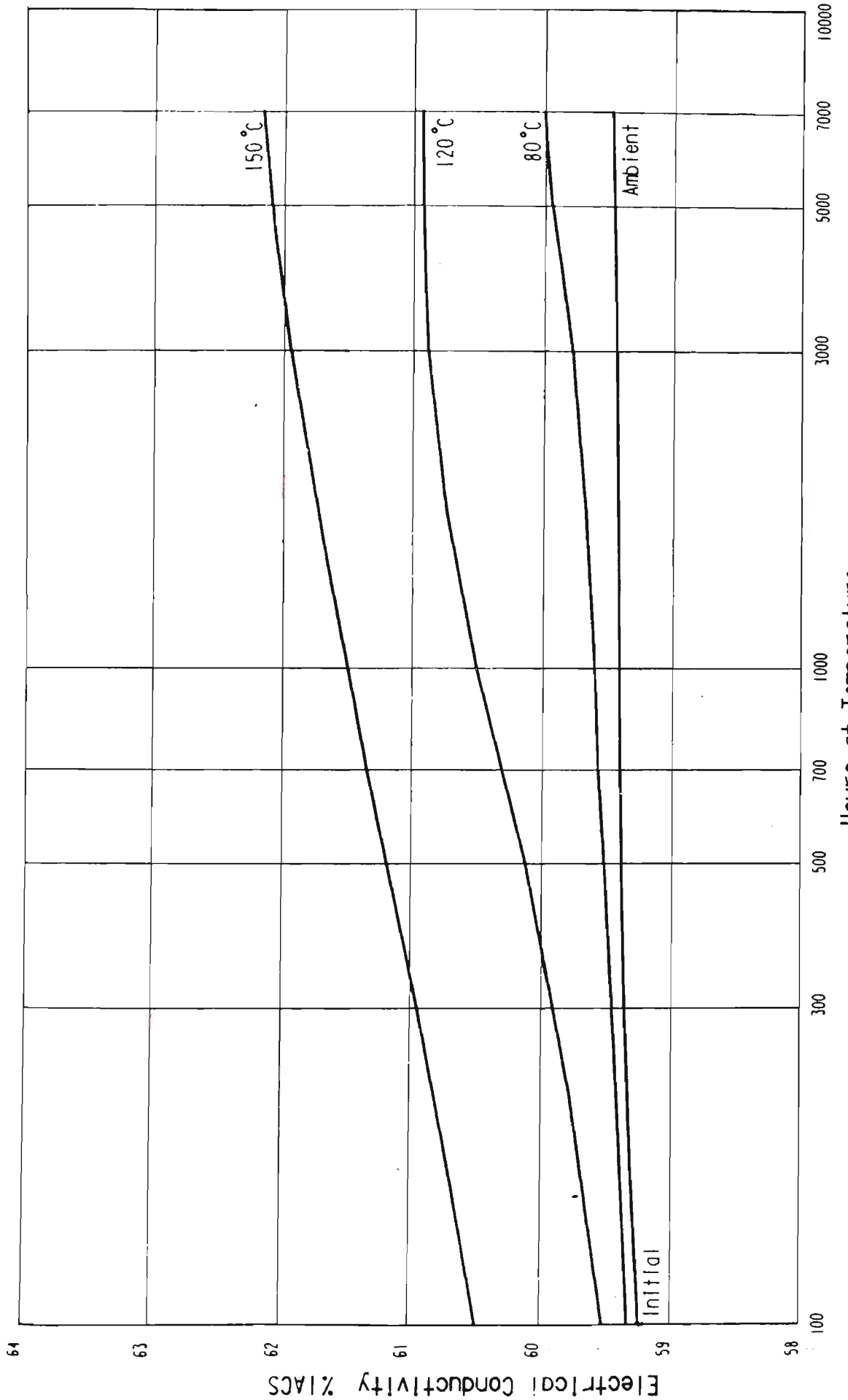

FIGURE 3.9 ELECTRICAL CONDUCTIVITY FOR ALLOY 1120 vs TIME AND TEMPERATURE

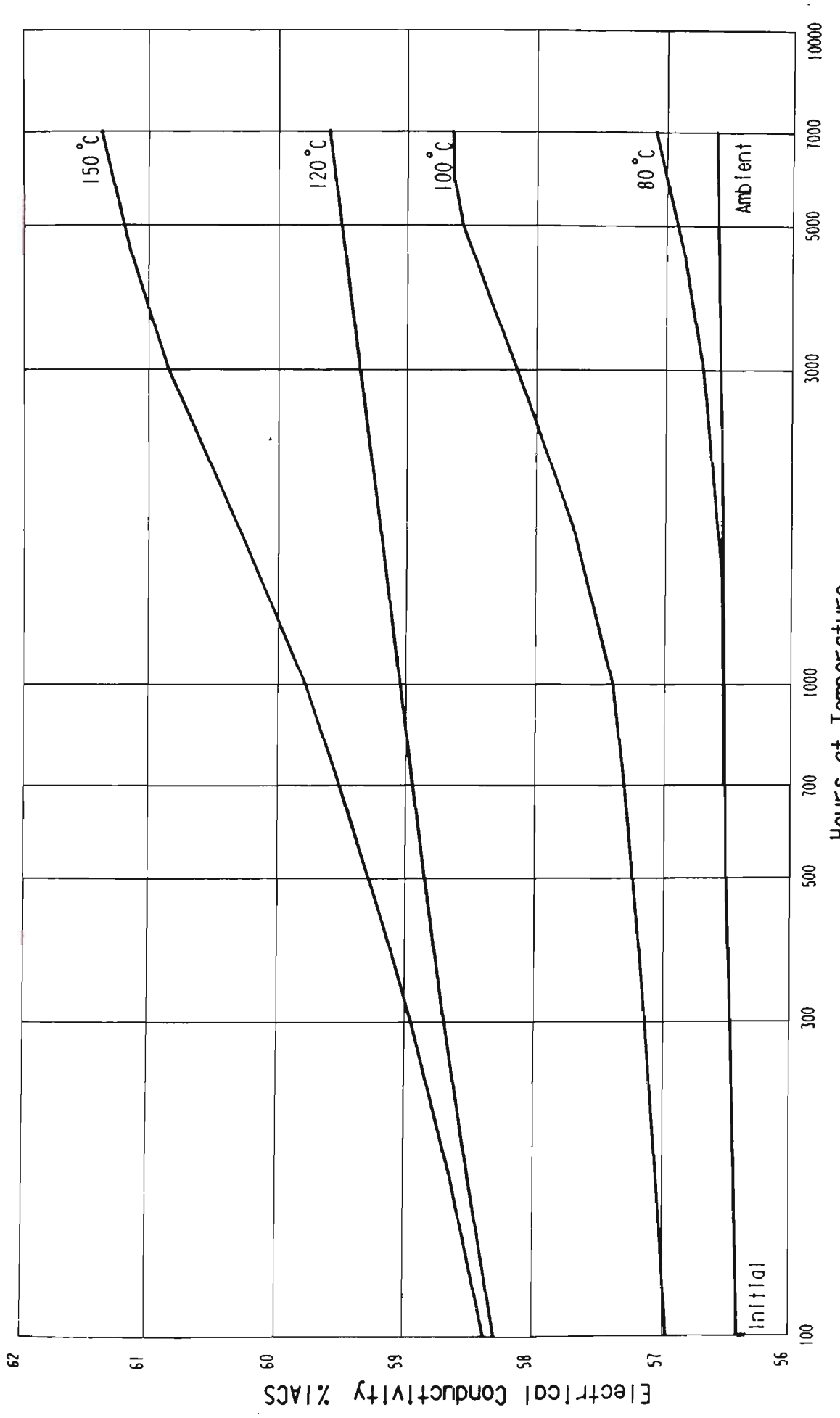

FIGURE 3.10 ELECTRICAL CONDUCTIVITY FOR ALLOY 6201 vs TIME AND TEMPERATURE

The details of the resistivity of the wires that constitute the conductor samples from the Avon to Kemps Creek, Dapto to Springhill, Tomago to Taree and Bellambi to Heathcote transmission lines are given in Appendix 3.

All samples of the conductor used for the electrical property determination were taken from areas away from the suspension point. A summary of the findings of the wire resistivity are given in Tables 3.10.

Regarding the aluminium wire resistivity for the,

1. Avon to Kemps Creek transmission line conductor sample complied with the maximum resistivity criteria and the mean resistivity was 1.3, 1.6 and 1.3% less than the minimum requirement for the 24, 18 and 12 wire layers respectively;

2. Dapto to Springhill transmission line conductor sample complied with the maximum resistivity criteria with the exception of two wires from the 24 wire layer. The mean resistivity was 0, 0.9 and 1.3% less than the minimum requirement for the 24, 18 and 12 wire layers respectively;

3. Tomago to Taree transmission line conductor sample complied with the maximum resistivity criteria and the mean resistivity was 3.1% less than the minimum requirement for both the 18 and 12 wire layers; and

Transmission Line	Nominal Wire Diameter	Mean Resistivity at 20°C um			Maximum Resistivity at 20°C		
		24 Wire Layer	18 Wire Layer	12 Wire Layer	24 Wire Layer	18 Wire Layer	12 Wire Layer
Avon-Kemps Creek	3.531	0.0279	0.0278	0.0279	0.0280	0.0279	0.0280
Dapto-Springhill	3.531	0.0283	0.0280	0.0279	0.0286	0.0281	0.0281
Tomago-Taree	2.997	-	0.0274	0.0274	-	0.0276	0.0276
Bellambi-Heathcote	3.708	-	0.0288	0.0278	-	0.0288	0.0279
Australian Standard							
C75.1 1963	3.531		-			0.028264	
	2.997		-			0.028264	
	3.708		-			0.028264	

TABLE 3.10 - SUMMARY OF ALUMINIUM WIRE TEST RESULTS
RESISTIVITY

* Two samples from the 18 wire layer and two samples from the 12 wire layer were measured.

4. Bellambi to Heathcote transmission line conductor sample, all the wires from the 12 wire layer complied with the maximum resistivity criteria. The mean resistivity for the 12 wire layer was 1.64% less than the minimum requirement. The average resistivity of the 18 wire layer was 1.90% in excess of the minimum requirement and subsequent chemical test revealed an average of 0.174% silicon component in the aluminium. This is in excess of the maximum silicon component at 0.100% and accounts for the higher than normal resistivity. High silicon components is consistent with the hot rolled production process probably used to manufacturer this conductor.

3.4.1.4 Steel Wire Galvanising Properties

The steel wire galvanising properties are assessed by determining the mass of the zinc coating and the adherence quality.

The mass of the zinc coating is determined by measuring the mass of a wire specimen. The zinc coating is then chemically removed and a further measurement of mass as well as diameter is carried out. From these measurements the mass per metre of zinc coating may be determined.

Changes in the galvanising mass may be caused by the zinc being sacrificial to the aluminium under certain circumstances and/or abrasion of the zinc caused by the movement of strands over the galvanised wire surface. Poor adhesion of the zinc to the parent steel wire is another likely cause of degradation of the zinc

coating mass. An example of this poor adhesion is illustrated in Plate 3.11. Poor adhesion is assessed by traditional wrap tests.

Forrest and Ward (39) published results of the loss of zinc coating mass of 30/7 ACSR/GZ construction for various environments for transmission lines being 16 to 20 years old. Whilst it is appreciated that extrapolation beyond this age range can lead to significant errors in predicted results particularly in view of the large scatter in the data, linear regression of the date suggests that after 42 years of service 25% of the zinc coating may be lost. The test results and the linear regression line are given in Figure 3.12.

This compares favourable with Occassione, Britton and Collins (65) results for 7/1 ACSR/GZ construction which suggests that after 20 years exposure to various environments no evidence of rust initiation had occurred.

As part of these studies further investigations suggest a greater loss of zinc coating mass occurs at the suspension clamp site compared with that of a site away from the suspension site (nominally termed the midspan site). This is probably caused by the constrained movement of the aluminium wires over the galvanised wire surface causing an abrasion and subsequent loss of the zinc. Linear regression of the test results of 27 year old 30/7/2.99 mm ACSR/GZ construction is given in Figure 3.13 illustrates this effect.

PLATE 3.11 SEM OF 30/7/2.997 MM ACSR/GZ
6 WIRE LAYER STEEL STRANDS
POOR ZINC ADHESION

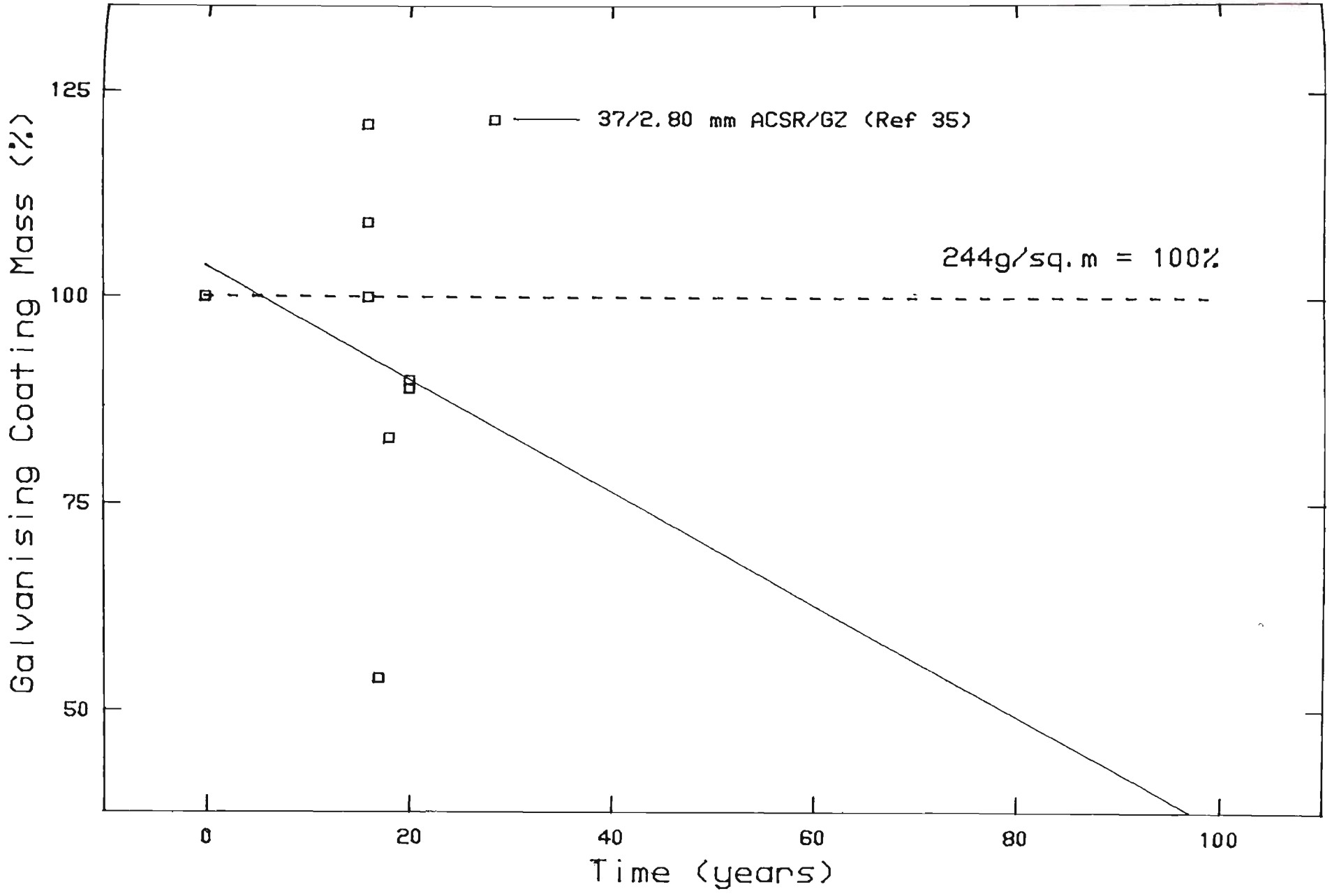

FIGURE 3.12 DEGRADATION OF GALVANISING COATING FOR ACSR/GZ CONDUCTOR

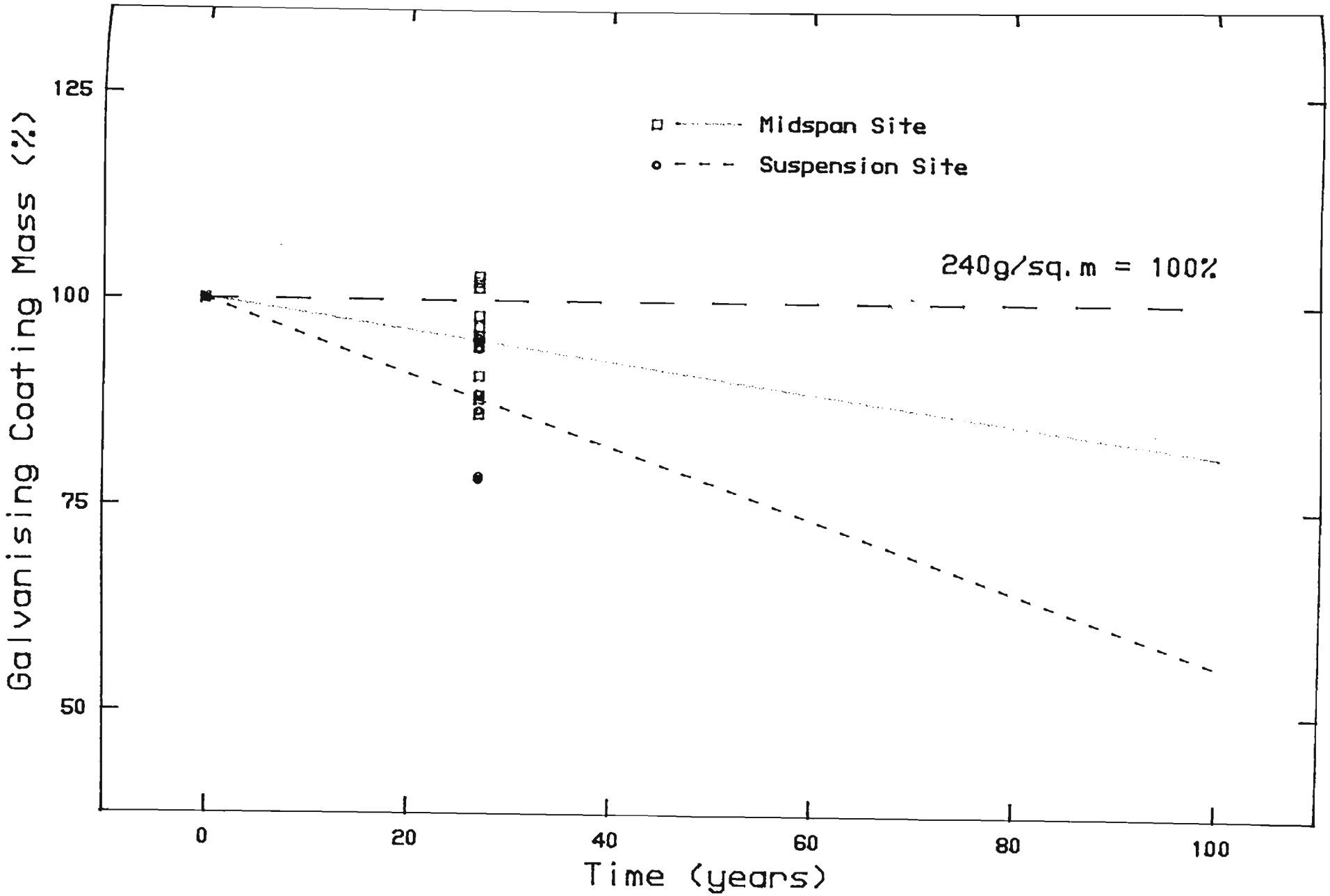

FIGURE 3.13 DEGRADATION OF GALVANISING COATING FOR 3/7/3.00MM ACSR/GZ

mm wires, generally accordance with ANSI/ASTM B117-73 (4). The aged samples were 27 years old and the tar was applied to the penultimate aluminium layer. The grease was only applied to the 6 steel wire layer.

The test consisted of exposing the samples to an atomised salt solution having a pH range of 6.5 to 7.2 and an environment temperature of 35^{o}C.

The results of the test are as follows:

1. For aged 2.99 mm and new 3.00 mm GZ wires, brown stains appeared on the surface of the wires after 144 and 672 hours exposure respectively with an average loss of wire mass of 3.16% and 3.46% respectively. The results of the wire mass loss and linear regression plots are given in Figure 3.14.

2. For the aged and tarred 7/2.99 mm and new and greased 7/3.00 mm GZ wires brown stains appeared on the surface of the stranded section after 408 and 864 hours exposure respectively. The aged and tarred 7/2.99 mm GZ wire as found and the new and greased 7/3.00 mm GZ wires as found is shown in Plates 3.12 and 3.13 respectively;

3. After 864 hours, on destranding the aged and tarred 30/7/2.99 mm and new and greased 30/7/3.00 mm ACSR/GZ construction some discolouration of the steel core was present. The tar and grease was removed from the steel core using a brush and trichlorethane. On the aged steel core brown stains were

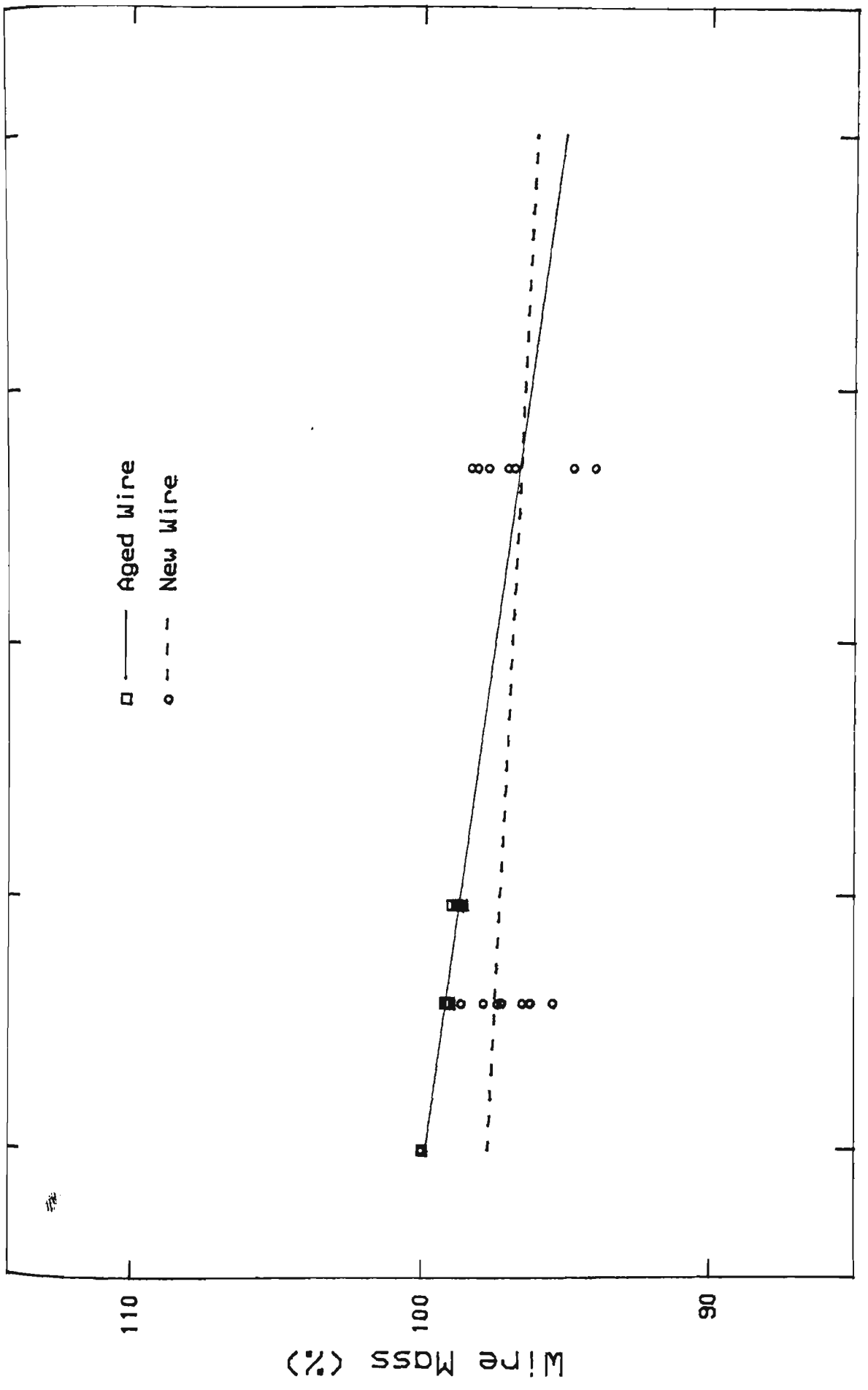

FIGURE 3.14 DEGRADATION OF GALVANISING MASS 3.00MM WIRE

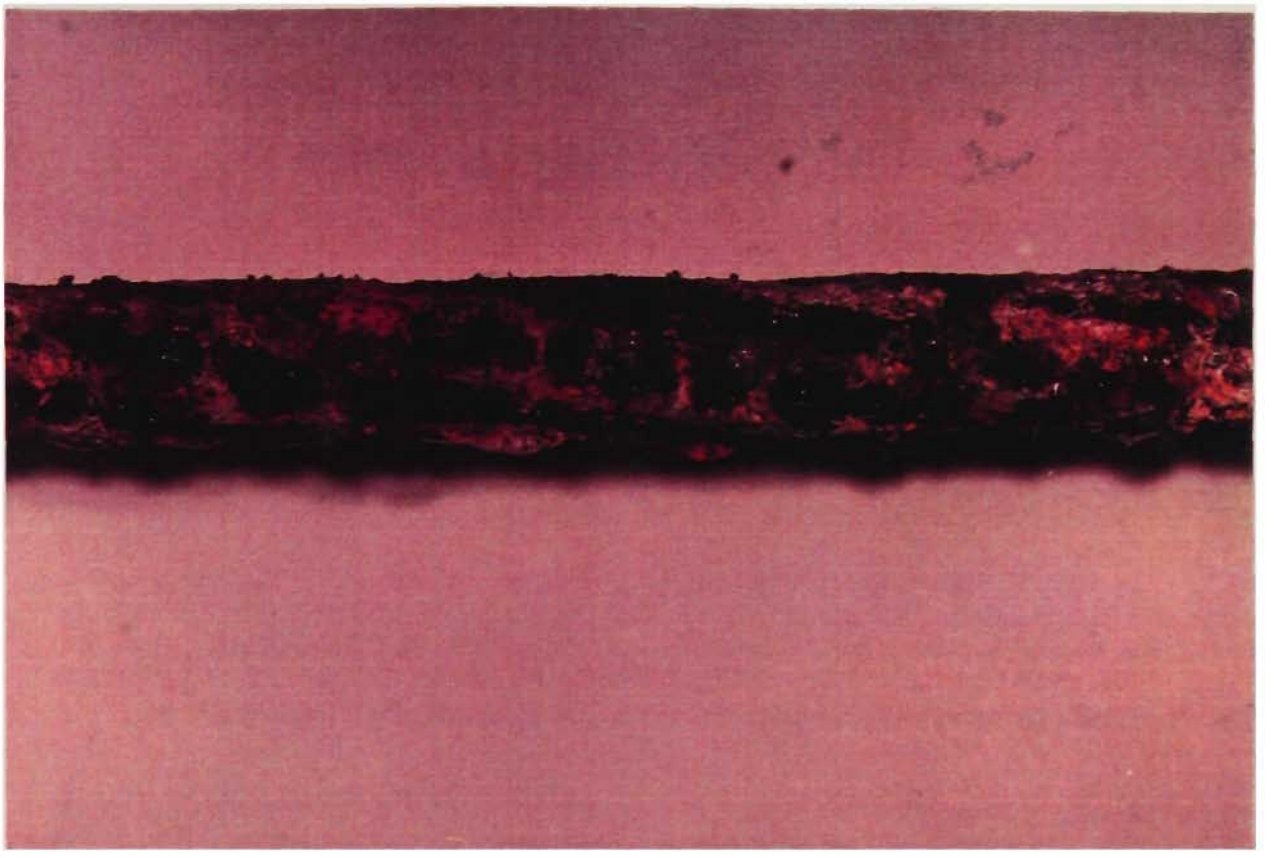

PLATE 3.12 7/2.99 MM TARRED AND AGED GZ WIRE
AFTER 408 HOURS SALT SPRAY EXPOSURE
AS FOUND SAMPLE

PLATE 3.13 7/3.00 MM NEW AND GREASED GZ WIRE
AFTER 864 HOURS SALT SPRAY EXPOSURE
AS FOUND SAMPLE

present and on the new steel core an area of dull grey galvanising with ingrest of accumulated salt was present. The aged and tarred 30/7.299 mm and the new and greased 30/7/3.00 mm ACSR/GZ construction destranded samples are as illustrated in Plates 3.14 to 3.21.

The salt spray test result suggest that:

1. After a mass loss of approximately 3% for GZ wires that brown stains will appear on the surface of wires irrespective of age or service history.

2. Whilst tar and grease afford an additional corrosion protection that after an incubation period brown stains will appear on the surface of the stranded wires. Greased stranded new wire samples performed better than tarred stranded wire samples.

3. The stranding construction of aluminium layers over the steel wires did provide additional protection. Furthermore tar applied to the penultimate layer also provided an additional barrier for salt ingrest and possible long term rust initiation.

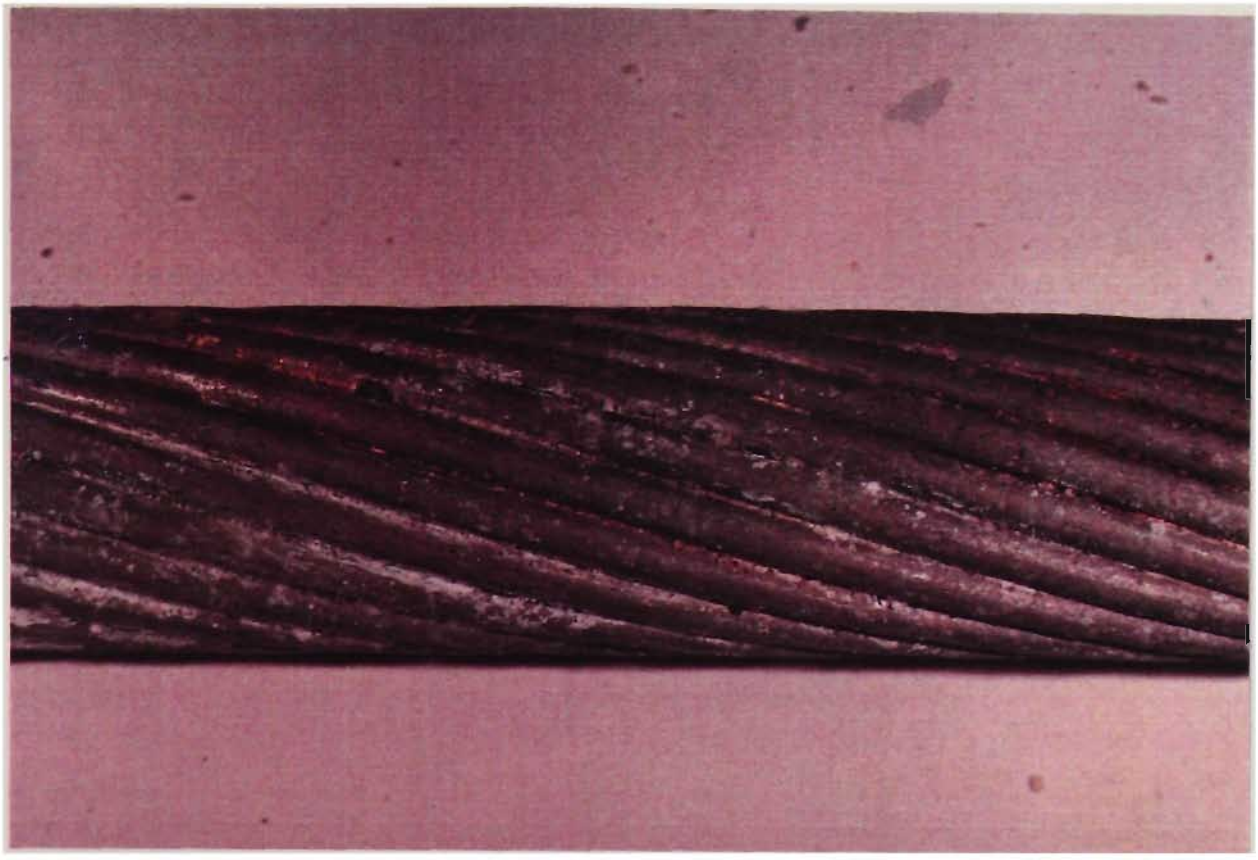

PLATE 3.14 30/7/2.99 MM ACSR/GZ 18 WIRE LAYER
AGED AND TARRED SAMPLE
AFTER 864 HOURS SALT SPRAY EXPOSURE

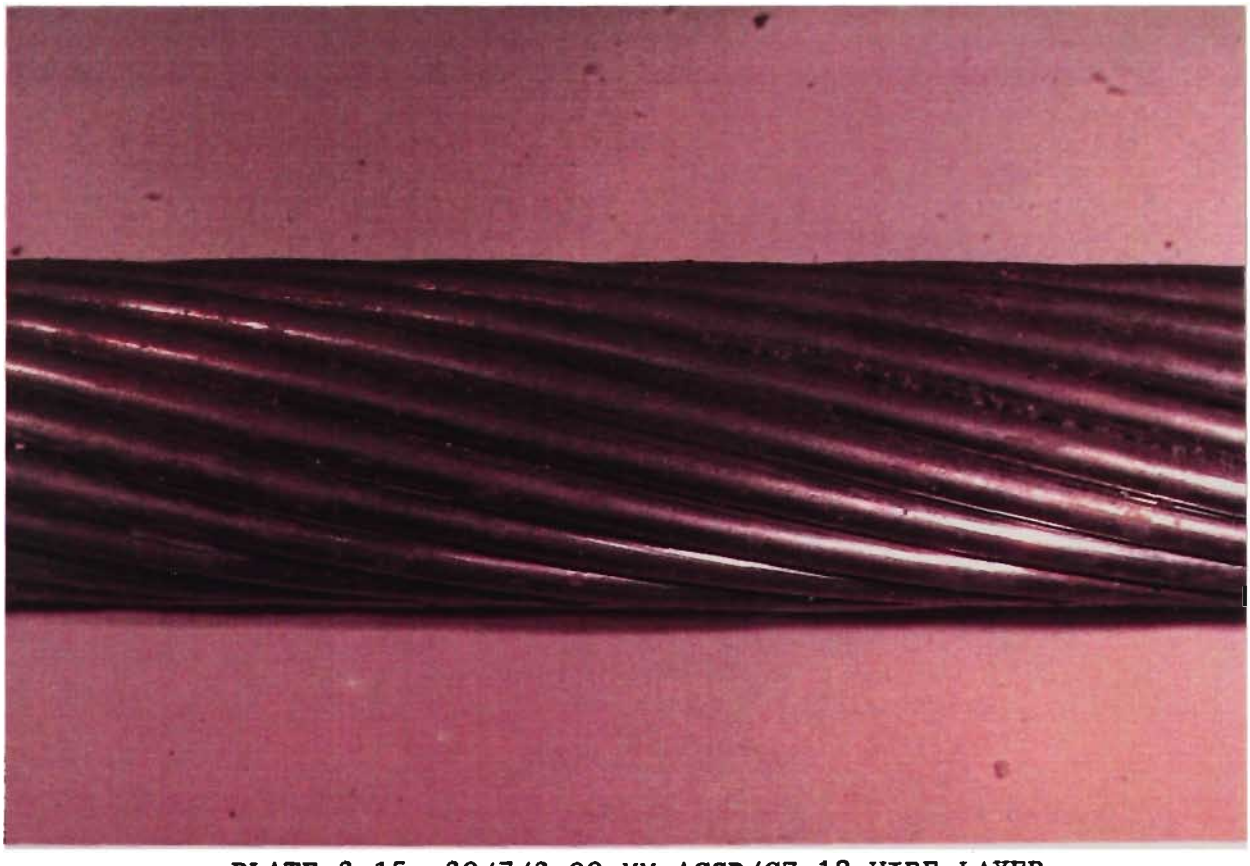

PLATE 3.15 30/7/3.00 MM ACSR/GZ 18 WIRE LAYER
NEW AND GREASES SAMPLE
AFTER 864 HOURS SALT SPRAY EXPOSURE

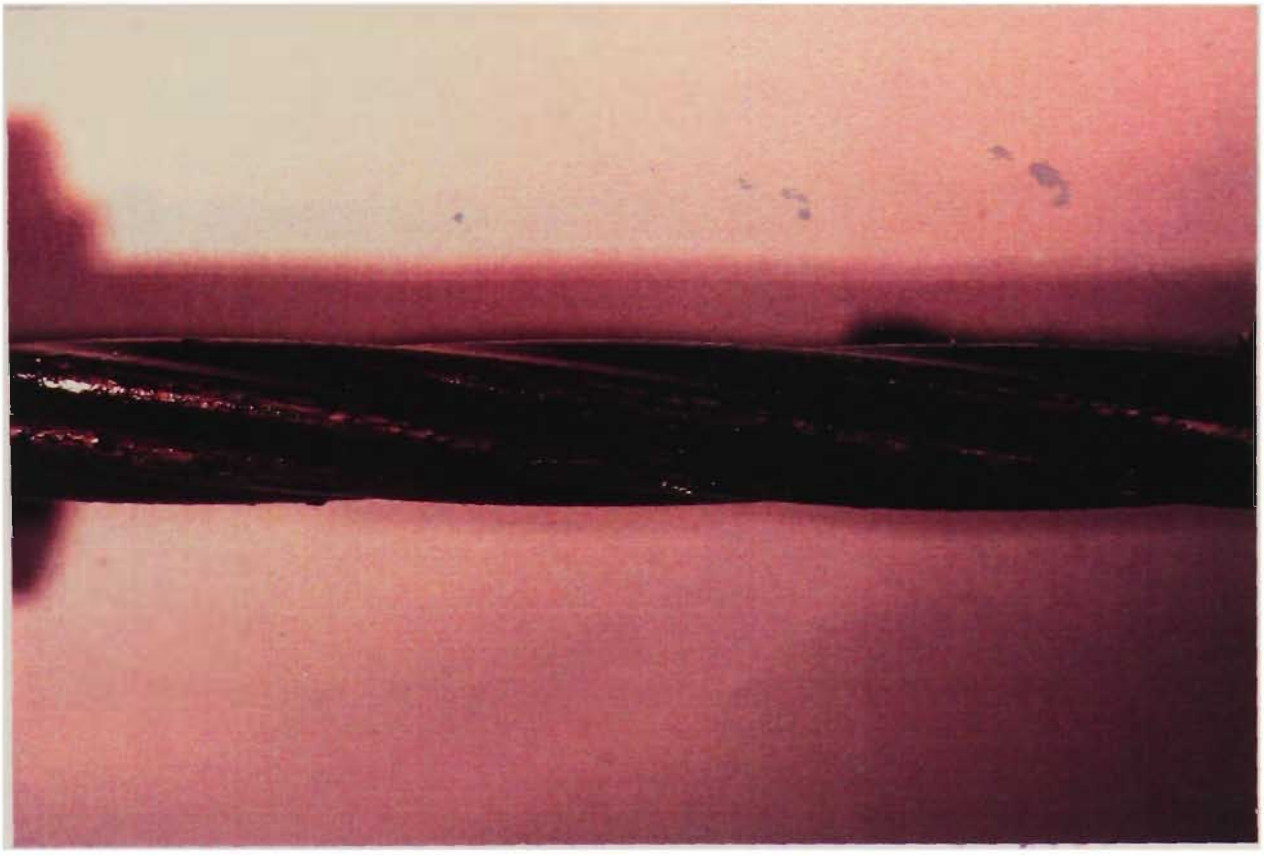

PLATE 3.16 30/7/2.99 MM ACSR/GZ 6 WIRE LAYER
AGED AND TARRED SAMPLE
AFTER 864 HOURS SALT SPRAY EXPOSURE

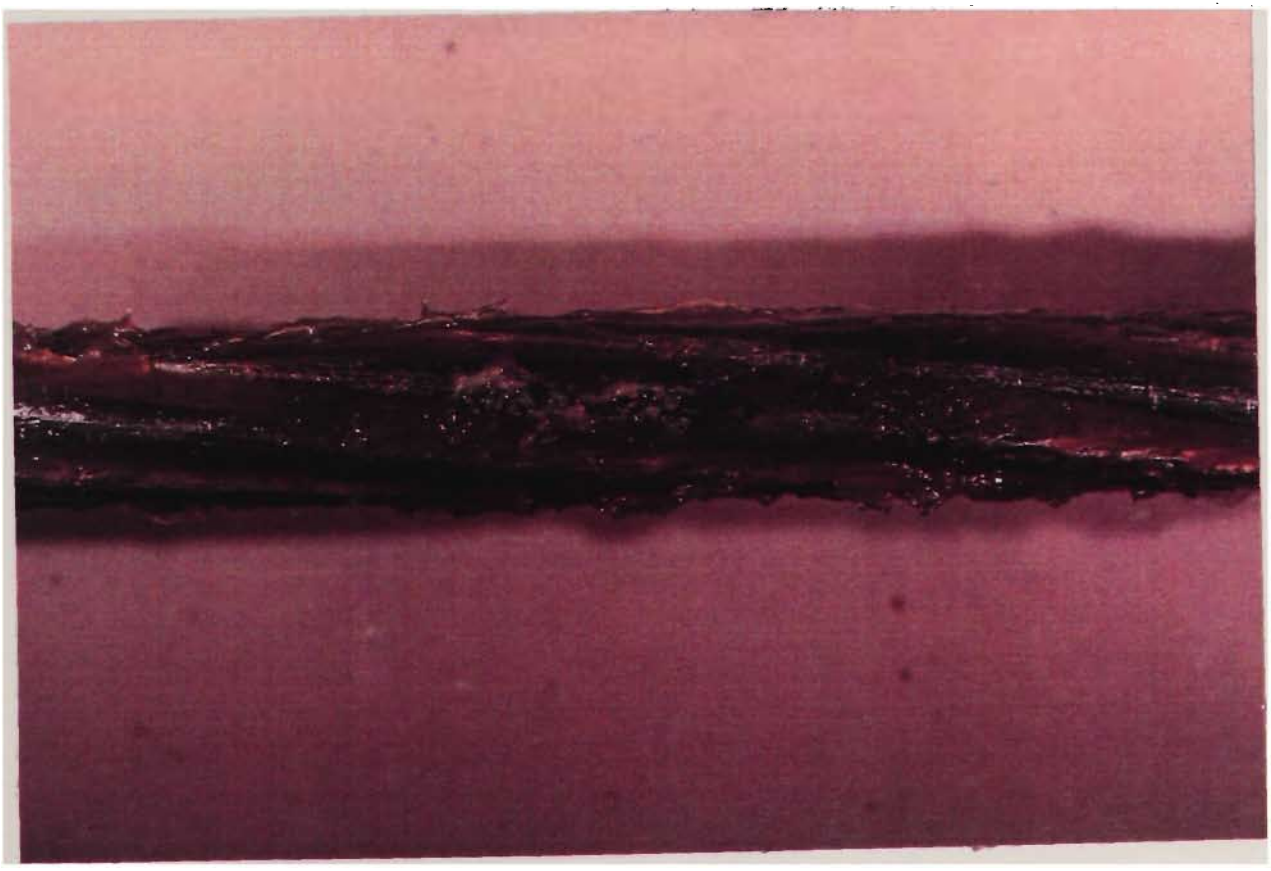

PLATE 3.17 30/7/3.00 MM ACSR/GZ 6 WIRE LAYER
NEW AND GREASED SAMPLE
AFTER 864 HOURS SALT SPRAY EXPOSURE

PLATE 3.18 30/7/2.99 MM ACSR/GZ 6 WIRE LAYER
AGED AND TARRED SAMPLE
AFTER 864 HOURS SALT SPRAY EXPOSURE
LOCALISED BROWN STRAINING

PLATE 3.19 30/7/3.00 MM ACSR/GZ 6 WIRE LAYER
NEW AND GREASED SAMPLE
AFTER 864 HOURS SALT SPRAY EXPOSURE
LOCALIZED DISCOLOURATION OF ZINC COATING

PLATE 3.20 30/7/2.99 MM ACSR/GZ 6 WIRE LAYER AGED AND TARRED SAMPLE AFTER 864 HOURS SALT SPRAY EXPOSURE CROSS SECTION SHOWING LOCALISED LOSS OF ZINC COATING

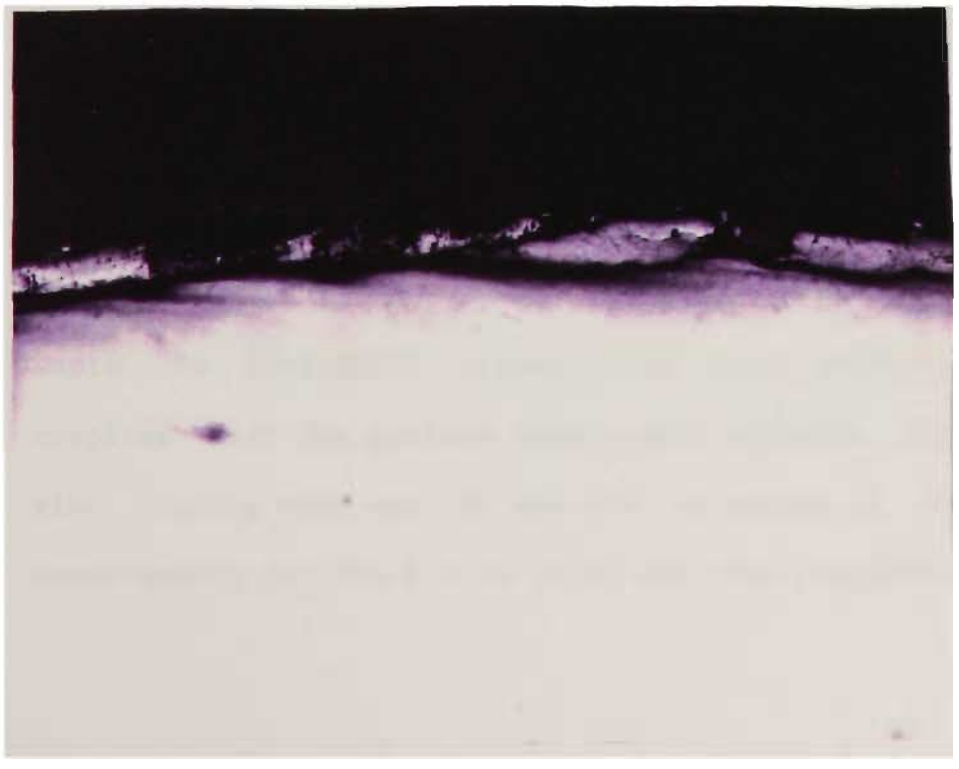

PLATE 3.21 30/7/3.00 MM ACSR/GZ 6 WIRE LAYER NEW AND GREASED SAMPLE AFTER 864 HOURS SALT SPRAY EXPOSURE CROSS SECTION SHOWING LOCALISED LOSS OF ZINC COATING

The detailed zinc coating mass and wrap test results of the wires that constitute the conductor samples from the Avon to Kemps Creek, Dapto to Springhill, Tomago to Taree and Bellambi to Heathcote transmission lines are given in Appendix 3. All wire samples except that of the Bellambi to Heathcote transmission line were taken from a suspension site.

The minimum requirement for the zinc coating mass given in AS C75.1 - 1963 is 240 $g.m^{-2}$ and 260 $g.m^{-2}$ for nominal diameter of coated wires in the range of 2.85 - 3.61 mm and 3.62 - 3.86 mm respectively. The minimum wrap test requirements is 6 wraps.

Regarding the test results for the,

1. Avon to Kemps Creek transmission line conductor sample complied with the minimum requirement criteria and the mean zinc coating mass was 50.2 and 51.1% in excess of the minimum requirements for the 6 wire layer and core respectively;

2. Dapto to Springhill transmission line conductor sample complied with the minimum requirement criteria and the mean zinc coating mass was 69 and 60% in excess of the minimum requirements for the 6 wire layer and core respectively;

3. Tomago to Taree transmission line conductor sample, five wires, four from the 6 wire layer and the core did not comply with the minimum zinc coating mass requirement. The mean zinc coating mass was 4 and 11% less than the minimum requirements for the 6 wire layer and core respectively. The minimum zinc coating mass was 14% less than the minimum requirement; and

4. Bellambi to Heathcote transmission line conductor sample complied with the minimum requirement criteria and the mean zinc coating mass was 15.3 and 37.5% in excess of the minimum requirements for the 6 wire layer and the core respectively.

3.4.2 Conductor Tests

The mechanical behavour of a conductor differs considerably from that of a wire because of the stranding factors of lay length, lay angle and diameter of lay. Individual wire tests on destranded conductors provide valuable information on the mechanical and electrical performance of the components of the conductor, however this information needs to be translated into an overall conductor performance.

In the past conductor data used to design transmission lines was generally theoretically determined and on some occassions confirmed by actual tests. In more recent times, as a result of supply authorities operating conductors at the excursions of the known electrical and mechanical parameters, a greater understanding of the overall conductor performance has been demanded.

In the case of aged transmission line conductors, actual conductor tests provide a complete picture of the continued serviceability of conductors. Several examples are discussed to show cause for the need of conductor tests.

Reviewing the wire breaking load test results, it is difficult to conclude the effect of an individual or several wires having low tensile strengths to the overall degradation of the strength of the conductor. In the past the breaking load of a conductor has been determined by in the case of an ACSR as 98% of the sum of the strengths of the aluminium wires plus 85% of the sum of

strength of the steel wires. The calculated breaking load may comply with the minimum criteria with many low strength wires offset with an equivalent number of high strength wires. In an actual breaking load test, the conductor may not reach the the calculated breaking load because of the premature failure of some of the low strength wires. In this case, clearly a breaking load test provides additional information on the overall performance of the conductor and the effects of low strength wires.

Furthermore, wire tests do not provide information on the permanent elongation of the conductor with regard to aged transmission line conductors. In other words has the aluminium wires permanently elongated over the steel in an ACSR construction to such to such an extent that aluminium wires no longer support their proportional share of the conductor stress.

Tests carried out on new or aged conductors are normally restricted to mechanical tests such as stress-strain, coefficient of linear expansion, creep, breaking load and lay length.

Testing equipment to determine actual DC and AC resistance is expensive, and some doubt is raised to the accuracy of such measurements. In addition it is questioned whether any degradation of the conductor can be assessed by the DC and AC resistance measurements. Consequently electrical tests on conductors were not carried as part of these studies.

Conductor samples used for the tests are approximately 14 m in length and terminated using special designed epoxy resin terminations. In preparation of the conductor for termination, the conductor is clamped at several locations at the test length end. The conductor is carefully destranded and the individual strands are cleaned to remove any dirt, grease and wire drawing lubricants. The conductor is then restranded and fitted with a steel sleeve. In the case of an ACSR construction, an additional steel sleeve compression fitting is applied to the steel core. The termination is completed by bonding the conductor to the steel sleeve using epoxy resin.

3.4.2.1 Stress Strain

The basic data of the mechanical properties of a conductor are obtained from a stress strain test in which a prepared conductor sample is subjected to an increasing axial load to 30% of the calculated breaking load after which the load is held constant for 30 minutes. The load is then gradually released until approximately 2% of the calculated breaking load is reached. The axial load is immediately reapplied gradually to the conductor sample until 50% of the calculated breaking load is reached and again the load is held constant for 30 minutes. The load is further gradually released until approximately 2% of the calculated breaking load is reached. The procedure is repeated a third time until 70% of the calculated breaking load is reached and the load is held constant for 1 hour. At the completion of this hold period the load is gradually released to zero.

In an ACSR construction the test procedure is repeated on a steel core sample to allow computation of the distribution of the loads in the steel core and aluminium.

The stress strain test is performed at ambient temperature and the conductor temperature differential over the gauge length is minimised by immersion of the conductor sample in a bath containing re-circulating oil. During the coarse of the test, measurements of conductor extension, conductor load and temperature are carried out.

Typical raw data plots for a composite 30/7/2.50 mm ACSR/GZ/1120 and a steel core 30/7/2.50 mm ACSR/GZ/1120 are given in Figures 3.15 and 3.16 respectively.

A zero correction of the raw data, to account for any wire slack or looseness in the wires during the sample preparation, is determined by choosing a line of best fit for the initial loading curve to 30% of the calculated breaking load. Linear regression is used to determine the line of best fit and the slope of the line for the composite and the weighted steel core is defined as E_{ci} and $^{m}E_{si}$, respectively. Using epoxy resin termination the zero correction is normally small and generally does not exceed 150 $mm.km^{-1}$. Aluminium compression fitting which if fitted to a short test length of conductor may extrude considerable aluminium into the test length and increase the slack component. For short test lengths aluminium compression fittings should not be used.

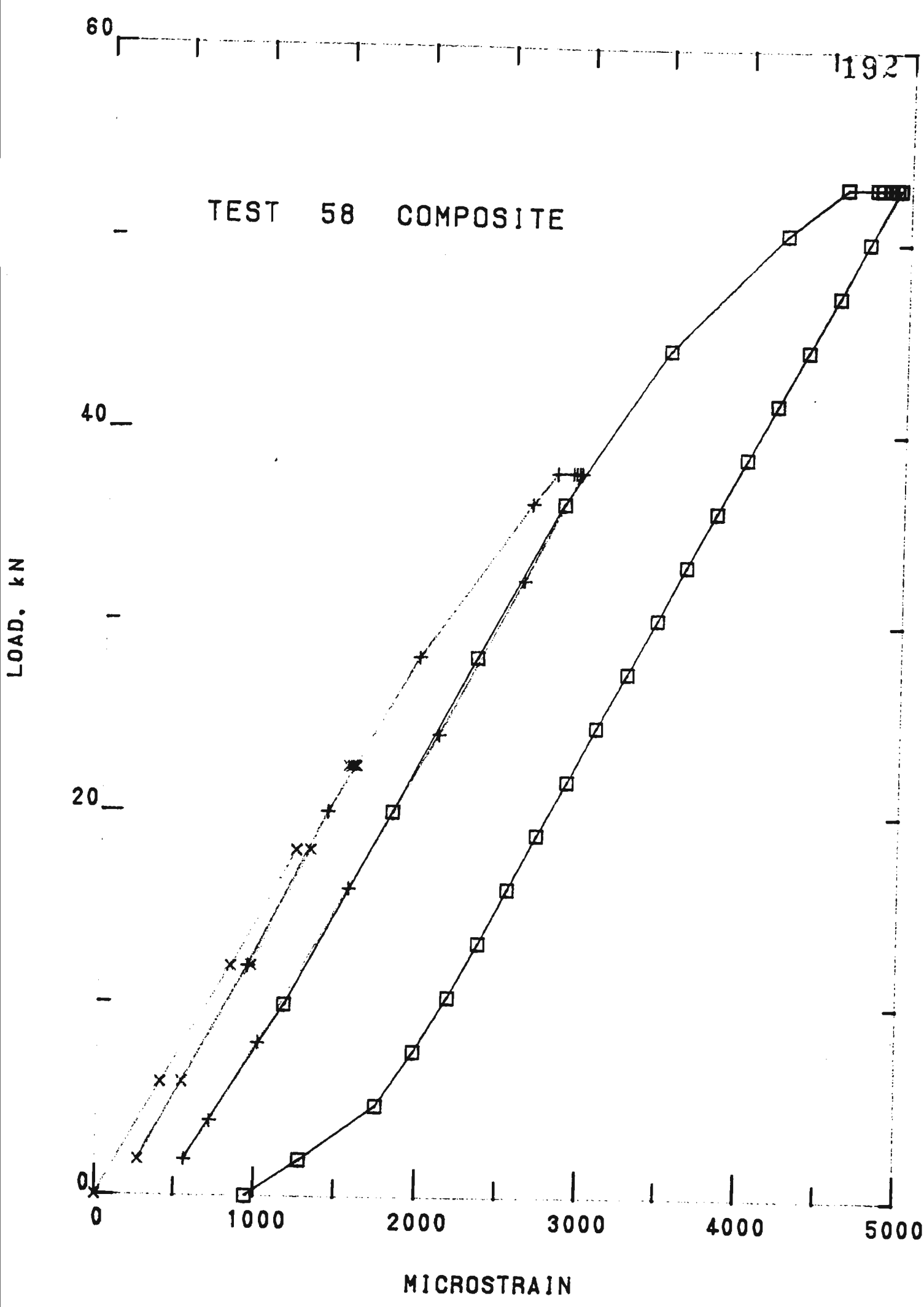

FIGURE 3.15 30/7/2.50 MM ACSR/GZ/1120
STRESS STRAIN TEST RESULT
RAW DATA PLOT

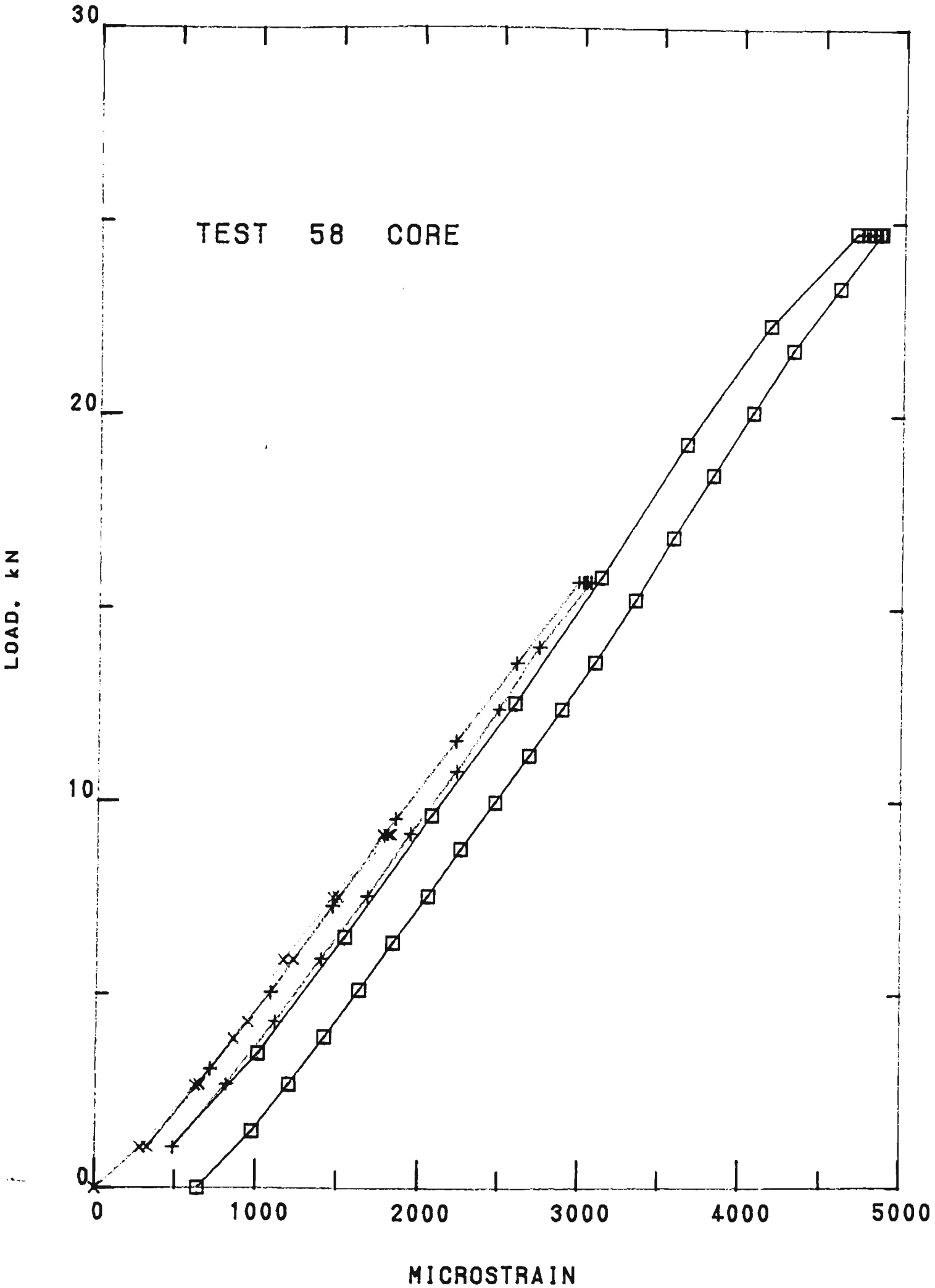

FIGURE 3.16 30/7/2.50 MM ACSR/GZ/1120
STRESS STRAIN TEST RESULT
RAW DATA PLOT

For zero corrected plots the initial 30% loading curve commence at the origin of zero load and zero elongation. All data points are corrected by the amount of the zero correction. Zero corrected plots are illustrated in Figure 3.17 and 3.18 for a composite 30/7/2.50 mm ACSR/GZ/1120 and a steel core 30/7/2.50 ACSR/GZ/1120 respectively. The zero correction is 7.06 and 95.8 $mm.km^{-1}$ respectively.

The master stress strain curves are derived from the zero corrected plots and for the 30/7/2.50 mm ACSR/GZ/1120 construction at the given test temperature are illustrated in Figure 3.19. The curves of three loops are, one for the composite construction, one for the steel core and a derived loop for the aluminium component. The ordinate of the composite loop is derived by dividing the load points by the total area of conductor. The ordinates of the aluminium and steel loops are weighted by the ratios of the respective areas to the composite areas, or mathematically A_a/A_c and A_s/A_c respectively.

The initial modulus curve of the composite construction is derived using a method of least squares applied to the three data points from the end of each hold period. The least squares solution provides an nth order polynominal equations given as,

$$\mu\varepsilon = A_0 + A_1S + A_2S^2 + A_3S^3 + A_4S^4 + ... \text{ etc} \qquad (3.1)$$

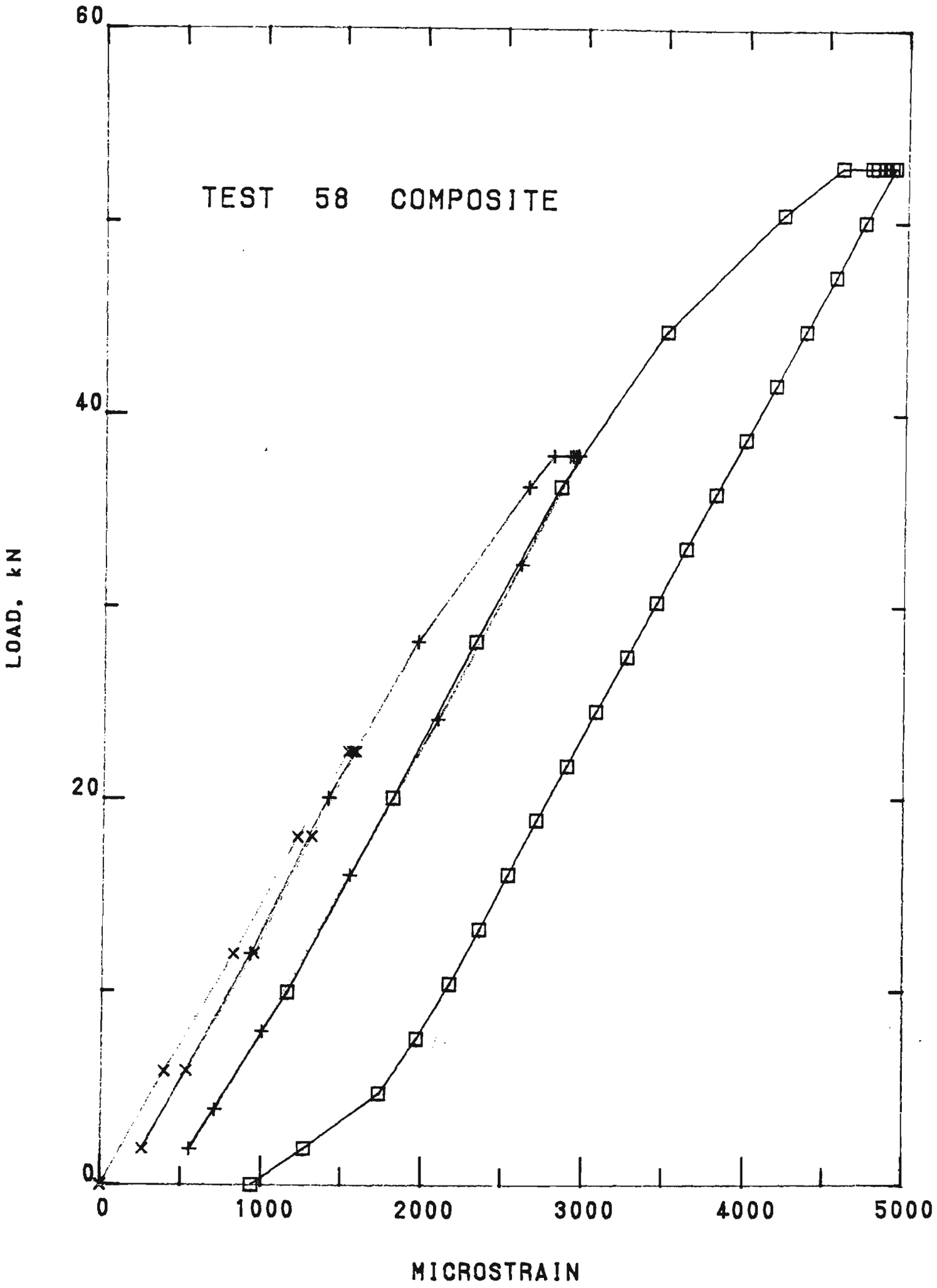

FIGURE 3.17 30/7/2.50 MM ACSR/GZ/1120
STRESS STRAIN TEST RESULT
ZERO CORRECTED PLOT

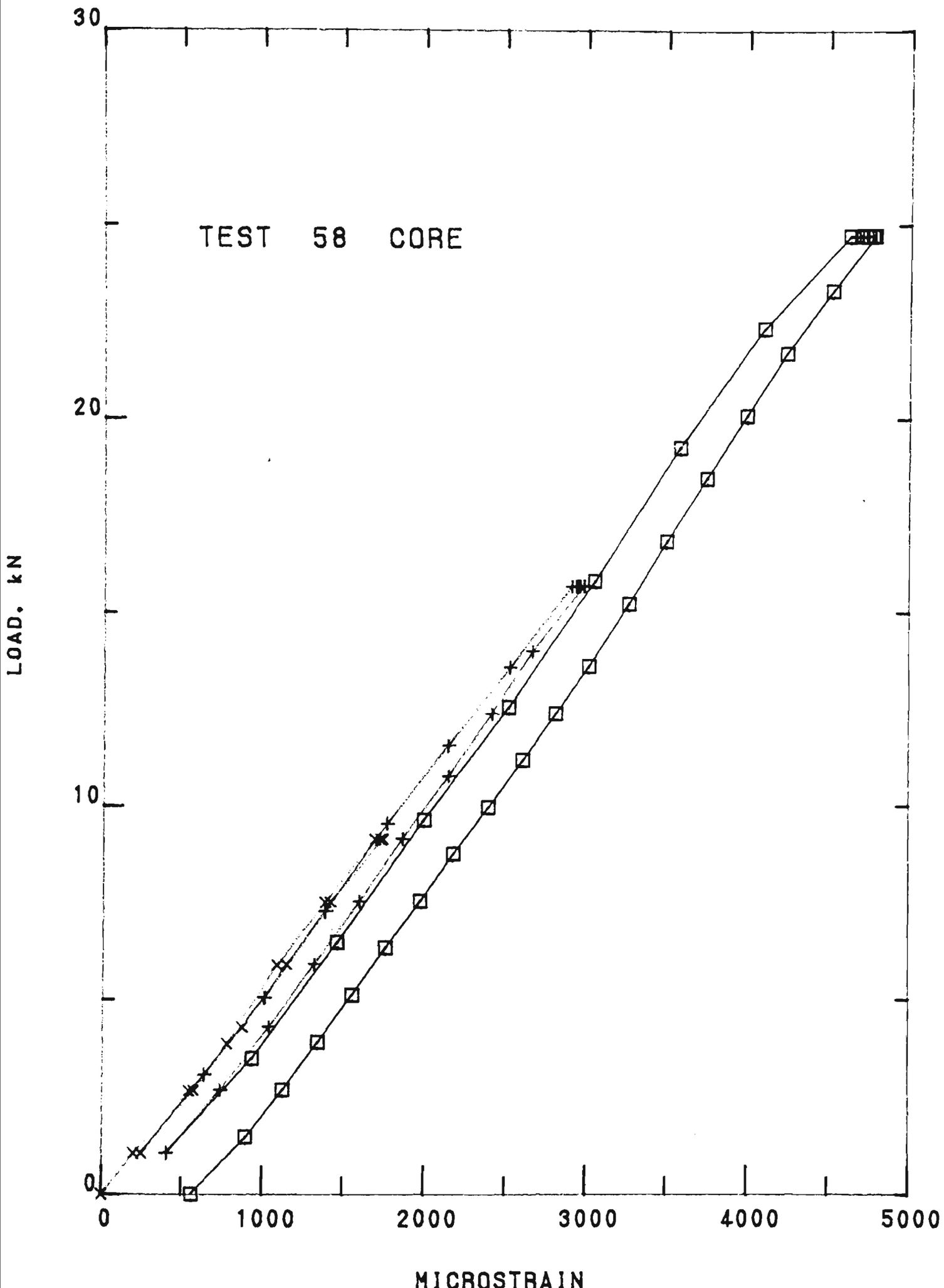

FIGURE 3.18 30/7/2.50 MM ACSR/GZ/1120
STRESS STRAIN TEST RESULT
ZERO CORRECTED PLOT

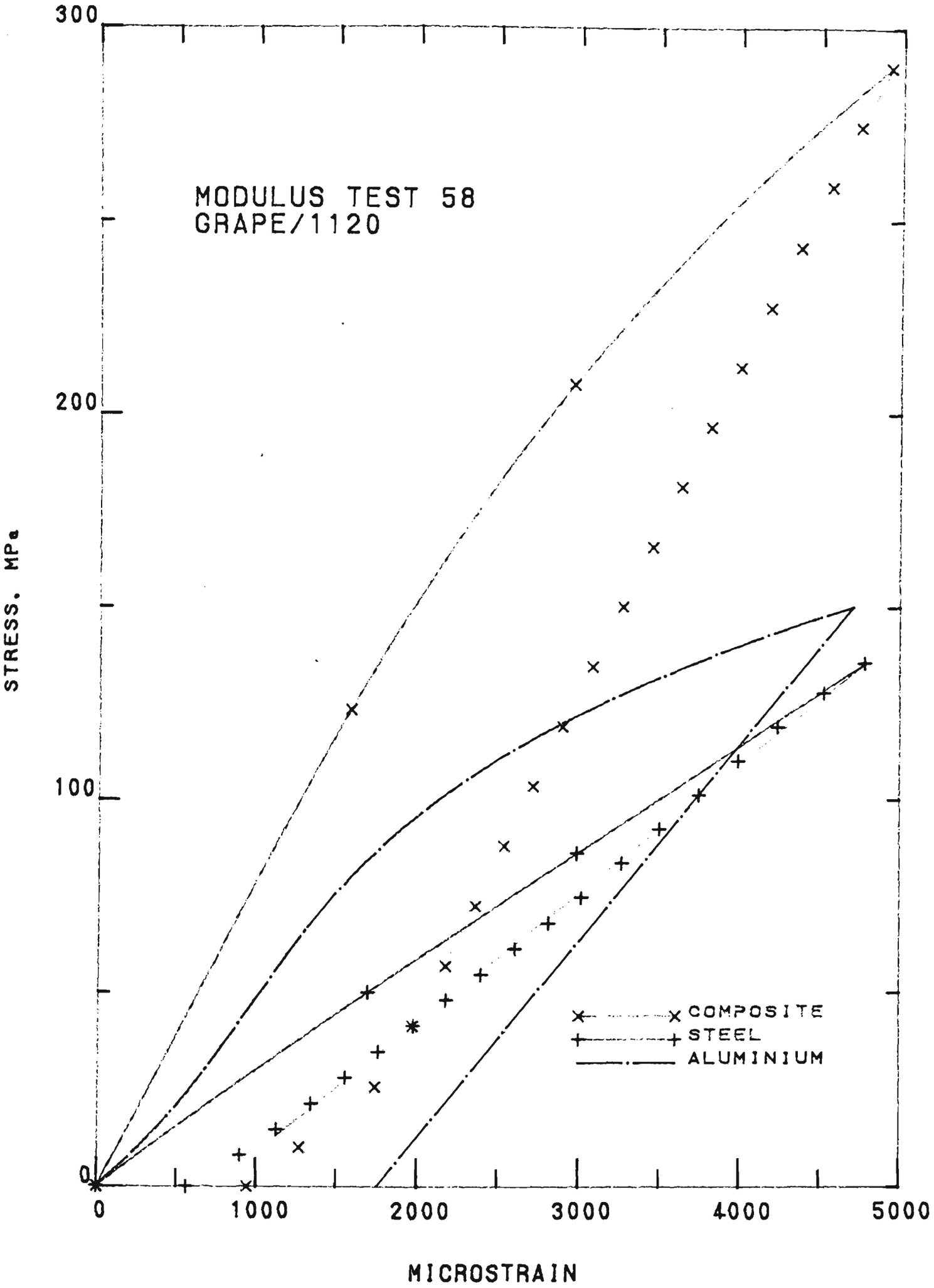

FIGURE 3.19 30/7/2.50 MM ACSR/GZ/1120
STRESS STRAIN TEST RESULT
MASTER STRESS STRAIN CURVES

A_o is general very small and can be ignored. Usually a 3rd order polynominal describes the data adequately, however in some cases other orders may be more appropriate. Similar polynominals are derived for the initial curves of the steel core and the aluminium.

The final modulus of the conductor is the slope of the regression line fitted to unloading curve from the final hold point at 70% of calculated breaking load to the slope transition point. The slope of the composite final modulus is designated E_{cf}. The slope of the final modulus for the aluminium curve may be expressed in terms of material modulus, E_{af} or the reduced final modular mE_{af}. Similarly, the slope of the final modulus for the steel curve may be expressed in terms of material modulus, E_{sf} or the reduced final modulus, mE_{sf}.

In the past the final modulus of elasticity of the composite conductor has been theoretically determined knowing the weighted ratios of the aluminium and steel components to the composite conductor and the material modulus of aluminium and steel. Considering a change in elongation from $x = x_1$ to $x = x_2$ where x_1 and x_2 are both greater than the transition microstrain (i.e. the linear part of the final curves) and at constant temperature the change in stress is given as,

$$S_s = mE_s (x_2 - x_1) \qquad (3.2)$$

$$S_a = nE_a (x_2 - x_1) \qquad (3.3)$$

$$S_c = E_{cf} (x_2 - x_1) \qquad (3.4)$$

The total stress change is given as,

$$\Delta S_c = \Delta S_a + \Delta S_s \tag{3.5}$$

By substitution of equations (3.2) to (3.4) into (3.5) and the values of m and n then,

$$E_{cf} = \frac{A_a}{A_c} E_a + \frac{A_s}{A_c} E_s$$

or the composite modulus is theoretically determined by,

$$E_{cf} = \frac{A_a E_a + A_s E_s}{A_c} \tag{3.6}$$

The final modulus of elasticity equation of a composite conductor may also be derived by considering a length of conductor clamped firmly at each end so that no slip occurs between the two dissimilar materials. Thus the strain will be the same for the two dissimilar materials. If the conductor is of ACSR construction having no initial condition tension and a force is applied to the conductor then,

$$F = S_s A_s + S_a A_a \tag{3.7}$$

The average stress is given as,

$$S_{av} = \frac{F}{A_s + A_a} \tag{3.8}$$

and the strain is given as,

$$\varepsilon = \frac{S_s}{E_s} = \frac{S_a}{E_a} \tag{3.9}$$

The modulus of elasticity of the composite construction is defined as,

$$E_{cf} = F\varepsilon \tag{3.10}$$

and by substitution of equations (3.7), (3.8) and (3.9) into (3.10)

$$E_{cf} = \frac{A_a E_a + A_s E_s}{A_c} \tag{3.11}$$

Equation (3.11) is identical to that of equation (3.6). In both these derivations the critical factor is that of the slope of the final modulus curves (i.e. mEs and nEa), the assumption that no slip occurs between the dissimilar materials and the wires are straight.

In more recent times Nigol and Barrett (62) discovered that the stress and strains in a helically stranded aluminium wires of a conductor were not the same as those of the individual straight wires. By examining the wire geometry of a helically stranded wire, Nigol and Barrett derived an equation for the conductor strain ε related to the wire ε_L and to the change of layer radius R by,

$$\varepsilon = \frac{1}{\lambda}\left[\frac{\partial\lambda}{\partial L}\Delta L + \frac{\partial\lambda}{\partial R}\Delta R\right]$$

$$= \frac{1}{\cos^2\sigma}\varepsilon_1 - \tan^2\sigma\frac{\Delta R}{R} \qquad (3.12)$$

Equation (3.12) consists of two parts, the thermal, elastic and plastic strain and the axial elongation of the layer as a result of a decreasing layer radius. By substitution of the uniaxial stress equation into equation (3.12) the true modulus of the wire material the layer modulus in the axial direction was derived and is given as,

$$\frac{1}{E_{axial}} = \frac{1}{E_x} = \frac{1}{\cos^3\sigma}E_w + \frac{\tan^2\sigma}{R}\left[\frac{-\Delta R}{S}\right] \qquad (3.13)$$

Thus the total layer modulus in the axial direction was defined as,

$$\frac{1}{E_N} = \frac{1}{E_{helical}} + \frac{1}{E_{radial}} \tag{3.14}$$

where,

$$E_{helical} = E_w \cos^3\theta_n \tag{3.15}$$

$$E_{radial} = \frac{R_n}{\tan^2\sigma_n}\left[\frac{S_n}{-\Delta R_n}\right] \tag{3.16}$$

In terms of the layer i and the material j, the lay angle is given as,

$$\tan\sigma_i = \frac{2\pi r_i}{L_i D_i} \tag{3.17}$$

the wire layer modulus of elasticity is given as,

$$E_{ij} = E_{wij} \cos^3\theta_i \tag{3.18}$$

and the composite modulus is given as,

$$E_{cf} = \frac{1}{A_c}\left[E_s A_s + \sum_{j=1}^{N_i}\left[\sum_{i=1}^{n}\left(n_{ij} A_{ij} E_{ij}\right)\right]\right] \tag{3.19}$$

Equations (3.17), (3.18) and (3.19) have been recently adopted by Australian Standards for inclusion into revision of AS1220 - 1973(7).

The next item of interest in the master stress strain curve of an ACSR construction is the critical tension/stress load defined as the point of the final modulus composite conductor curve where the slope of the curve changes from E_{cf} to that of mE_{sf}. In other words, the point where the aluminium because of permanent elongation does not support its share of the total conductor stresses during further unloading. The critical tension/stress load is determined by linear regression of the data points above the transition point and linear regression of data points below the transition point. Data points immediately adjacent the transition are discounted. From the linear regression equations the intercept of critical tension/stress and strain are determined.

Of particular interest is the change in the critical tension/stress load with a change in temperature. Jordon (54) derived a linear equation that related in increasing critical tension/stress with an increasing temperature and is given by,

$$S_{kt} = S_{co} - \frac{E_{cf}}{nE_a} S_{ao} + mE_s\alpha_s\Delta T \qquad (3.20)$$

This deviation is based on the final modulus of elasticity previously derived and given in equations (3.6) and (3.11). Figure 3.20 illustrates the linear relationship of transition tension and conductor temperature for a 54/7/3.53 + 1/3.71 mm ACSR/GZ construction. Everyday tension for this conductor is approximately 32 kN. As the conductor temperature increases for a given span length the tension will decrease as determined by

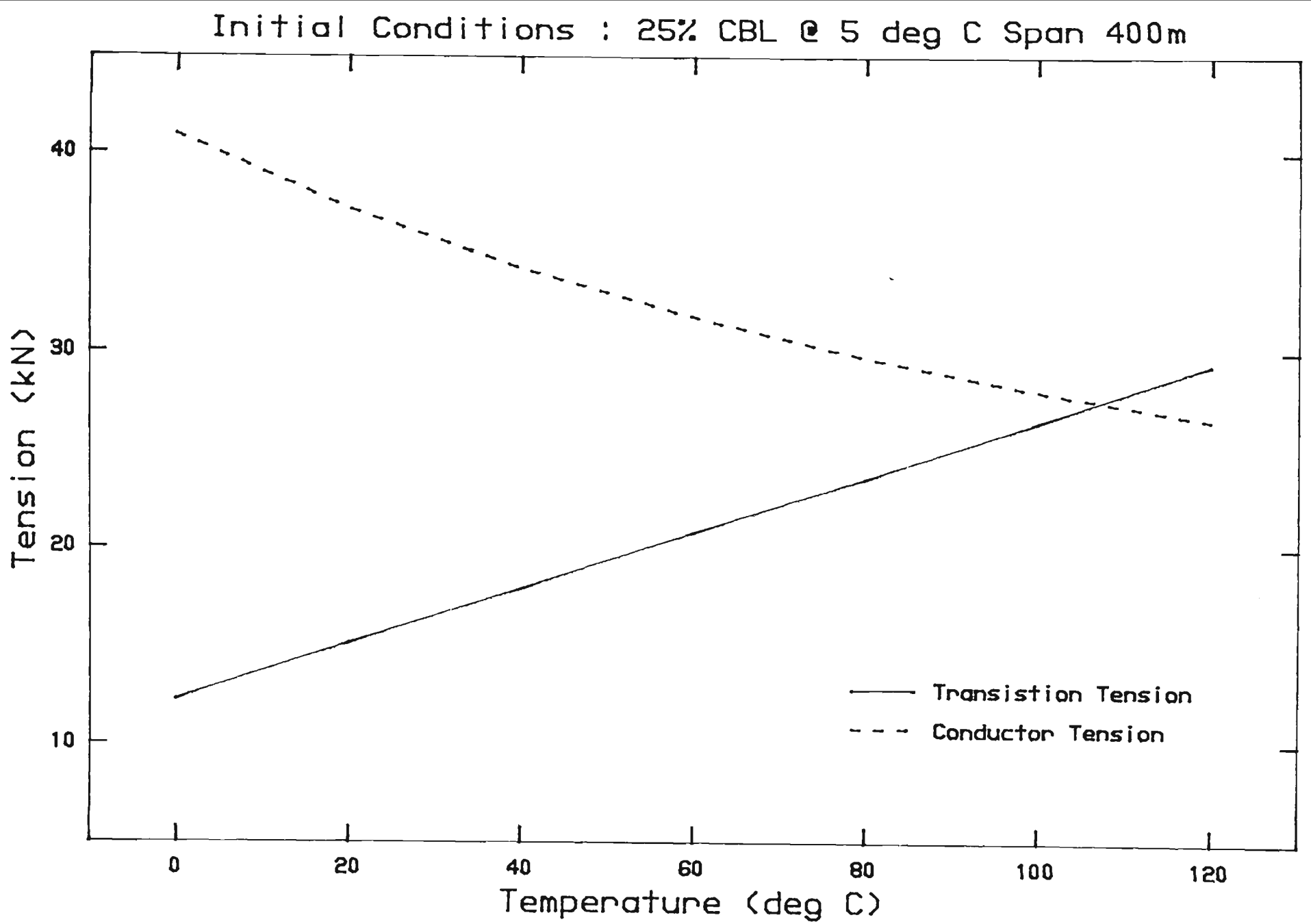

FIGURE 3.20 54/6/3.53 + 1/3.71 ACSR/GZ
Transition Tension and Conductor Tension Change
With Change in Temperature

equations given in Figures 2.5 or 2.6. This change in conductor tension with temperature is illustrated in Figure 3.20. An interesting phenomena occurs when the two curves intersect at 107°C. This phenomena was reported by Nigol Barrett (62) known as the birdcaging temperature is, when above this temperature the conductor expands at the rate of the steel core. With increasing tensions the birdcaging temperature will increase because additional thermal expansion is required in the aluminium before the load is transferred wholly to the steel core. Nigol and Barrett (62) derived an equation for the birdcaging stress and is given as,

$$S_b = \frac{mE_sE_a}{E_{cf}} \left[\frac{S_{co}}{mS_{so}} - (\alpha_a - \alpha_s)\Delta T - (C_a - C_s) \right] \quad (3.21)$$

The last item of interest of the master stress strain curve is the ability to determine the coefficient of linear expansion of the steel core in an ACSR construction. The equation was derived by Jordon (54) and is given by,

$$\alpha_s = \alpha_{cf} \frac{E_{cf}}{E_{cf} + nE_a} \quad (3.22)$$

The detailed conductor stress strain test results and data for the samples from the Avon to Kemps Creek, Dapto to Springhill and Tomago to Taree transmission lines are given in Appendix 3. A summary of the findings of the stress strain tests are given in Tables 3.11 and 3.12 respectively.

Modulus of Elasticity (GPa)		Avon-Kemps Creek Test No. 62	Dapto-Springhill Test No. 61	Tomago-Taree Test No. 52	Tomago-Taree Test No. 53
E_{cf}	ASC75-1963	82.6	82.6	91.8	91.8
	Equation (3.6)	82.6	82.7	91.6	91.6
	Equation (3.19)	77.2	77.0	88.6	88.6
	Test Result	81.0	81.5	77.9	80.0
nE_{af}		52.1	51.3	42.9	39.8
E_{af}	Test Result	59.0	58.0	52.9	49.1
	ASC75-1963	68.0	68.0	68.0	68.0
mE_{sf}		22.2	22.2	36.1	36.1
E_{sf}	Test Result	190	190	191	191
	ACS75-1963	193	193	193	193

TABLE 3.11 - SUMMARY OF CONDUCTOR TEST RESULTS MODULUS OF ELASTICITY

Initial Modulus Curve Polynominal Coefficient		Avon-Kemps Creek Test No. 62	Dapto-Springhill Test No. 61	Tomago-Taree Test No. 52	Tomago-Taree Test No. 53
Composite	A_1	0.161×10^{-4}	0.180×10^{-4}	0.224×10^{-4}	0.232×10^{-4}
	A_2	-0.564×10^{-7}	-0.689×10^{-7}	-0.789×10^{-7}	-0.819×10^{-7}
	A_3	0.384×10^{-9}	0.395×10^{-9}	0.274×10^{-9}	0.294×10^{-9}
Steel	A_1	0.524×10^{-4}	0.489×10^{-4}	0.391×10^{-4}	0.315×10^{-4}
	A_2	-0.265×10^{-6}	-0.198×10^{-6}	-0.196×10^{-6}	-0.115×10^{-6}
	A_3	0.250×10^{-8}	0.244×10^{-8}	0.998×10^{-9}	0.727×10^{-9}
Aluminium	A_1	0.302×10^{-6}	0.317×10^{-4}	0.558×10^{-4}	0.810×10^{-4}
	A_2	-0.420×10^{-6}	0.345×10^{-6}	-0.689×10^{-6}	-0.118×10^{-5}
	A_3	0.390×10^{-8}	0.302×10^{-8}	0.652×10^{-8}	0.110×10^{-7}
Critical Point					
Tension (kN)		19.6	15.4	18.1	19.2
Strain (mm/km)		1430	1480	2500	2570
% CBL		12.3	9.6	20.1	21.3

TABLE 3.12 - SUMMARY OF CONDUCTOR TEST RESULTS STRESS STRAIN

The final composite modulus of elasticity for the conductor samples from the Avon to Kemps Creek and Dapto to Springhill transmission lines is in good agreement with that of AS C75 1963 and equations (3.6) and (3.19). The Tomago to Taree transmission line conductor samples test results, suggests a change of an instrinsic property of modulus of the conductor. Unfortunately when the conductor sample was removed from service no precautions were taken to prevent relative wire movements. This wire movement is confirmed by the critical tension/stress as a percentage of calculated breaking load being as high as 20%. Accordingly it is hypothesised that the instrinic property of modulus has not changed however the lay of the wires and the relative position to each other has changed causing a significant change in the final modulus of the composite conductor. This is also supported by the significant difference in the final modulus of the aluminium and to a lesser extent the final modulus of the steel.

3.4.2.2 Coefficient of Linear Expansion

The coefficient of linear expansion properties of a conductor are obtained from a thermal test in which a prepared conductor sample is heated and during the course of the test, measurements of conductor extension as a function of temperature are carried out for a constant load.

To remove varience in extension due to conductor settlement or initial metallurgical creep the conductor sample is preconditioned by performing a stress strain test or holding the sample at 70% calculated breaking load for one hour prior to the thermal test.

To minimise the effects of high temperature creep, the constant load of 20% calculated breaking load is only applied at the instant of the measurement of extension.

The conductor sample is heated in a recirculating oil bath and measurements of extension are taken at approximately $10^{o}C$ intervals to $100^{o}C$. At each temperature interval the differential temperature over the gauge length is minimised by allowing an approximate 10 minute stabilising period before measurements are taken.

After the conductor sample reaches $100^{o}C$ the temperature is allowed to cool to room temperature. Additional extension measurements are taken at approximately $15^{o}C$ intervals during the cooling period. In the early stages of the cooling cycle stabilised heating periods may be necessary to ensure a minimum temperature differential over the gauge length.

The gauge length of the conductor sample is approximately 10 m in length and the conductor temperature is measured by means of thermocouples attached to the conductor sample within the gauge length every 1.5 m.

The constant load of 20% calculated breaking load is chosen such that in an ACSR construction the conductor load will be in excess of the critical tension/stress and thermal elongation will be that of the composite construction and not of the steel component.

Typical raw data plots for an all aluminium construction 7/4.75 mm AAC is given in Figure 3.21. Linear regression is used to determine the line of best fit and the slope of the line is defined as the coefficient of linear expansion.

In the past the coefficient of linear expansion of a composite conductor has been determined knowing the weighted ratios of the aluminium and steel components, the moduli of aluminium and steel components and the coefficient of linear expansion of the aluminium and steel components. An expression for the coefficient of linear expansion of a composite conductor may be derived, if we consider for a temperature change of ΔT which in effect is a change of elongation providing the initial and final elongation is greater than critical strain then the change in the steel stress is given as,

$$\Delta S_s = mE_s\alpha_s\Delta T \qquad (3.23)$$

and the change in aluminium stress is given as,

$$\Delta S_a = nE_a\alpha_a\Delta T \qquad (3.24)$$

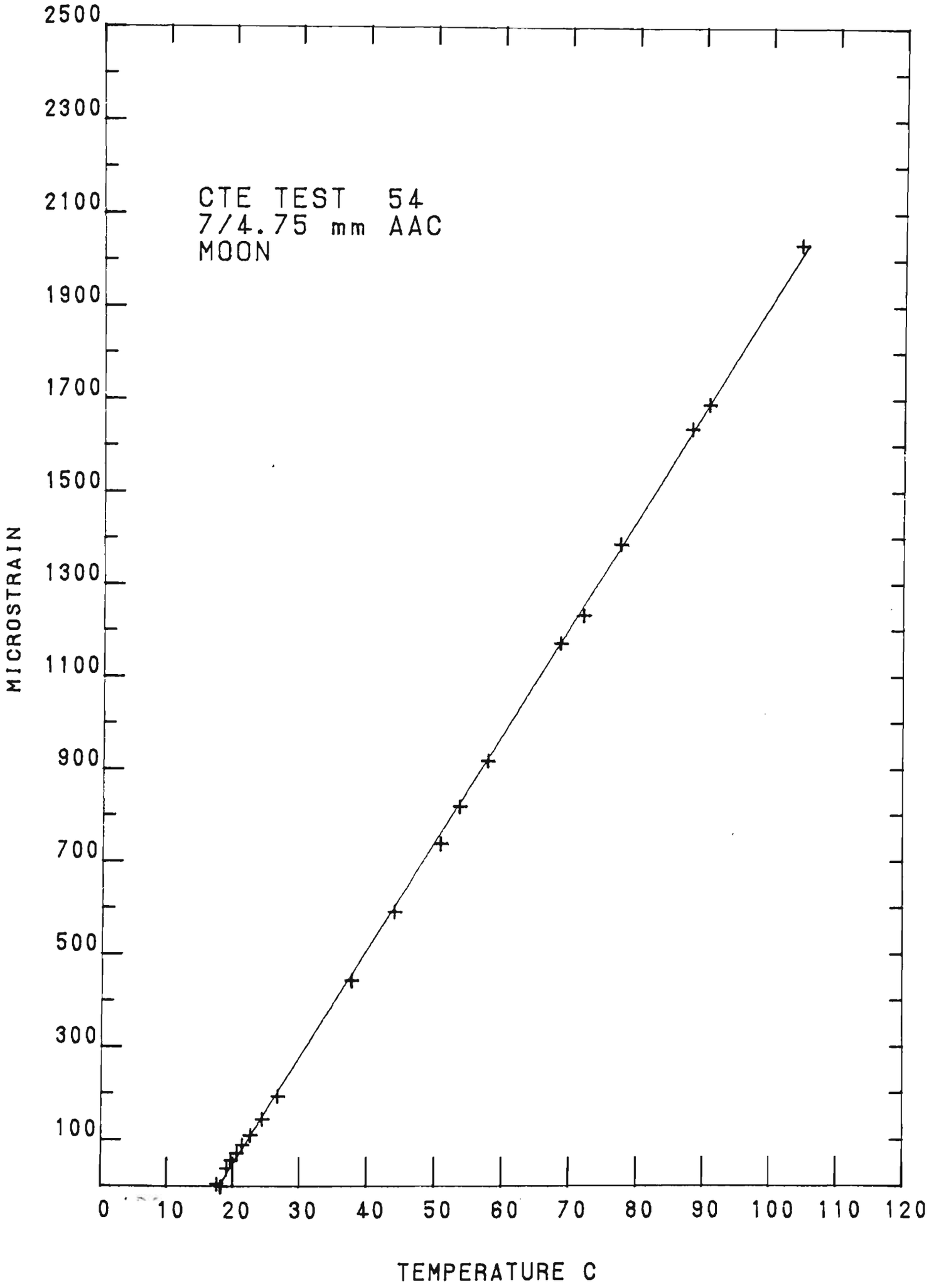

FIG. 3.21 7/4.75 MM AAC
COEFFICIENT OF LINEAR EXPANSION
TEST RESULTS
RAW DATA AND LINEAR REGRESSION PLOT

The change in the composite stress is given as,

$$\Delta S_c = mE_{cf}\alpha_{cf}\Delta T \tag{3.25}$$

By substitution of equations (3.23), (3.24) and (3.25) into equation (3.5) and the values of m and n,

$$E_{cf}\alpha_{cf}\Delta T = mE_s\alpha_s\Delta T + nE_a\alpha_a\Delta T \tag{3.26}$$

$$E_{cf}\alpha_{cf} = \frac{A_s}{A_c} E_s\alpha_s + \frac{A_a}{A_c} E_a\alpha_a \tag{3.27}$$

$$\alpha_{cf} = \frac{A_sE_s\alpha_s + A_aE_a\alpha_a}{A_cE_{cf}} \tag{3.28}$$

By substitution of equation (3.6) into (3.28), the composite coefficient of linear expansion is given as,

$$\alpha_{cf} = \frac{A_sE_s\alpha_s + A_aE_a\alpha_a}{A_sE_s + A_aE_a} \tag{3.29}$$

Equation (3.29) does not account of the wire geometry of a helical stranded conductor and will always over estimate the coefficient of linear expansion. By examination of the wire geometry of Figure 3.22 an increase in temperature will cause an increase in wire length of ΔL, resulting in an increase in lay length. The lay length change in terms of the lay angle is given as,

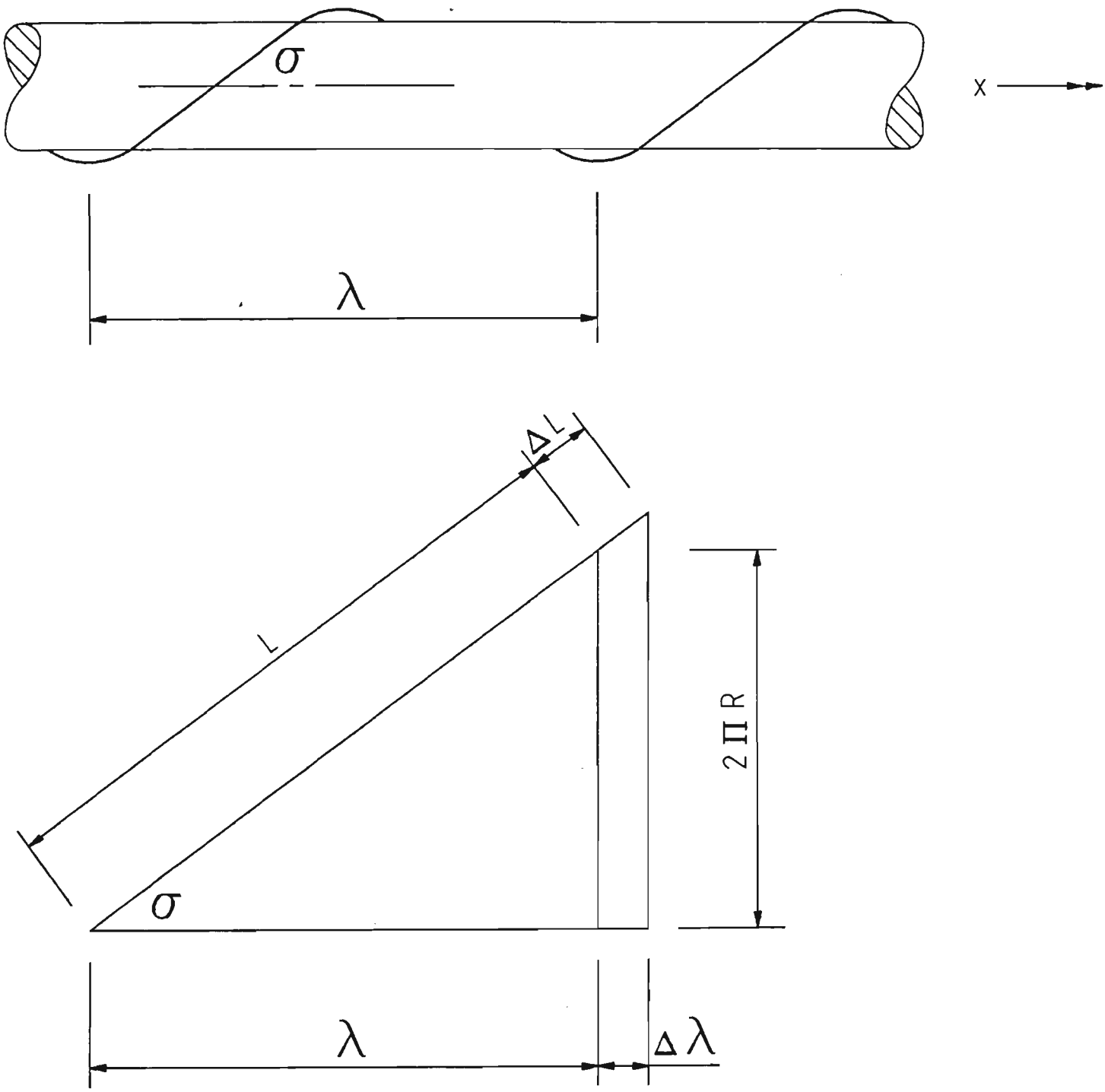

FIGURE 3.22 WIRE GEOMETRY IN A HELICALLY-STRANDED CONDUCTOR

$$\Delta\lambda = \frac{\alpha\Delta T\lambda}{1} = \alpha\Delta T \cos\sigma$$

$$= \alpha\Delta T \cos\left[\tan^{-1}\frac{2\pi R}{\lambda}\right] \qquad (3.30)$$

Using the layer and material notation, equation (3.30) may be written as,

$$\alpha_{ij}' = \alpha_j \cos\left[\tan^{-1}\frac{2\pi R}{L_i D_i}\right] \qquad (3.31)$$

The stress in the centre wire for a temperature change of ΔT is given as,

$$\Delta S_s = \frac{A_s}{A_c} E_s \alpha_s \Delta T \qquad (3.32)$$

and the stress in successive layers i is given as,

$$\Delta S_i = \frac{A_{ij}}{A_c} E_{ij} \alpha_{ij}' \Delta T \qquad (3.33)$$

By substituting equations (3.32), (3.33) and (3.25) into equation (3.5),

$$E_{cf} A_c \alpha_{cf} \Delta T = E_s A_s \alpha_s \Delta T + E_{ij} A_{ij} \alpha_{ij}' \Delta T \qquad (3.34)$$

and summating for all materials j and layers i, the final composite construction coefficient of thermal expansion is given as,

$$\alpha_{cf} = \frac{1}{E_{cf}A}\left[E_s A_s \alpha_s + \sum_{j=1}^{N_i}\left[\sum_{i=1}^{n}(n_{ij}A_{ij}\alpha_{ij}')\right]\right] \quad (3.35)$$

The detailed coefficient of thermal expansion conductor test results and data for the samples from the Avon to Kemps Creek, Dapto to Springhill and Tomago to Taree transmission lines are given in Appendix 3. A summary of the findings of the coefficient of thermal expansion tests are given in Table 3.13.

The coefficient of linear expansion for the conductor samples from the Avon to Kemps Creek and Dapto to Springhill transmission lines is in good agreement with that of AS C75 1963 and equations (3.29) and (3.33). The Tomago to Taree transmission line conductor sample test number 43 and 44 supports the findings of the stress strain test results.

Test Number	Avon-Kemps Creek	Dapto-Springhill 50	Tomago-Taree 43	Tomago-Taree 44
Test Load				
Tension	31.9	31.9	18.0	36.0
% CBL	20	20	20	40
Coefficient of Linear Expansion $1^{o}C$				
Equation (3.29)	19.86×10^{-6}	19.86×10^{-6}	18.42×10^{-6}	18.42×10^{-6}
Equation (3.33)	19.22×10^{-6}	19.21×10^{-6}	18.06×10^{-6}	18.06×10^{-6}
Test Results	18.31×10^{-6}	18.27×10^{-6}	12.58×10^{-6}	18.45×10^{-6}

TABLE 3.13 - SUMMARY OF CONDUCTOR TEST RESULTS COEFFICIENT OF LINEAR EXPANSION

3.4.2.3 Creep

Conductor creep has been previously defined as non recoverable or inelastic plastic deformation sometimes termed permanent elongation, that occurs under tensile load and increases with both temperature and stress. Permanent elongation begins at the instant of applied axial tensile load and continues at a decreasing rate providing tension and temperature remain constant.

Conductor creep data has, in the past generally been determined from CIGRE (27) empirical equations and constants, however in more recent times conductor creep testing facilities have become available to supply authorities in Australia. Accordingly, more accurate predictions of permanent elongation of conductors and determination of inelastic stretch allowances are now possible for conductor constructions manufactured in Australia.

Two regimes of metallurgical creep exist, low temperature and high temperatures for temperatures greater than 0.4 of the material melting point. Schematic representation of these regimes for typical strain time creep curves is given in Figure 3.23.

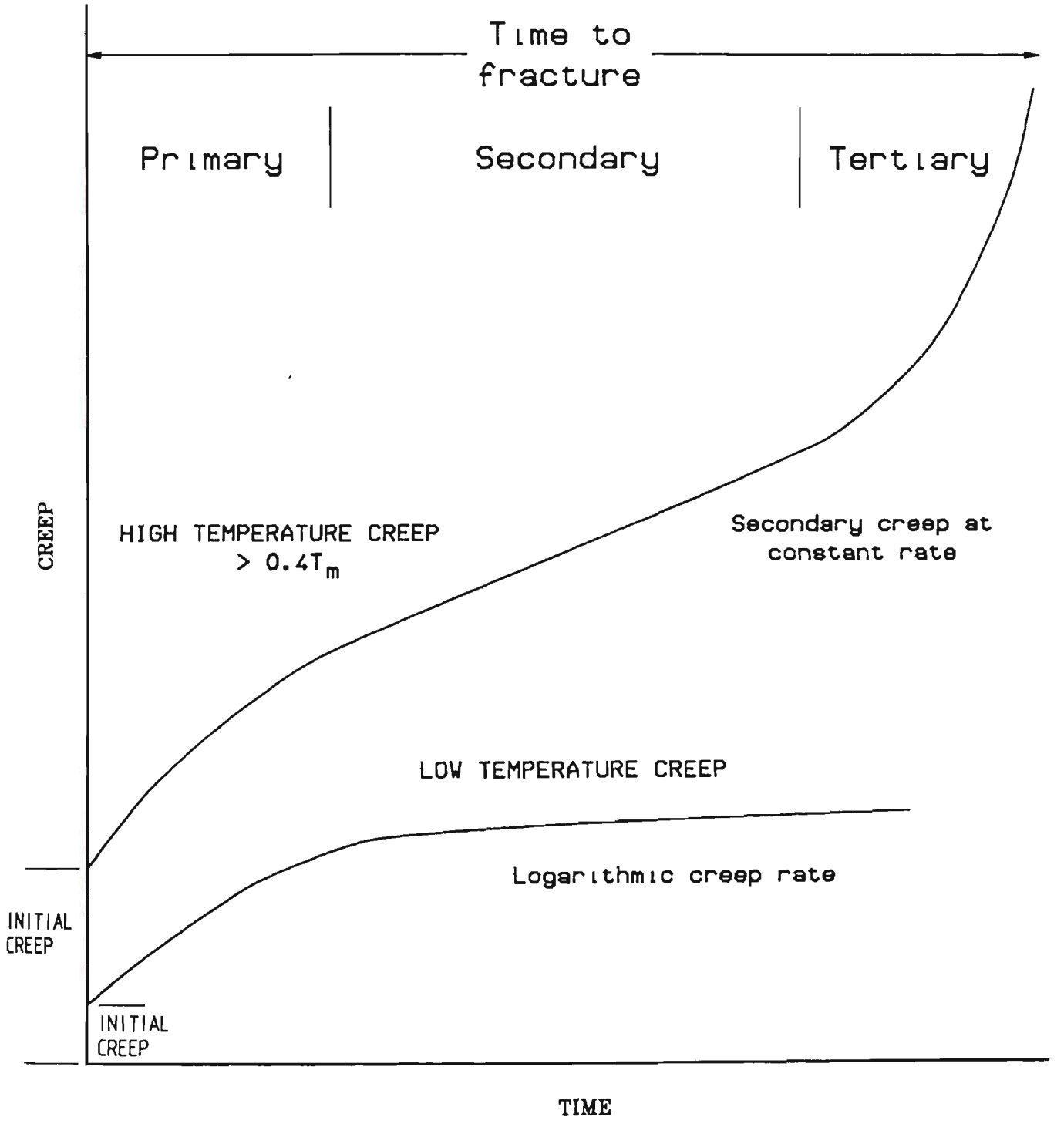

FIG. 3.23 LOW AND HIGH TEMPERATURE CREEP

To delineate between both creep curves, the melting point of the most commonly used aluminium and aluminium alloys is given in Table 3.14. The maximum design temperatures typically used by supply authorities are 323, 358 and 393°K, 50, 85 and 120°C respectively. The majority of these temperatures fall in or close to the logarithmic creep regime, consequently long term creep rupture is highly unlikely.

Conductor creep is attributed to geometric settling of the wires moving both radially and tangentially and initial metallurgical creep during the initial loading period. The creep strain as a function of time, stress and temperature is described by the logarithmic equation is given as,

$$\mu\varepsilon = A_2 \, t^{n_1} \, S^{n_2} \, e^{n_3 (T-21.4)} \qquad (3.36)$$

where the parameters A_2, n_1, n_2 and n_3 define the creep behaviour of the conductor and are determined by test. The constant n_3 is determined from a high temperature creep test.

Interestingly, an analysis of the creep data for all the tests performed for these studies from 500 hrs results in a better correlation coefficient determined by regression analysis for a linear equation than the logarithmic equation. In other words the linear equation predicts a better line of best fit of the

Aluminium	Melting Temperature T_m ^oK	0.4 T_m ^oK
1350	917	367
1120	917	367
6201	887	355

TABLE 3.14 - ALUMINIUM AND ALUMINIUM ALLOY MELTING TEMPERATURES

test data than the logarithmic equation. Accordingly, it could easily be hypotherized that the conductors are in a secondary stage of creep.

To put this into perspective, creep predicted for the Moose ACSR/GZ conductor test results given in Appendix 3 by the logarithmic and linear equations is 254 and 1553 $mm.km^{-1}$ respectively for a load of 20% CBL after 10 years. Translated into conductor sag for a 400 m span at $120^{o}C$, this creep difference is equivalent to a sag of 2.53 m.

The sag tension results presented in Chapter Two would not support such a large departure in sag measurements unless a significant amount of prestressing of the conductor had occurred at installation.

These arguments aside, the discussions depicts the difficulties of designing for long times based on the predication of mathematical models. A further constraint is introduced when one considers the wide deversity of service conditions and the need for material properties of conductors after long and varying service histories. It is these service histories that are difficult to duplicate under laboratory conditions to obtain adequate design data. The empirical models do permit interpolation in the regions bounded by the experimental data, however extrapolation to predict conductor creep behaviour beyond measured data is considered hazardous.

CIGRE (27) suggest that the conductor creep test duration should be a minimum 2000 hour. Using creep data from such tests and considering a transmission line service life of 30 years, extrapolation of the logarithmic data 1.65 times is required. Extrapolation with confidence in these circumstances is thought to be reasonably reliable particularly when one considers the confidence limits of the test data.

Little work has been carried out in the area of long term conductor creep measurements to confirm the use of the traditional logarithmic equation to predict creep behaviour. Nakayima and Kojima (61) performed a series of field measurements of the creep of overhead line conductors on a test line and the results were correlated with those of laboratory creep tests. The duration of the field test was 4 1/2 years annd the laborating tests was 1000 hours. Whilst the predicted results

> "are quite similar in terms of the order after a lapse of 10^4 to 10^5 hours,"

no regression analysis was reported to establish which mathematical model best describes the test results.

The methods presented in Chapter Two of these studies do provide a method to measure conductor creep for "in service" transmission lines. A monitoring program, not unlike that for dam wall movements, can now be readily carried out in the future that would confirm long term conductor creep behaviour.

The basic data of the creep properties of a conductor test is obtained in an elongation test in which a prepared conductor sample is subjected to a constant axial load for the given duration of the test. The duration of the test is usually 2000 hours. Three conductor samples are normally tested simultaneously with axial loads of 20, 30 and 40% of calculated breaking load.

The creep tests are performed at a constant temperature and the conductor temperature differential over the gauge length is minimised by providing circulating cooled air. In the case of high temperature creep, test a recirculating oil bath is used as the heating medium, but one must question the validity of such test results, given the possible temperature differentials and subsequent wire stress variations likely to occur if heating was via an electrical source. No high temperature creep tests were carried out as part of these studies.

During the course of the creep tests, measurements of conductor extension conductor load and temperature are carried out.

Typical raw data linear linear plots and raw data log log plots with regression lines are given in Figures 3.24 and 3.25 respectively for Moon AAC 7/4.75 mm construction.

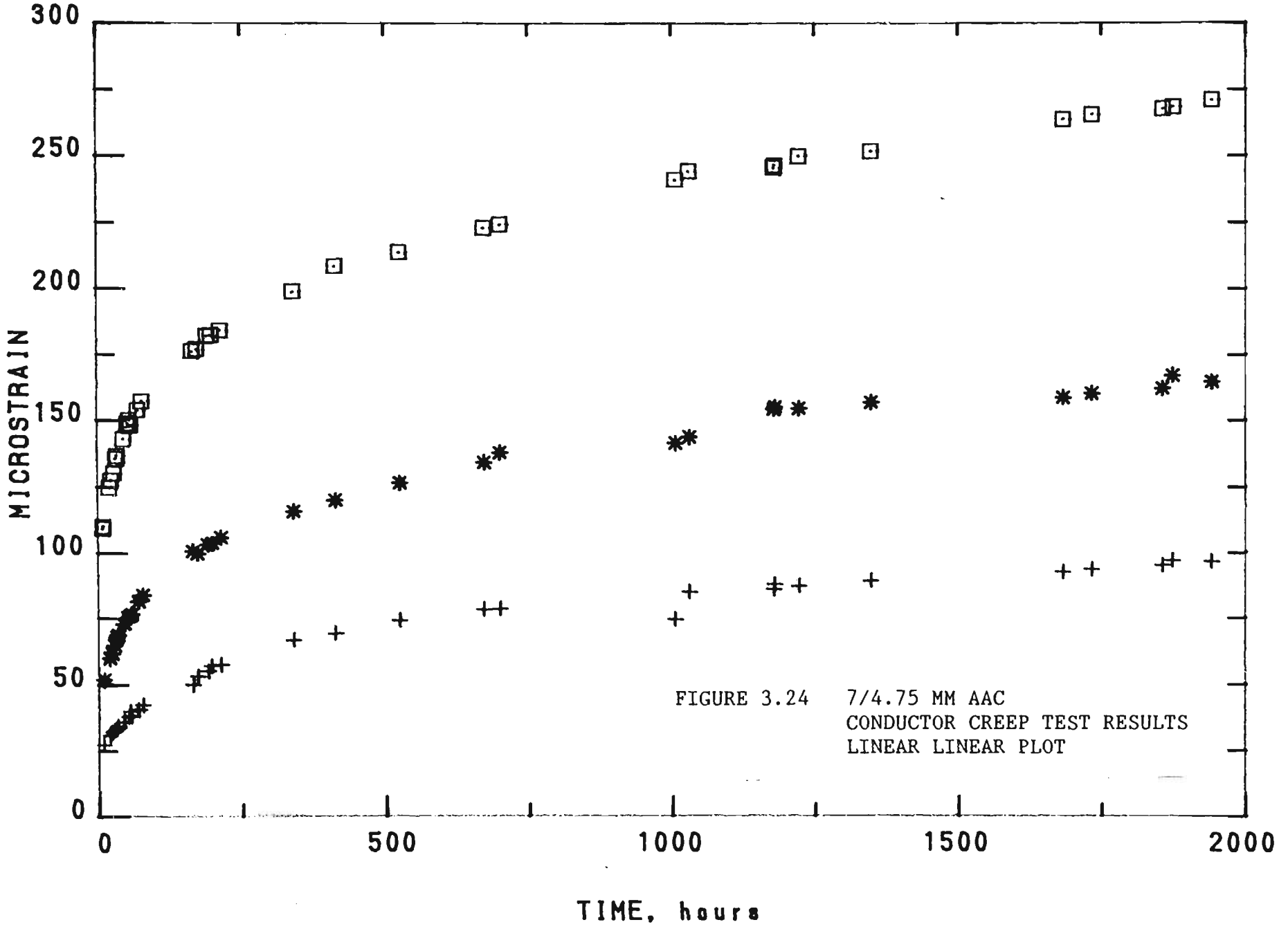

FIGURE 3.24 7/4.75 MM AAC
CONDUCTOR CREEP TEST RESULTS
LINEAR LINEAR PLOT

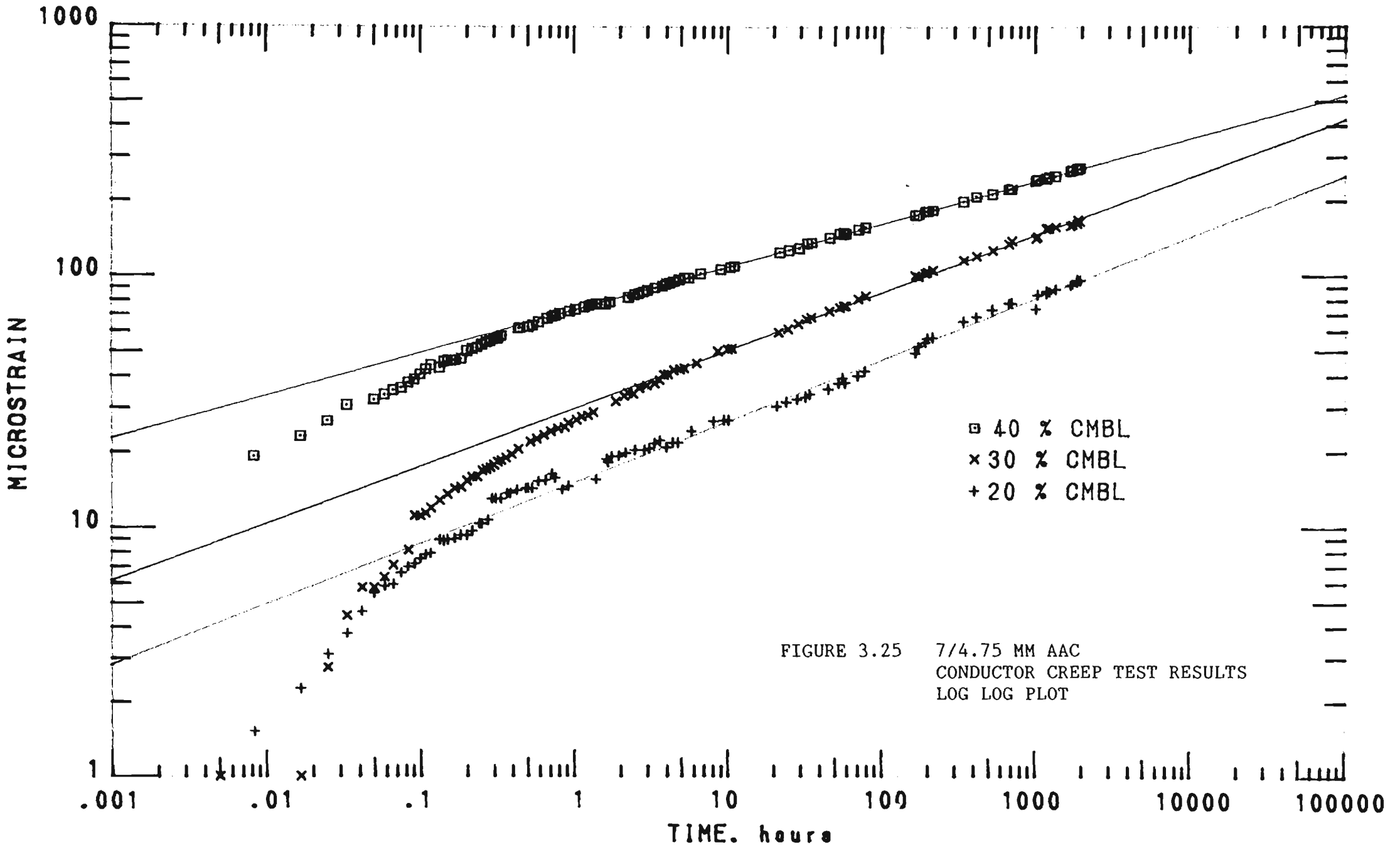

FIGURE 3.25 7/4.75 MM AAC
CONDUCTOR CREEP TEST RESULTS
LOG LOG PLOT

Since the long term effect of conductor creep is to reduce tensions and increase sag thus reduce ground clearance, an allowance must be made for creep in sag tension calculations. Once creep data is available four ways of interpretation of the results is possible to compensate for the effects of creep.

1. PRESTRESSING CONDUCTORS - It has been established for some time now, that after a period of time inelastic stretch rate decreases with time. To accelerate the creep behaviour of the conductor, over stressing at a predetermined tension is carried out for a nominated period of time. This removes a significant amount of creep because the initial rate of creep at the higher stress level is much more rapid than at a low stress level. Figure 3.26 illustrates the creep rates for stress levels of 20, 30 and 40% of calculated breaking load for Moon AAC 7/4.75 mm. Prestressing the Moon conductor at 30% of calculated breaking load for 5 hours reduces the possible final sag change in 30 years for an 80 m span at 85^{o}C by 50%.

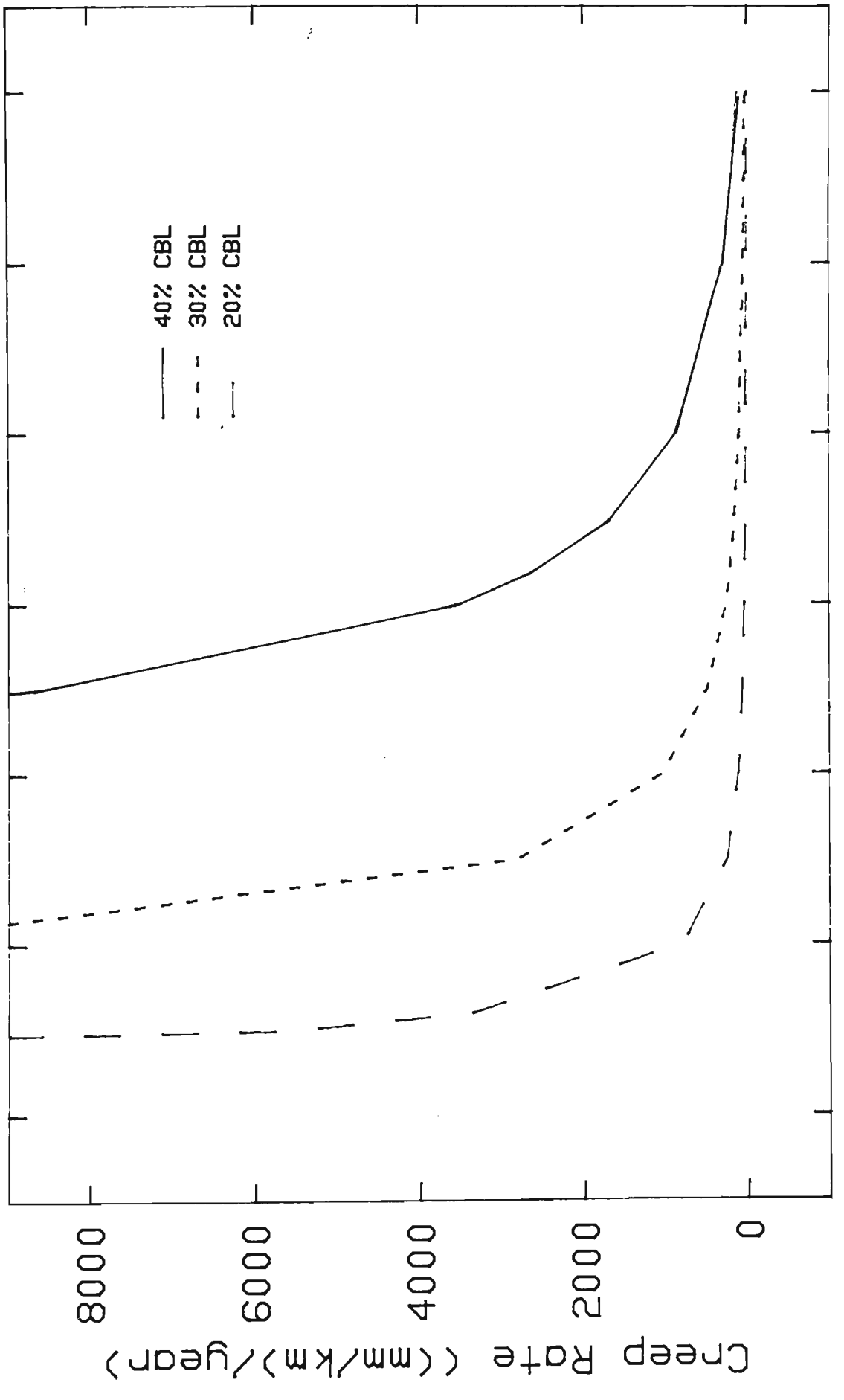

FIGURE 3.26 Conductor Creep Rate

2. OVERTENSIONING - In this compensating method the conductor is overtensioned at final stringing to make an allowance for the long term stress relaxation or permanent elongation of the conductor. Figure 3.27 illustrates the change in tension and sag for Moon AAC 7/4.75 mm for a 30 year service life. The tension change during this period is 40N representing a sag change of 74 mm. Overtensioning of 40N at final stringing compensates for this stress relaxation. In longer spans using larger conductors overtensioning loads can be considerable higher than the calculated 40N for the Moon AAC construction and span combination.

3. MARGINAL CLEARANCE ALLOWANCE - In the overtensioning compensating method for Moon AAC construction and span combination previously discussed a sag change of 74 mm occurred in a 30 year service life. The marginal clearance allowance compensating method provides for an additional 74 mm at the conductor attachment reduced level to provide for long term sag change.

4. TEMPERATURE ALLOWANCE - Creep may be interpreted as permanent extension in length similarly to that of the elastic extension due to temperature. Consequently it is possible to say that a certain amount of creep will produce an identical increase in conductor length as a certain temperature rise. This temperature may be added to the stringing temperature and after creep has taken place and at maximum operating temmperature no infringement of statutory ground clearances will occur. In the Moon AAC construction and span

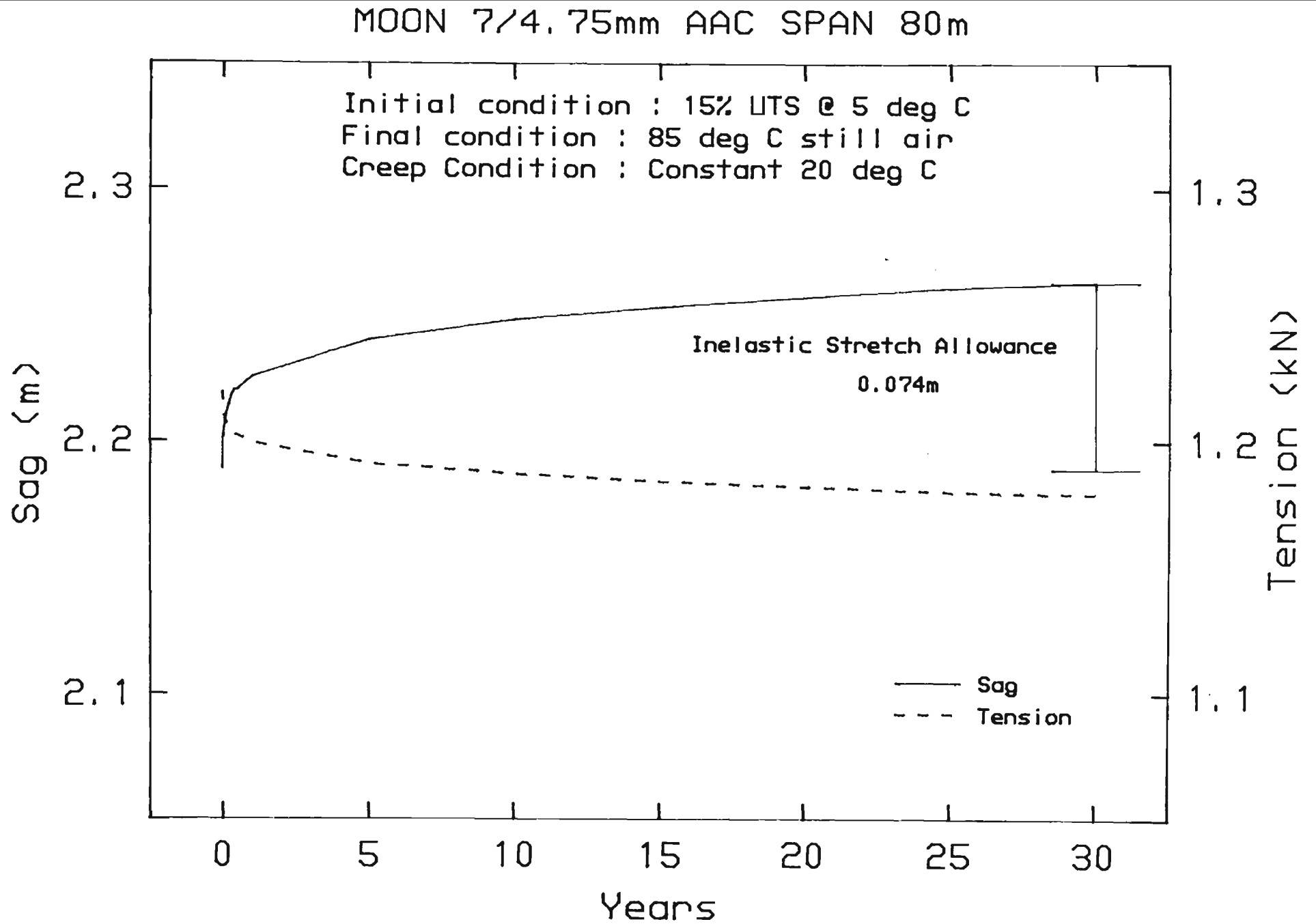

FIGURE 3.27 Conductor Tension & Sag Change With Change in Time

combination, the initial chord length at maximum operating temperature is 80.160 m. The chord length at 30 years service life and maximum operating temperature is 80.171 m representing an additional thermal expansion of 6°C. Accordingly if the temperature at sagging is 26°C, the sagging is carried out 20°C.

Degradation of conductors with time due to creep is considered unlikely and the possibility of long term conductor rupture must be extremely small. It is more probably that as a result of long term creep and inadequate creep compensation, statutory ground clearance are likely to be infringed.

The creep results for the conductor samples from the Avon to Kemps Creek and Dapto to Springhill transmission lines are not in agreement with those predicted by the CIGRE equations. The differing results for the Avon to Kemps Creek and Dapto to Springhill transmission lines is hypotherized as the effect of preforming the steel wires. The Dapto to Springhill transmission line did not have preformed steel wires and has exhibitied less creep than that of Avon to Kemps Creek transmission line with preformed steel wires. Two reasons are sited for the difference in the creep rates.

1. Creep has already been partly attributed to strand movement in the radial and axial directions. In the non preformed steel wire conductor sample a considerable back or unstranding torque is present. This back torque has the effect of straightening the steel wires at the initial

stranding stage and continuing throughout the service history. In comparison the preformed steel wires do not have the same level of back torque and when axial load is applied strand movement is likely to be greater. In other words, more strand movement occurs in the preformed steel wire sample than that of no preformed steel wire sample.

2. Although great care is taken in the preparation of the conductor samples, some back torque in the non preformed steel wire conductor sample after the conductor termination clamps were removed may have occurred in the test length. This has the effect of straightening the steel core wires and reducing the amount of strand movement likely to occur during the creep test.

When comparing the CIGRE (27) predictor equation (7) with that of the test results of Figure 3.29 and discounting the Dapto to Springhill transmission line conductor sample, there is good agreement in the slope of creep curve. The Dapto to Springhill transmission line conductor sample is discounted as the preforming the steel core wires has been carried out for a considerable period of time and the CIGRE conductor construction constants have probably been determined from creep test on ACSR/GZ construction with preformed steel core wires. Considerable departures in the CIGRE temperature and stress constants lead to the offset of the creep curves by as much as 600 $mm.km^{-1}$ at 50 years.

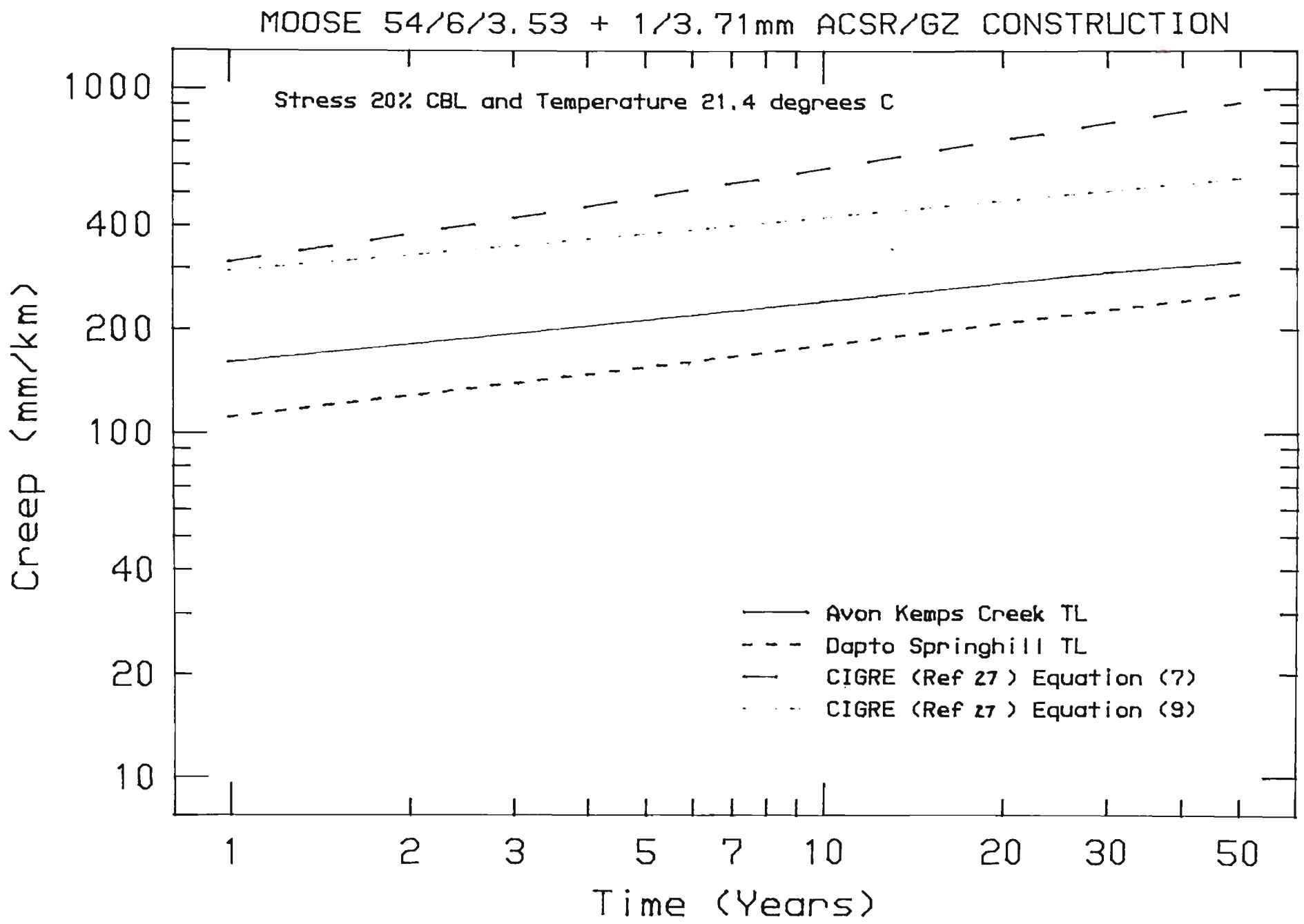

FIGURE 3.29 Summary of Conductor Test Results

Creep

Finally, Figures 3.30 and 3.31 illustrates the change in tension and sag for the Moose ACSR/GZ construction with time for the conductor samples from the Avon to Kemps Creek and Dapto to Springhill transmission line respectively for an every day service condition of 20°C, no ice and no wind. In addition the required creep or inelastic stretch allowance is given for each conductor sample.

To complete an accurate picture of the necessary inelastic stretch allowance additional knowledge of high temperature creep data is necessary and a stress and temperature history or more appropriate, prediction of the service stress and temmperature of the conductor is required. The later is probably the most difficult to obtain although some work in this field has been carried out by Beers, Gilligan Lis and Schamberger (13).

3.4.2.4 Breaking Load Tests

The breaking load or ultimate tensile strength (UTS) of a conductor is determined by a breaking load test similar to that for a wire obtained in a tensile test. However, because of the nature and difficulty of the test, prepared conductor samples are placed in a specially designed bench provided with a mechanical means of elongating the conductor until failure occurs.

Historically, the breaking load of a conductor is determined by calculations based on the premise that the aluminium strands will break at 1% strain with a suitable derating factors to account for the lay angle of the various layers. For ACSR constructions,

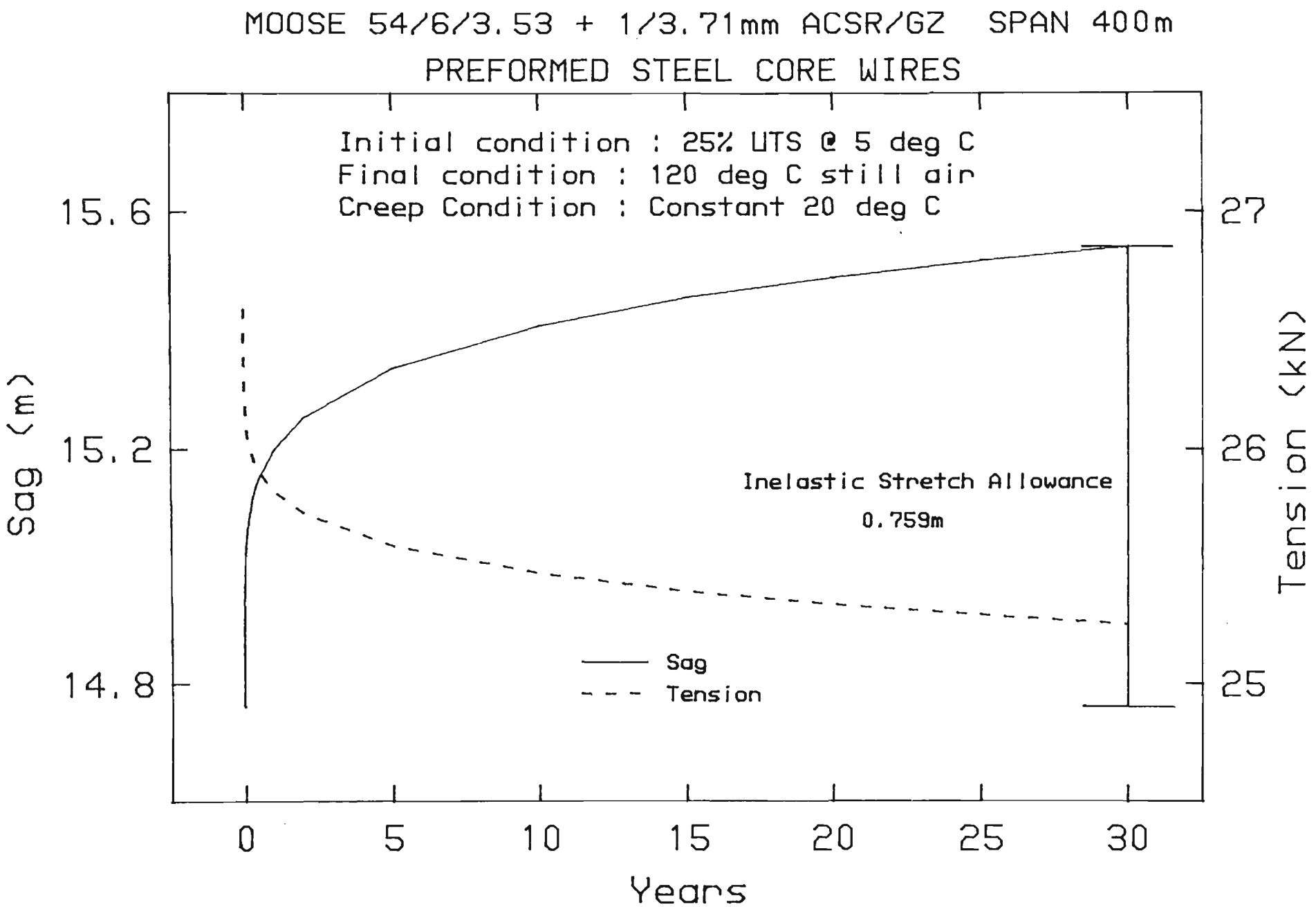

FIGURE 3.30 Conductor Tension & Sag Change With Change in Time

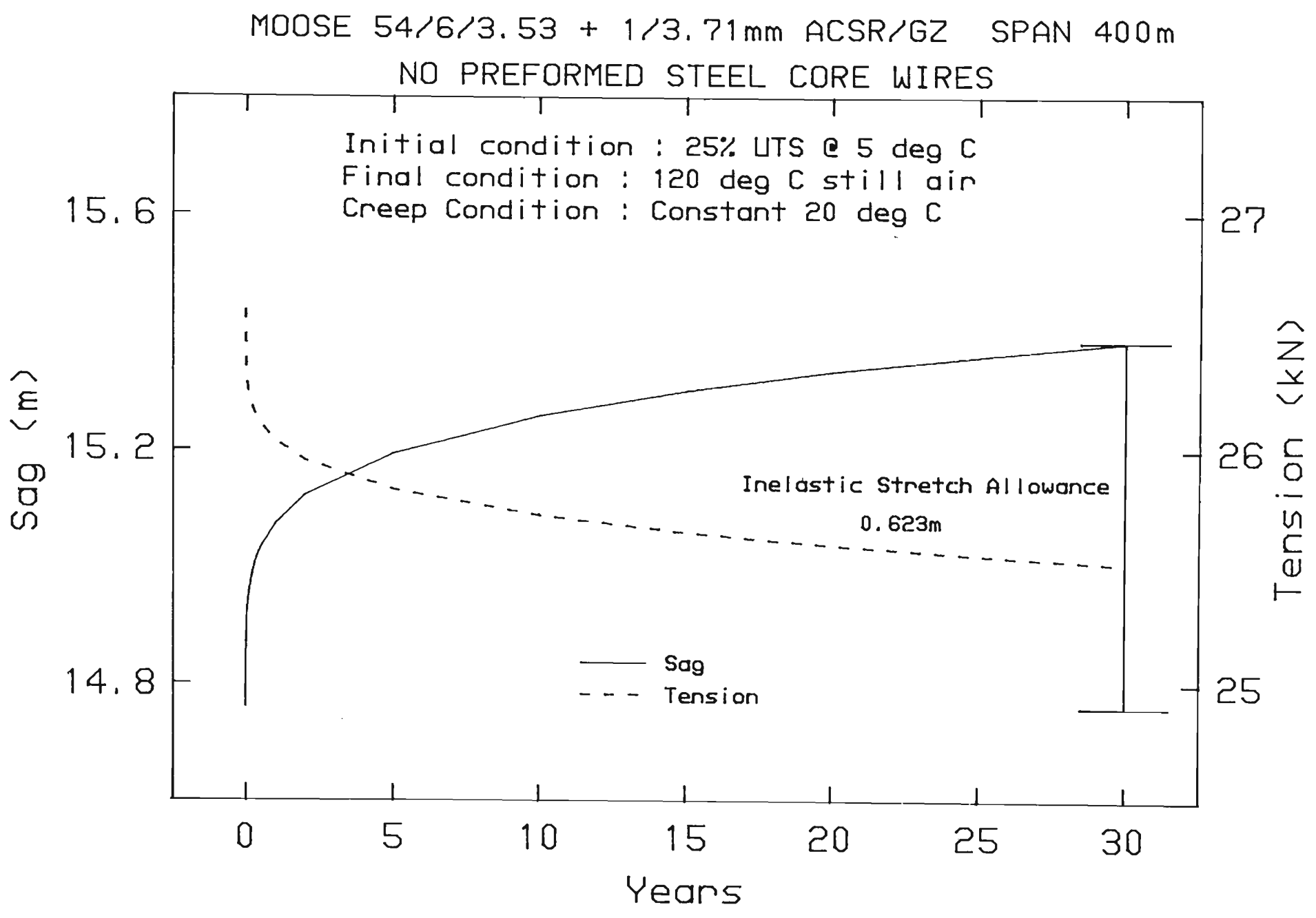

FIGURE 3.31 Conductor Tension & Sag Change With Change in Time

the strength of the steel wire core is included by measurements of the steel wire strength at 1% strain in a tensile test. Like the aluminium wires an appropriate derating factor to account for the lay of the steel wires is applied. The total calculated breaking load of the composite construction is then taken as the sum of the aluminium and steel components.

British and Australia Standards, whilst recognising the failure criteria of 1% strain do not require the measurement of the steel wire at 1% strain. Appropriate derating factors based on breaking load test data are applied to the strength of the aluminium and steel wires. In the case of an ACSR construction, the derating factors for aluminium and steel wires are 98% and 89% respectively when the samples are taken from the stranded conductor. During the manufacturing of a conductor, it is more convenient to test the wires before stranding as part of a quality assurance program. In this case, because of the probability of wire damage, particularly that of a reduction of cross sectional area caused by the back torque on the strander bobbins, a derating of the steel wire of 85% is applied.

Theoretically, if the layer stranding constant was determined and knowing the strand breaking load along the helix lay axis, the calculated breaking load along the composite conductor axis direction could be determined by the relationship,

$$CBL = BL_s + \sum_{j=1}^{N} \sum_{i=1}^{n_i} \cos\left[\tan^{-1}\frac{\pi}{MLR_{ij}}\right] n_{ij} BL_{ij} \qquad (3.37)$$

Unfortunately equation (3.37) assumes a simple transformation theory and does not recognise the complex combination of shear, torsion and tension that each wire in a composite construction is being subjected to in a breaking load test. Correlation between equation (3.37) and calculated breaking load test results is poor.

It has already been discussed in Chapter Two of these studies, the influence that the breaking load or UTS of the conductor has on tension and sag determinations. Put into perspective, a 2.5% reduction in the breaking load is translated into almost a 4% increase in sag for Lemon ACSR/GZ construction and a 300 m span.

Accordingly, supply authorities are slowly recognising this situation and requesting the verification of the calculated breaking load by actual breaking load tests.

Changes with time of the breaking load of a composite construction may be attributed to a loss of cross sectional by corrosion, fatigue crack initiation and/or annealing of the wires that constitute the conductor.

The detailed conductor breaking load test results for the samples of conductor from the Avon - Kemps Creek, Dapto - Springhill and Tomago - Taree transmission lines are given in Appendix 3. A summary of the findings of the Brealaimg Load tests are given in Table 3.15.

The breaking loads for the conductor samples from the Avon - Kemps Creek and Dapto - Springhill transmission lines are in good agreement with that of the value quoted in AS C75 - 1963, despite the premature termination failures. The breaking load for the conductor sample from the Tomago - Taree transmission line suggests a 6.5% degradation which supports the wire mechanical property tests. However cecause of the premature termination failure the breaking load tests for this conductor sample is not conclusive. Unfortunately an additional conductor sample was not available for further breaking load tests.

Premature termination failures are defined as the failures that occur outside the gauge test length. The gauge test length is the length of test specimen less 3 times the epoxy termination length at each end of the specimen. It is in this region that strands become disturbed during the preparation of the conductor termination that may influence the breaking load test results Typical sections of an epoxy termination are given in Plates 3.22 and 3.23.

	Avon-Kemps Creek		Dapto-Springhill		Tomago-Taree	
Test No.	205	206	207	208	163	164
Breaking Load (kN)						
ASC75-1963	159.5	159.5	159.5	159.5	89.2	89.2
Calculated[1]	178.9	178.9	184.6	184.6	96.3	96.3
Test Result	153.11[2]	158.9[2]	170.4[2]	159.5[2]	83.4[2]	83.3[2]
Failure Strain (%)	0.69	0.85	0.88	0.76	0.61	0.67

TABLE 3.15 - SUMMARY OF CONDUCTOR TEST RESULTS BREAKING LOAD

Notes:

1. Calculated value is determined from actual wire breaking loads and employing the methods of ASC75-1963.

2. Premature termination failure.

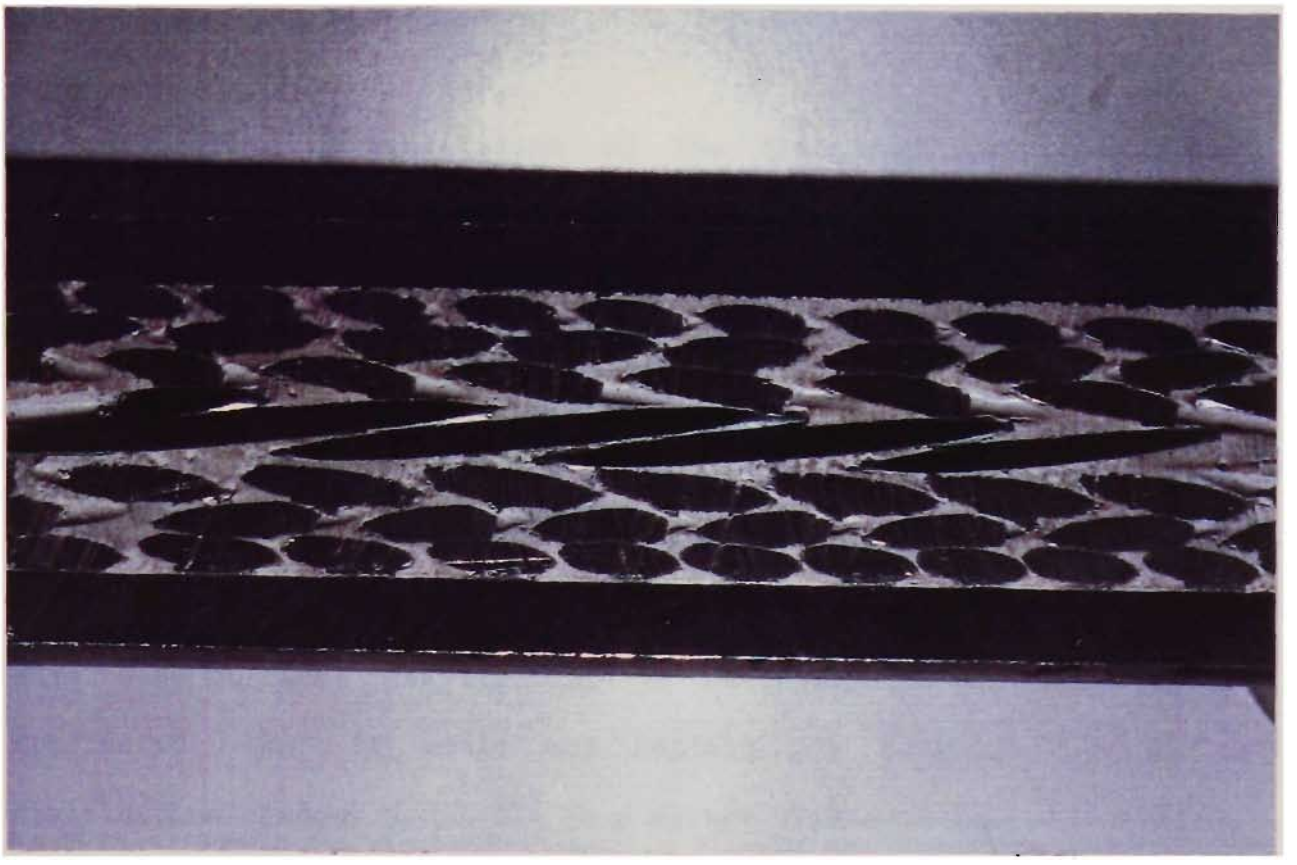

PLATE 3.22 - SECTION OF EPOXY/COMPRESSION TERMINATION
OF AN ACSR CONSTRUCTION

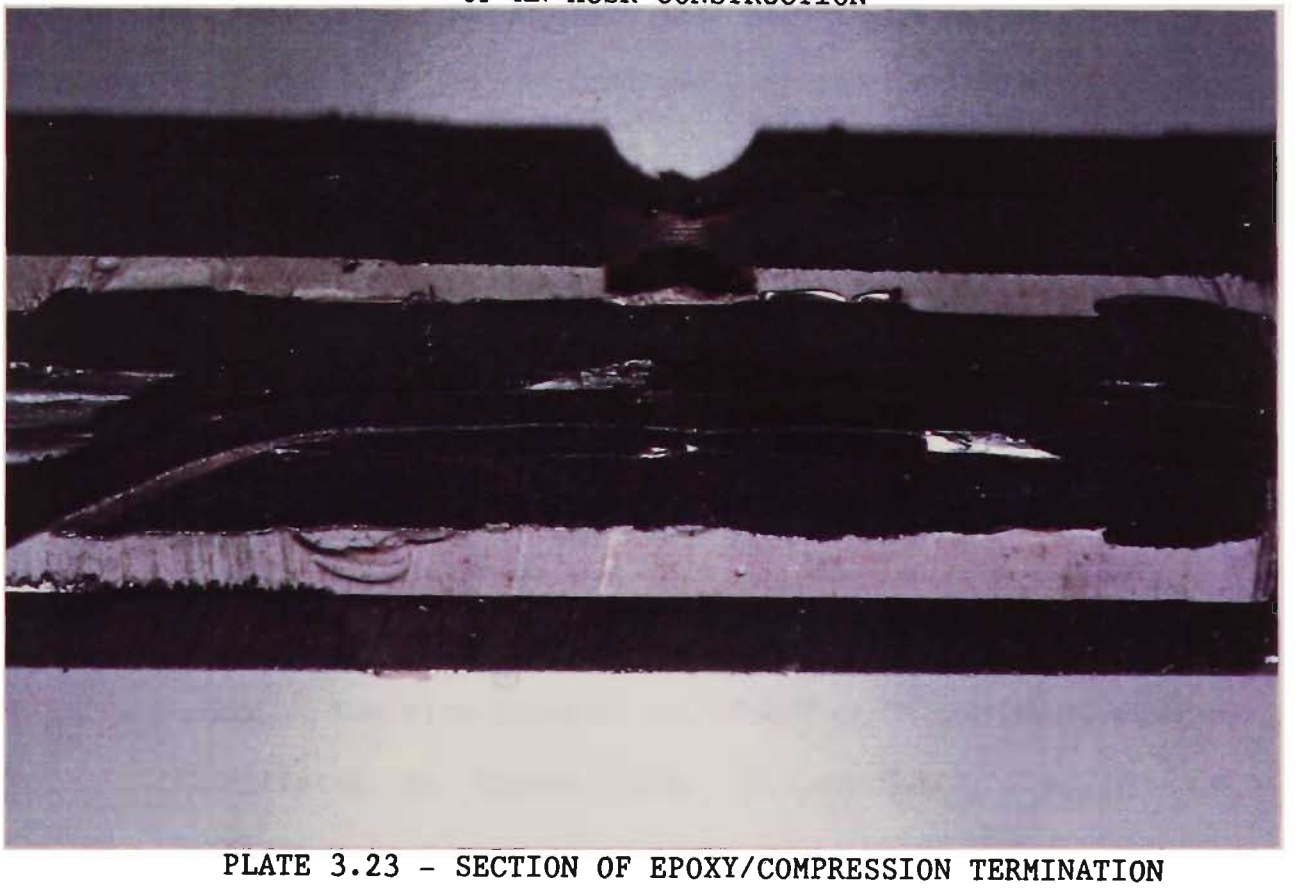

PLATE 3.23 - SECTION OF EPOXY/COMPRESSION TERMINATION
OF AN ACSR CONSTRUCTION
SHOWING COMPRESSION SLEEVE

An interesting interpretation of the breaking load test result is polynominal modelling of the stress strain curve. The polynominal model is given as,

$$\text{Load} = B_0 + B_1 S + B_2 S^2 + B_3 S^3 \ldots B_n S^n \quad (3.38)$$

Changes in the stress distribution with time in an ACSR construction may exhibit differing polynominal constants caused by the creep of aluminium wires. Unfortunately for this assessment to be successful a substantial data base of test results would be necessary and at this stage it is considered that it would not replace the determination of stress distribution changes available in a stress strain test.

Polynominal modelling of Panther and Moose ACSR/GZ is illustrated in Figures 3.32 and 3.33 and the constants of the polynominal equations are given in Table 3.16.

3.4.2.5 Lay Ratio

The lay ratio is defined as the ratio of axial length of one complete turn of the helix formed by an individual wire in a stranded conductor to the external diameter of the helix. In the past the lay ratio was determined from the mean diameter of the helix. The wire geometry of a helically stranded conductor is illustrated in Figure 3.34. Mathematically the lay ratio is defined as,

$$LR = \frac{L}{2R} \quad (3.39)$$

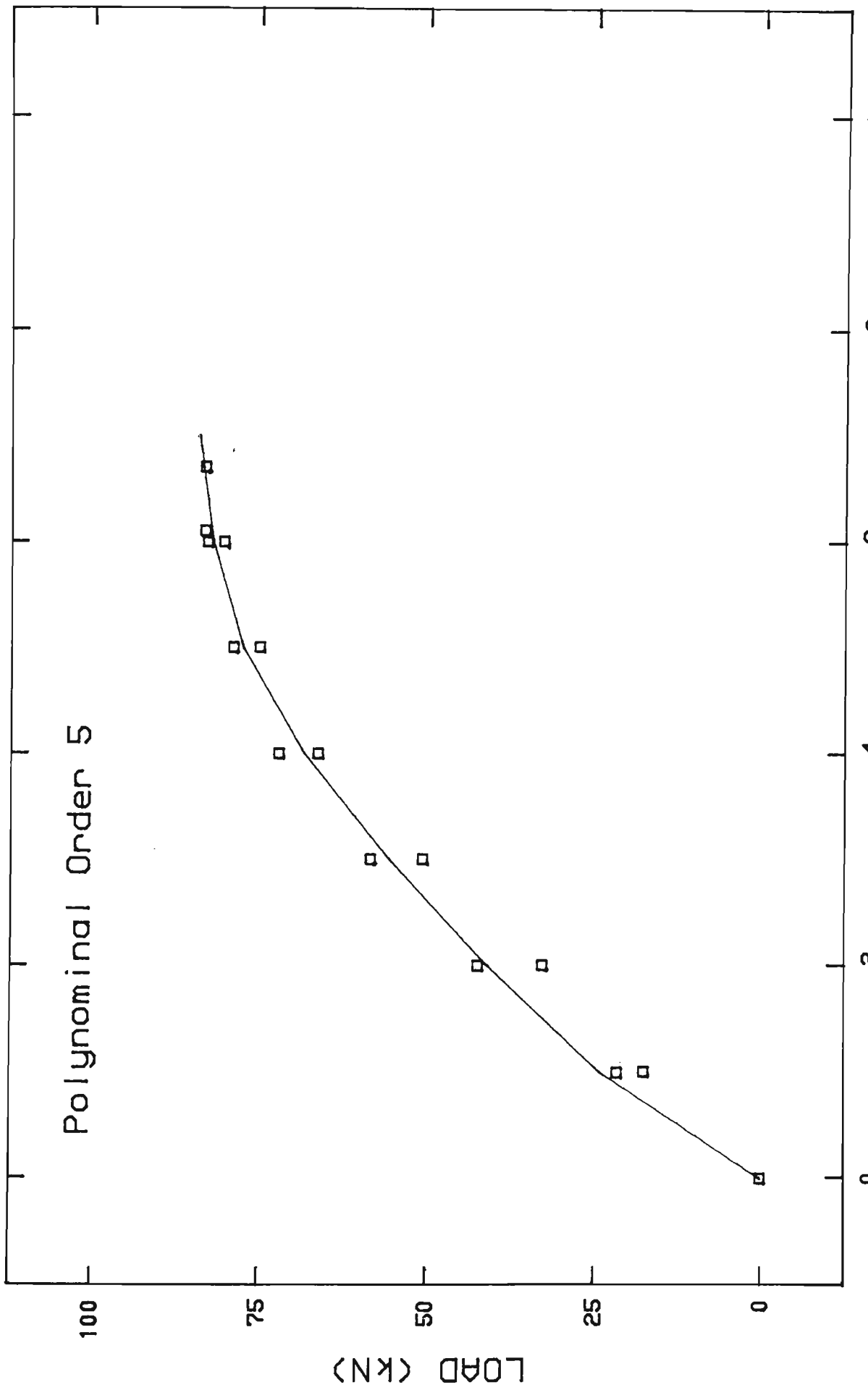

FIGURE 3.32 POLYNOMINAL MODELLING OF BREAKING LOAD TESTS

PANTHER ACSR/GZ 30/7/2.99mm CONDUCTOR

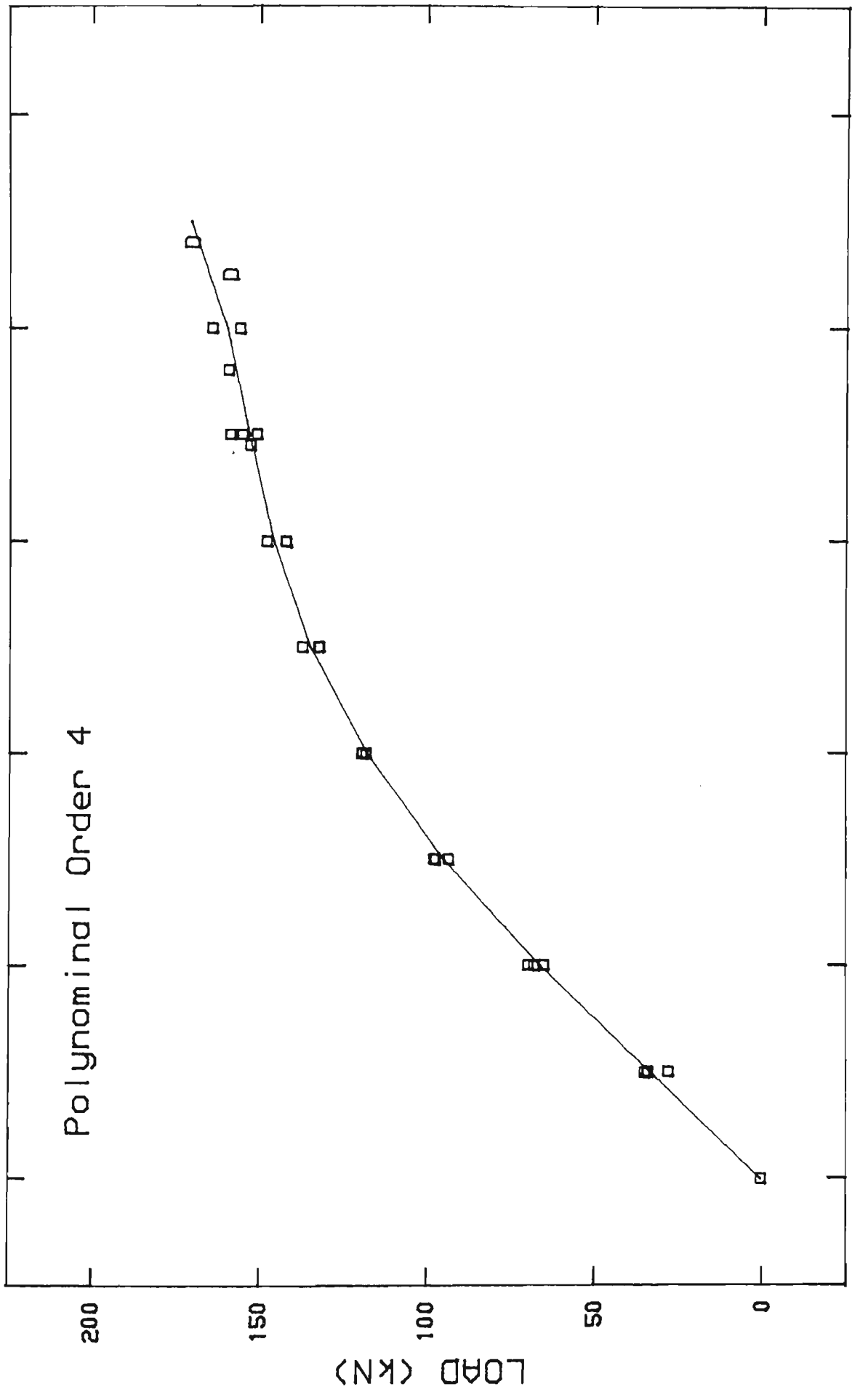

FIGURE 3.33 POLYNOMINAL MODELLING OF BREAKING LOAD TESTS

MOOSE ACSR/GZ 54/6/3.53 + 1/3.71 CONDUCTOR

Coefficient	Panther ACSR/GZ	Moose ACSR/GZ
B'_o	-0.00587	0.0765
B_1	206	317
B_2	-187	218
B_3	851	-904
B_4	-2050	561
B_5	1390	-

TABLE 3.16 - POLYNOMINAL MODELLING OF BREAKING LOAD TESTS
TABLE OF COEFFICIENTS

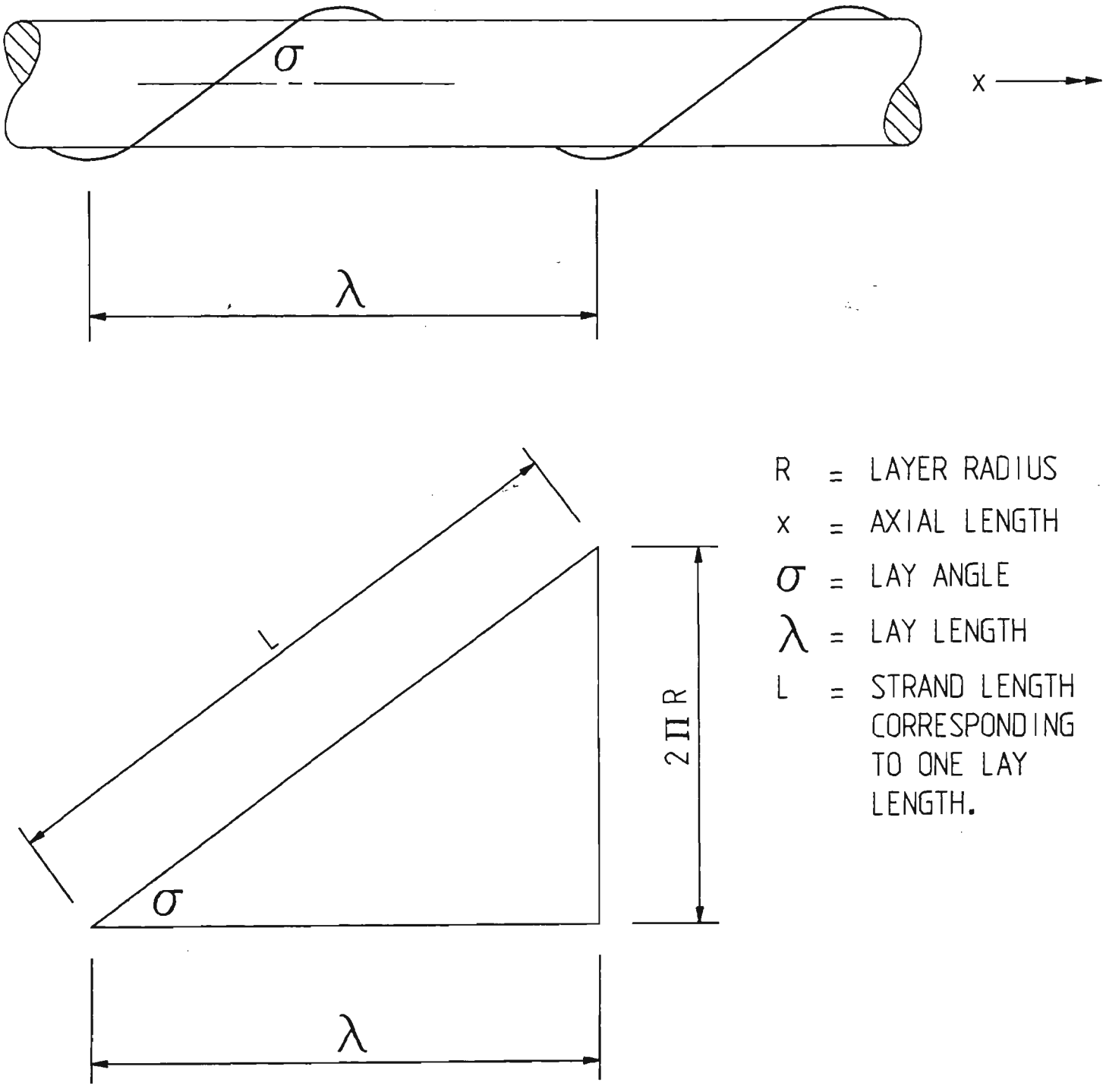

FIGURE 3.34 WIRE GEOMETRY IN A HELICALLY-STRANDED CONDUCTOR

The lay angle of the helix is defined as,

$$\sigma = \tan^{-1}\left[\frac{2\pi R}{L}\right] \qquad (3.40)$$

The lay ratio describes the amount that one wire of a particular layer of the conductor is longer than the length of the conductor. This is applicable to all layers of a conductor with the exception of the core wire.

Depending on the lay ratio, number of wires in a construction and the size of the wires, the lay of the wires has the effect of increasing the bulk mass and resistance of the conductor compared with that of the sum of the individual straight strands. In addition, the conductor parameters of calculated equivalent aluminium area which compares the area of a solid aluminium rod having the same d.c. resistance as the conductor is influence by the lay of the wires.

Unit less constants are determined for particular stranding construction and published in Standards (6, 7, & 8). These constant for mass, resistance and calculated aluminium area for layer i are given as,

$$m_{ci} = \left[\cos\left[\tan^{-1}\frac{\pi}{LR_i}\right]\right]^{-1} \qquad (3.41)$$

$$R_{ci} = \frac{m_{ci}}{2n_i} \qquad (3.42)$$

$$A_{ci} = \frac{1}{R_{ci}} \qquad (3.43)$$

respectively.

Changes in the lay ratio with time are attributed to radial and axial movements of the wires. In an ACSR conductor, particularly one with non preformed steel wires, the back torque on the 6 wire layer has the effect of unravelling this layer. This unravelling will increase the lay ratio for those layer with the same direction of lay or the 6 wire layers steel core and decrease the lay ratio for those layers with the opposite direction of lay as the 6 wire layer steel core.

One of the main difficulties in assessing a change in the lay ratios is the broad range of lay ratios allowed in the appropriate manufacturing standard. Even if a bench mark lay ratio could be established and a significant change occurred, this would not represent a serious degradation to the conductor unless the conductor layers had unravelled to such an extent that the conductor elongated and ground clearance statutory requirements were infringed. This situation is not likely to

occur since successive layer in the conductor have opposite directions of lay, so an increase in lay ratio in one layer when translated to the next layer represents a decrease in lay ratio.

These discussions aside for one moment, unravelling of the conductor may actually enhance and improve the conductor performance with regard to a.c. resistance.

The details of the lay ratios of the layers that constitute the conductor samples from the Avon to Kemps Creek and Dapto to Springhill transmission lines are given in Appendix 3. The lay ratios were not measured on the conductor sample from the Tomago to Taree transmission line as consequence of the stress train test results. A summary of the findings of the lay ratio and a comparison of the appropriate Australian Standard are given in Table 3.17.

3.5 CHEMICAL TESTS

The chemical tests that are possible on an aged transmission conductor fall into three areas, material composition, grease drop point and grease mass.

Layer	AS C75.1-1963	Avon-Kemps Creek Transmission Line	Dapto-Springhill Transmission Line
6 Wire	20-30	25.83	24.31
12 Wire	14-21	16.75	16.22
18 Wire	11.25-18	14.56	14.79
24 Wire	11.25-14	10.84	10.82

TABLE 3.17 - SUMMARY OF CONDUCTOR TEST RESULTS LAY RATIO

3.5.1 Material Composition

The material properties of a conductor are function of the composition and structure of the material. Fundamentally, if the material intrinsic properties are suspected of changing with time then either or both the metallurgical structure and the chemical composition have changed.

However, it is not possible for the chemical composition of a conductor to change with time. To eliminate chemical composition as a possible factor in determining a property change it is necessary to carry out chemical composition tests on a sample of conductor to establish the material bench mark.

To illustrate the possible misinterpretation of wire or conductor test results, the resistivity of aluminium wires that constitute the conductor sample from the Bellambi to Heathcote transmission line was high because of a high silicon component consistant with a hot rolled production process. This could have easily been interpretated as loss of conductivity due to high operating temperatures for extended periods causing an intrinsic property change.

The chemical composition of the three currently available conductor aluminiums is given in Table 3.18.

Aluminium Designation	Si	Fe	Cu	Mn	Mg	Cr	Zn	Ga	B	T+Ti+V	Al
1350	0.10	0.40	0.05	0.01	-	0.01	0.05	0.03	0.05	0.02	99.5
1120	0.10	0.40	0.05-0.35	0.01	0.20	0.01	0.05	0.03	0.05	0.02	99.2
6201A	0.5-0.7	0.50	0.04	-	0.6-0.9	-	-	-	0.06	-	REM

TABLE 3.18 - CHEMICAL COMPOSITE LIMITS OF ALUMINIUM AND ALUMINIUM ALLOYS (2)

3.5.2 Grease/Tar Drop Point

The principal reason of including a grease or tar in a conductor is to provide corrosion resistance to the wires that constitute the conductor. It has been previously discussed in Section 3.3.1 that the zinc coating of the steel wire under some conditions is sacrificial to the aluminium. The grease/tar plays an important role in providing a barrier to this zinc aluminium interface, thus preventing the possibility of corrosion.

Another important property of the grease/tar is to restrict the loss of grease/tar when the conductor is operating at high temperatures. Accordingly the grease/tar drop point should be greater than the maximum design operating temperature of the transmission line.

The grease/tar drop point is determined in accordance with the requirement of ASTM D566.*

* ASTM Designation D566-64 "Dropping Point of Lubricating Grease". IP Standards for Petroleum and its Product Part I Mothods for Analysis and Testing Section 1 IP Methods 1

The details of the grease/tar drop point of the conductor samples from the Avon to Kemps Creek, Dapto to Springhill, Tomago to Taree and Bellambi to Heathcote transmission lines are given in Appendix 3. A summary of the findings of the grease/tar drop point and the maximum design operating temperature of the transmission lines is given in Table 3.19.

In the case of the Avon - Kemps Creek and Dapto to Springhill conductor grease drop points were less than the maximum design operating temperature. Accordingly, loss of grease may occur if the conductor temperature was greater than grease drop point for a sufficient time for migration of the grease from the core to the surface to occur.

Two stages of grease/tar flow are likely to occur.

1. The grease/tar migrates from the top of the conductor to the bottom.

2. The grease/tar accumulates at the bottom of the conductor and then flows to the span low point or to a point where the mass of the grease/tar droplets is sufficiently large that discharge from the conductor will occur.

Transmission Line	Avon-Kemps Creek	Dapto-Springhill	Tomago-Taree	Bellambi-Heathcote
Corrosion Prevention				
Material	Grease	Grease	Tar	Tar
Extent (wire layer)	6	6	6 & 12	6 & 12
Material Drop Point				
(^{o}C)	65	65	74	70
Material Mass				
($g.m^{-1}$)	11.6	11.4	37	36.8
Maximum Design				
Operating Temperature (^{o}C)	120	120	50	50

TABLE 3.19 - SUMMARY OF CHEMICAL TEST RESULTS
CORROSION PROTECTION MATERIAL DROP POINT AND MASS
AND MAXIMUM DESIGN OPERATING TEMPERATURE

The effects of grease/tar flow are:

1. The creation of voids where water and corrosive products will accumulate and may result in wire corrosion.

2. The loss of the protection interface between the aluminium and zinc materials and the subsequent electrolytic corrosion.

3. Radio interference voltage caused by electrostatic discharge from the droplets.

4. Property damage directly beneath the transmission line.

To minimise the grease/tar loss a series of tests need to be carried out to quantify the duration at elevated temperatures for the grease/tar migration to occur in a conductor. This will be the subject of a future study.

3.5.3 Grease/Tar Mass

To quantify the grease/tar loss, the grease/tar mass may be measured to determine the extent of any loss.

The grease/tar is given by,

$$m_g = \frac{m_c - \sum_{i=1}^{n} w_i}{l_c} \qquad (3.44)$$

Current typical grease masses for various conductor constructions is given in Table 3.20. Unfortunately past tar mass data is not available, however good correlation between the Tomago to Taree and Bellambi to Heathcote transmission line conductor samples would indicate for tarring of 6 and 12 wire layers a tar mass in the order of 36-37 $g.m^{-1}$ is likely.

A comparison of the grease mass per metre for the Avon to Kemps Creek and Dapto to Springhill transmission lines given in Table 3.19 and the typical grease mass per metre for conductor constructions suggests no loss of grease.

3.6 METHODOLOGY FOR TESTING AGED CONDUCTORS

Conductor degradation with time can be attributed to one or all of five mechanisms, corrosion, fatigue, annealing, electrical and mechanical. In an ACSR construction stress distribution changes can occur due to creep of the aluminium wires over the steel wire. Furthermore, overall transmission line degradation caused by the infringement of statutory ground clearances is attributed to conductor creep.

A methodology for conductor sampling, testing and assessing the level of degradation of each of these mechanisms and a simple life expectancy model is discussed as follows.

Construction	Grease Mass, Mg[1] % M_c
3/4	0.2-0.3
4/3	0.2-0.3
6/1	0.3-0.4
6/7	1.0
30/7	1.0-1.5
54/7	1.0
54/19	1.0

TABLE 3.20 - TYPICAL GREASE MASS IN CONDUCTORS

3.6.1 Corrosion

The level of corrosion in a conductor is a function of the pollution level of the environment and the topography of the route of the transmission line. Climatic factors can also influence the extent of the corrosion in a conductor. Results of the samples of conductor suggests negligible corrosion will occur in pollution environments ranging from light to heavy.

Experience would indicate sampling of the conductor is necessary at the suspension point where foreign materials are likely to accumulate beneath the armour rods and deterioration of the aluminium wires and the galvanizing zinc of the steel wires is more likely.

Corrosion of a homogeneous conductor will normally be restricted to pit corrosion, with pit growth rates generally small. Experience also would suggest catastrophic localised corrosion is not likely to occur because of the presence of the hard aluminium oxide surface film, even in environments with a heavy pollution level. The overall effect of pit growth would be the gradual loss of cross sectional area and the development of marginal thermal hot spots.

In non homogeneous conductors such as ACSR/GZ construction internal corrosion is an additional consideration and will occur in several stages. Initially, in the presence of an electrolyte a cell is established between a zinc anode and an aluminium cathode. The zinc corrodes exposing the steel core. Secondary

cell action is then established where the aluminium behaves as the anode and the steel as the cathode. As the aluminium deteriorates bulges will form and with the flow of electric current and the gradual loss of cross sectional area, thermal hot spots will develop that may lead to ultimate failure of the aluminium and steel wires.

Steel wire galvanising properties discussed in Section 3.4.1.4 indicates that with a 3% loss of wire mass that onset of brown strains on the wire will occur. The most effective way to prevent this onset occurring is insuring an adequate corrosion prevention material such as a grease or tar is present. These materials have the effect of providing an insulating barrier to the zinc aluminium interface and excluding any electrolyte from the interstitials. Typical grease masses for various conductor constructions are given in Table 3.20. Tar masses are unavailable, however for a 30/7 ACSR construction with tar on 6 & 12 wire layers, the results of these studies, assuming no loss had occurred in the service life of the samples, suggest that 36 $g.m^{-1}$ is an appropriate value.

Conductor life expectancy is predicted by a simply philosophy. If negligible degradation has occurred in the grease and zinc coating for a particular service history, then provided the environment remains the same, one would expect a similar future exposure period without significant additional degradation to occur from the time of initial sampling. In the case of measurable degradation, annual visible inspections of evidence of conductor bulging combined with conductor sampling at the rate of

one quarter the period from the time of initial sampling is considered appropriate.

A methodology for testing for the degradation of steel wires due to corrosion is given in Figure 3.35. A methodology for testing for the degradation of aluminium wires due to corrosion is restricted to tensile tests where results need to comply with the appropriate manufacturing standards. In the event of that one or more wires did not meet the appropriate criteria then a conductor breaking load test would provide an overall performance indicator on the conductor degradation.

3.6.2 Fatigue

Two design philosophies are used to account for material fatigue, damage tolerant and damage free. Damage tolerant designs permit fatigue crack initiation and predicts an acceptable crack propogation period before material replacement is necessary. On the other hand, the damage free designs determines a critical value of stress in the material, which if not exceeded, inhibits fatigue crack initiation.

With the use of vibration dampers, transmission line conductor designs are based on the damage free criteria. The rule of thumb critical dynamic strain is 150 $mm.km^{-1}$. However even with such damage free designs, as transmission line conductors age and in

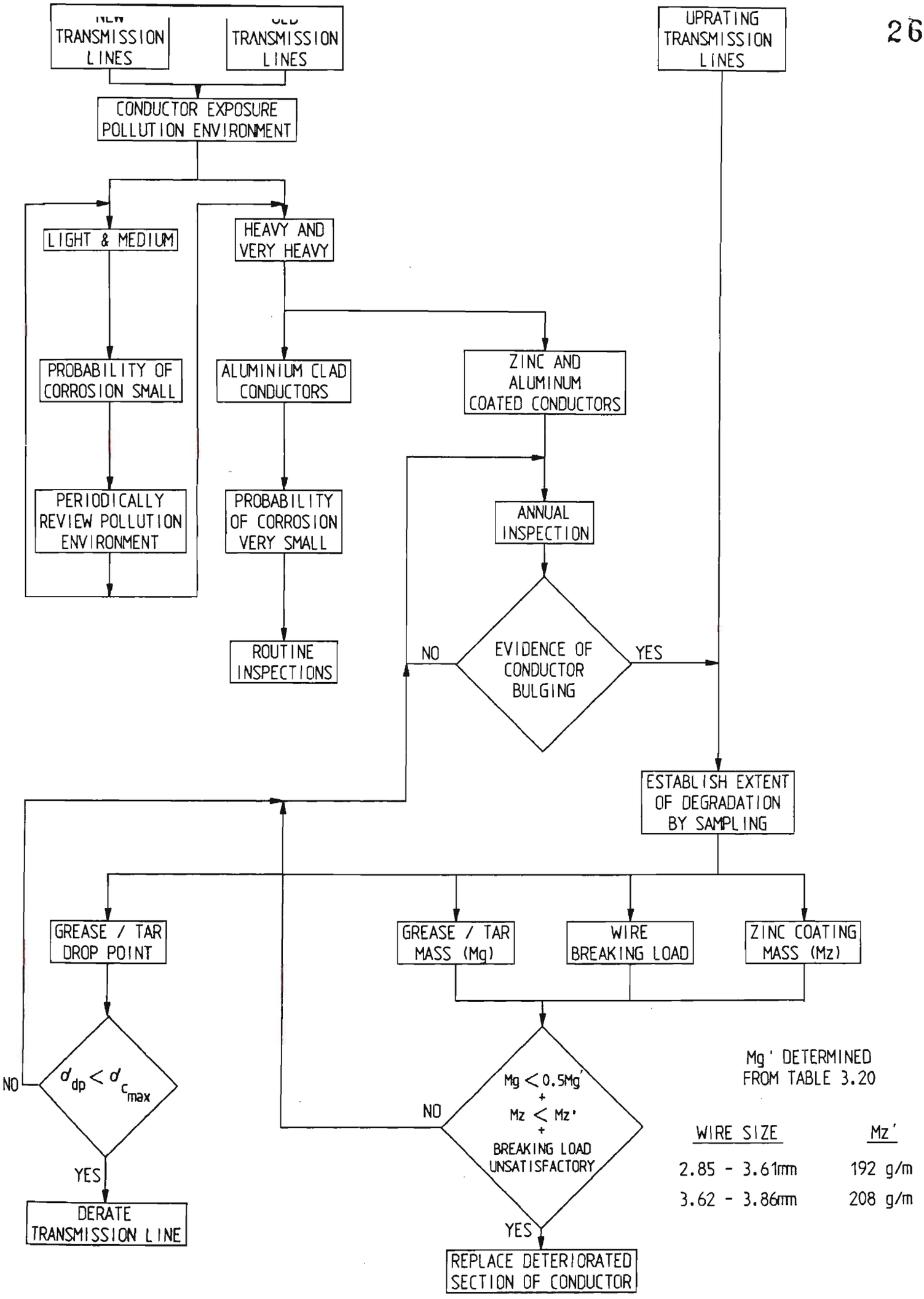

FIGURE 3.35 METHODOLOGY FOR TESTING STEEL WIRES IN AGED CONDUCTORS

view of the wide spectrum of service conditions, the complex nature of stranded conductors and the instrinsic fretting action of the component wires, it is prudent to investigate for evidence of fatigue crack initiation.

The first evidence of wire fatigue is abrasion or fretting and the presence of aluminium oxide. Wire fretting is more prone to occur where radial wire movement is restricted such as suspension points, conductor spacers and vibration damper locations. At the suspension point the addition of the bending stress over the suspension clamp, particularly at the top of the conductor makes this site the most likely location for fatigue cracks to be present.

Samples of fretted wires are examined with an optical microscope and a scanning election microscope to establish the presence of fatigue cracks in the fretted areas and longitudinal section are prepared to measure the depth of any fatigue cracks. Tensile tests on fatigued wires were not conclusive as to whether such tests are sufficiently sensitive to indicate fatigue crack initiation.

The samples of conductors examined as part of these studies did reveal wire fretting without fatigue cracks. However with such a small sampling rate the likelihood of finding fatigue cracks must be considered small. Even so, with no evidence of fatigue cracks and a current history of fatigue free service of transmission line conductors in NSW, such results are reassuring.

These discussions aside, it could be hypotherized that all the conductors in service to date are in an incubation period and future wire breaks are possible. If this scenario did eventuate, then the remedial action necessary would consist of placing the conductor in stringing sheaves and relocating the damaged section of conductor away from the suspension point. Armour repair rods fitted to the damage section of conductor would provide insurance against loss of cross sectional, if other wires were subsequently damaged.

Future life expectancy of conductors in the event of wire fatigue failure is considered limited without remedial action. This is due to the cumulative damage already occurred in the remaining wires and the increased stress that the remaining wires will be subjected. In other words the increased stress levels in the remaining wires is likely to accelerate the propogation of fatigue cracks in any other damaged wires.

A methodology for testing for the degradation of aluminium wires due to fatigue is given in Figure 3.36.

3.6.3 Annealing

Annealing is the heating of a material generally followed by a cooling period. During this process the material experiences a change in the microstructure and for aluminium this includes a reduction in tensile strength and an increase in conductivity.

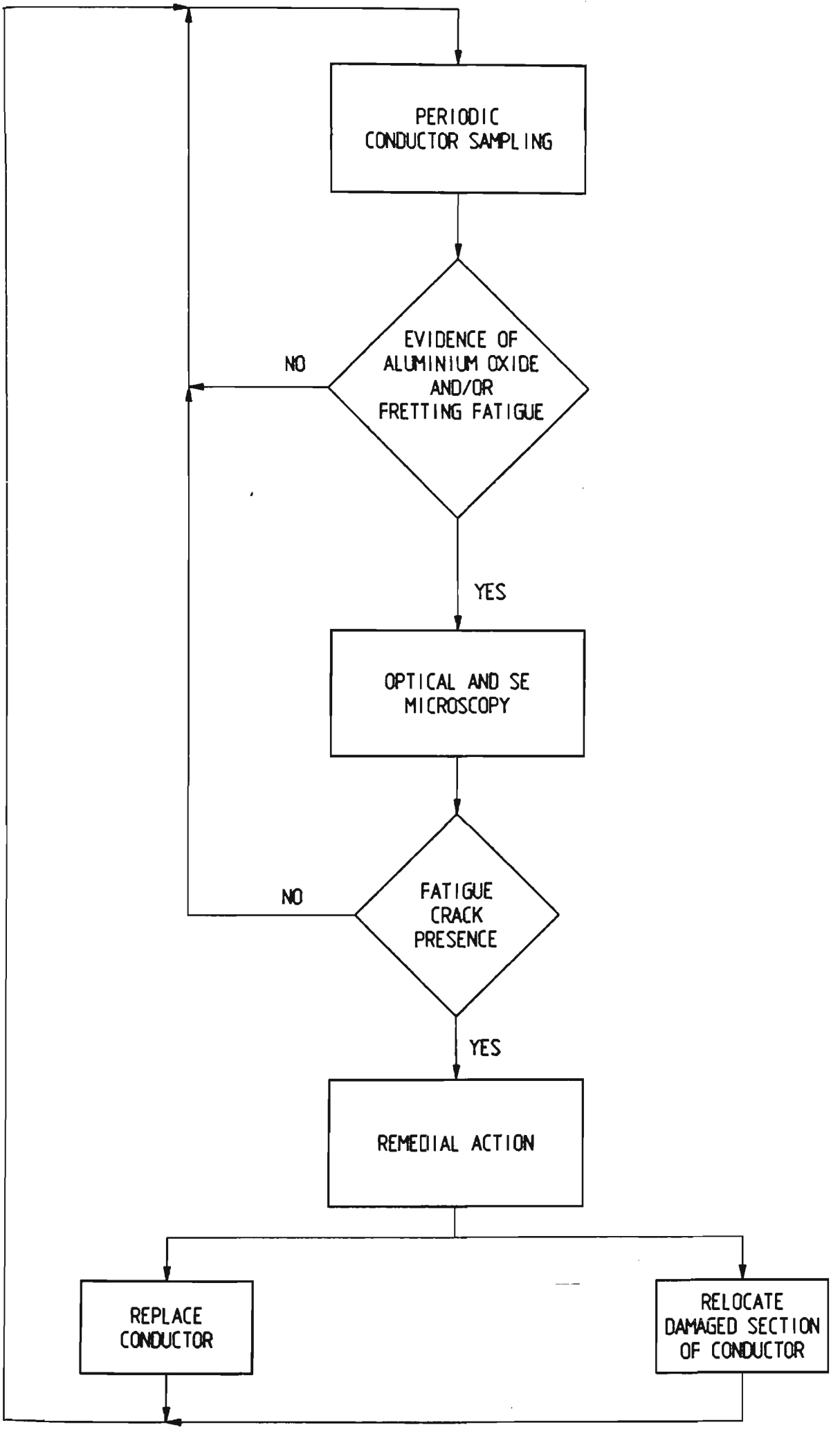

FIGURE 3.36 METHODOLOGY FOR TESTING FATIGUE OF ALUMINIUM WIRES IN AGED CONDUCTORS

Such changes have already been illustrated in Figures 3.5 to 3.7 and 3.8 to 3.10 for tensile strength and conductivity respectively.

It is clear from these illustrations that significant changes in the tensile strength and conductivity only occur when conductors are subjected to operating temperatures greater than 80^{o}C with corresponding long exposure times. Normal maximum design temperatures only marginally exceed this value, however transient short circuit currents will increase the conductor temperature considerably. This high temperature excursions are thought not to have a large impact on annealing of conductors as the exposure times are limited to less than 0.2 seconds by high speed protection systems. Even with cumulative annealing during the lifetime of conductors large excursions of property changes are not likely.

The results of these studies support this and suggest the current operating policies of the Electricity Commission of NSW that the likelihood of conductor annealing is small.

The extent of annealing is determined by tensile testing of a destranded conductor and the extent of degradation measured using the appropriate manufacturing standard minimum criteria. In the event, that several wires did not meet the criteria, a composite breaking load test would give an overall performance indicator

and the effect of individual low strength wires. If the conductor did not meet the breaking load criteria, the results of lower conductor statutory safety factors would need examination.

Conductivity tests may be carried out to determine the extent of the annealing, however given the likely initial manufacturing tolerances, it is considered that such tests would be inconclusive.

Life expectancy is measured by determining the future date when statutory safety factors could not be achieved. Even though the tensile strength deterioration rate is complicated by an increasing conductivity, a linear degradation model is suggested.

A more complex model that would account for the combined effects of conductor temperature, exposure time, increasing conductivity and decreasing tensile strength could be established by determining equations for loss of strength and resistivity by mathematically modelling the curves of Figures 3.5 to to 3.10 using multiple regression. However this is not considered appropriate unless it is necessary to operate conductors at temperatures in excess of $80^{o}C$ for long periods of time.

A methodology for testing for the effects of annealing of aluminium wires is given in Figure 3.37.

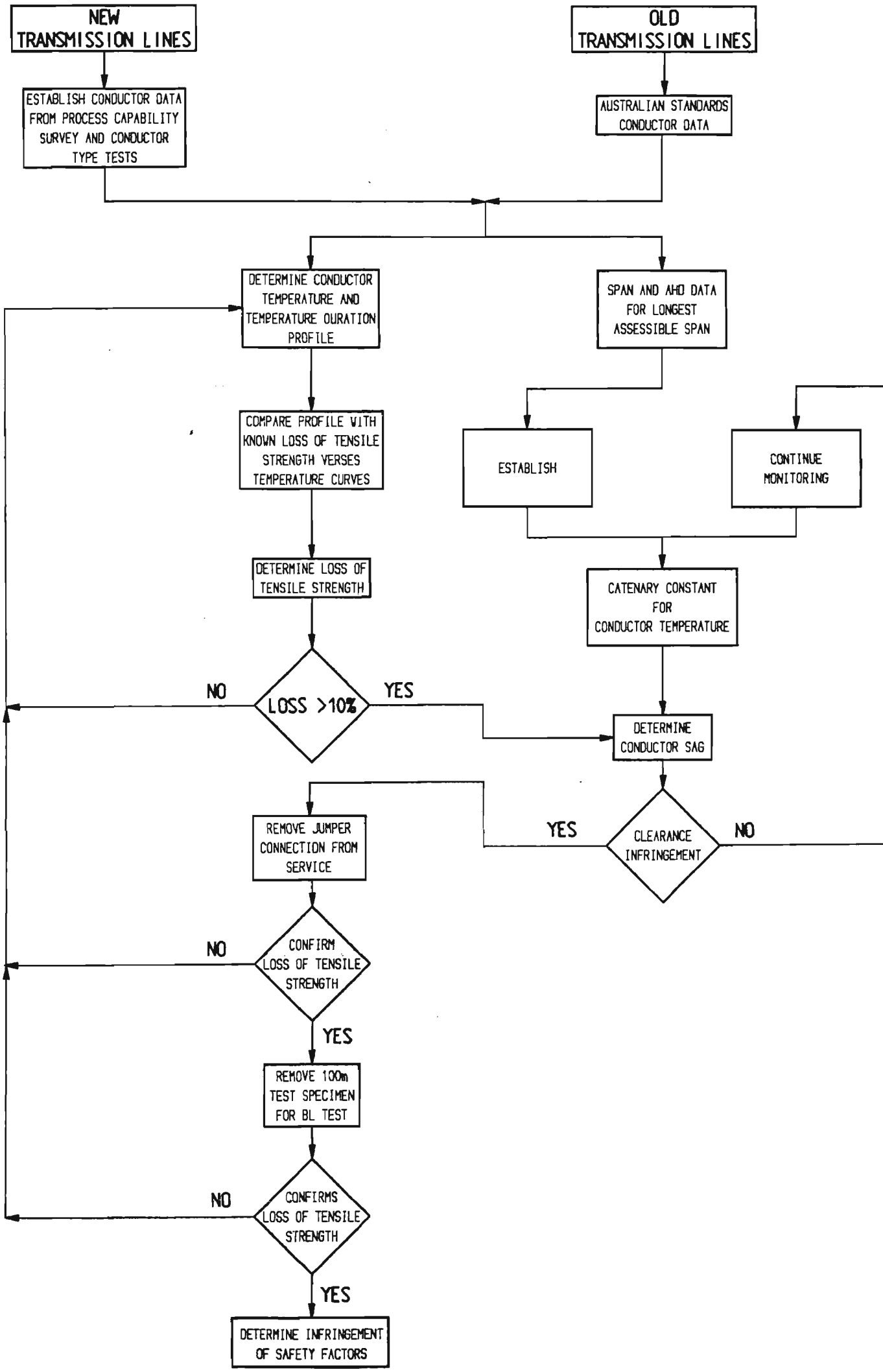

FIGURE 3.37 METHODOLOGY FOR TESTING OF AGED CONDUCTORS
=ANNEALING OF ALUMINIUM WIRES

3.6.4 Creep

Various stages of conductor creep have previously discussed and considering the operating temperatures typically used by supply authorities creep rupture is considered unlikely.

Like fatigue, conductor creep requires a design philosophy and four methods are given in Section 3.4.2.3.

The results of long term conductor creep is an increasing sag with time. In the event of inadequate creep compensation, statutory ground clearance will be infringed.

A methodology for testing for the effects of conductor creep and statutory ground clearance infringements is given in Table 3.38. The methods used to measure conductor sag have previously been given in Chapter 2.

3.6.5 Electrical

Insulation co-ordination designs of a power system as far as economically reasonable are based on minimising the effects of over-voltages. However, over-voltage transients such as direct lightning strikes, interphase conductor clashing and insulator flashovers may result in the damage of conductors. The damage of the conductor is the destructive power of electric arcs which generate high localised temperatures that vapourise conductor materials.

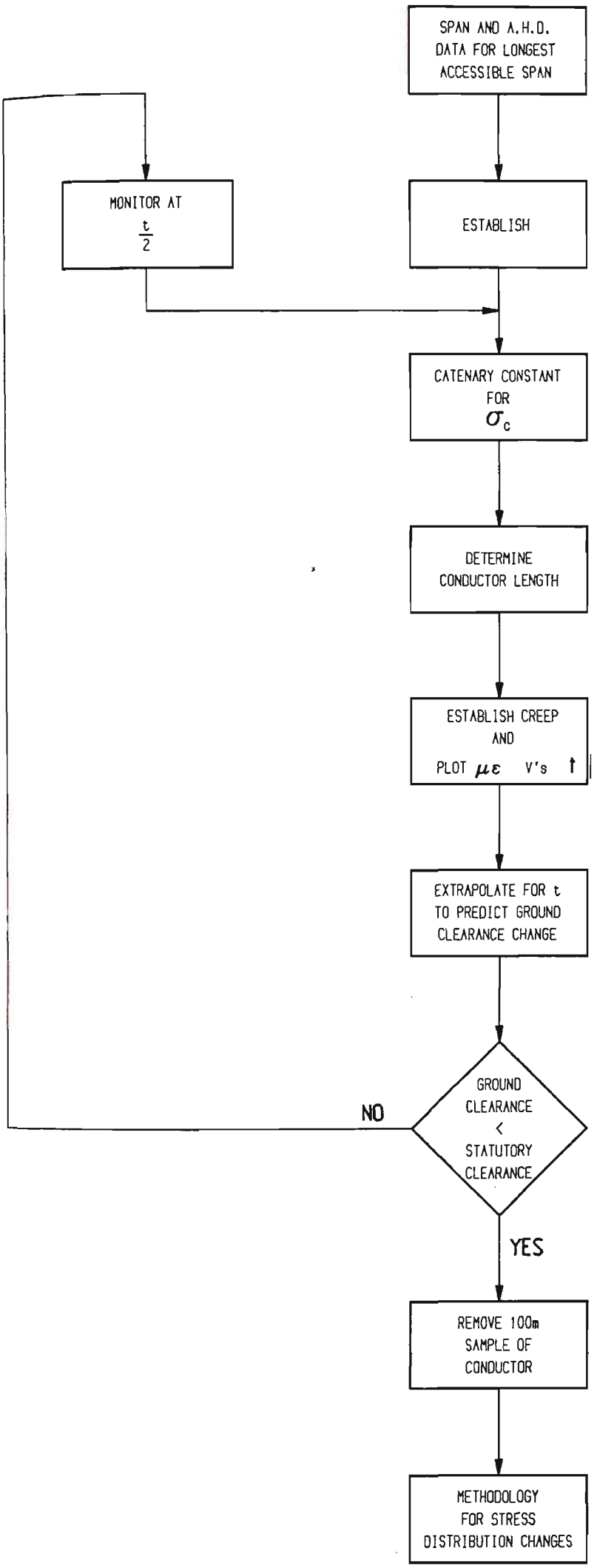

FIGURE 3.38 METHODOLOGY FOR TESTING CREEP IN AGED CONDUCTORS

Evidence of such damage is the pitting and deposit of arc products and discolouration of the conductor. The effect of this degradation is the reduction of cross sectional area, localised annealing, wire breaks and even conductor failure.

Remedial action depends on the nature and extent of the damage and may range from the application of repair rods to the replacement of the damaged sections of conductor.

3.6.6 Mechanical

Degradation due to a mechanical source resulting in the failure of the conductor is generally attributed to flying objects coming in contact with the conductor. In rare circumstances, structure or foundation failure may be attributed to conductor failure.

In this situations the conductor is likely to sustain considerable mechanical damage and may even fail. Depending on the magnitude of the forces of the failure, necking damage may have occurred in the affected section of conductor. This effective cross sectional area reduction will reduce the mechanical integrity of the transmission line, consequently it is considered prudent to replace the affected sections of conductor.

3.6.7 Stress Distribution Degradation

With time, the stress distribution of the aluminium and steel wires in an ACSR construction changes. At high transient mechanical loads the aluminium wires will permanently elongate at a greater rate than the steel wires. When the transient mechanical load is removed, the aluminium wires can be longer than that of the steel thus the conductor will not share the applied stress appropriately. Accordingly, the steel wires may be in a situation of being overloaded even though the conductor ultimate tensile strength has not been degraded.

The advantage of such changes occuring is the resultant coefficient of thermal expansion being two thirds that of the ACSR construction at high temperature and corresponding low stress levels. In other words, the ACSR construction develops a coefficient of thermal expansion of steel because the steel is the only component that is mechanically loaded.

Unfortunately, to assess for stress distribution changes with time one needs to have bench mark values of critical strain and stress determined from of stress strain test. Manufacturing standards do not require the publication of stress strain data other than the modulus of elasticity of the composite and the components. Consequently this information is generally not available.

The only measure available to determine suspected stress distribution change is the coefficient of linear expansion test at a load corresponding to the minimum tension of maximum design temperature condition. Coefficient of linear expansion results should be similar to that determined by equation (3.33). It would seem prudent at the same time to carry out a stress strain test to establish a data base of critical stresses and strains.

Conductor sampling techniques have previously been described in section 3.2. It is emphasised that without proper sampling techniques, incorrect results will result as indicated in the Tomago to Taree transmission line conductor sample.

A methodology for testing for the effects of stress distribution changes is given in Figure 3.39.

3.7 CONCLUSION

A transmission line conductor having numerous span lengths, passing through varying topography, with mechanically simple but mathematically complex suspension and tension supports and exposed to the excursions of climates from low velocity winds inducing aeolian vibration to destructive winds and bushfires truly represents a complex physical and mathematical problem. In addition, the transmission line represents a large structural system incorporating conductors with a wide range of material behaviour that includes such as corrosion, annealing, fatigue and creep. In

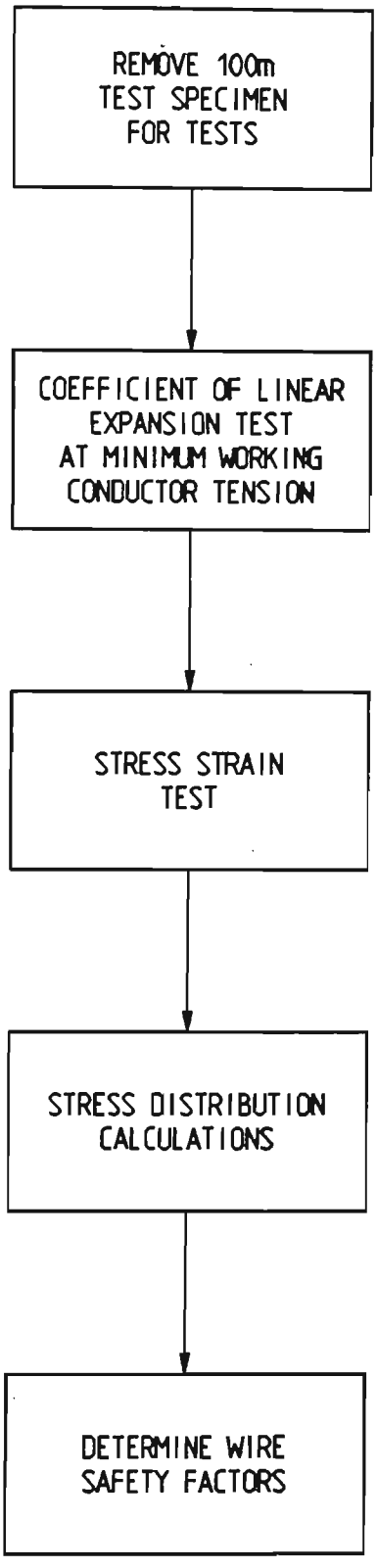

FIGURE 3.39 METHODOLOGY FOR TESTING STRESS DISTRIBUTION CHANGES IN AGED CONDUCTORS

particular in an ACSR construction, the stress in the aluminium wires decreases due to time dependent creep, inducing stress changes from the aluminium to the steel components.

It is these material properties and behavioural changes with time that are assessed for the degradation determination and the continued serviceability of aged conductors. Such deterioration assessments are carried out in several steps commencing with the most important stage, sampling.

When choosing the site for the subsequent removal of transmission line conductor sample, one must decide on a location that is representative of the exposures to the extremes of pollution and frequent low velocity winds. Topography and climatic conditions will also have a major influence on the degradation of conductor and must be included in the sampling criteria.

If it is necessary to remove other than a jumper connection, proper care must be taken to insure no wire relative movements take place prior to the cutting of the conductor. Satisfactory methods of conductor removal have been developed and described herein to ensure such movements are minimised.

Once the conductor sample is available the difficulty in assessing for the degradation of the aged conductor commences when an acceptance criteria is established. With early manufactured conductors the acceptance criteria is the appropriate manufacturing standard. In time, a data base of test

results will replace this acceptance criteria for old conductors. Conductors manufactured after the mid 80's will employ process capability studies as the acceptance criteria.

For wire tests the criteria is readily available and a methodology for assessing degradation by the mechanisms of corrosion, fatigue and annealing has been discussed and contained herein. It is unlikely that conductors with operating temperatures of less than 80^{o}C will incur annealing. Furthermore, conductors exposed to light pollution levels are not likely to deteriorate by corrosion.

Unfortunately, unlike wire data, actual conductor data other than theoretical predictions is generally not available. However test procedures have been developed herein to provide sufficient information to assess the level of degradation caused by annealing, wire stress redistribution and creep of aged conductors.

In the future, as supply authorities operate conductors at the excursions of their mechanical properties some demand will be placed on establishing actual conductor parameters. Conductor criteria such as stress strain, coefficient of linear expansion, creep, fatigue and breaking load information will become available allowing for accurate aged conductor degradation assessments.

Creep and fatigue mechanisms of conductor degradation need to be treated as design parameters rather than allowing with time a level of acceptable degradation to occur. Conductor creep testing facilities are available which permit predications of long term inelastic stretch and the necessary allowances. Differences between CIGRE predictor equations and actual

creep results are considerable placing emphasis on the need for actual conductor creep tests.

As a direct result of these studies, conductor fatigue testing facilities are now available and in the future fatigue curves (S-N) will become available. This will enable known fatigue endurance designs to be implemented.

These degradation free design philosophies aside, it is considered prudent to examine conductor samples and transmission line spans for evidence of fatigue and creep respectively. Favourable results are reassuring and a measure of successful design practises.

A summary of the degradation mechanisms and assessment for aged conductors is given in Figure 3.40.

Life expectancy models developed are simple in nature and in some instances require routine annual inspections to provide assurance of the continued serviceability and integrity of the conductor. Such inspections are useful because of the complex nature of a conductor, deterioration rates may in some circumstances be indeterminate and unpredictable.

3.7.1 Avon to Kemps Creek Transmission Line

The conductor sample tested being representative of a low pollution, environment suggested no degradation of corrosion resistance and the strength of the conductor and wire stress distribution were satisfactory. Sag measurements revealed no

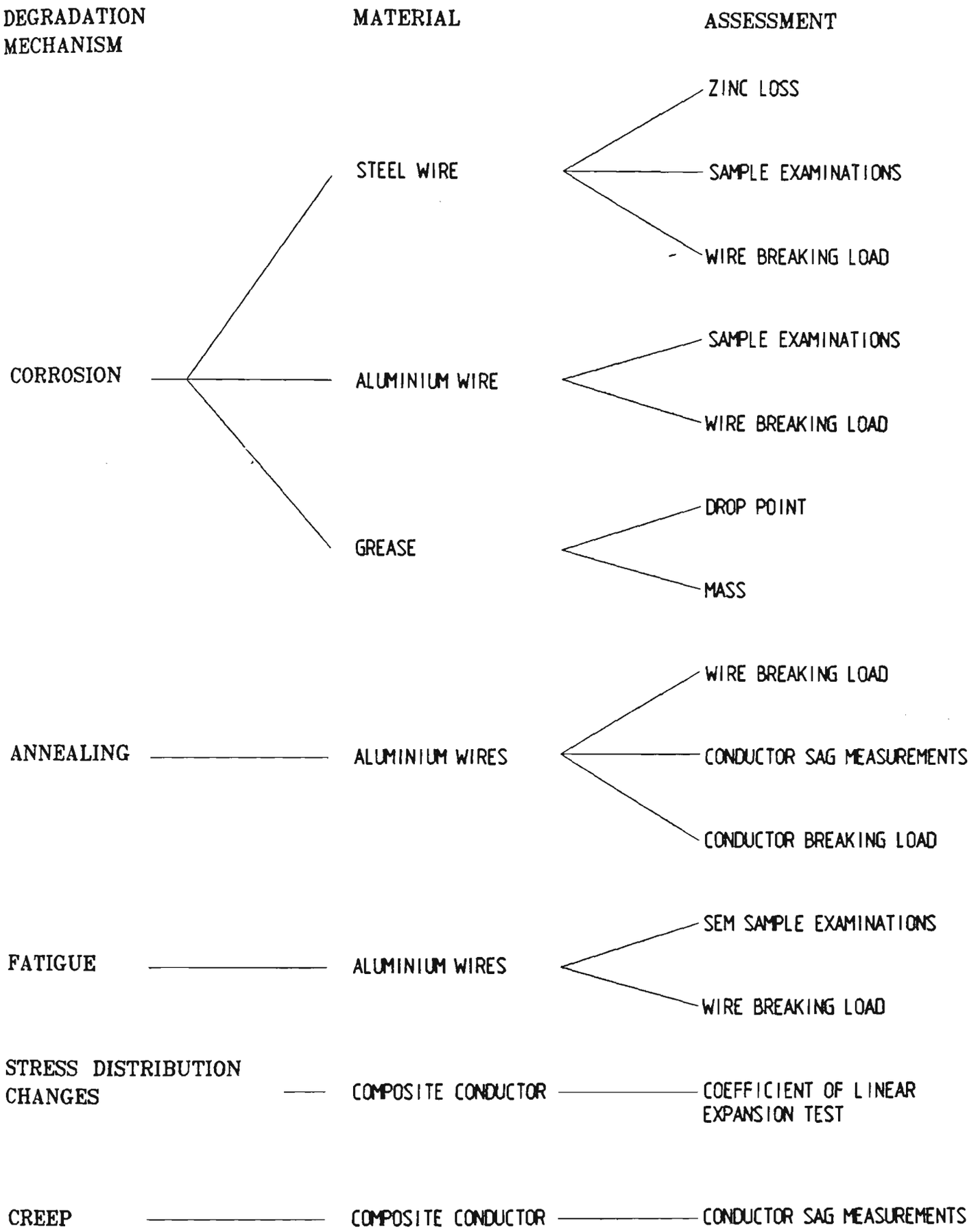

FIGURE 3.40 SUMMARY OF DEGRADATION MECHANISMS AND MENT PROCEDURES FOR AGED CONDUCTORS

significant evidence of creep deformation and wire sample examination concluded that there was minimal fretting damage and there was no fatigue crack initiation.

The drop point of the grease dictated that the operating temperature of the transmission line should be restricted to 60°C. A risk of loss of grease and accelerated corrosion may occur if operation in excess of 60°C is necessary.

Accordingly, if cumulative fatigue damage is minimal then it is expected that the transmission line conductor will remain serviceable for a further 24 years for similar operating conditions and pollution environments.

3.7.2 Dapto to Springhill Transmission Line

The conductor sample tested being representative of pollution environment suggested no degradation of corrosion resistance and the strength of the conductor and wire stress distribution were satisfactory. Sag measurements revealed no significant evidence of creep deformation and wire sample examination concluded that there was minimal fretting damage and there was no fatigue crack initiation.

The drop point of the grease dictated that the operating temperature of the transmission line should be restricted to 60°C. A risk of loss of grease and accelerated corrosion may occur if operation in excess of 60°C is necessary.

Accordingly, if cumulative fatigue damage is minimal then it is expected that the transmission line conductor will remain serviceable for a further 24 years base on similar operating conditions and pollution environment.

3.7.3 Tomago to Taree Transmission Line

Additional sampling and testing is necessary to allow more conclusive coefficient of linear expansion and breaking load test to be carried out. On the basis that the location of the sampling was unknown, one cannot assess whether the sample condition is representative of the extremes of pollution. In the absence of further tests it is concluded that:

(i) the breaking load is 83.3 kN a mechanical derating of 6.6%;

(ii) the coefficient of linear expansion for tensions less than 19.2 kN is $12.6 \times 10^{-6}.C^{-1}$;

(iii) the conductor thermal rating be restricted to $70^{o}C$. A risk of loss of tar and accelerated corrosion may occur if operation in excess of $70^{o}C$ is necessary; and

(iv) routine annual inspection policy be implemented.

Wire sample examination concluded that there was minimal fretting damage and there was no fatigue crack initiation. Accordingly, if cumulative fatigue damage is minimal then it is expected the transmission line will remain serviceable for a further 6 years

base as similar operating conditions and pollution environments. After 6 years further additional sampling is necessary to provide reassurance of the continued serviceability of the conductor.

3.7.4 Bellambi to Heathcote Transmission Line

Additional sampling and testing is necessary to allow more conclusive coefficient of linear expansion and breaking load tests to be carried out. On the basis that the location of the sampling was unknown, one cannot assess whether the sample condition is representative of the extremes of pollution. In the absence of further tests it is concluded that:

(i) the a composite breaking load test will probably not meet the minimum criteria. Accordingly, the conductor requires mechanical derating; and

(ii) the conductor thermal rating be restricted to 65^{o}C. A risk of loss of tar and accelerated corrosion may occur if operation in excess of 70^{o}C is necessary.

Examination for wire fretting was not carried out since the conductor sample was a jumper connection not subjected to aeolian vibration inducing fatigue.

CHAPTER FOUR

TRANSMISSION LINE CONDUCTOR FATIGUE

4.1 INTRODUCTION

Two approaches are possible when one designs for conductor fatigue and the appropriate conductor static and dynamic stress levels. The first approach is the fatigue free philosophy where conductor stress levels are restricted to give a predicted infinite conductor life and the second approach, is a cumulative damage approach were conductor stress levels are generally higher than the fatigue free philosophy, however known sustained fatigue damage occurs that will result in conductors having a finite life.

Both design philosophies require a knowledge of the conductor strength or fatigue characteristics known as S-N curves. In addition, the cumulative damage approach requires a knowledge of the stress or load history and a suitable cumulative damage theory.

In the past, the accepted design practise for fatigue endurance assumes an every day tension (EDT) of a conductor at approximately 20% of calculated breaking load. Limited conductor fatigue data available from overseas sources suggests the fatigue free limit of aluminium is approximately 30-40 MPa while other researchers (23) claim, a non asymptotic behaviour because of the influence of wire fretting. Further to this situation, no conductor fatigue tests have been carried out in Australia on conductors manufactured to Australian Standards.

Accordingly it is now appropriate to review the conductor every day stress design philosophies and initiate a conductor fatigue testing program for Australian manufactured conductors. The objective of these studies is as follows:

1. Examine the available conductor vibration theory;

2. Design and commission a conductor fatigue testing apparatus;

3. Initiate a conductor fatigue testing program which will enable an understanding of the effects of alloying aluminium on the fatigue limit of electrical grade aluminium; and

4. Investigate the effects of conductor fittings on the conductor S-N curves.

4.2 FUNDAMENTAL CONDUCTOR VIBRATION THEORY

4.2.1 Aeolian Vibration

When a constant velocity wind passes across a transmission line conductor under tension, vortices are detached at regular and alternating intervals from the top and bottom sides of the conductor. The rate of detachment of the vortices is a function of the wind velocity and each detachment is associated with a small vertical force induced into the conductor.

Experience has shown that conductor vibration is generated with winds having laminar flow with velocities between 0.5 $m.s^{-1}$ to 7.0 $m.s^{-1}$. Wind velocities below this regime do not have sufficient energy to produce vortex shedding and induce an alternating forces. Wind velocities above 7.0 $m.s^{-1}$ are generally turbulent in nature and do not produced the periodic vortex shedding.

The behaviour of the air flowing past a cylinder changes with the Reynolds number. The corresponding Strouhal number that covers the regime of vibration inducing wind velocities and conductor diameters is 0.185 (79). The Strouhal number is a dimensionless number that relates the medium velocity, cylinder diameter and vortex frequency or in the case of a transmission line, wind velocity, conductor velocity and vibration frequency respectively. The Strouhal number is given by the equation,

$$S = \frac{f d_c}{v} \qquad (4.1)$$

When Stroudal equation is rearranged with S = 0.185, the frequency of conductor vibration is given as,

$$f = 0.185 \frac{v}{d_c} \qquad (4.2)$$

Accordingly for large conductors and low wind velocities, low frequencies are produced, however the highest frequencies of vibration exist in small conductors at relatively high wind velocities. This relationship is illustrated in Figure 4.1 for various wind velocities.

In the case of a transmission line span with negligible damping at the support points, the vibrations will take the form of a standing wave with fixed nodes. Assuming the conductor has negligible stiffness with regard to the vibration loop length and the effect of variations in tension in a span is small than the loop length is given by,

$$L = \frac{1}{2f}\sqrt{\frac{T}{m}} \qquad (4.3)$$

The behaviour of a conductor in terms of wind velocity is predicted by substituting equation (4.2) into equation (4.3) yielding,

$$\frac{L}{d_c} = \frac{2.703}{v}\sqrt{\frac{T}{m}} \qquad (4.4)$$

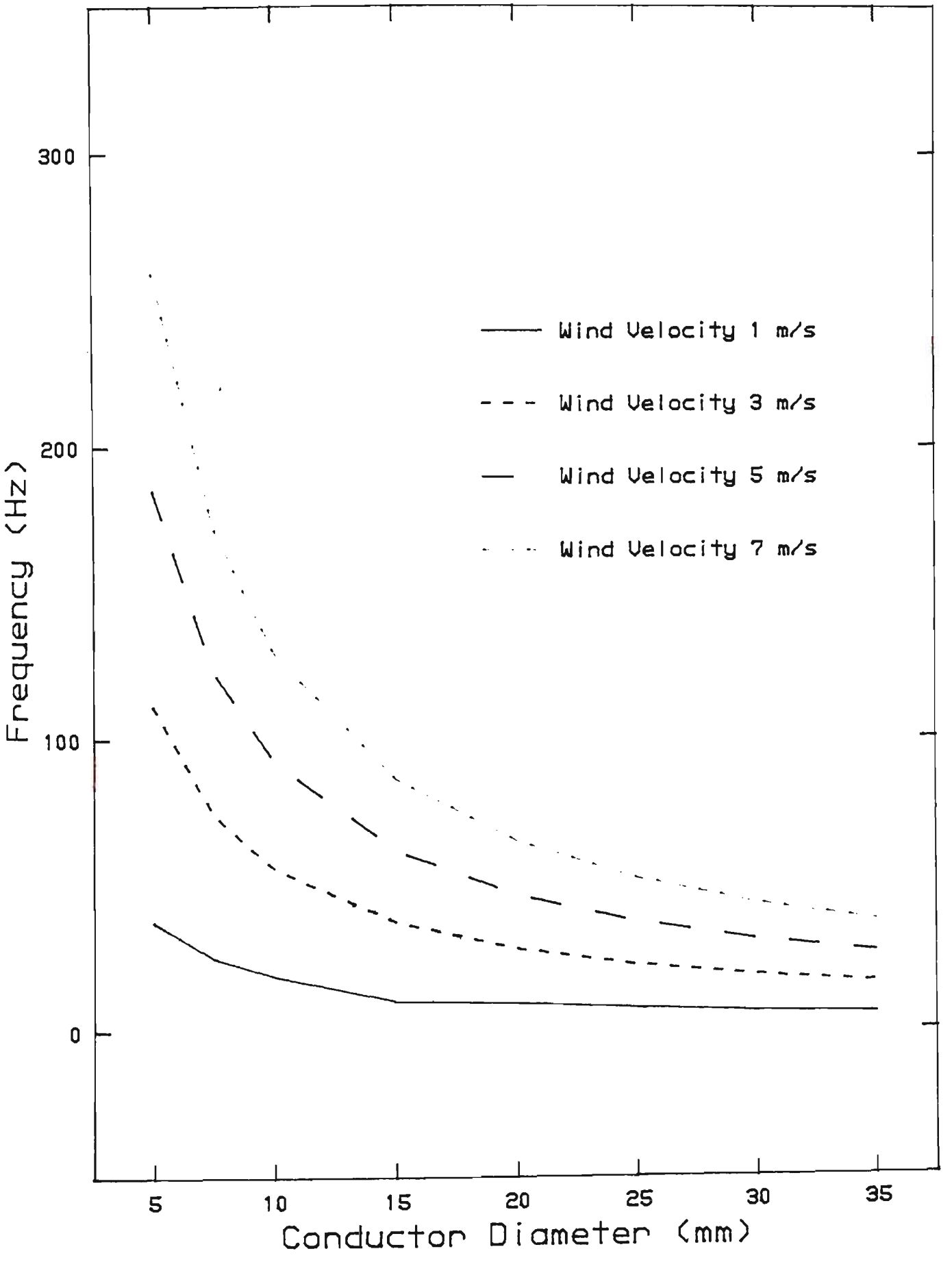

FIG 4.1 Relationship of Vibration Frequency to Conductor Diameter

Thus, for small conductors at high wind velocities, small loop lengths are generated and for large conductors and low wind velocities loop lengths can be greater than 10 m. The ratios of loop length to conductor diameter and conductor tension to conductor mass for various wind velocities is illustrated in Figure 4.2

4.2.2 Wind Velocity and Conductor Displacement Relationship

The dynamic stress in a conductor at the support point is a function of the amplitude of vibration. The amplitude of vibration of the conductor is determined from a balance of the conductor self dissipation characteristic and the wind input power. Interpretation of the input power and conductor self-dissipation is given by Diana and Alcoa, published in the Transmission Line Reference Book Wind - Induced Conductor Motion (36) and is illustrated in Figure 4.3.

An analysis of this data by plotting the Diana prediction curve with logarithmic logarithmic scales yields Figure 4.4 and has an equation, derived by linear regression analysis with a correlation coefficient of 0.9983, as

$$f = 7.509 \left[\frac{d_c}{Y} \right]^{0.4865} \qquad (4.5)$$

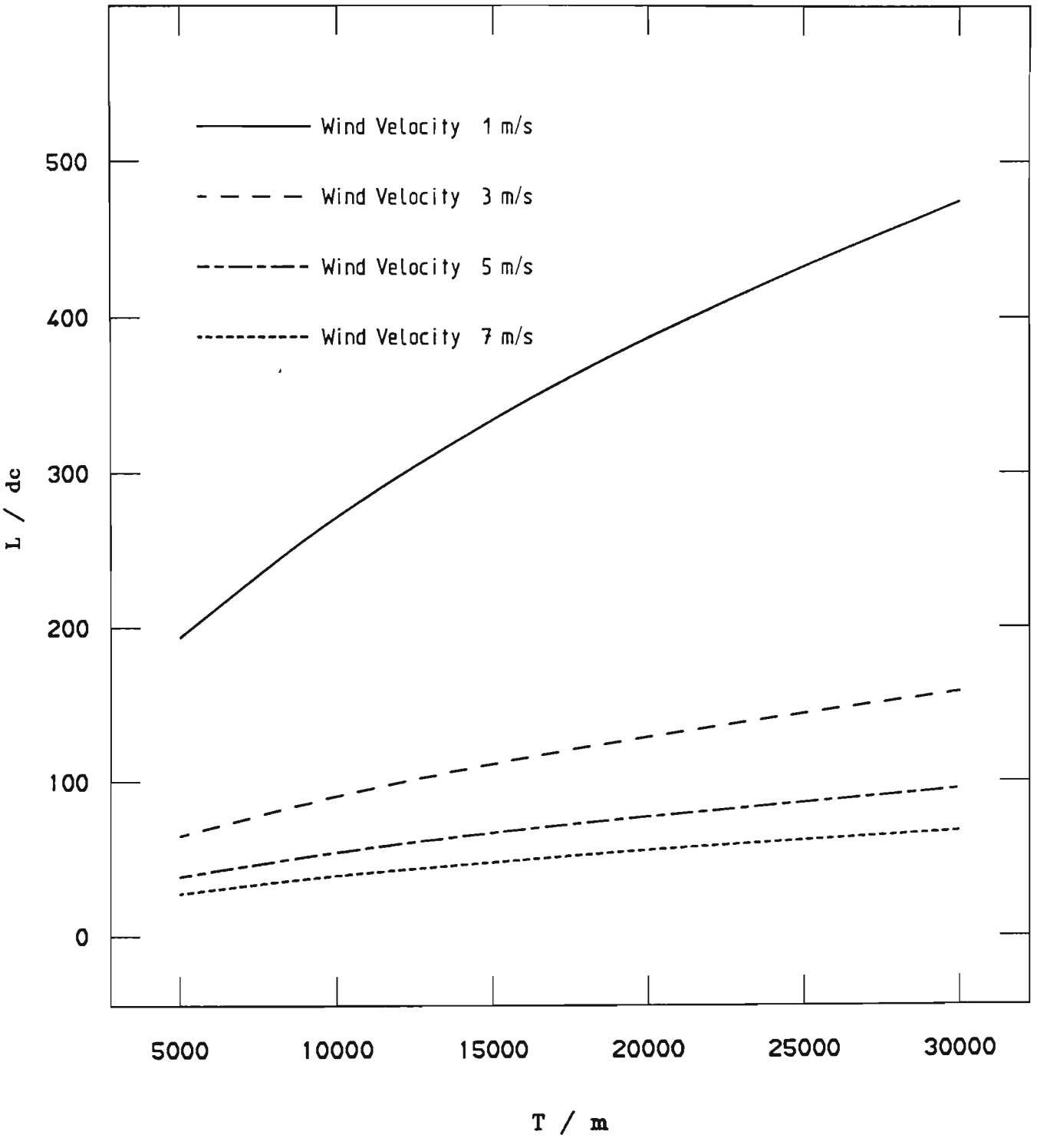

FIG. 4.2 RELATIONSHIP OF CONDUCTOR PARAMETERS TO CONDUCTOR VIBRATION LOOP LENGTH

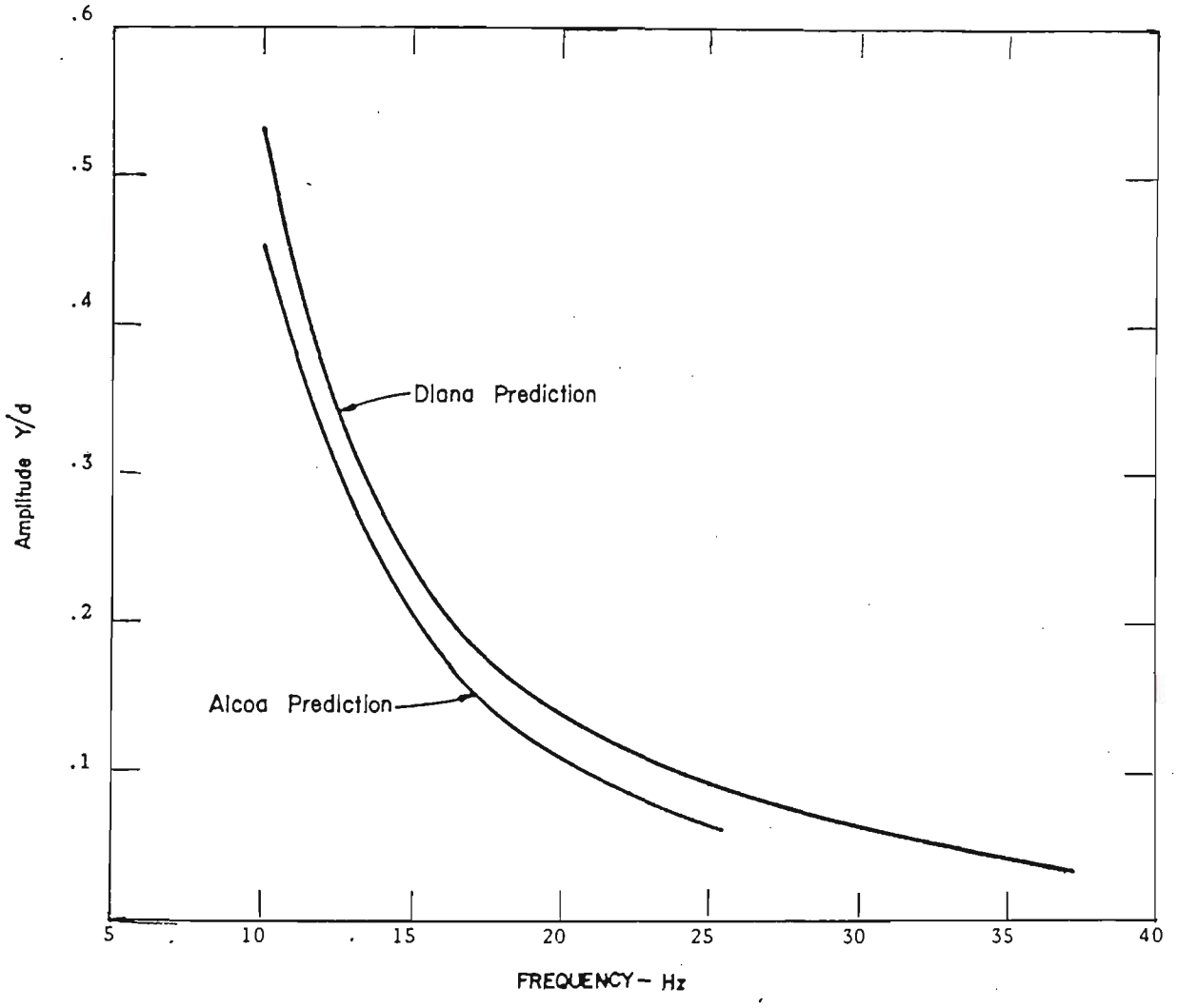

FIGURE 4.3 PREDICTED CONDUCTOR VIBRATION AND AMPLITUDE (36)

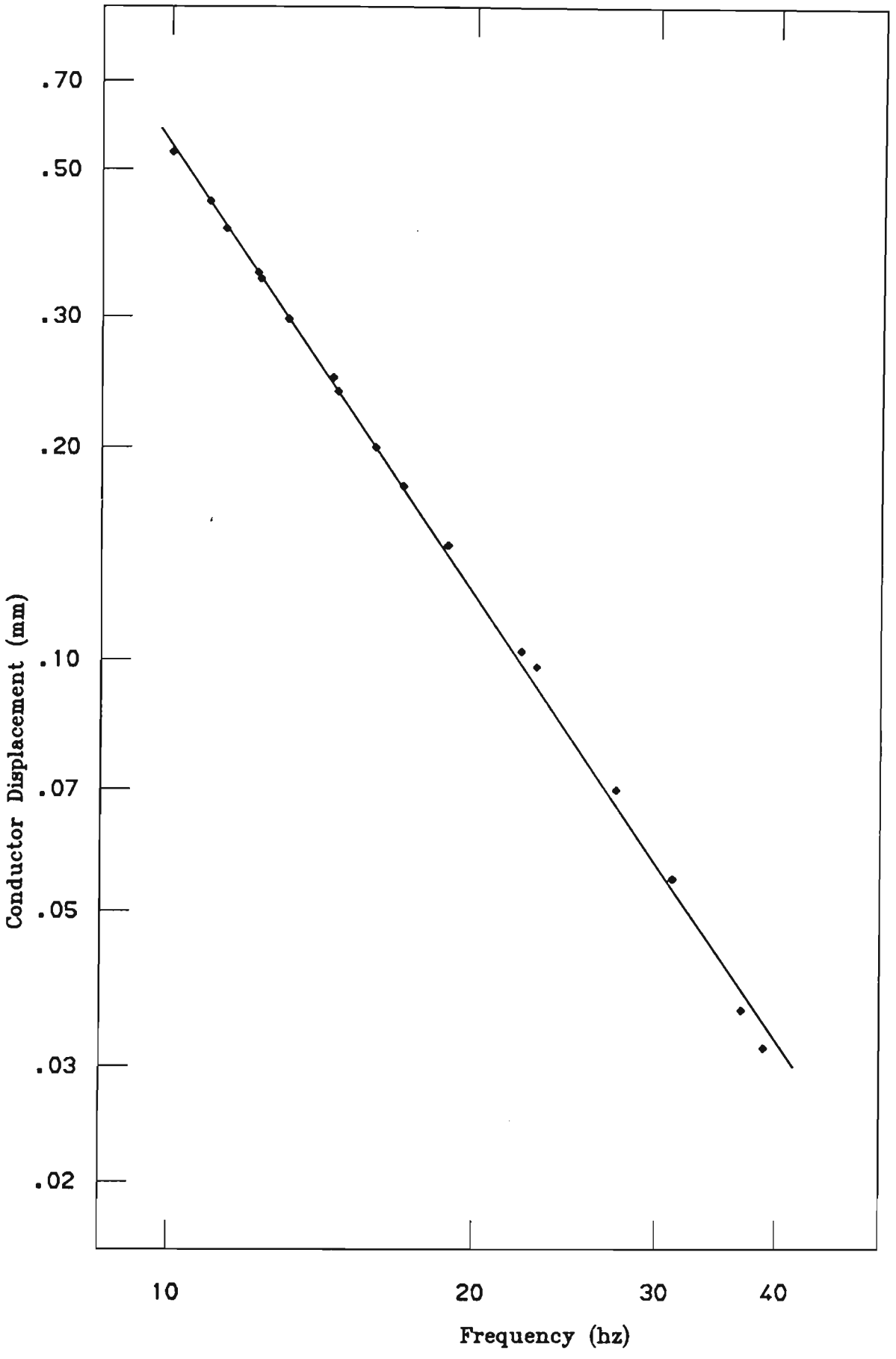

FIG. 4.4 DIANA FREQUENCY AND AMPLITUDE PREDICATION

A relationship of peak amplitude in terms of conductor diameter and wind velocity is derived by substituting equation (4.2) into equation (4.5) and is given as,

$$Y' = 1012\, d_c^{3.055}\, v^{-2.055} \qquad (4.6)$$

The conductor displacement behaviour as a function of conductor diameter for various wind velocities as given in equation (4.6) is illustrated in Figure 4.5.

4.2.3 Wind Velocity and Conductor Dynamic Stress Relationship

The fatigue of aluminium wires is generally attributed to the dynamic stress induced by aeolion vibration. The addition of the static load stress to the dynamic load stress makes the top of the conductor at the support point, the site most likely to sustain fatigue.

An equation to describe the dynamic stress in the top wires of the conductor at the conductor support as a function of the conductor mid loop displacement was derived by Claren and Diana (30) and is given as,

$$\sigma = \pi\, d_w\, E_a \sqrt{\frac{m}{EI}}\, f\, Y' \qquad (4.7)$$

By substitution of equations (4.2) and (4.6) into equation (4.7) the conductor dynamic stress in terms of wind velocity is given as,

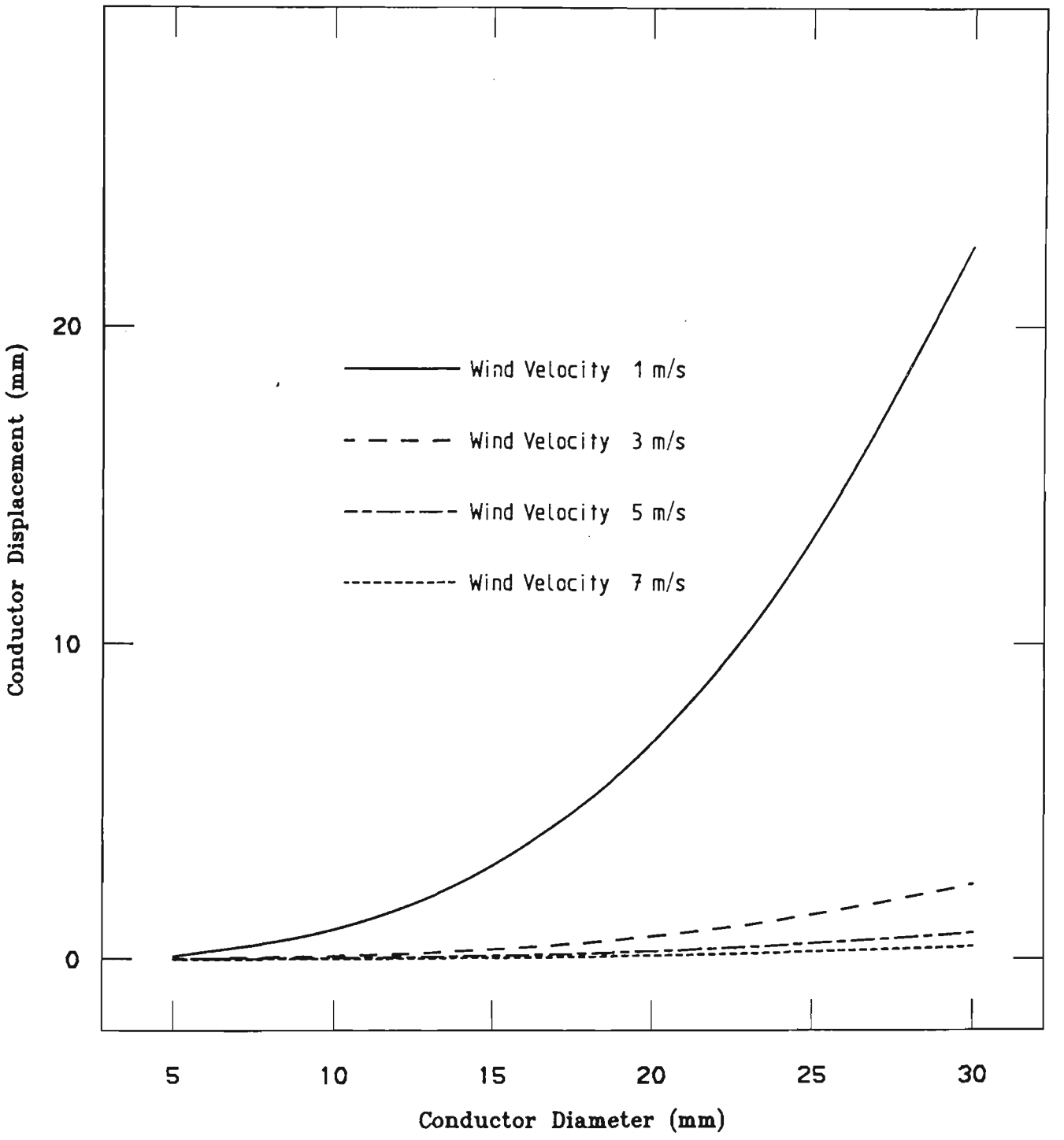

FIG. 4.5 RELATIONSHIP OF CONDUCTOR DEFLECTION TO CONDUCTOR DIAMETER

$$\sigma_w = 588\, d_a E \sqrt{\frac{m}{EI}}\, d_c^{2.055}\, v^{-1.055} \qquad (4.8)$$

All conductors have self damping characteristics that vary with size and construction parameters. The self clamping characteristics of a conductor decreases as tension increases. It is interesting to note that using the Diana predication of Figure 4.3 to derive the dynamic stress equation (4.8), the conductor tension is not a critical factor.

The conductor dynamic stress is a function of the flexural rigidity (EI) of the conductor. Two models may be employed in evaluating the flexual rigidity of a conductor,

1. the wires act individually and independent from one another with no friction between the wires; and

2. the wires act as a solid homogenous body.

In practise the conductor behaviour will vary within these models for a given span. At the suspension site the conductor will act as a homogenous body and the flexural rigidity will be a minimum. Away from the suspension site the wires have two degrees of freedom longitudinal and radially, hence the wires will act individually and the flexural rigidity will be at a maximum.

A comparison of calculated values with experimental values given by Gopolan (45) suggests that an appropriate value of half the maximum flexural rigidity should be employed for designs at the suspension site.

The minimum flexural rigidity for an ACSR construction is given as,

$$EI_{min} = n_s E_s \frac{\pi d_s^4}{64} + n_a E_a \frac{\pi d_a^4}{64} \qquad (4.9)$$

and the maximum flexural rigidity is given as,

$$EI_{max} = \sum_{j=1}^{N_i} \left[\sum_{i=1}^{n_j} E_{ij} \frac{m_{ij} \pi d_{ij}}{8} \left[\frac{d_{ij}^2}{8} + r_{ij} \right] \right] \qquad (4.10)$$

Typical values of flexural rigidity of transmission line conductors are given in Table 4.1.

Conductor		Flexural Rigidity ($N.m^2$)	
Code Name	Stranding	min	max
Grape	30/7/2.50	6.50	243
Lemon	30/7/3.00	13.50	505
Lime	30/7/3.50	25.0	935
Mango	54/7/3.00	20.0	1340
Orange	54/7/3.25	27.5	1850
Olive	54/7/3.50	37.0	2490

TABLE 4.1 - TRANSMISSION LINE CONDUCTOR FLEXURAL RIGIDITY

4.2.4 Conductor Displacement and Dynamic Stress Relationship.

In contrast to the design dynamic stress equation (4.8) in terms of wind velocity, Poffenberger and Swart (67) derived an equation which relates conductor displacement adjacent to the conductor support to the conductor stress. This relationship is used in conjunction with displacement transducers fitted to the suspension point to record conductor deflection.

The dynamic stress in the top surface of the conductor at the suspension point as a result of deflection y_a at A distance from the suspension point is given as,

$$\sigma'_d = \frac{1000\, y_a\, d\, E_c\, a}{2j^2 \left[e^{-A/j} - 1 + A/j \right]} \qquad (4.11)$$

where

$$j = \sqrt{EI/T} \qquad (4.12)$$

The international accepted distance A is 3 1/2 inches or 89 mm.

Equation 4.11 is used to determine the conductor dynamic stress for all fatigue tests results given in Appendix 4.

4.2.5 Conductor Static Load Stresses

The conductor static load stress consists of two components, the stringing stress and the bending stress over the suspension clamp.

The aluminium wire stringing stress is simply given as,

$$\sigma_a = \sigma \frac{A_a E_a}{A_c E_c} \qquad (4.13)$$

and the bending stress over the suspension clamp (35) is given as,

$$\sigma_b = \frac{E_a c}{R} \qquad (4.14)$$

The bending stress is a function of the inverse of the conductor radius. Thus if the radius is small the resultant bending stress is large. An overall interpretation of equations (4.13) and (4.14) suggests that as conductor tension is increased, the mean stringing stress increases however the bending stress decreases. Such net effects have been revealed in fatigue test results (34) and described as,

> "the level of tension in the conductor seems to have little effect upon the S-N relationship given the conductor and its supporting clamp."

4.3 FATIGUE CHARACTERISTICS OF CONDUCTORS

4.3.1 Fatigue Properties of Aluminium

In high purity form, the aluminium is a soft and durabile material and is generally classified by two main groups of manufacturing process, wrought and cast. In the commercially pure form aluminium has a tensile strength of approximately 90 MPa (2).

Several metallurgical factors contribute to the overall strength of fully annealed aluminium. These include solid solutions hardening, cold working and precipitation hardening.

Three aluminium and aluminium alloy parent materials are used to manufacture conductors namely 1350, 1120 and 6201A. The chemical composition of the aluminium and aluminium alloys is given in Table 3.18.

Aluminium 1350 is the electrical grade aluminium characterised by excellent corrosion, resistance, high thermal and electrical conductivity, low mechanical properties and excellent work ability. The conductivity of aluminium 1350 is 61.0% IACS, the ultimate tensile strength is in the range of 159-188 MPa and maximum resistivity of 0.0283 μ.m (53).

Aluminium alloy 1120 is a relatively high purity aluminium alloy containing small additions of copper and magnesium and has similar properties of 1350 aluminium. The conductivity of aluminium alloy 1120 is 59.0% IACS, the ultimate tensile strength is in the range of 230-250 MPa and maximum resistivity of 0.0293 μ.m (53).

Lastly, aluminium alloy 6201A contain small additions of silicon and magnesium which enables heat treatment, while precipitation hardening is achieved by a combination of cold working and heat treatment. The magnesium silicon alloys possess good formability and corrosion resistance with medium strength and electrical properties. The conductivity of 6201A aluminium alloy is 52.6% IACS, the ultimate tensile strength is of the order of 315-325 MPa and maximum resistivity of 0.0328 μ.m (53).

Fatigue endurance is related to tensile strength suggesting that the aluminium alloys have better fatigue characteristics than the electrical grade aluminium. Fatigue curves for commercially pure aluminium tend to be asymptotic and the Electric Power Research Institute (35) suggested that,

> "in general, it may be said that for heat treatable alloys a fatigue limit is doubtful; whereas, for non-heat-treatable alloys there is possibly a definite fatigue limit."

The fatigue limit of aluminium is expressed as the fatigue strength at $5x10^8$ cycles. In addition, the fatigue ratio (ratio of fatigue strength to ultimate strength) for 1350 and 1120 aluminium lies between 0.45 and 0.60.

However this fatigue ratio has to be addressed in the context of the conductor fatigue mechanism.

4.3.2 Conductor Fatigue Mechanism

It is generally accepted that any fatigue mechanism consists of two stages, crack nucleation and crack propogation.

The probability of the crack nucleation depends on the combination of stress and strength factors. The stress factors are the presence of stress concentration, temperature and stress combinations. The strength factors are the grain size effects, surface finish and notch effects.

In a conductor the process of crack nucleation is influenced by the repetitive dynamic stress action on the aluminium wires and the fatigue characteristics of aluminium.

It has been previously discussed that a constant wind velocity passing over the conductor induces an alternating vertical motion in the conductor. The normal mode shape for other than at the support locations is approximately a sine wave. At the support locations, due to the partial rigidity of the conductor, distortion of the mode shape occurs. The addition of the bending

stress over the suspension clamp to the static load stress and the dynamic load stress makes the top of the conductor at the support point, the site most likely to fatigue.

Other factors such as the additional tension caused by the increased length of the curved form of the vibrating loop, bearing stress due to the conductor mass and bearing stress due to radial clamping pressures are considered small, however they will aggravate and accelerate the fatigue action.

The dynamic motion of the conductor is responsible for an additional longitudinal force in the wires of the conductor. When the longitudinal force is sufficient to overcome the frictional and compressive force of adjacent wires, small longitudinal movements will occur. Since the dynamic motion of the conductor is cyclic, the longitudinal movements will be cyclic. Fretting is a particular type of damage which occurs when two surfaces in contact, experience slight relative motion and such motions can often be only a few microns.

In the free loop the longitudinal movement is not large enough to overcome the friction and compressive force, so no movement of the wires will occur. However, in the region adjacent to the suspension site, longitudinal movements will occur and for this reason fretting damage is only found a short distance on either side of the suspension site. Other sites, such as at the location of vibration dammper and mid span spacers may also experience fretting damage.

Rawlins and Ficke (41) suggested that the fretting occurs in a series of stages,

> "In the first stage, surface oxide films are disrupted and bare metal rubs against bare metal. Minute projections from one metal surface become welded to similar asperities of the other metal surface. When the two metal surfaces move relative to each other, the weld junctions are broken. Because the tips of the asperities had been distorted before the welds were established, however, they were work-hardened and are somewhat stronger than the bulk material. The welds break, therefore, not at the weld injunction itself, but slightly back from the junction. Metal is transferred from one surface to another.
>
> Continued welding and breaking-off of asperities between mating parts leads to transfer of the material alternately from one surface to the other. Gradually, a layer is built up on the material surface composed of the remnants of the asperities which have been passed back and forth."

A by product of the fretting action is the immediate replacement of newly exposed aluminium surface with a fresh coating of aluminium oxide. This aluminium oxide is harder than the parent material and will probably accelerate the fretting action. Further fretting will dislodge the aluminium oxide and evidence of fretting fatigue is quite often indicated by the accumulation of aluminium oxide (black powder) in the region of the suspension point.

Classical wire fretting is illustrated in Plate 4.1 for Neptune 19/3.25 AAC construction.

PLATE 4.1 FRETTING FATIGUE
19/3.25 AAC CONSTRUCTION

The cyclic action of the wires on the microscopic cracks will cause

> "highly localised plastic deformation at the crack tips. If the fatigue deformation becomes large enough, a fatigue crack may nucleate and eventually propogate throughout the wire". (35)

The mulitple initiation of fatigue cracks in the fretted areas and propogation at 45^{o} to the stress axis is common feature of fretting fatigue. This is illustrated in Plate 4.2 and previously illustrated in Plate 3.7.

The action of wire fretting has a significant impact on fatigue curves and this illustrated in Figure 4.6 (29).

Unfortunately little quantitiative information is available on the relative duration of crack nucleation and crack propogation. However, prediction of wire failure can be achieved by a cumulative damage theory.

4.3.3 Cumulative Damage Theory

Several cumulative damage theories are available and most theories generally assume that,

1. Operation at any given cyclic stress amplitude will produce fatigue damage;

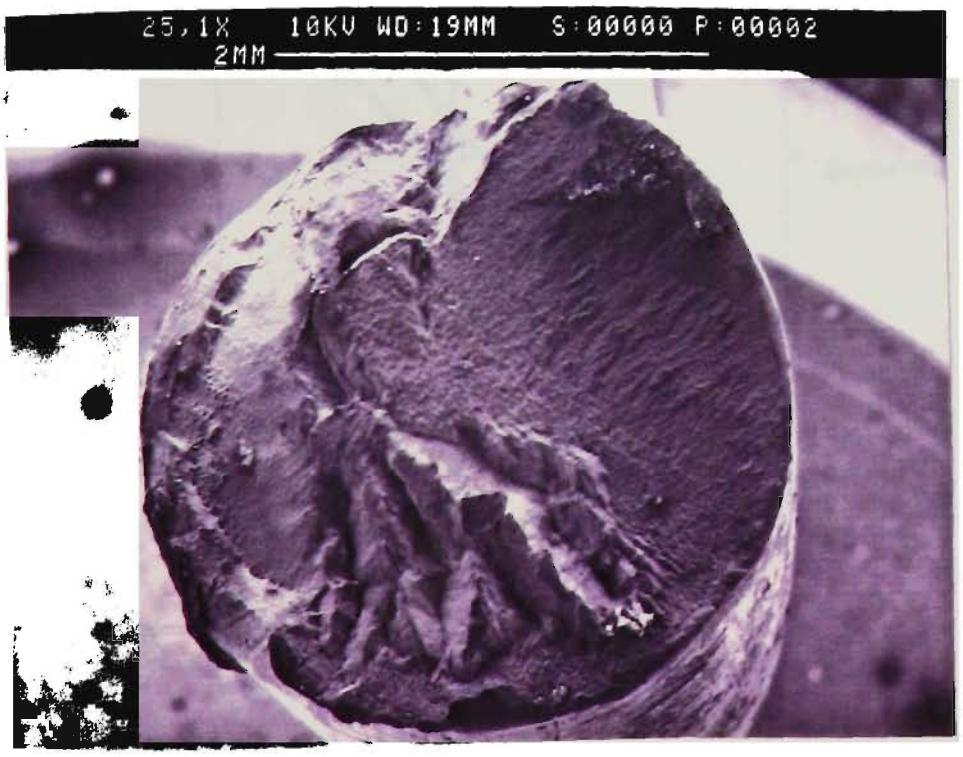

PLATE 4.2 FATIGUE FAILURE
19/3.25 AAC CONSTRUCTION

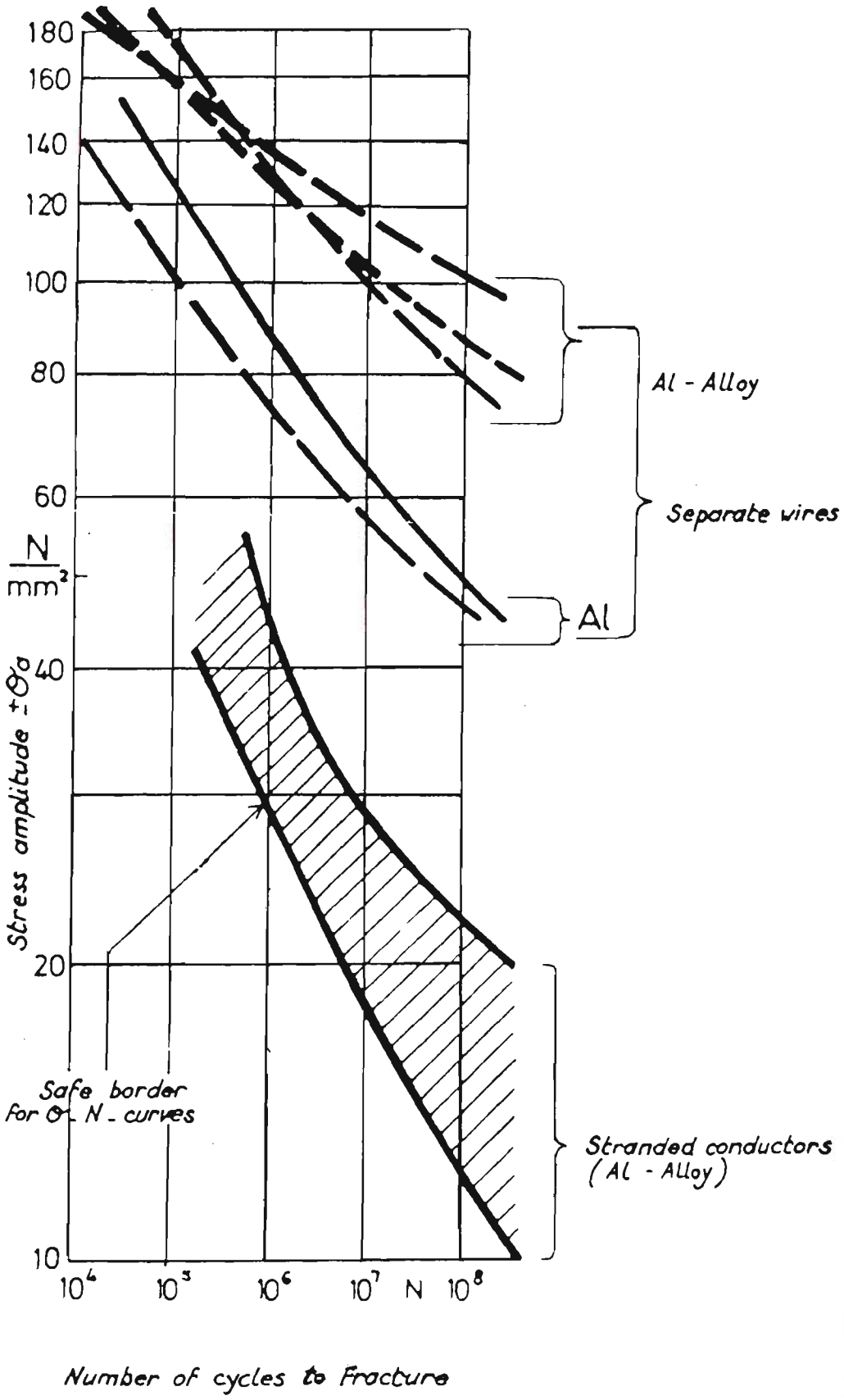

FIGURE 4.6 FATIGUE CURVES OF SEPARATE WIRES AND STRANDED CONDUCTORS (29)

2. Damage incurred is permanent; and

3. Exposure to several differing stress levels will result in an accumulation of total damage equal to the sum of the damage increments accrued at each individual stress level.

Miner's cumulative damage theory (58) has been shown to be a valid cumulative fatigue damage model for conductor fatigue tests carried out as part of EPRI's research efforts (35).

Miner's theory is illustrated in Figure 4.7 and is simply given as

$$\frac{n_1}{N_1} + \frac{n_2}{N_2} + \cdots\cdots\cdots + \frac{n_n}{N_n} = 1 \qquad (4.15)$$

In addition to the previous mentioned assumptions, Miner followed four additional assumptions to validate the theory,

1. the loading cycle is sinusoidal;

2. the total amount of work that can be absorbed produces failure (that is no work hardening occurs);

3. the relationship between various stress ratios is approximately as described by the modified-Goodman relationship and S-N experimental work;

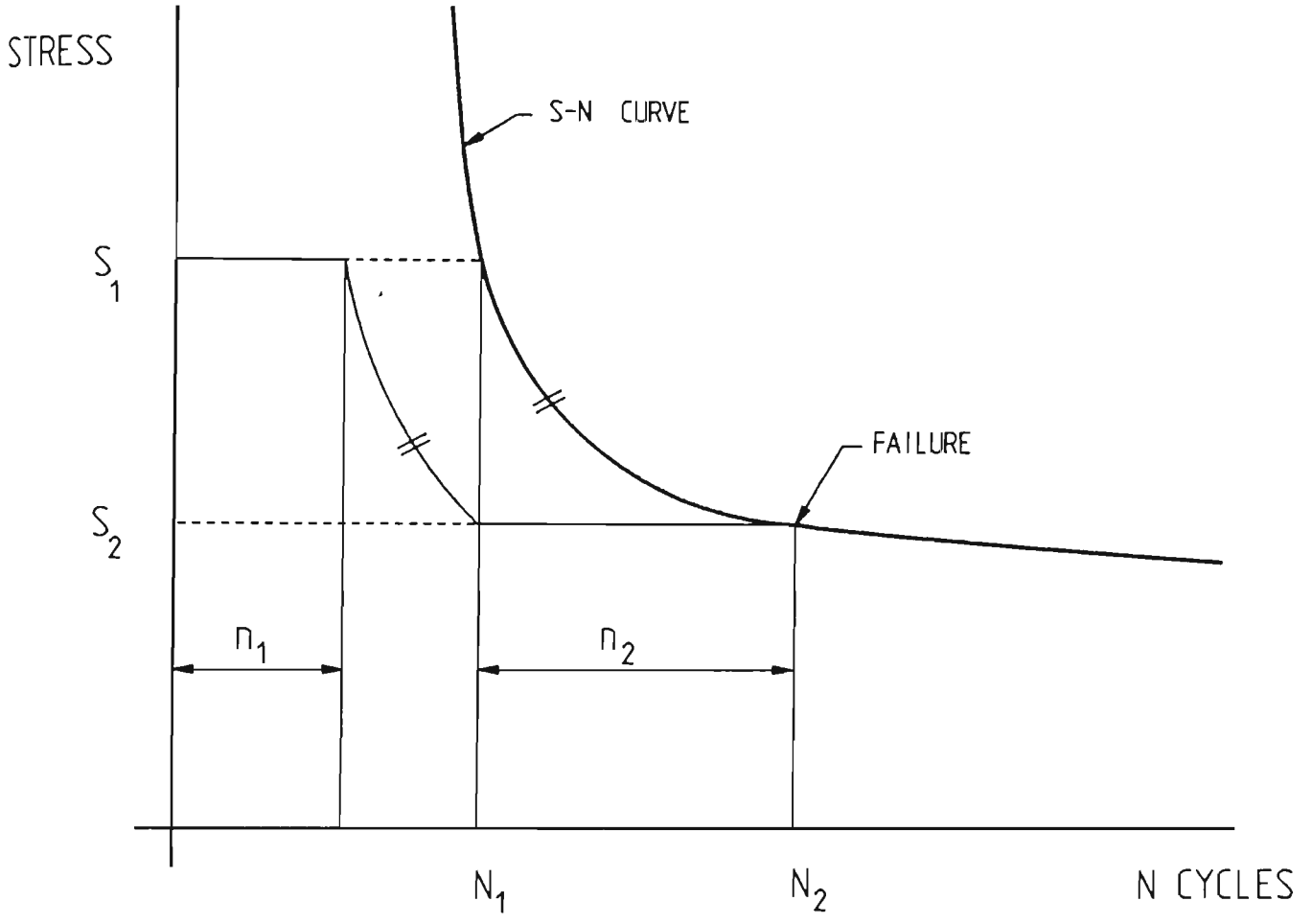

FIGURE 4.7 MINERS CUMULATIVE DAMAGE THEORY

4. the inception of a crack when observed is considered to constitute a failure.

The later assumption is difficult to detect in a conductor fatigue test because of the very nature of the test and the sample. This implies that for a conductor the sum of cumulative damage is likely to be greater than one.

In addition some evidence exists (35) that the load sequence can affect the life predications by the Miner's Theory.

4.3 FATIGUE TESTS

The primary objective of this part of the study was to design and Commission a conductor fatigue test apparatus that would induce aeolian vibration standing waves into conductor samples.

4.3.1 Test Apparatus

The test apparatus consists of 15 metres bench manufactured from a redundant overhead crane I steel section. At each end of the bench a pulley arrangement provides a mechanical connection between the conductor sample and an adjustable static mass. The static mass provides the conductor static tension. The static mass consists of a fixed steel mass of approximately 250 kg and adjustable mass of up to 1000 kg. The adjustable mass generally consists of a combination of sand and water. Plates 4.3

PLATE 4.3 GENERAL ARRANGEMENT OF CONDUCTOR FATIGUE TESTER

illustrates the general arrangement of the fatigue test apparatus and the static mass arrangement.

Mounted on the bench is two moveable conductor termination blocks and a movable conductor mechanical actuator.

The conductor termination block is in two parts that permits disassembly to allow conductor samples to be loaded and unloaded from the test bench. To prevent metal to metal contract, nylon sleeves are used as means of mechanically insulating the conductor sample and the termination block. The conductor termination arrangement is illustrated in Plate 4.4.

A similar arrangement of mechanically insulating the conductor is used at the mechanical actuator. The mechanical actuator consists of a 1 kV 3 phase motor, a five speed adjustable pulley, an offset cam, a drive shaft and a yoke plate mounted on linear bearings. Like the termination block, the yoke plate is in two parts that permits loading and unloading of conductor samples. The conductor mechanical actuator is illustrated in Plate 4.5.

In addition to the speed adjustable pulley an electronic speed controller allows precise vibration frequency settings in the range of 1 Hz to 50 Hz.

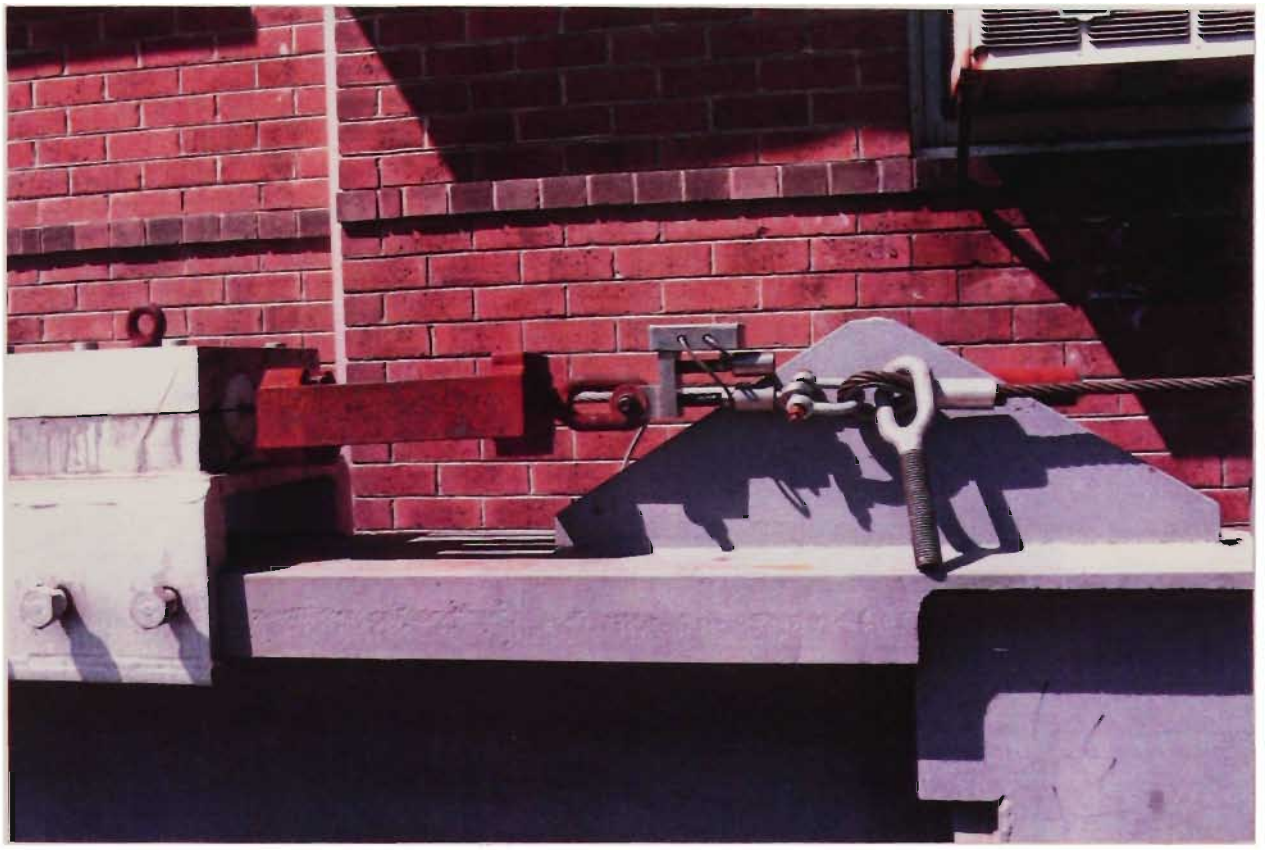

PLATE 4.4 CONDUCTOR TERMINATION BLOCK AND STATIC STRESS STRAIN GAUGE ARRANGEMENT

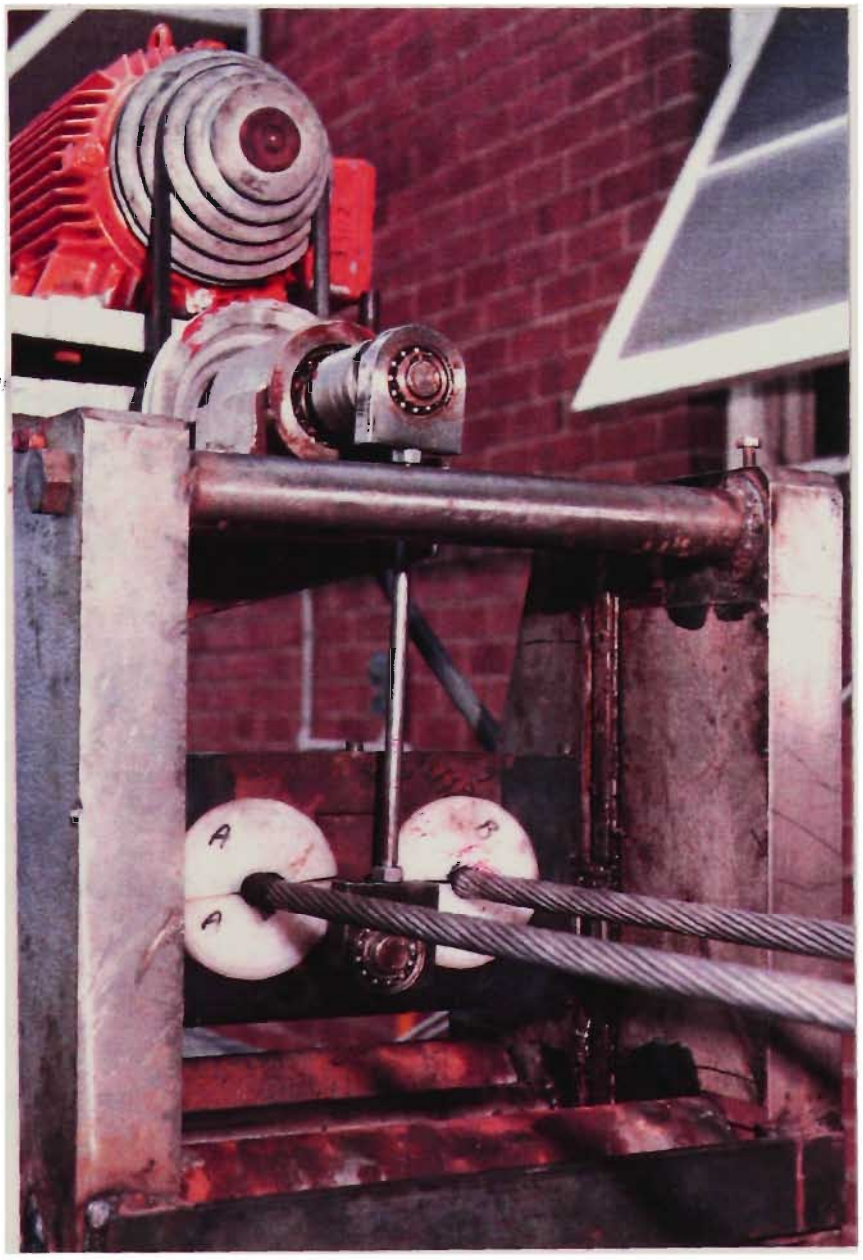

PLATE 4.5 CONDUCTOR FATIGUE TESTER
CONDUCTOR MECHANICAL ACTUATOR

Conductor standing wave deflection is controlled by precisely locating the termination blocks and the mechanical actuator. Further adjustments of offset cam and vibration frequency also allows accurate deflection control.

4.3.2 Instrumentation

4.3.2.1 Wire Break Detection

The wire detection system was designed to perform two critical functions, detect breaks of wires without test interruption and provide a reference time of each break, hence the number of cycles to each break.

Resolving the tensile force in the conductor results in three components, the tensile force in the wire, the force vertical to the axis and the force producing torque around the axis. These forces are illustrated in Figure 4.8. The torque on the wire at radius r is given as,

$$M = T_4 r = T r \sin \theta \cos \theta \qquad (4.16)$$

or in terms of individual stresses on the wire assuming the simple homogeneous conductor case (that is $T = \sigma a_c$) is given as,

$$M = \sigma a_c r \sin \theta \cos \theta \qquad (4.17)$$

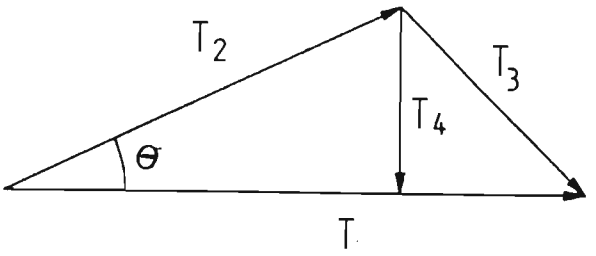

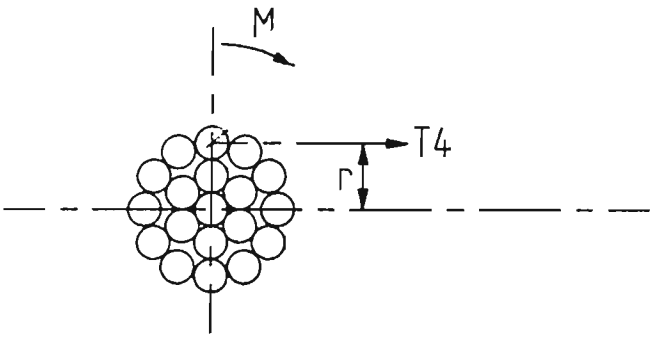

FIGURE 4.8 CONDUCTOR ROTATING TORQUE

For a multi-layer homogenous conductor with successive layers having differing lay directions and assuming a uniform stress distribution in the wires, the rotating torque is given as,

$$M = \sum_{i=1}^{n_i} \sigma_i N_i a_i r_i \sin\theta_i \cos\theta_i - \sum_{j=1}^{n_j} \sigma_j N_j a_j r_j \sin\theta_j \cos\theta_j \quad (4.18)$$

In the event of a wire break a change of rotating torque occurs. The direction of the change of rotating torque is dependent on the layer in which a wire breaks. It is this directional change that is detected via a moment arm located at node point and sensitive detection microswitches. The state of the microswitches is detected by TTL logic via an online datataker.

The wire break detection arrangement is illustated in Plate 4.6.

4.3.2.2 Conductor Amplitude Detection

To determine the conductor dynamic stress from either equation (4.7) or (4.11) it is necessary to measure the conductor amplitude at the appropriate location applicable to the equation.

Initially the conductor amplitude was determined using an accelerometer. However this method was discounted as expensive and unneccessarily complicated. Simply V-scopes were developed that enable conductor minimum peak to peak deflections of 100 μm to be measured. A range of V-scopes were developed for various

PLATE 4.6 CONDUCTOR FATIGUE TESTER
WIRE BREAK DETECTION ARRANGEMENT

deflection ranges and Plate 4.7 illustrates the V-scope measurement technique based on the image of the intersection of the apparent two triangles.

The V-scopes were attached to the conductor by means of a paper bull dog clip.

4.3.2.3 Conductor Frequency

Since the first wire break was chosen as the failure criteria of the conductor, the number of vibration cycles is recorded to allow the appropriate data point to be plotted on the fatigue curve.

Accordingly it is necessary to measure the vibration frequency and this was achieved by a combination of a proximity transducer and a spectrum analyser.

The proximity transducer was mounted adjacent to the conductor. In addition to the vibration frequency, the spectrum analyser determined the sinusoidal distortion of the induced mechanical vibration by providing the harmonic components of the vibration. Hard copies of the vibration frequency spectrum were obtained by means of an X-Y plotter.

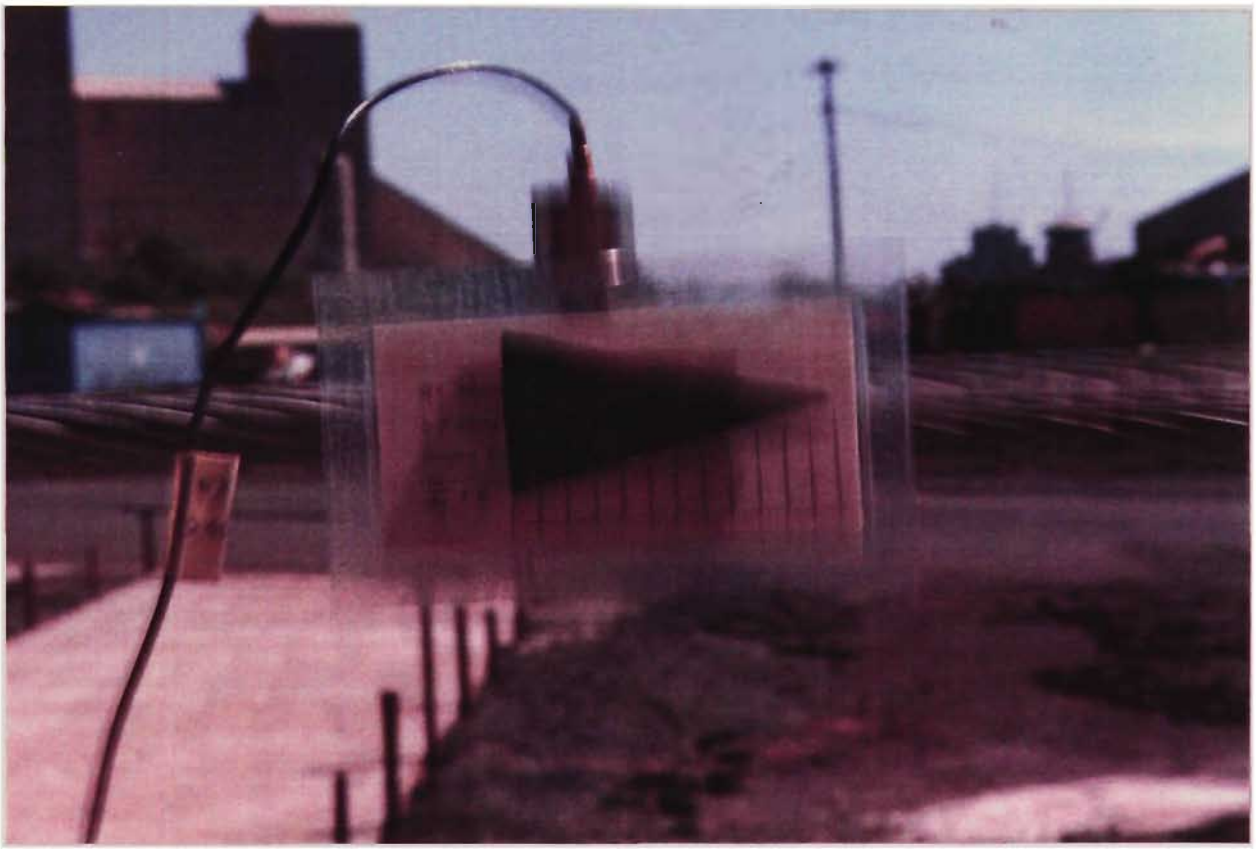

PLATE 4.7 CONDUCTOR FATIGUE TESTER
V-SCOPE MEASUREMENT TECHNIQUE

4.3.2.4 Data Logging

Data logging of wire breaks, conductor frequency and duration to wire breaks was performed by a commercially available CMOS and TTL electronic datataker. The output of the datataker was logged to an online terminal and echoed to a line printer.

4.4.4 Test Program

The test program consists of two stages, firstly to determine the fatigue free stress of aluminium and aluminium alloy conductors and secondly, to determine the effect of suspension fittings on the fatigue free stress. The details of the test program are,

1. Carry out sufficient fatigue tests to establish S-N curves for an identical conductor construction with the exception of the differing aluminium and aluminium alloys component wires namely 1350, 1120 and 6201A; and

2. Using the similar conductor construction used in the abovementioned tests, establish the effect of an armour grip suspension units, armour rods/suspension clamp combination and a suspension clamp on the S-N curves.

It was intended as part of these studies to complete stage one of the test program and establish the fatigue curves. The details of the conductors selected for the tests and the test program are given in Figure 4.10.

Paramater	Australian Standard Code Name		
	Neptune	Krypton	Opal
Mechanical			
Alloy	1350	1120	6201A
Cross Sectional Area (mm^2)	157.6	157.6	157.6
Overall diameter (mm)	16.3	16.3	16.3
Stranding	19/3.25	19/3.25	19/3.25
Mass $kg.m^{-1}$	0.433	0.433	0.433
Ultimate Tensile Strength (kN)	24.7	37.4	44.2
Final Modulas of Elasticity (GPa)	56	56	56
Coefficient of Linear Expansion ($^oC^{-1}$)	$23x10^{-6}$	$23x10^{-6}$	$23x10^{-6}$
Electrical			
Cross Sectional Area			
Aluminium	155	150	134
Copper Equivalent	94.6	88.2	70.5
Resistance DC at 20^oC	0.183	0.189	0.212
Fatigue Testing Program			
Conductor Static Tension (%CBL)	35	35	35
Dynamic Stress Range (MPa)	100-500	100-700	100-900
Maximum Test Duration (cycles)	10^7	10^7	10^7

FIGURE 4.10 - CONDUCTOR FATIGUE TEST PROGRAM

4.4.4 Test Results

The details of the fatigue test results for 19/3.25 mm 1350 AAC construction are given in Appendix Four and a summary of the test results are given in Table 4.2 and illustrated in the S-N fatigue curve of Figure 4.11.

Fatigue Test No.	Dynamic Stress MPa	No. of Cycles to failure $x10^6$
NEP/1	511	4.22
NEP/2	511	3.17
NEP/3	511	Inconclusive
NEP/4	114	10.36
NEP/5	248	10.3
NEP/6	393	6.71

TABLE 4.2 - SUMMARY OF FATIGUE TEST RESULTS
NEPTUNE 19/3.25 AAC

As a result of delays caused by fatigue failures of the testing apparatus and the tenure of the research and development secondment expiring, the condutor fatigue testing program was not completed. However it is anticipated that further funding from the Electrical Research Board may be forthcoming to complete the program.

4.5 CONCLUSION

The conductor stress consists of three primary components, stringing stress, bending stress and dynamic stress. Quantitive relationships have been presented for the stress components and in particular the dynamic

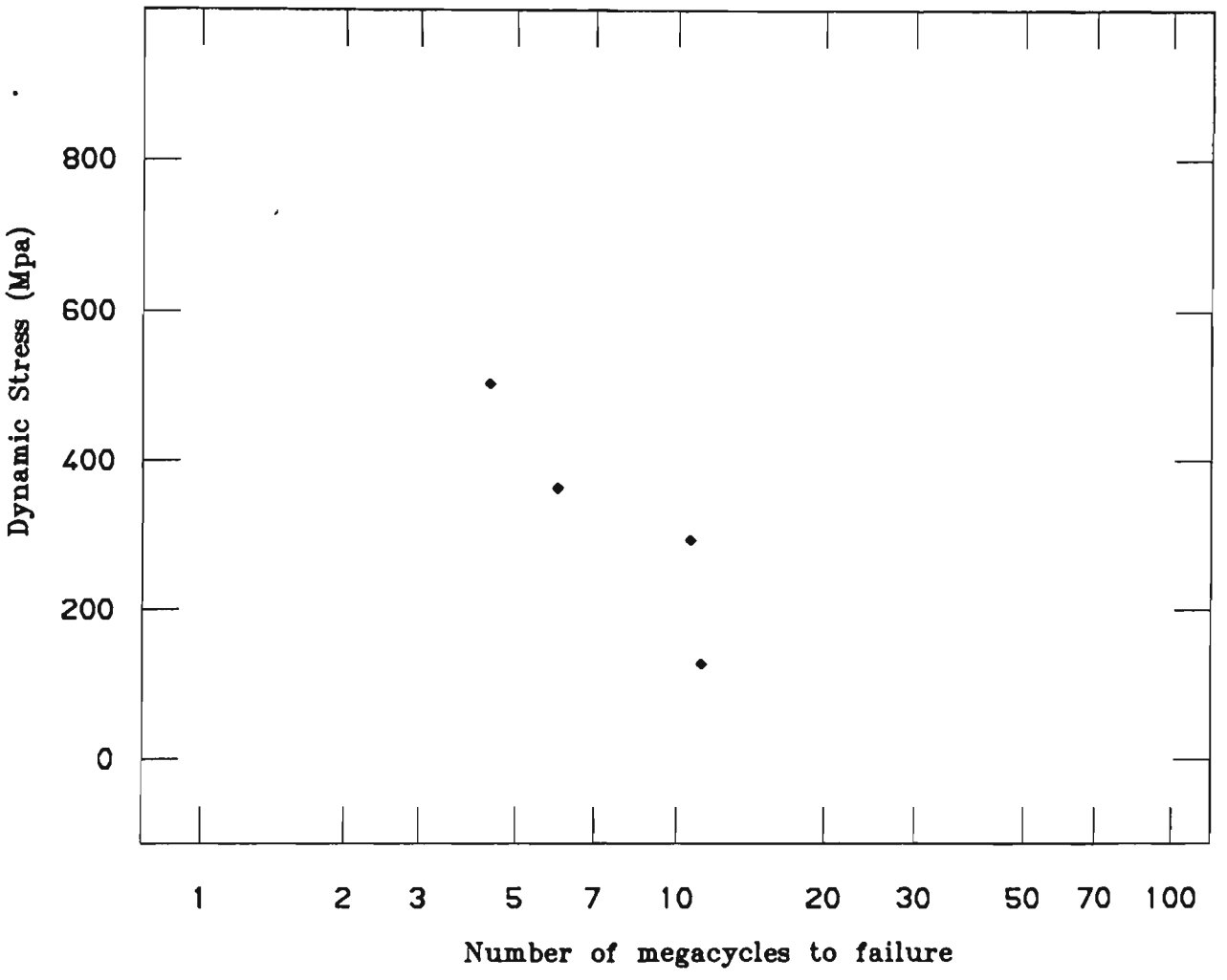

FIG. 4.11 S–N FATIGUE RESULTS
FOR 19/3.25 AAC CONDUCTOR

stress relationship as a function of wire and conductor properties and wind velocity has been derived.

It is suggested, like many researchers and is illustrated by the empirical equations presented that conductor stringing stress is not a critical factor in the fatigue design of conductors. Accordingly the stringing stress design should be based on an appropriate safety factors on aluminium wires ultimate stress, allowances for fittings and consideration given to the environmental influences.

A conductor fatigue testing apparatus was commissioned and appropriate instrumentation developed. Fatigue tests to permit the understanding of the effects of alloying aluminium on the fatigue limit of electrical grade aluminium have commenced. However, as a result of time constraints and fatigue failures of the testing apparatus, to date the fatigue limits have not been quantified.

REFERENCES

1. Alcoa Aluminimum — Graphic Methods for Sag Tension Calculations for ACSR and other Conductors. Overhead Conductor Engineering Data Section 8, Rome Cable Division Aluminum Company of America.

2. Aluminium Development Council of Australia. — Aluminium Standards and Data - Wought Products. Fourth Edition June 1983.

3. ANSI/IEEE Standard — IEEE Guide to the Installation of Overhead Transmission Line Conductors. ANSI/IEEE Std 524-1980, The Inst. of Electrical and Electronics Engineers, Dec 1980.

4. ANSI/ASTM B117-73 — Standard Method of Salt Spray (Fog) Testing.

5. Ash, D.O., Dey, P., Gaylard, B. & Gibbon, R.R — "Conductor Systems for Overhead Lines: Some Considerations in Their Selection." IEE Proc Vol 126, No. 4, April 1979, pp 333-341.

6. Australian Standard — Aluminium Conductors Steel Reinforced for Transmission Purposes. AS C75, Part 1 1963.

7. Australian Standard — Aluminium Conductors Steel Reinforced for Overhead Transmission Purposes. AS 1220, Parts 1, 2 & 3, 1973.

8. Australian Standard — Aluminium Conductors for Overhead Transmission Purposes. AS 1531, Parts 1, 2 & 3, 1974.

9. Barrett, J.S., Dutta, S. & Nigol, O. — "A New Computer Model of Conductors." IEEE Trans on PAS Vol PAS-102 No. 3, March 1983, pp 614-618

10. Barrett, J.S., Ralston, P. & Nigol, O. — "Mechanical Behaviour of ACSR Conductors." CIGRE 22-09, Ontario Hydro Canada. Paper presented to the Sept, 1982 Session.

11. Barrett, J.S. & Nigol, O. — "A New Model of AC Resistance in ACSR Conductors." IEEE Trans on PAS, Vol PWRD-1, No. 2, April 1986, pp 198-208.

12. Barrien, J. "Precise Sags and Tensions in Multiple Span Transmission Lines." Elec. Eng. Trans. IEAust, Vol EE II No.1, 1975, pp 6-11.

13. Beers, G.M., Gilligan, S.R., Lis, H.W. & Schamberger, J.M. "Transmission Conductor Rating." AIEE Trans. Pt III, Oct 1963, pp 767-775.

14. Boal, G.R. "Precise Sag-Tension Calculations of Overhead Conductors." Wire Journal, Aug 1977, pp 56-60

15. Bogardus K.O., Hunter, M.S., Holt, M. & Frank, Jr, G.R. "Effects of Prior Creep on the Tensile Properties of Cold Worked Unalloyed Aluminium."

16. Booker, J.R. "Natural Aging of Non-Energised Alumunium Conductors." IEEE Trans on PAS Vol PWRD-1, No. 4, Oct 1986, pp 269-274.

17. Boyse, C.O. & Simpson, N.G. "The Problem of Conductor Sagging on Overhead Transmission Lines." Journal of the Inst. of Elec. Eng. Vol 91, Pt II, Dec 1944, pp 219-231.

18. Bradbury, J., Kuska, G.F. & Tarr, D.J. "Sag and Tension Calculations For Mountanious Terrain." IEE Proc. C, Gen., Trans & Distrib, 1982, pp 213-220.

19. Bradbury, J. "The Creep of Steel-Cored Aluminium Conductors." Lab Report No. RD/L/R 1438 Central Electricity Research Laboratories. 31 Jan 1967.

20. Bradbury, J. "Creep of SCA Conductors at Elevated Temperatures." Lab Report No. RD/L/N 134/69 Central Electricity Research Laboratories 5 March 1970.

21. Bradbury, J., Dey, P. Orawski, G. & Pickup, K.H. "Long Term Creep Assessment for Overhead-Line Conductors." IEE Proc Vol 122, No. 10, Oct 1975, pp 1146-1151.

22. British Standard Aluminium Conductors Steel Reinforced for Transmission Purposes. BS 215 Part 2, 1956.

23. Buckner, W.F., Helm, R. Papailiou, K.O. "The Effect of Ageing of Overhead Line Conductors Due to Aeolian Vibration." Int. Conf. on Revitalising Transmission and Distribution Systems, London England, 1986, pp 39-43.

24. Cahill, T. "Development of a Low-Creep ACSR Conductor." Wire Journal, July 1973.

25. Carter, R.D. "Corrosion Resistance of Aluminium Conductors in Overhead Service." MM Metals Report released by the Aluminium Development Council.

26. Carter, R.A. & Quick, D.G. "NDT of High Voltage Transmission Lines." Non-Destructive Testing-Aust, Jan/Feb, 1979, pp23-25.

27. CIGRE Working Group 22.05 of Study Committee No. 22. "Permanent Elongation of Conductors. Predictor Equation and Evaluation Methods." CIGRE Electra No. 75 March 1981.

28. CIGRE Working Group 22.04 of Study Committee No.22 "Guide for Endurance Tests of Conductors Inside Clamps." CIGRE Electra No. 100, May 1985.

29. CIGRE Working Group 22.04 of Study Committee No.22 "Recommendation for the Evaluation of the Lifetime of Transmission Line Conductors." CIGRE Electra No. 63, March 1979.

30. Claren, R. & Diana, G. "Dynamic Strain Distribution on Loaded Stranded Conductors." IEEE Trans on PAS Vol PAS-88, No. 11, Nov 1969, pp 1678-1690.

31. Commellini, E. "Some Comments About Creep Evaluations In Overhead Line Design." CIGRE 22-72 (WG05) 03, May 1971.

32. Dwight, H.B. "Sag Calculations for Transmission Lines." AIEE Trans. Vol 45, May 1926, pp 796-805.

33. Douglass, D.A. "Radial and Axial Temperature Gradients in Bare Stranded Conductors." IEEE Trans on PAS Vol PWRD-1, No. 2, April 1986, pp 7-15.

34. Ehrenburg, D.O. "Transmission Line Catenary Calculations." AIEE Trans. Vol 54, July 1935, pp 719-728.

35. Electric Power Research Institute Conductor Fatigue Life. EPRI EL-4744 Project 1278-1 Final Report, Jan 1987.

36. Electric Power Research Institute Transmission Line Reference Book Wind Induced Conductor Motion. Based on EPRI Research Project 792 1973.

37. Electricity Development Act 1945 "Overhead Line Construction and Maintenance Regulations, 1962." NSW, as amended.

38. Elton, M.B., Hard, A.R. & Shealy, A.N. "Transmission Conductor Vibration Tests." AIEE Trans on PAS Vol 77 Pt III, Aug 1959, pp 528-537.

39. Forrest, J.S. & Ward, J.M. "Service Experience of the Effect of Corrosion on Steel Cored Aluminium Overhead Line Conductors." IEC Vol 101 Pt II No. 81, June 1954, pp 271-283.

40. Foat, D., Lin, S.H. & Carberry, R. "Signifance of Conductor Radial Temperature Gradient within a dynamic Line Rating Methodology." IEEE Trans on PD, Vol PWRD-2, No. 2, April 1987, pp 502-511.

41. Ficke, W.G. & Rawlins, C.B. "Importance of Fretting in Vibration of Stranded Conductors." IEEE Trans PAS Vol PAS-87, No. 6, June 1968, pp 1381-1384.

42. Fritz, E. "The Effect of tighter Conductor Tensions on TL Costs." IEEE Trans Paper Vol PAS 79 1960, pp 513-527.

43. Goldman, A. & Sigmond, A.S. "Corona Corrosion of Aluminium in Air." Journal of the Electrochemical Society, Dec 1985, pp 2842-2853.

44. Gouch, A.J. & Johnston, G.H. "Creep, Modulus of Elasticity and Coefficient of Thermal Expansion of Aluminium Based Overhead Conductors." MM Metals Technical Department, Report No. Development Council.

45. Gopalan, T.V. "Fatigue Damage Criterion for ACSR." IE Journal EL Vol 65, April 1985, pp 164-166.

46. Hard, A.R. "Studies of Conductor Vibration in Laboratory Span, Outdoor Test Span and Actual Transmission Lines." CIGRE Report No. 404, 1958.

47. Harvey, J.R. "Creep of Transmission Line Conductors." IEEE Trans on PAS Vol PAS-88 No. 4, April 1969, pp 281-286.

48. Harvey, J.R. "Effect of Elevated Temperature Operation on the Strength of Aluminium Conductors." IEEE Trans on PAS Vol PAS-91 No. 5, Sept/Oct 1972, pp 1769-1772.

49. Harvey, J.R. & Larson, R.E. "Use of Elevated-Temperature Creep Data in Sag-Tension Calculations." IEEE Trans on PAS Vol PAS-89 No. 3, March 1970, pp 380-386.

50. Haughton, B.A. & Cole, A. "Site Corrosion Tests of Aluminium and Aldery and Overhead Line Conductors. Pt 7: Results of 10 Years Exposure at UK Sites and at Karachi." BICC Research and Engineering Ltd., Peport No. CO/T.263, April 1979.

51. Helms, R. & Ziebs, J. "Investigations on Aluminium Conductors Steel Reainforced (ACSR) Under Tensile and Creep Load." CIGRE 22-71 (WG05) 05, Federal Institute For Materials Testing, Paper Presented to CIGRE Study Committee No. 22 May 1971.

52. Hooker, R.J. & Humphurys W. "Damping of Electrical Transmission Lines Part II - Field and Laboratory Studies."

53. Johnston, G.H. & Stewart, W.H. "Properties Of Aluminium Alloy Conductors." MM Metals Technical Department, Paper presented to the Conference of the ESEA of NSW, Sydney August, 1985.

54. Jordan, C.A. "A Simplified Sag-Tension Method for Steel-Reinforced Aluminium Conductor." AIEE Trans. Vol 71 Pt III, Dec 1952, pp 1108-1117

55. Landau, M. "Incremental Method for Sag-Tension Calculations." AIEE Trans. Vol 70, Pt II, 1951, pp 1594-1571.

56. Little, J.C., MacMillian, D. & Majeriah, J.V. "Vibration and Fatigue Life of Steel Strands." AIEE Trans Vol 69, 1950, pp 1473-1479.

57. Maddock, B.J.,Allnut, G.R. Ferguson, J.M., Lewis, K.G., Swift, D.A., Teare, P.W. & Tunsatll, M.J. "Some Investigations of the Aging of Overhead Lines." CIGRE 22-09 Paper Presented 1986 session.

58. Miner, M.A. "Cumulative Damage in Fatigue." Proc. Amer. Soc. Mech.Eng. Metals 67(1945) S.A.-159/64, pp A159-A164.

59. Morgan, V.T. "Rating of Overhead Conductors for Continuous Currents." IEE Proc Vol 114, No. 10, Oct 1967, pp 1473-1482.

60. Morgan, V.T. "The Loss of Tensile Strength of Hard Drawn Conductors by Annealing in Service." IEEE Trans on PAS Vol PAS-98 No. 3, June 1979, pp 700-709.

61. Nakayama, Y. & Kojima, T. "Field Measurements of the Creep of Overhead Line Conductors." CSC 22-70 (WG05) 02, The Furukawa Electric Co., Ltd. Tokyo, Japan, May 1970.

62. Nigol, O. & Barrett, J.S. "Characteristics of ACSR Conductors at High Temperatures and Stresses." IEEE Trans on PAS, Vol PAS-100, No. 2, Feb 1981, pp 485-493.

63. Nigol, O. & Barrett, J.S. "Development for an Accurate Model of ACSR Conductors for Calculating Sags at High Temperature - Part II: Sag-Tension Program - STESS." Report Prepared for the Canadian Electrical Association, Nov 1980.

64. Nigol, O. & Barrett, J.S. "Development of an Accurate Model of ACSR Conductors for Calculating Sags at High Temperatures - Part III." Report Prepared for the Canadian Electrical Association, March 1980.

65. Occasione, J.F., Britton, Jr, T. C. & Collins, R.C. "Atmospheric Corrosion Investigations of Aluminium-Coated, Zinc-Coated, and Steel Wire and Copper-Bearing Steel and Wire Products: A Technical Publication 585A, Aug 1984.

66. Overhead Conductor Design BICC Wire Mill Division Prescot Lancashire England, 1st Edition, Sept 1967.

67. Poffenberger, J.C. & Swart, R.L. "Differential Displacement and Dynamic Conductor Strain." IEEE Trans on PAS Pt III April 1965, pp 281-289.

68. Philippe, W., Carlshem, W. & Buckner W. "The Endurance Capability of Single and Bundle Transmission Line Conductors and its Evaluation." Report Presented to CIGRE Study Committee 22, Working Group 04.

69. Pickins, B.M. "Sag-Tension Calculation Program for Digitial Computers." AIEE Trans on PAS Vol PAS 77 Pt III, Feb 1958, pp 1308-1315.

70. Reding, J.L. "Development and Installation of BPA's New Generation Transmission Conductors." IEEE Trans on PD Vol PWRD-2, No. 3, July 1987, pp 917-923.

71. Richardson, Jr, A.S. & Smith, F.S. "Some Effects of Tension on Static Wire Fatigue in New England." IEEE Trans on PAS, Vol PAS-100. No. 2, Feb 1981, pp 646-654.

72. Rickard, J.R. & Sproule, J. "Thermal Rating of Overhead Transmission Lines." ECNSW Internal Document 1/6/61.

73. Roche, J.B. & Dziedzic, E. "Some Factors Affecting Creep and Sag In EHV Transmisson Lines." Pacific Coast Electrical Association San Francisco, California, 28 March 1968.

74. Roman, G.J. "Dynamic Thermal Line Rating Summary and Status of the State-of-the-Art Technology." IEEE Trans on PD, Vol PWRD-2, No. 3, July 1987, pp 851-858.

75. Sakakibara, A., Iisaka, H., Mori, N., Okumura, T. & Kawamura, T. "Development of Low Wind Pressure Conductors for Compact Transmission Line." IEEE Trans on PAS Vol PAS-103, No. 10, Oct 1984, pp 3117-3123.

76. Steidel, R.F. "Factors Affecting Vibratory Stresses in Cables Near the Point of Support." AIEE Trans on PAS Vol PAS-77, Pt III, Dec 1959, pp 1207-1213.

77. Stickley, G.W. "Stress-Strain Studies of Transmission Line Conductors." Paper presented at Summer Convention of AIEE Cleveland Ohio, June 20-24, 1932.

78. Simmons, J.M., Gilmore, K.L. & Dulhunty, P.W. "Damping of Electrical Transmission Lines Part I - Analysis and Numerical Simulation."

79. Tomkins, J.S., Merrill, L.L. & Jones, B.L. "Quantitive Relationships in Conductor Vibration Damping." AIEE Trans on PAS Pt III, Oct 1956, pp 879-896.

80. Winkleman, P.F. "Sag-tension Computations and Field Measurements of Bonneville Power Administration." AIEE Trans. Pt III, Feb 1960, pp 1532-1548.

81. Varney, T. "The Vibration of TL Conductors." AIEE Trans, July 1928.

APPENDIX TWO

SAG TENSION TEST RESULTS

A2.1 SURVEY AND CALCULATED DATUM

A2.1.1 Avon Kemps Creek Transmission Line

The "as designed" and "as measured" span length, conductor attachment reduced level, curve constant, insulator longitudinal swing distance, conductor length and plotted profile for the stated conductor temperature and survey method for spans 51 to 52, 52 to 53 and 53 to 54 are given in Figures A2.1 to A2.3 respectively.

A2.1.2 Dapto Springhill Transmission Line

The "as designed" and "as measured" span length, conductor attachment reduced level, curve constant, insulator longitudinal swing distance, conductor length and plotted profile for the stated conductor temperature and survey method for spans 317A to 318A, 318A to 319A, 319A to 320A, 320A to 321A and 321A to 322A are given in Figures A2.4 to A2.8 respectively.

SURVEY METHOD : Tangent

- - as designed curve

- - - as measured curve

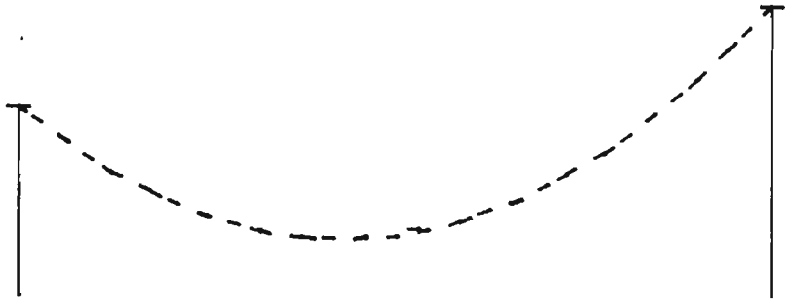

SCALES Vert 1:400
Hor 1:4000

Conductor Temperature 27.2 deg C

PARAMETER		AS DESIGNED	AS MEASURED
Span Length	m	363.20	363.20
Conductor Attachment RL Str 51	m	117.83	117.83
Str 52	m	123.03	123.03
Curve Constant	m	1777.4	1768.9
Insulator Longitudinal Swing Distance Str 51	mm	-	-
Str 52	mm	+13	-27
Conductor Length	m	363.869	363.876

Figure A2-1 Avon Kemps Creek Transmission Line
Profile
Structures 51 to 52

SURVEY METHOD : Tangent

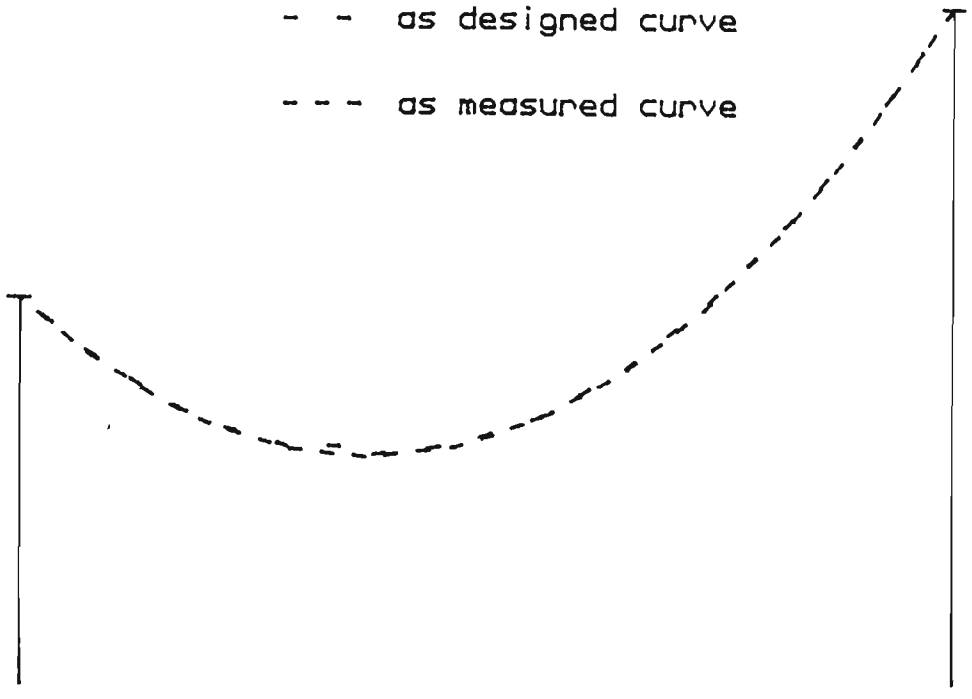

SCALES Vert 1:400
Hor 1:4000

Conductor Temperature 34.3 deg C

PARAMETER		AS DESIGNED	AS MEASURED
Span Length	m	448.32	448.32
Conductor Attachment RL Str 52	m	123.03	123.03
Str 53	m	137.89	137.89
Curve Constant	m	1717.5	1729.3
Insulator Longitudinal Swing Distance Str 52	mm	-75	-87
Str 53	mm	+27	+17
Conductor Length	m	449.839	449.822

Figure A2.2 Avon Kemps Creek Transmission Line
Profile
Structures 52 to 53

SURVEY METHOD : Satellite

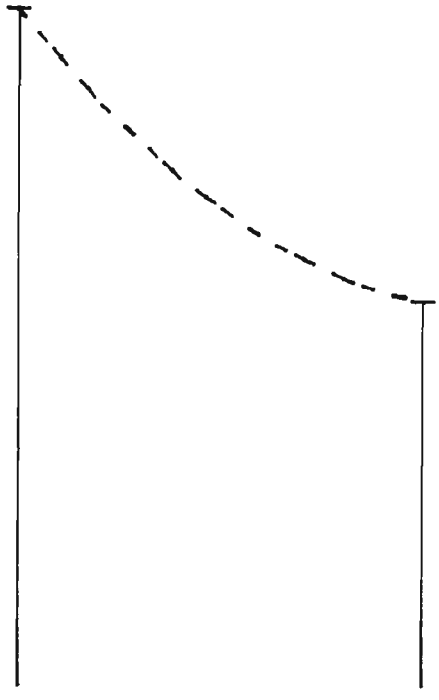

- - as designed curve

- - - as measured curve

SCALES Vert 1:400
Hor 1:4000

Conductor Temperature 34.3 deg C

PARAMETER		AS DESIGNED	AS MEASURED
Span Length	m	195.41	195.41
Conductor Attachment RL Str 53	m	137.89	137.89
Str 54	m	123.03	123.03
Curve Constant	m	1703.6	1702.8
Insulator Longitudinal Swing Distance Str 53	mm	-75	-87
Str 54	mm	-	-
Conductor Length	m	196.081	196.081

Figure A2.3 Avon Kemps Creek Transmission Line
Profile
Structures 53 to 54

SURVEY METHOD : Tangent

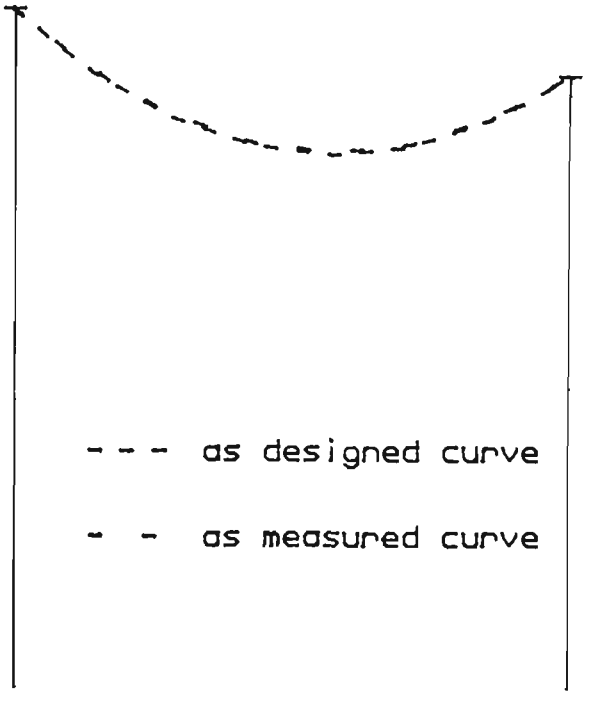

SCALES Vert 1:400
Hor 1:4000

Conductor Temperature 31.5 deg C

PARAMETER		AS DESIGNED	AS MEASURED
Span Length	m	266.66	266.66
Conductor Attachment RL	Str 317Am	128.30	128.30
	Str 317Am	125.05	125.05
Curve Constant	m	1574.0	1606.3
Insulator Longitudinal Swing Distance	Str 317Amm	-	-
	Str 318Amm	+11	+11
Conductor Length	m	266.999	266.986

Figure A2-4 Dapto Springhill Transmission Line
Profile
Structures 317A to 318A

SURVEY METHOD : Tangent

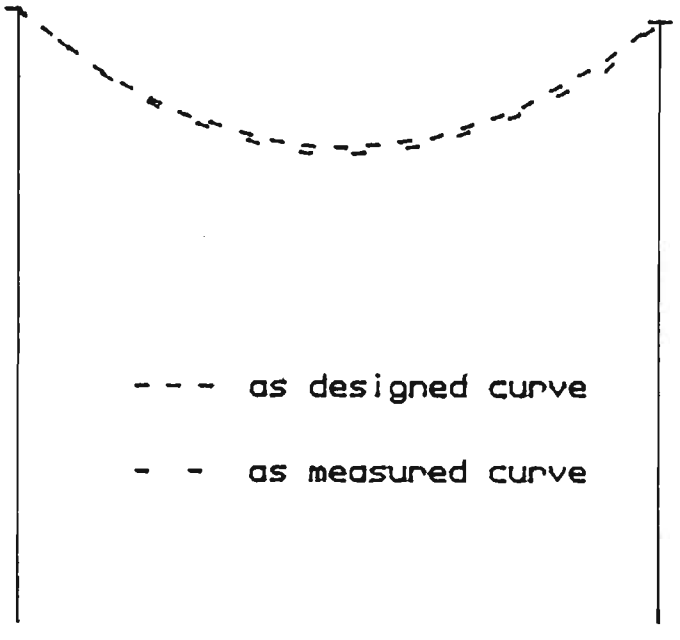

SCALES Vert 1:400
Hor 1:4000

Conductor Temperature 18.6 deg C

PARAMETER		AS DESIGNED	AS MEASURED
Span Length	m	308.62	308.62
Conductor Attachment RL	Str 318Am	125.05	125.05
	Str 319Am	124.54	124.54
Curve Constant	m	1752.3	1667.0
Insulator Longitudinal Swing Distance	Str 318A mm	+11	+11
	Str 319A mm	-12	-15
Conductor Length	m	309.019	309.061

Figure A2.5 Dapto Springhill Transmission Line
Profile
Structures 318A to 319A

SURVEY METHOD : Tangent

- - - as designed curve

- - as measured curve

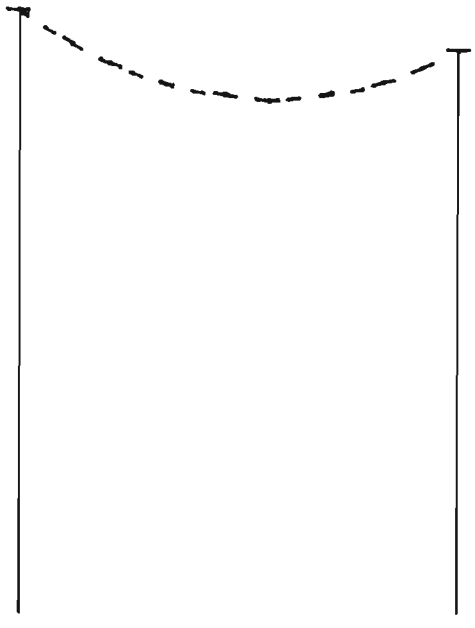

SCALES Vert 1:400
Hor 1:4000

Conductor Temperature 31.5 deg C

PARAMETER		AS DESIGNED	AS MEASURED
Span Length	m	210.91	210.91
Conductor Attachment RL Str 319Am		124.54	124.54
Str 320Am		122.54	122.54
Curve Constant	m	1573.2	1580.3
Insulator Longitudinal Swing Distance Str 319A	mm	-24	+14
Str 320A	mm	+23	+23
Conductor Length	m	211.077	211.076

Figure A2.6 Dapto Springhill Transmission Line
Profile
Structures 319A to 320A

SURVEY METHOD : Tangent

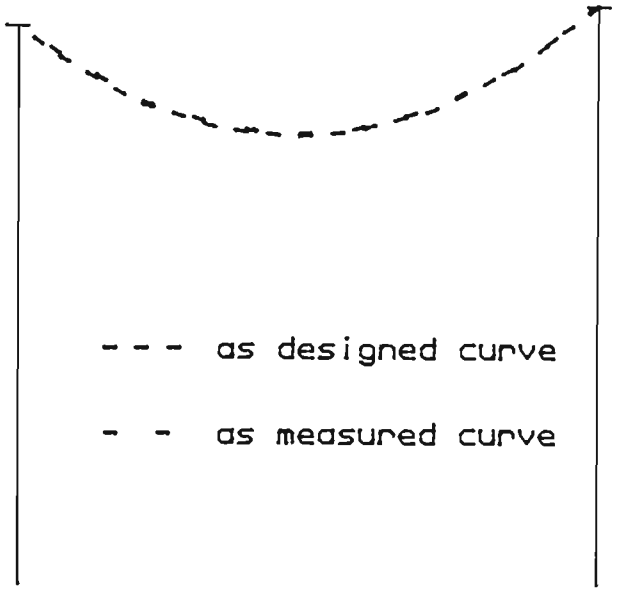

SCALES Vert 1:400
Hor 1:4000

Conductor Temperature 31.5 deg C

PARAMETER		AS DESIGNED	AS MEASURED
Span Length	m	278.68	278.68
Conductor Attachment RL	Str 320Am	122.54	122.54
	Str 321Am	123.58	123.58
Curve Constant	m	1576.5	1592.9
Insulator Longitudinal Swing Distance	Str 320A mm	+23	+23
	Str 321A mm	+24	+14
Conductor Length	m	279.045	279.037

Figure A2.7 Dapto Springhill Transmission Line
Profile
Structures 320A to 321A

SURVEY METHOD : Tangent

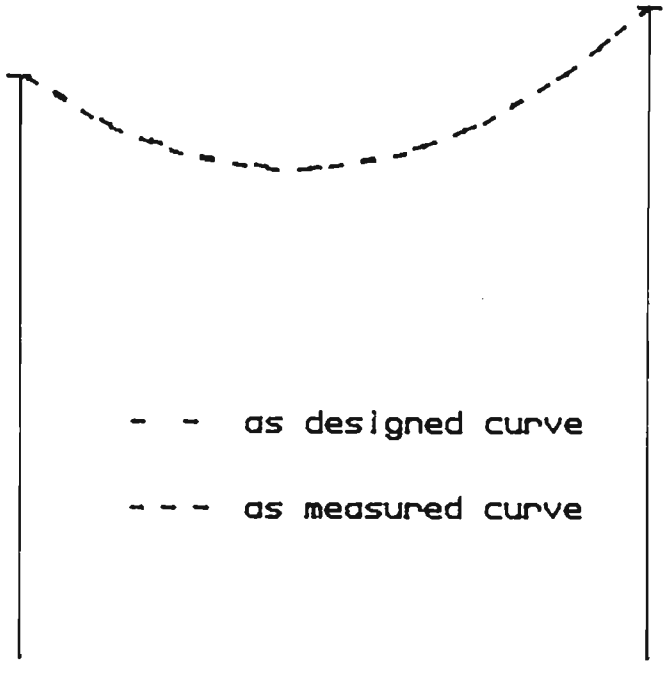

SCALES Vert 1:400
Hor 1:4000

Conductor Temperature 18.6 deg C

PARAMETER		AS DESIGNED	AS MEASURED
Span Length	m	302.19	302.19
Conductor Attachment RL	Str 321Am	123.58	123.58
	Str 322Am	127.16	127.16
Curve Constant	m	1754.6	1683.9
Insulator Longitudinal Swing Distance	Str 321A mm	+13	+14
	Str 322A mm	-	-
Conductor Length	m	302.585	302.617

Figure A2.8 Dapto Springhill Transmission Line
Profile
Structures 321A to 322A

APPENDIX THREE

MECHANICAL PROPERTIES OF AGED TRANSMISSION LINE CONDUCTORS

TEST RESULTS

A3.1 Metallographic Examination

A3.1.1 Macro Examination

A3.1.1.1 Avon to Kemps Creek Transmission Line

On destranding of the armour rod suspension grip revealed traces of white powder and the external surface of the conductor was matt grey in colour. In addition there was an accumulation of grit particles in gaps between the wires. With the exception of the white powder similar observations were made of the conductor away from the suspension point. The 24 wire layer or the outer layer is illustrated in Plate A3.1.

On destranding the 24 wire aluminium layer elliptical areas of surface damage could be seen on the underside of the 24 wire layer. A series of corresponding marks on the outside surface of the 18 wire layer were observed. These marks were unformly distributed over the conductor surface and consistent with marks formed by the closing die of a stranding

machine. The wires were all bright grey in colour. Similar observations were made of the conductor sample away from the suspension point. The 18 wire layer is illustrated in Plate A3.2.

On destranding the 18 wire aluminium layer similar observations were made for the destranding of the 24 wire layer with the exception that the number of elliptical areas observed on the wires was reduced. This is consistent with the decreased number of strands in contact with the 12 wire layer. The 12 wire layer is illustrated in Plate A3.3.

On destranding the 12 wire aluminium layer revealed copous quantities of grease on the underside of the 12 wire aluminium layer and the outside of the 6 wire steel layer. On removing the grease from the aluminium strands elliptical areas of surface damage previously described were observed on the underside of the 12 wire layer. These damaged areas were longer and deeper than previously mentioned. The 6 wire layer is illustrated in Plate A3.4.

On destranding the 6 wire steel layer revealed copous quantities of grease on the underside of 6 wire steel layer and on the surface of the core steel wire. On removing the grease from the destranded 6 wire steel layer and the core, the galvanized surface of the steel wires was bright grey. The core wire is illustrated in Plate A3.5.

A3.1.1.2 Dapto to Springhill Transmission Line

With the exception of the absence of white powder products mentioned in the destranding of the armour rods and the non preforming of the steel core, the macro examinations revealed similar observations for the various layers mentioned in section A3.1.1.1

Almost all elliptical areas of surface damage within 50 mm either side of the suspension clamp contained evidence of abrasion or aluminium fretting.

The 24, 18, 12, 6 wire layers and the core are illustrated in Plates A3.6, A3.7, A3.8, A3.9 and A3.10 respectively.

A3.1.1.3 Tomago to Taree Transmission Line

On destranding of the armour rod suspension grip revealed a voluminous quantity of white powder formed on the external surface of the conductor. The external surface of the conductor was matt grey and there was with evidence of pitting. Pitting and white powered deposits were not present on the conductor away from the suspension point. The 18 wire aluminium layer from a suspension site and away from the suspension site is illustrated in Plate A3.11 and A3.12 respectively.

On destranding the 18 wire aluminium layer revealed copous quantities of bituminous tar on the underside of the 18 wire aluminium layer and the outside of the 12 wire aluminium layer. The tar was bright black in colour and very sticky. On removing the tar from the 18 wire aluminium strands, elliptical areas of surface damage previously described were observed on the underside of the 18 wire layer. The 12 wire aluminium layer and the underside of the 18 wire aluminium layer is illustrated in Plate A3.13.

On destranding the 12 wire aluminium layer revealed copous quantities of bituminous tar on the underside of the 12 wire aluminium layer and the outside of the 6 wire steel layer. The tar was bright black in colour and very sticky. On removing the tar from the 12 wire aluminium strands elliptical areas of surface damage previously described were observed on the inside of 12 wire layer. These damaged areas were longer and deeper than those of 18 wire layer. The 6 wire steel layer and the underside of the 12 wire aluminium layer is illustrated in Plate A3.14.

On destranding the 6 wire steel layer revealed the steel core. Little bituminous tar was present on the core or the underside of the 6 wire steel layer. On removal of the tar from the destranded 6 wire layer and the core, the galvanised surface of the steel wires was dull grey with

some evidence of brown strains and rust sites. The destranded 6 wire steel layer and steel core as found and cleaned wires are illustrated in Plates A3.15 and A3.16 respectively.

A3.1.1.4 Bellambi to Heathcote Transmission Line

This sample was removed from a jumper connection, consequently no armour rods were fitted on the conductor and the sample was not subjected to stringing tension.

The external surface of the conductor was matt grey with minor pitting evidence. The 18 wire aluminium layer is illustrated in Plate A3.17.

On destranding the 18 wire layer aluminium layer revealed bituminous tar with an accumulation of dirt particles on the underside of the 18 wire layer and the outside of the 12 wire layer. The tar was matt black in colour and dry. On removing the tar similar but smaller elliptical areas of surface damage previously described were observed on the underside of the 18 wire layer. The 12 wire aluminium layer and the underside of the 18 wire aluminium layer are illustrated in Plates A3.18.

For the remainder of the macroexamination, the observations for the remaining layers were similar as mentioned in section A3.1.1.3 with the exception of the smaller elliptical areas of surface damage.

The 6 wire layer and core wire did not have any brown stains present and are illustrated in Plates A3.19 and A3.20 respectively. The destranded and cleaned 6 wire steel layer and core wire are illustrated in Plate A3.21.

A3.1.2 Microexamination

Scanning electron microscopy of the elliptical areas revealed no definite signs of fatigue crack formation on any of the abovementioned samples examined. Some scoring of the surface of the wire in the elliptical areas, as illustrated in Plate A3.22 was common.

Optical microscopy of longitudinal sections through a series of elliptical marks did not reveal fatigue cracks on any of the abovementioned samples examined. A typical longitudinal section is illustrated in Plate A3.23.

Longitudinal sections through the outside layer of the aluminium wires confirmed that some pitting existed but this was generally confined to less than 50 μm as illustrated in Plate A3.24. With the exception of the Tomago to Taree transmission line similar results were obtained on the abovementioned samples examined. The 18 wire aluminium layer from the Tomago to Taree transmission line sample revealed pitting corrosion to a depth of 0.6 mm as illustrated in Plate A3.25.

Longitudinal sections through the steel wires confirmed that some galvanising loss has taken place for all of the abovementioned samples examined. However, for the Tomago to Taree transmission line sample, in some areas the galvanising had eroded away leaving exposed steel that has commenced to corrode. Maximum pit depths were 180 µm. The loss of galvanising and corrosion of the steel core and wires from the 6 wire layer are illustrated in Plates A3.26 and A3.27 respectively.

A3.2 Wire Test

A3.2.1 Cross Sectional Area

The cross sectional area of wires that constitute the conductor samples from the Avon to Kemps Creek, Dapto to Springhill, Tomago to Taree and Bellambi to Heathcote transmission lines is given in Tables A3.1 to A3.4 respectively.

A3.2.2 Mechanical Properites

The breaking load, ultimate tensile strength and elongation of the wires that constitute the conductor samples from the Avon to Kemps Creek, Dapto to Springhill, Tomago to Taree and Bellambi to Heathcote transmission lines is given in Tables A3.5 to A3.8 respectively.

In addition to these test results all wires complied with the requirements of a wrap test.

A3.2.3 Electrical Properties

The resistivity of the aluminium wires that constitute the conductor samples from the Avon to Kemps Creek, Dapto to Springhill, Tomago to Taree and the Bellambi to Heathcote transmission lines is given in Tables A3.9 to A3.12 respectively.

A3.2.4 Galvanised Steel Wire Zinc Coating Mass

The zinc coating mass of the steel wires that constitute the conductor samples from the Avon to Kemps Creek, Dapto to Springhill, Tomago to Taree and Bellambi to Heathcote transmission lines is given in Tables A3.13 to A3.16 respectively.

A3.2.5 Galvanised Steel Wire Wrap test

The steel wire that constitute the conductor samples from the Avon to Kemps Creek, Dapto to Springhill, Tomago to Taree and Bellambi to Heathcote transmission lines complied with the requirements of BS443-1961.

A3.3 Conductor Tests

A3.3.1 Stress Strain

The raw data plots for the composite and core, derived stress strain plot and test result data for the conductor sample from the Tomago to Taree transmission line are given in Figures A3.1 to A3.3 and Table A3.17 respectively. An additional stress strain raw data and derived plots and test result data for a second conductor sample from the Tomago to Taree transmission line are given in Figures A3.4 to A3.6 and Table A3.18 respectively.

The raw data plots for the composite and core, derived stress strain plot and test result data for the conductor sample from the Dapto to Springhill transmission line are given in Figures A3.7 to A3.9 and Table A3.19 respectively.

The raw data plots for the composite and core, derived stress strain plot and test result data for the conductor sample from the Avon to Kemps Creek transmission line are given in Figures A3.10 to A3.12 and Table A3.20 respectively.

As a result of the inadequate sample length, no stress strain tests were carried out on the conductor sample from the Bellambi to Heathcote transmission line.

A3.3.2 Coefficient of Linear Expansion

The raw data plot and linear regression test result, and test result data for the Tomago to Taree transmission line with test load of 20% CBL is given in Figures A3.13 and Table A3.21, respectively. An additional raw data plot and linear regression test result, and test result data for the Tomago to Taree transmission line with test load of 40% CBL is given in Figure A3.14 and Table A3.22, respectively.

The raw data plot and linear regression test result, and test result data for the Dapto to Springhill transmission line with test load fo 20% CBL is given in Figure A3.15 and Table A3.23, respectively.

The raw data plot and linear regression test result, and test result data for the Avon to Kemps Creek transmission line with test load at 20% CBL is given in Figure A3.16 and Table A3.24, respectively.

As a result of the inadequate sample length, no coefficient of linear expansion tests were carried out on the conductor sample from the Bellambi to Heathcote transmission line.

A3.3.3 Creep

The raw data linear linear plot, raw data log log plot and regression lines, and test result data with test loads of 20 and 30% CBL for the conductor sample from the Avon to Kemps Creek transmission line is given in Figures A3.17 and A3.18 and Table A3.25, respectively.

The raw data linear linear plot, raw data log log plot and regression lines, and test result data with test loads of 20 and 30% CBL for the condcutor sample from the Dapto to Springhill transmission line is given in Figures A3.19 and A3.20 and Table A3.26, respectively.

The conductor temperature variation during the duration of the creep tests is given in Figure A3.21.

As a result of the stress strain test results for the conductor sample from the Tomago to Taree transmission line a creep test was not carried out.

Furthermore, as a result of the inadequate sample length, no creep test were carried out on the conductor sample from the Bellambi to Heathcote transmission line.

A3.3.4 Breaking Load

The test results and test result datum for the conductor sample from the Tomago to Taree transmission line are given in Figures A3.22 and A3.23 and Tables A3.27 and A3.28.

The test results and test result datum for the conductor sample from the Avon to Kemps Creek transmission line are given in Figure A3.24 and A3.25 and Tables A3.29 and A3.30.

The test result and test result datum for the conductor sample from the Dapto to Springhill transmission line are given in Figures A3.26 and A3.27 and Tables A3.31 and A3.32.

Breaking load tests was not carried out on the Bellambi to Heathcote transmission line conductor sample.

A3.3.5 Lay Lengths

The lay lengths for the conductor samples from the Dapto to Springhill and Avon to Kemps Creek transmission lines are given in Tables A3.33 and A3.34 respectively.

Lay lengths were not measured for the Bellambi to Heathcote and Tomago to Taree transmission line conductor samples.

A3.4 Chemical Tests

The tar drop point and tar mass test result data for the conductor sample from the Tomago to Taree and Bellambi to Heathcote transmission lines is given in Tables A3.35 and A3.36, respectively.

The grease drop point and grease mass test result data for the conductor sample from the Avon to Kemps Creek and the Dapto to Springhill transmission lines is given in Tables A3.37 and A3.38, respectively.

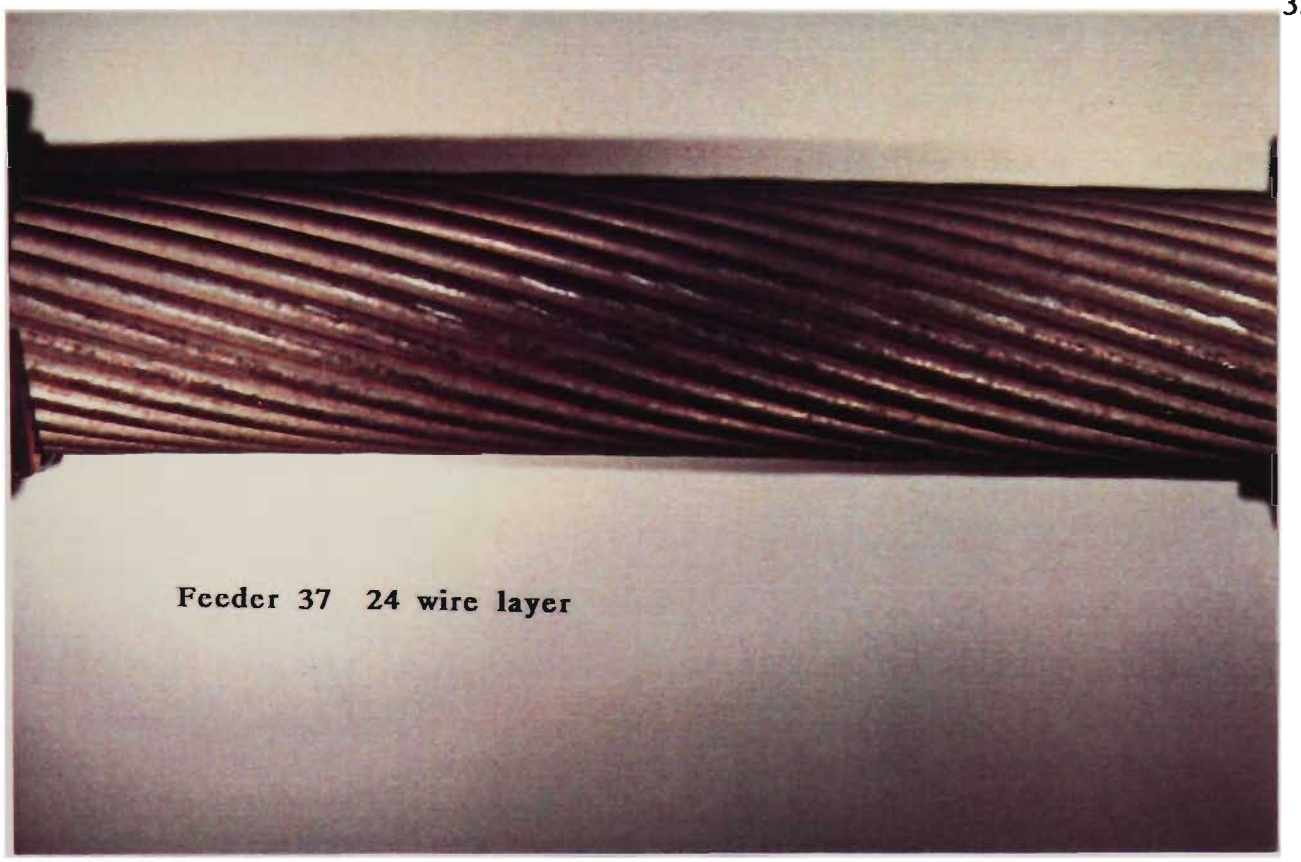

PLATE A3.1 - AVON TO KEMPS CREEK TRANSMISSION LINE
24 WIRE ALUMINIUM LAYER OR OUTSIDE LAYER

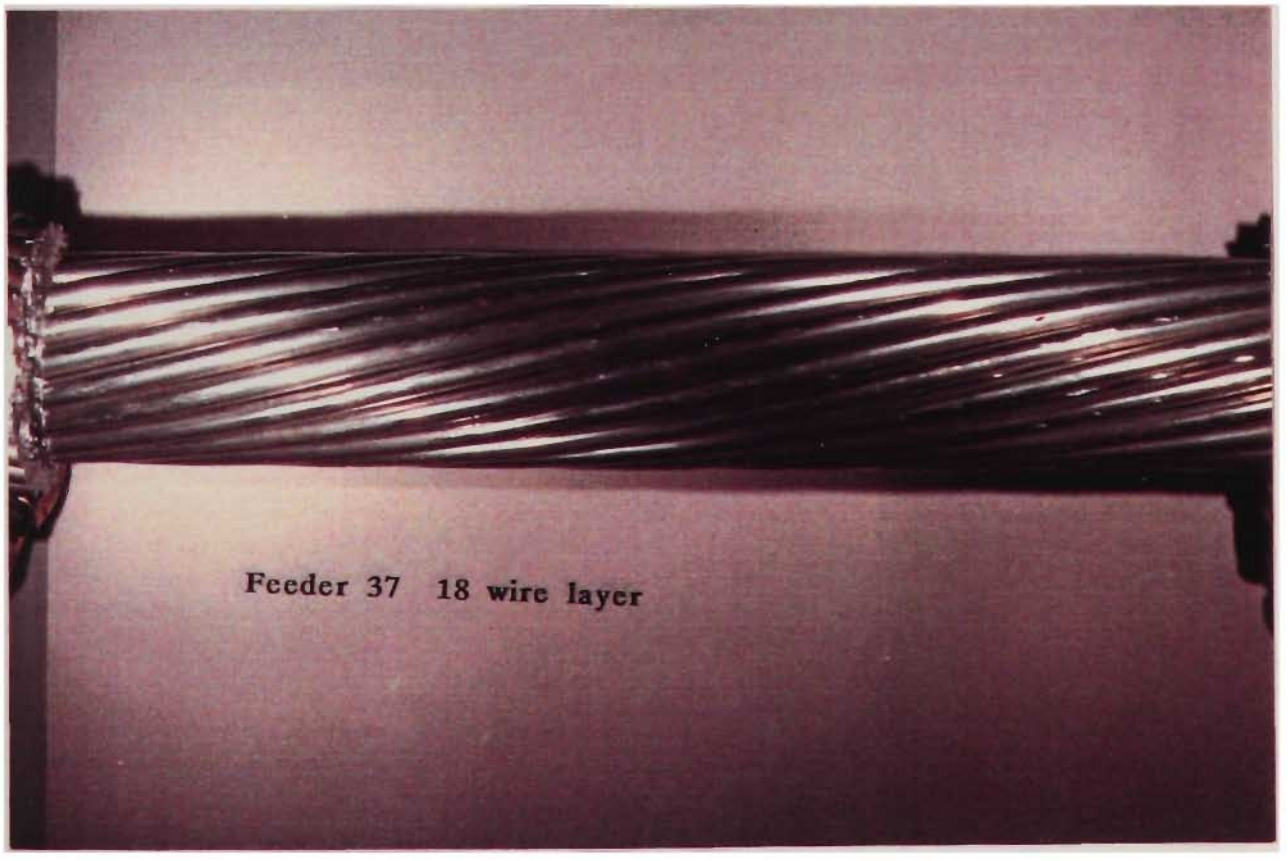

PLATE A3.2 - AVON TO KEMPS CREEK TRANSMISSION LINE
18 WIRE ALUMINIUM LAYER

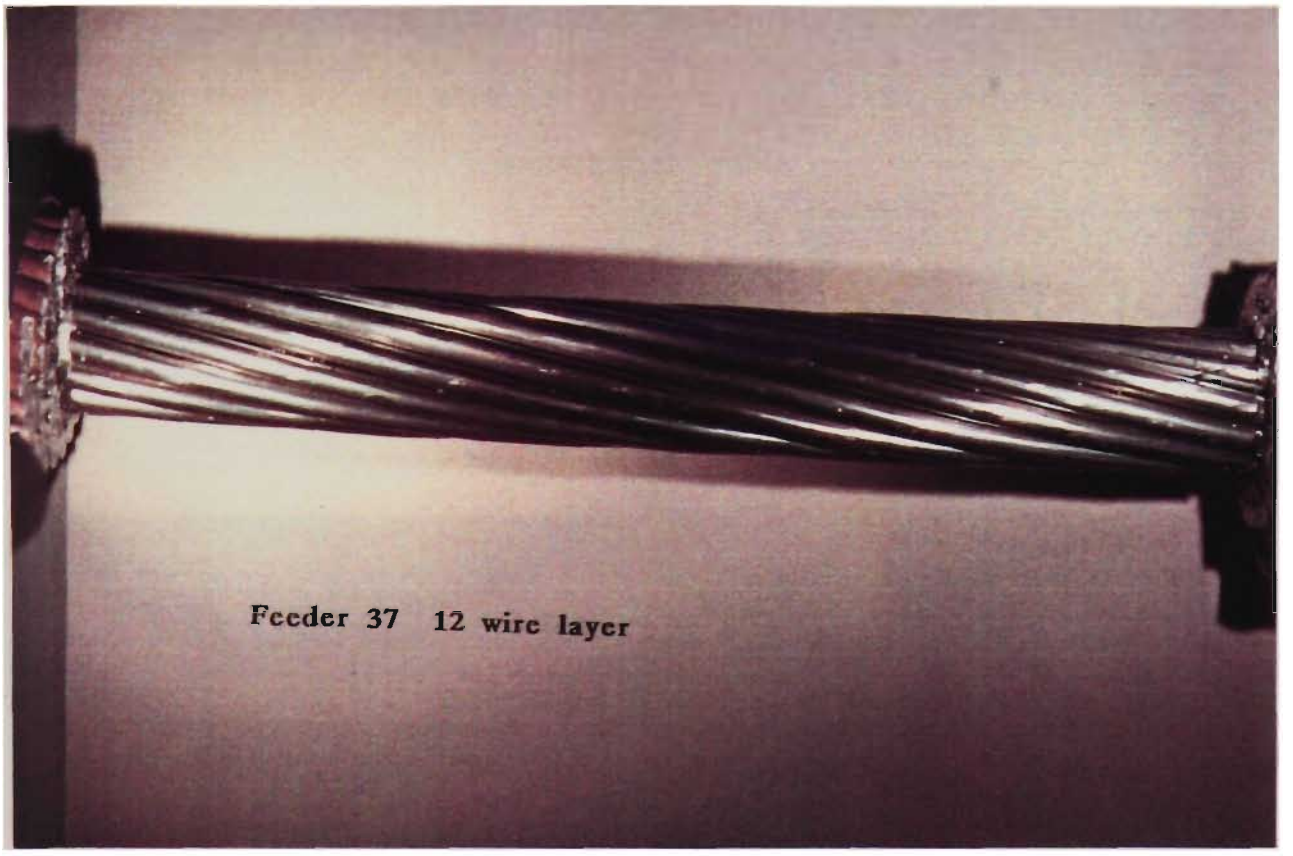

PLATE A3.3 - AVON TO KEMPS CREEK TRANSMISSION LINE
12 WIRE ALUMINIUM LAYER

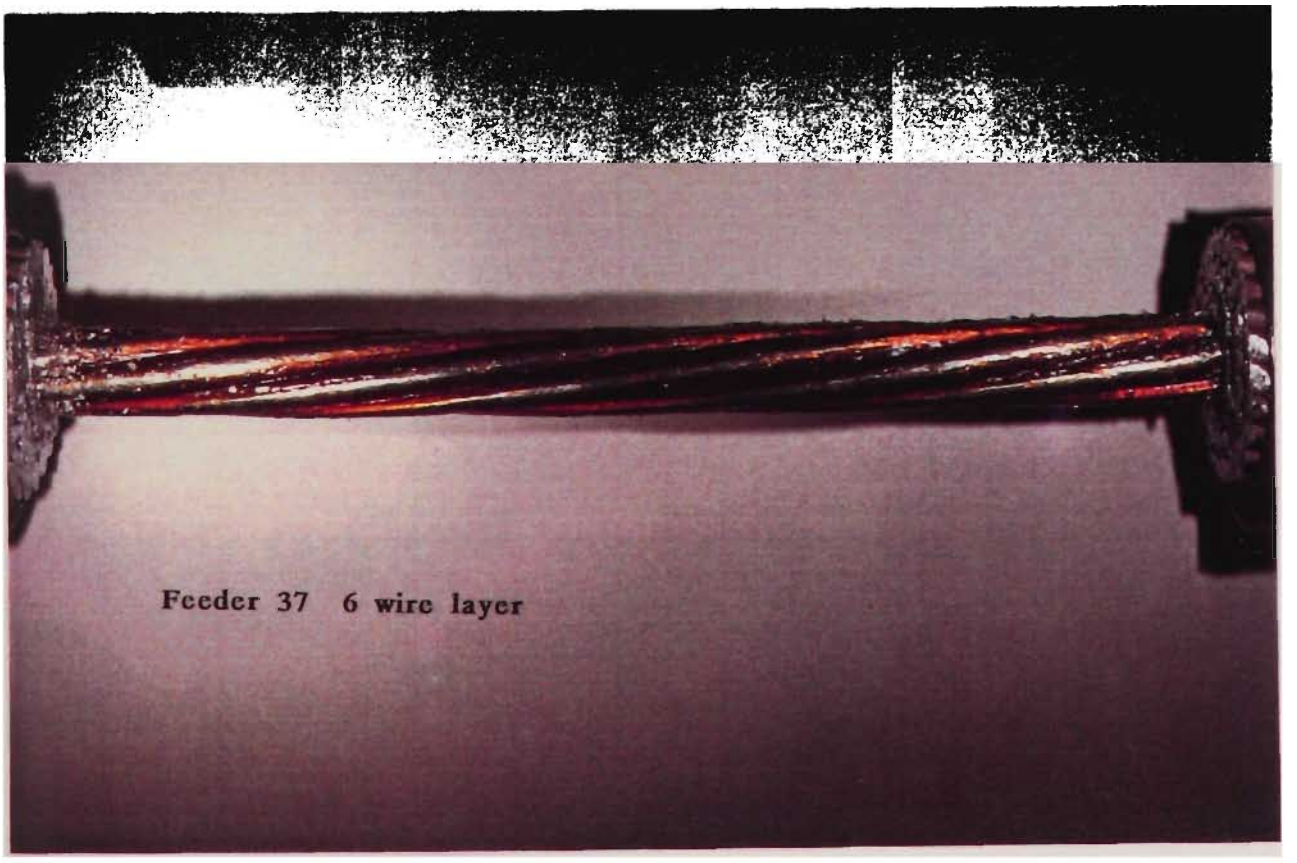

PLATE A3.4 - AVON TO KEMPS CREEK TRANSMISSION LINE
6 WIRE STEEL LAYER

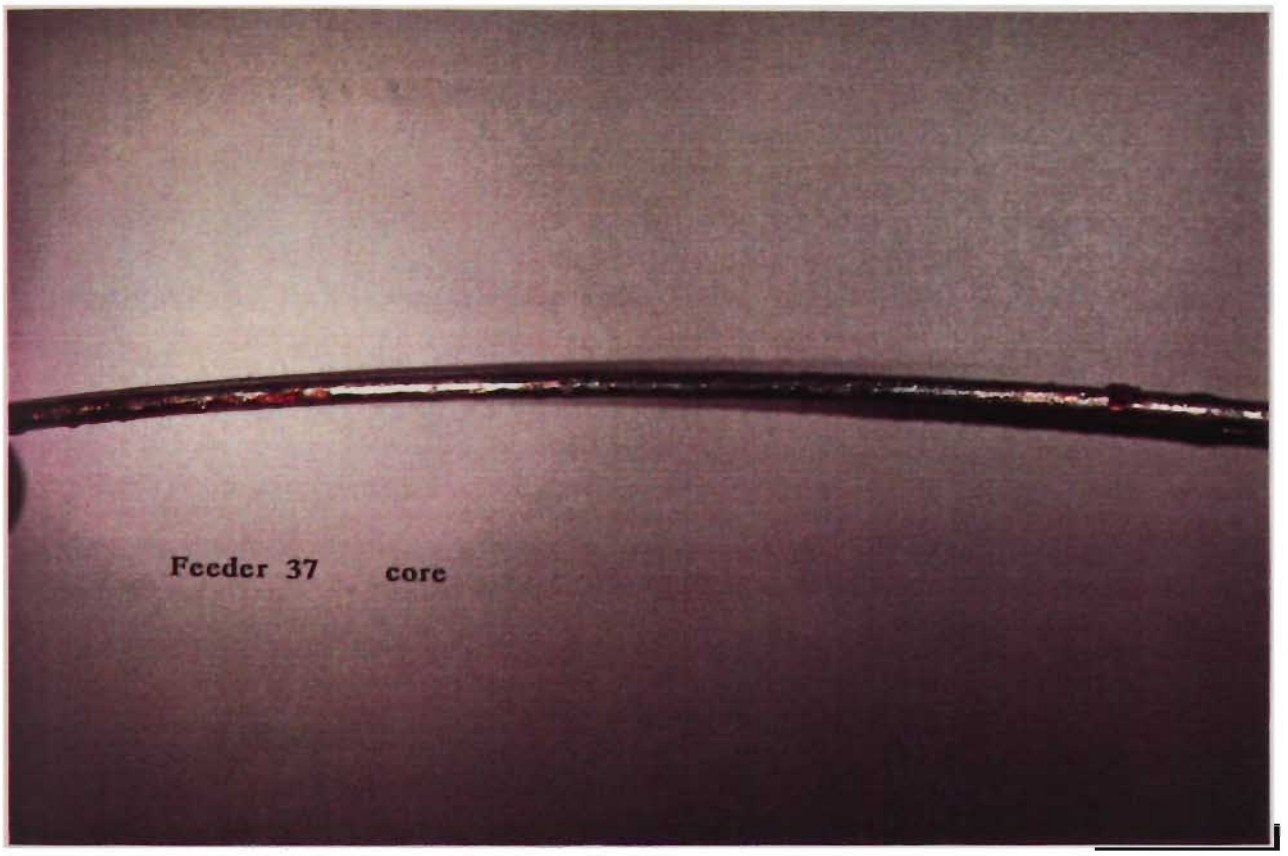

PLATE A3.5 - AVON TO KEMPS CREEK TRANSMISSION LINE
STEEL CORE

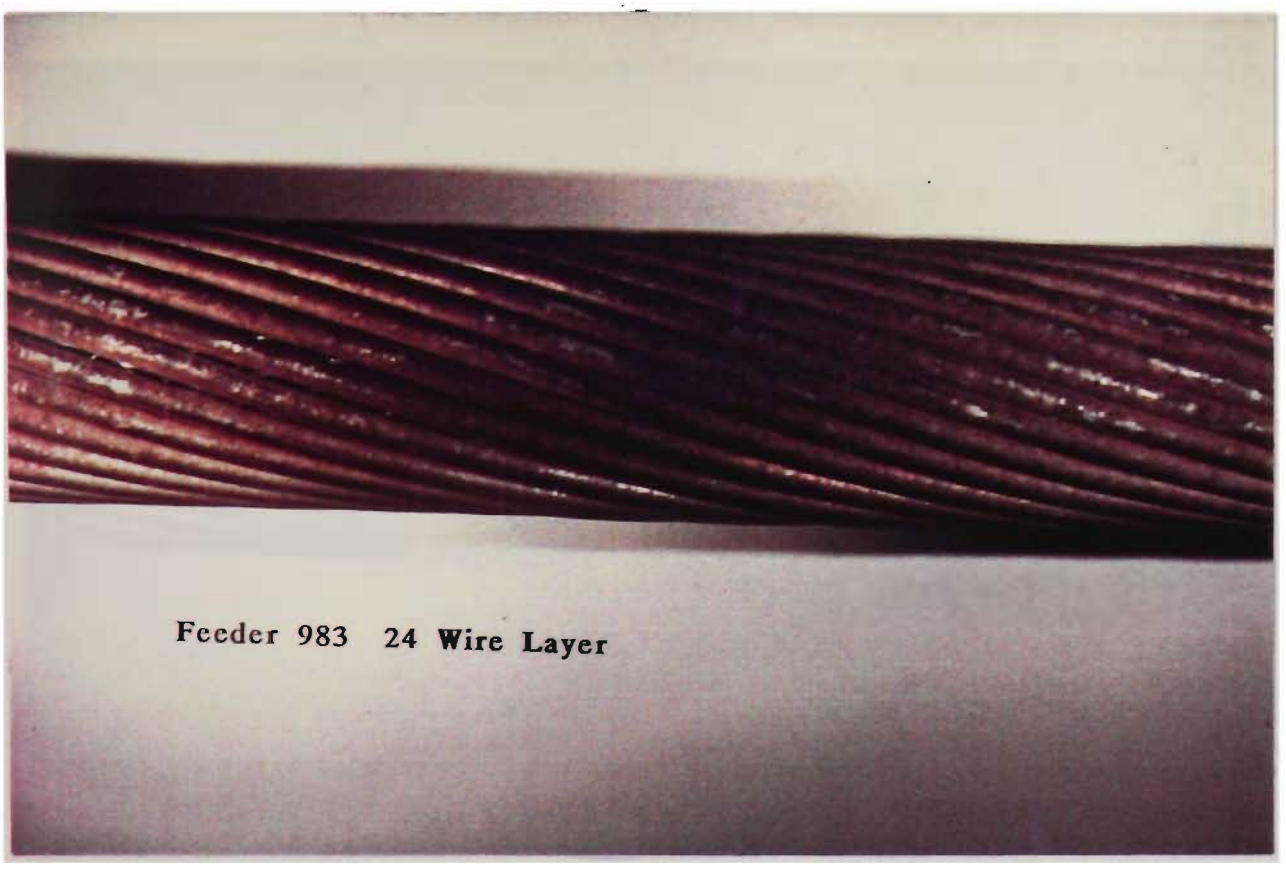

PLATE A3.6 - DAPTO TO SPRINGHILL TRANSMISSION LINE
24 WIRE ALUMINIUM LAYER OR OUTSIDE LAYER

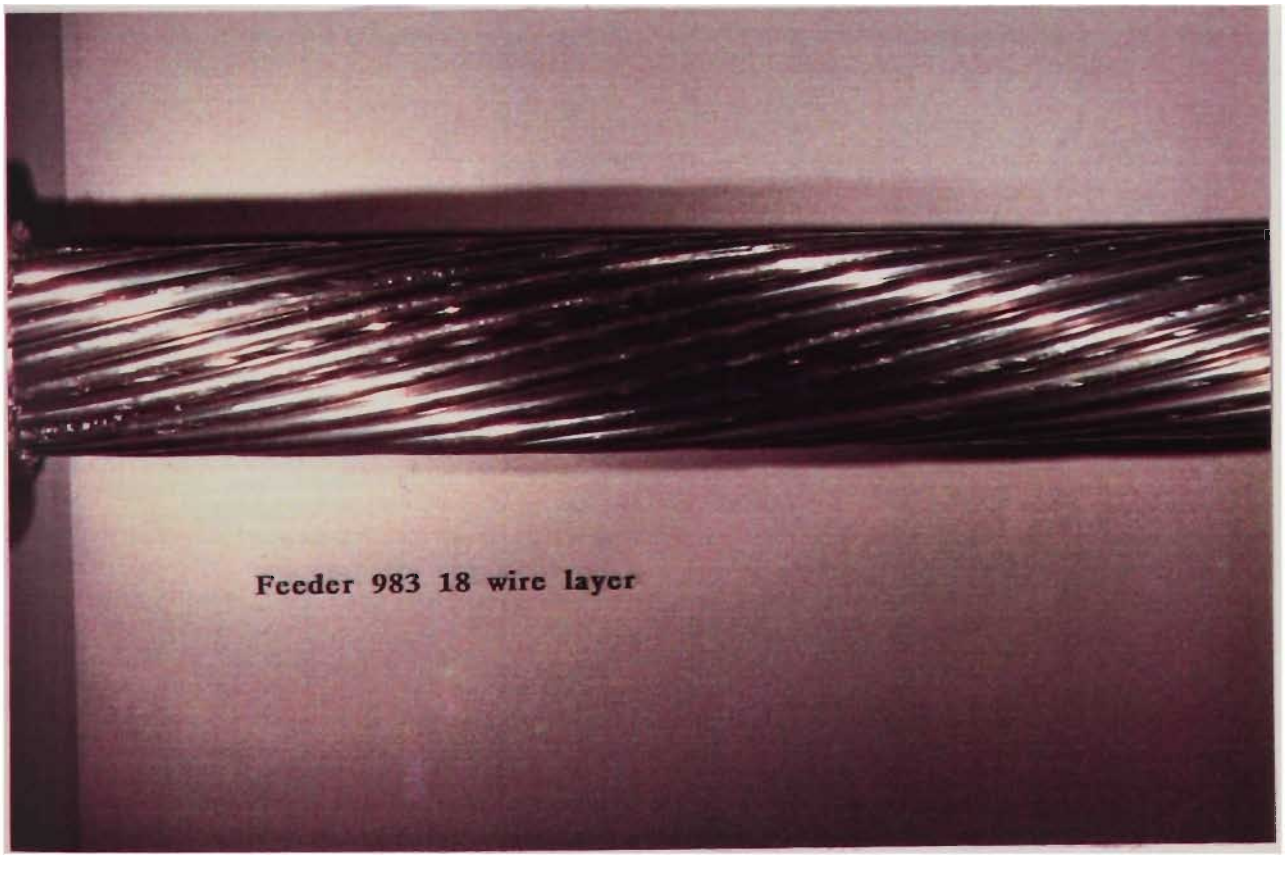

PLATE A3.7 - DAPTO TO SPRINGHILL TRANSMISSION LINE
18 WIRE ALUMINIUM LAYER

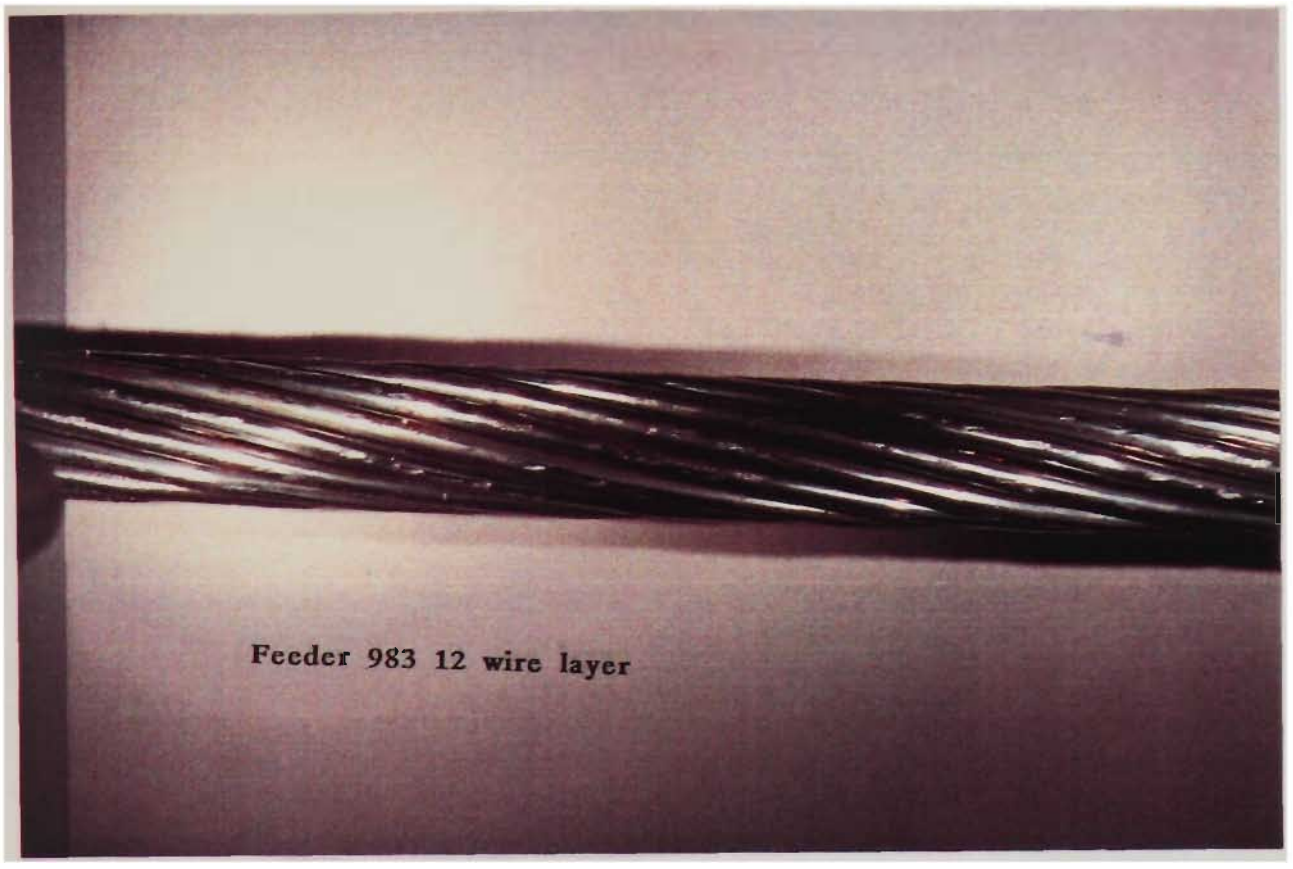

PLATE A3.8 - DAPTO TO SPRINGHILL TRANSMISSION LINE
12 WIRE ALUMINIUM LAYER

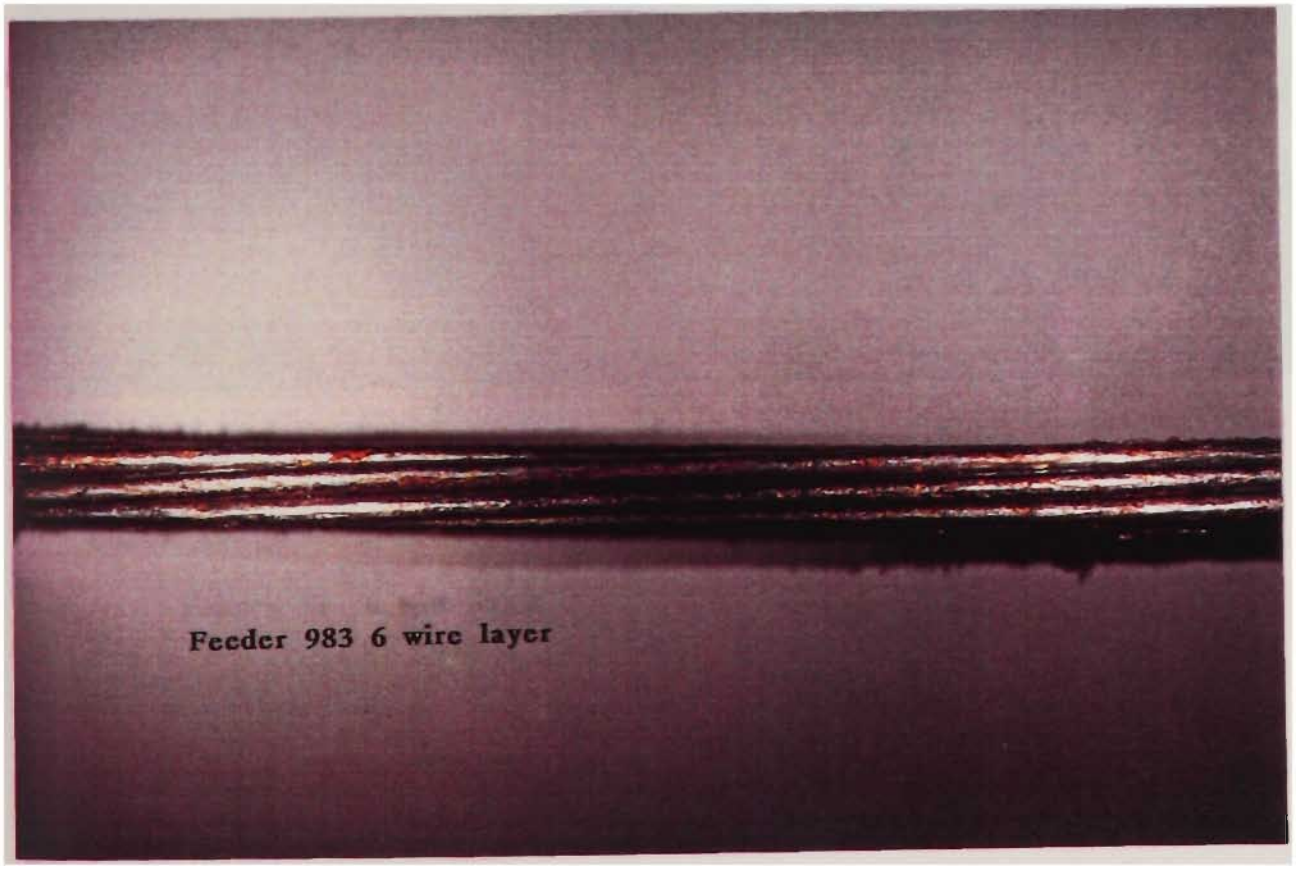

PLATE A3.9 - DAPTO TO SPRINGHILL TRANSMISSION LINE
6 WIRE STEEL LAYER WITHOUT PREFORM

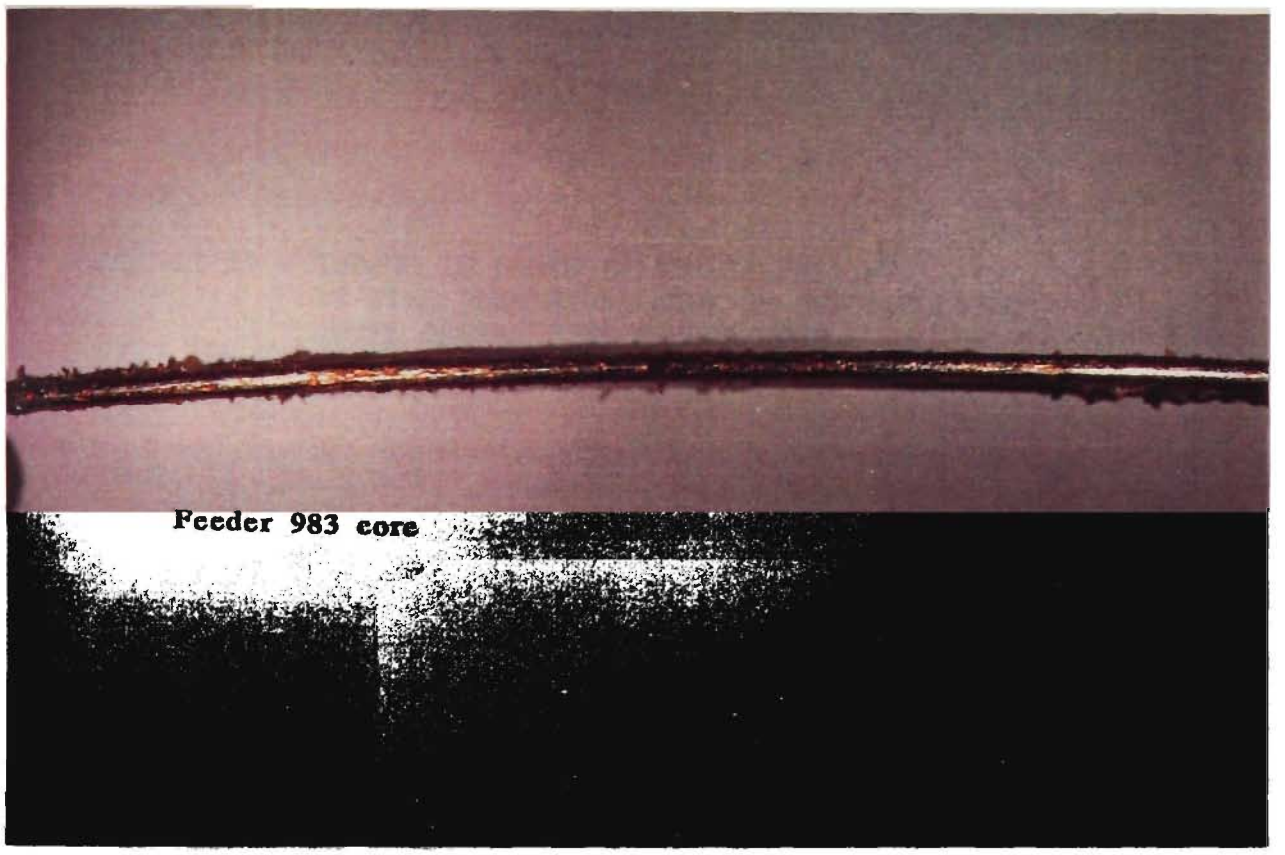

PLATE A3.10 - DAPTO TO SPRINGHILL TRANSMISSION LINE
STEEL CORE

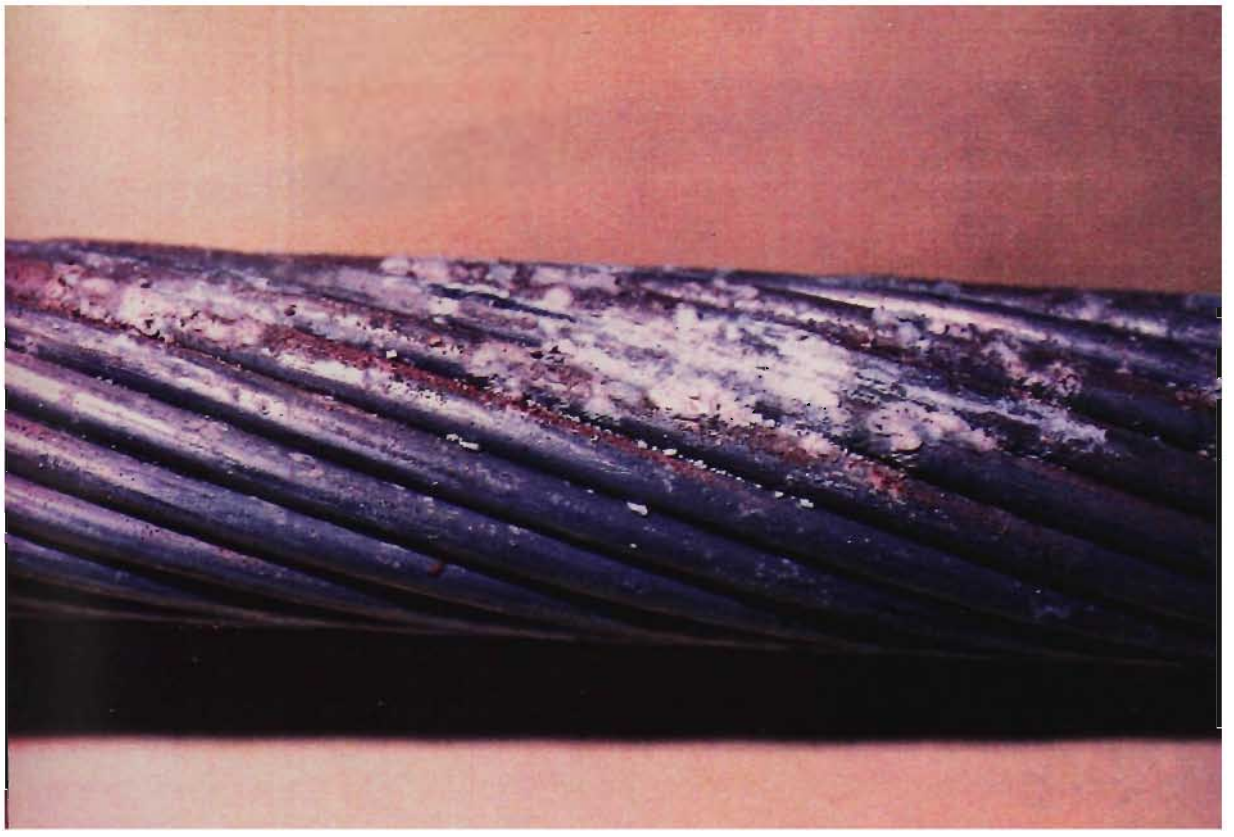

PLATE A3.11 - TOMAGO TO TAREE TRANSMISSION LINE
18 WIRE ALUMINIUM LAYER OR OUTSIDE LAYER
AFTER DESTRANDING ARMOUR RODS

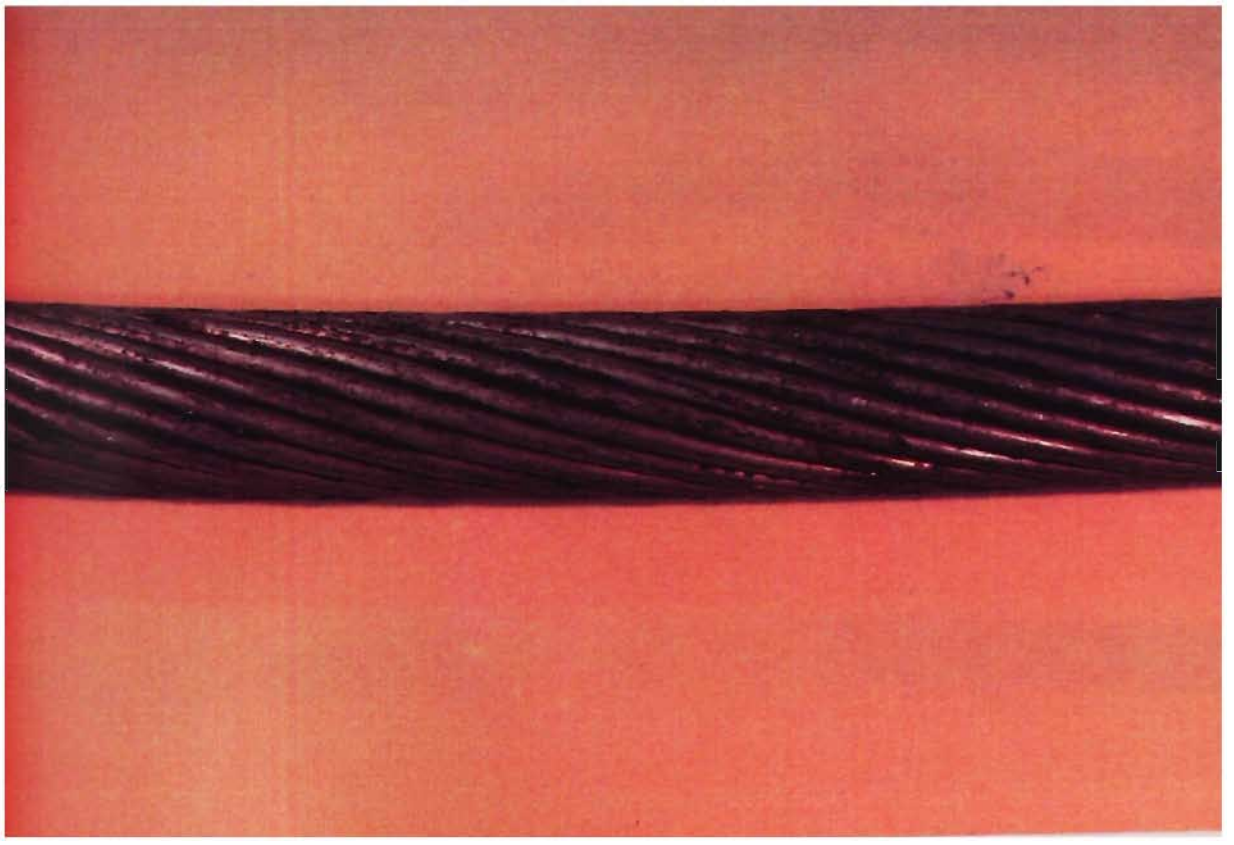

PLATE A3.12 - TOMAGO TO TAREE TRANSMISSION LINE
18 WIRE ALUMINIUM LAYER OR OUTSIDE LAYER

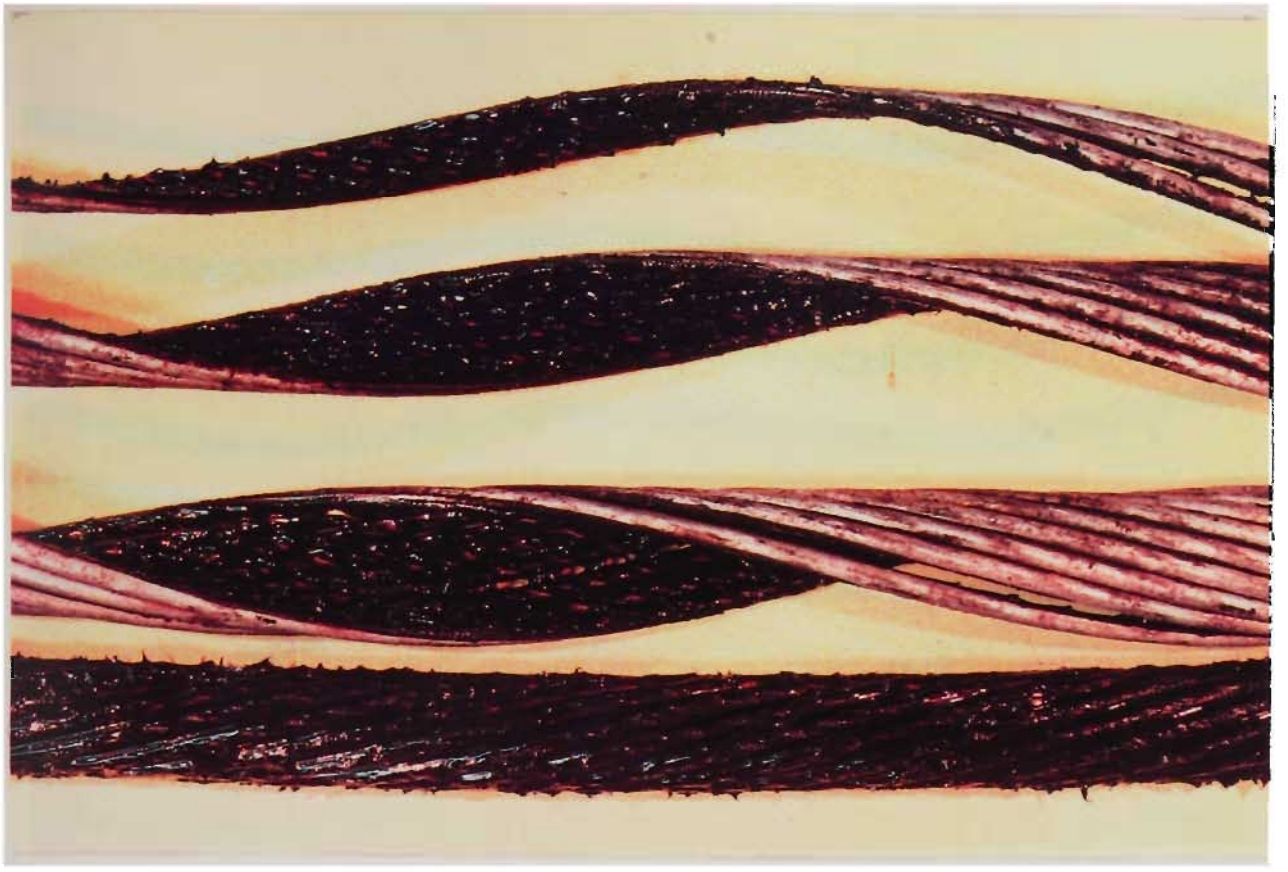

PLATE A3.13 - TOMAGO TO TAREE TRANSMISSION LINE
12 WIRE ALUMINIUM LAYER AND
UNDERSIDE OF 18 WIRE ALUMINIUM LAYER

PLATE A3.14 - TOMAGO TO TAREE TRANSMISSION LINE
6 WIRE STEEL LAYER AND
UNDERSIDE OF 12 WIRE ALUMINIUM LAYER

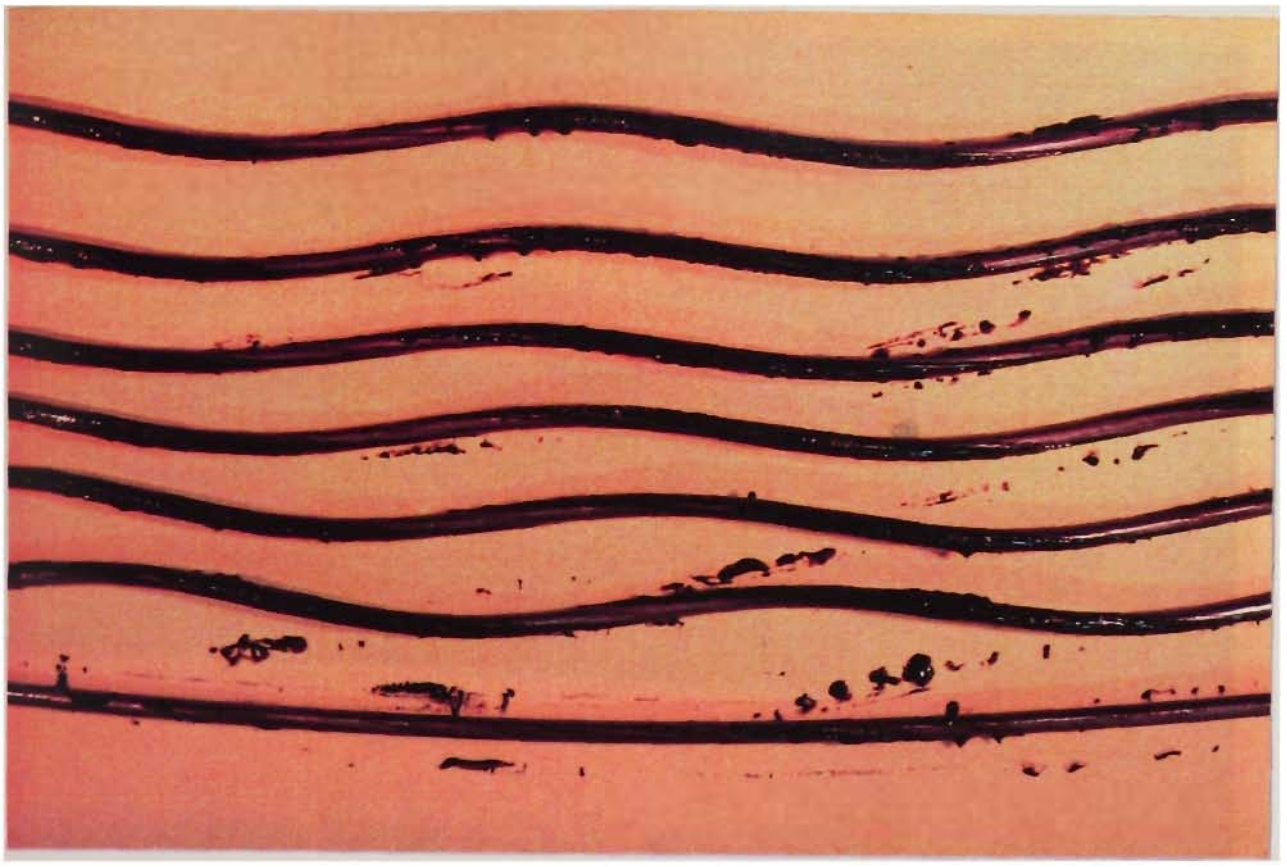

PLATE A3.15 - TOMAGO TO TAREE TRANSMISSION LINE
DESTRANDED 6 WIRE STEEL LAYER AND STEEL CORE

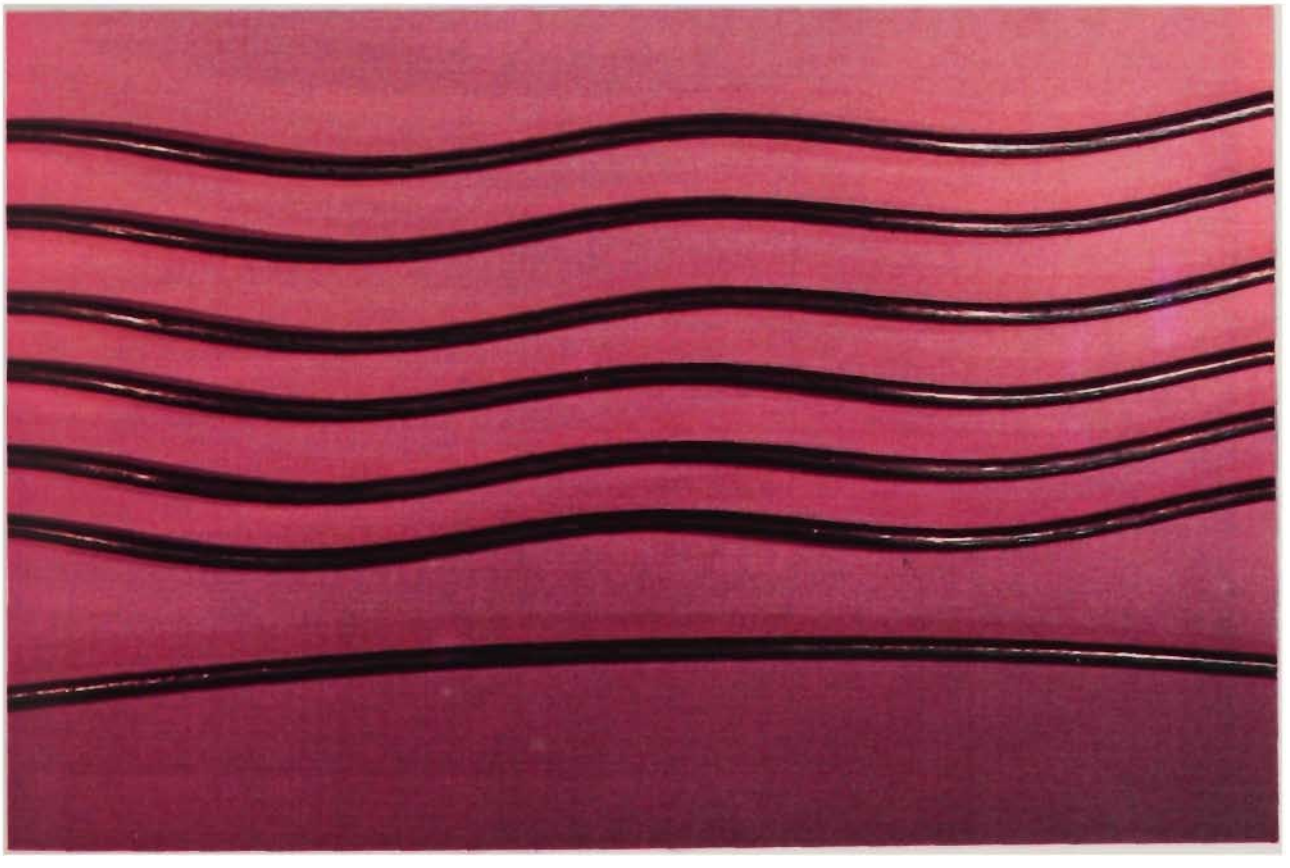

PLATE A3.16 - TOMAGO TO TAREE TRANSMISSION LINE
DESTRANDED AND CLEANED 6 WIRE STEEL
LAYER AND STEEL CORE

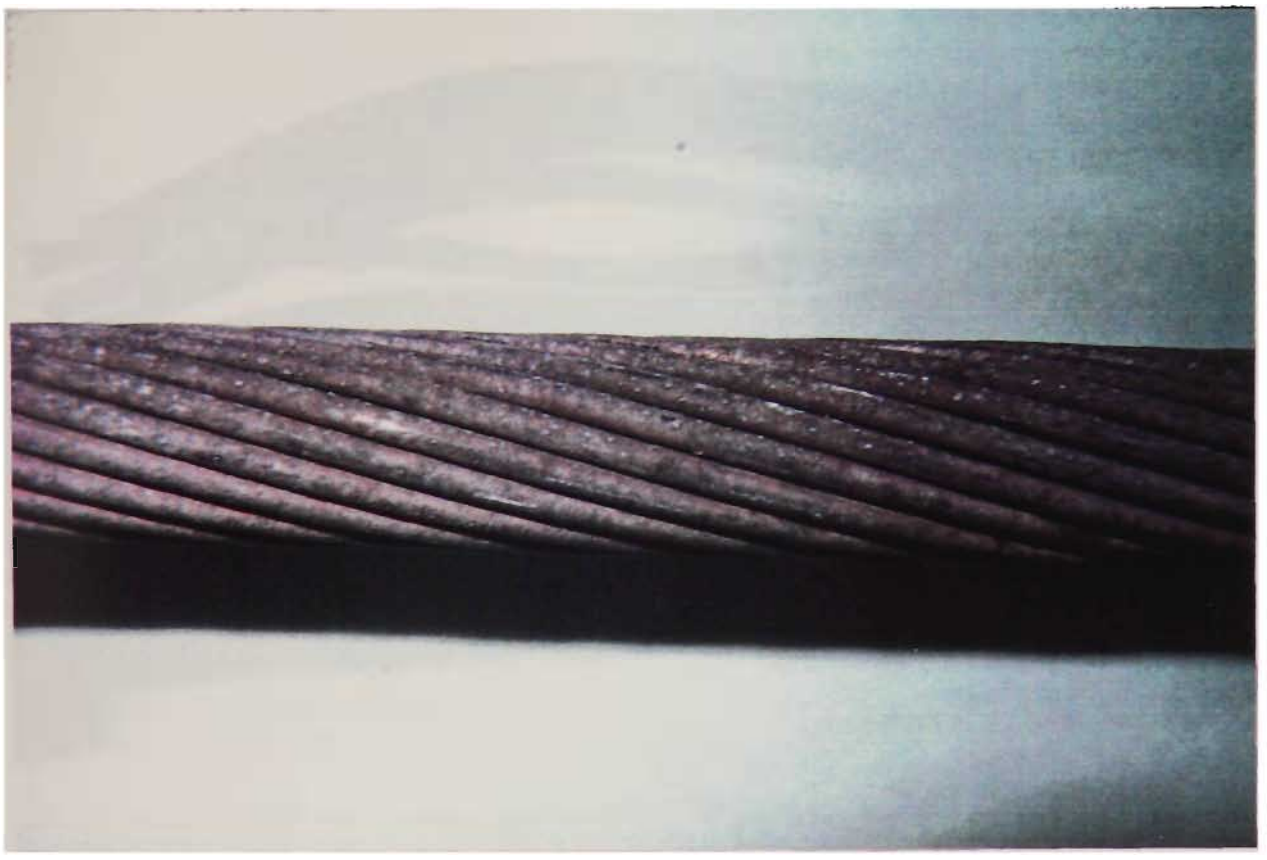

PLATE A3.17 - BELLAMBI TO HEATHCOTE TRANSMISSION LINE
18 WIRE ALUMINIUM LAYER OR OUTSIDE LAYER

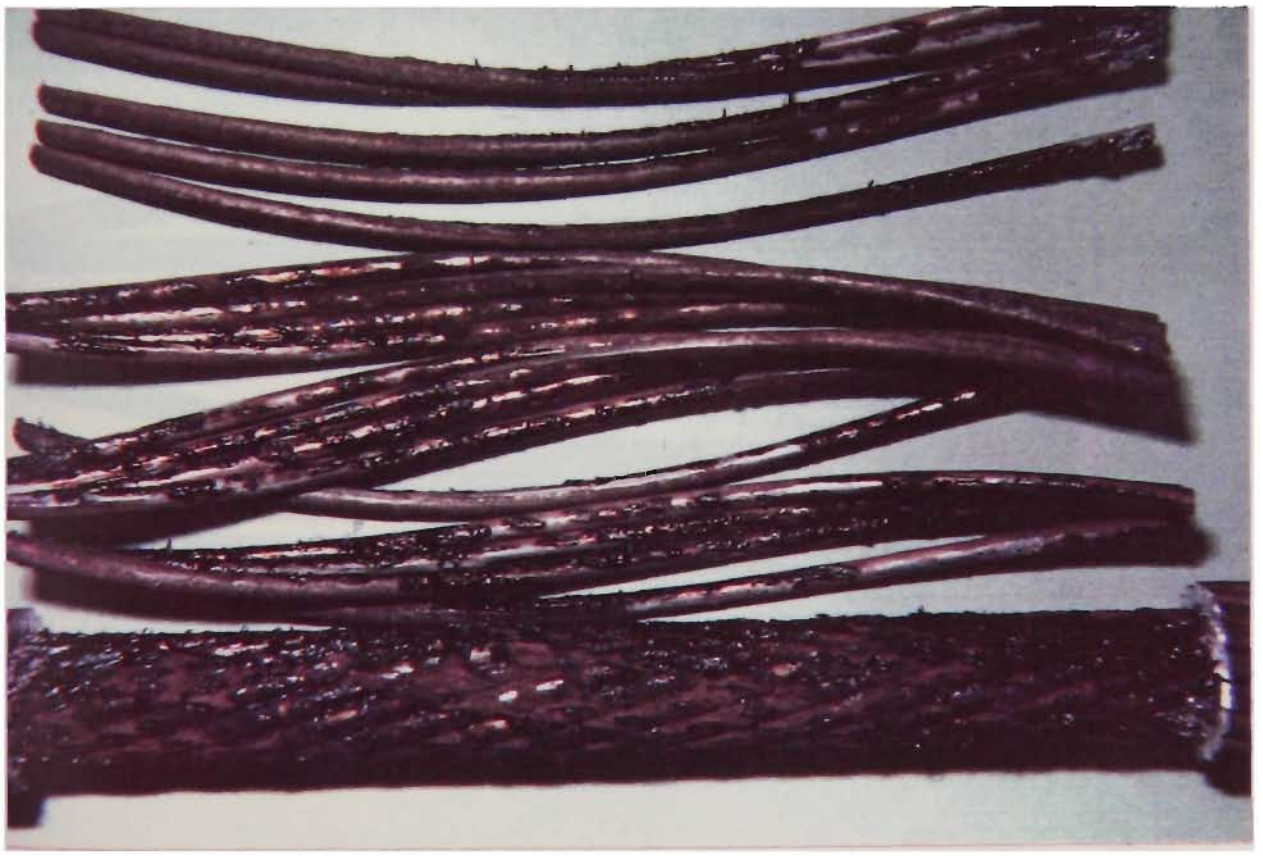

PLATE A3.18 - BELLAMBI TO HEATHCOTE TRANSMISSION LINE
12 WIRE ALUMINIUM LAYER AND
UNDERSIDE OF 18 WIRE ALUMINIUM LAYER

PLATE A3.19 - BELLAMBI TO HEATHCOTE TRANSMISSION LINE
6 WIRE STEEL LAYER AND
UNDERSIDE OF THE 12 WIRE ALUMINIUM LAYER

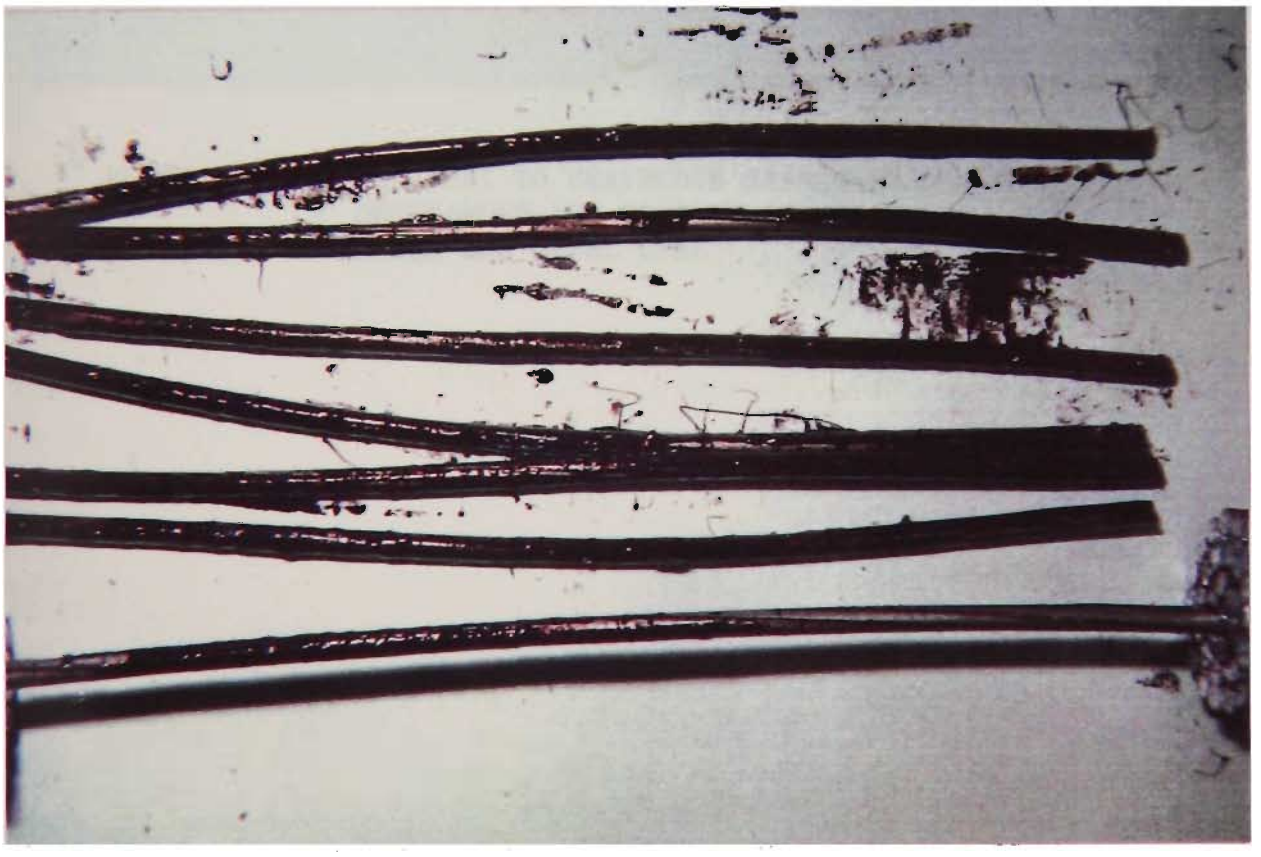

PLATE A3.20 - BELLAMBI TO HEATHCOTE TRANSMISSION LINE
DESTRANDED 6 WIRE STEEL LAYER AND
STEEL CORE

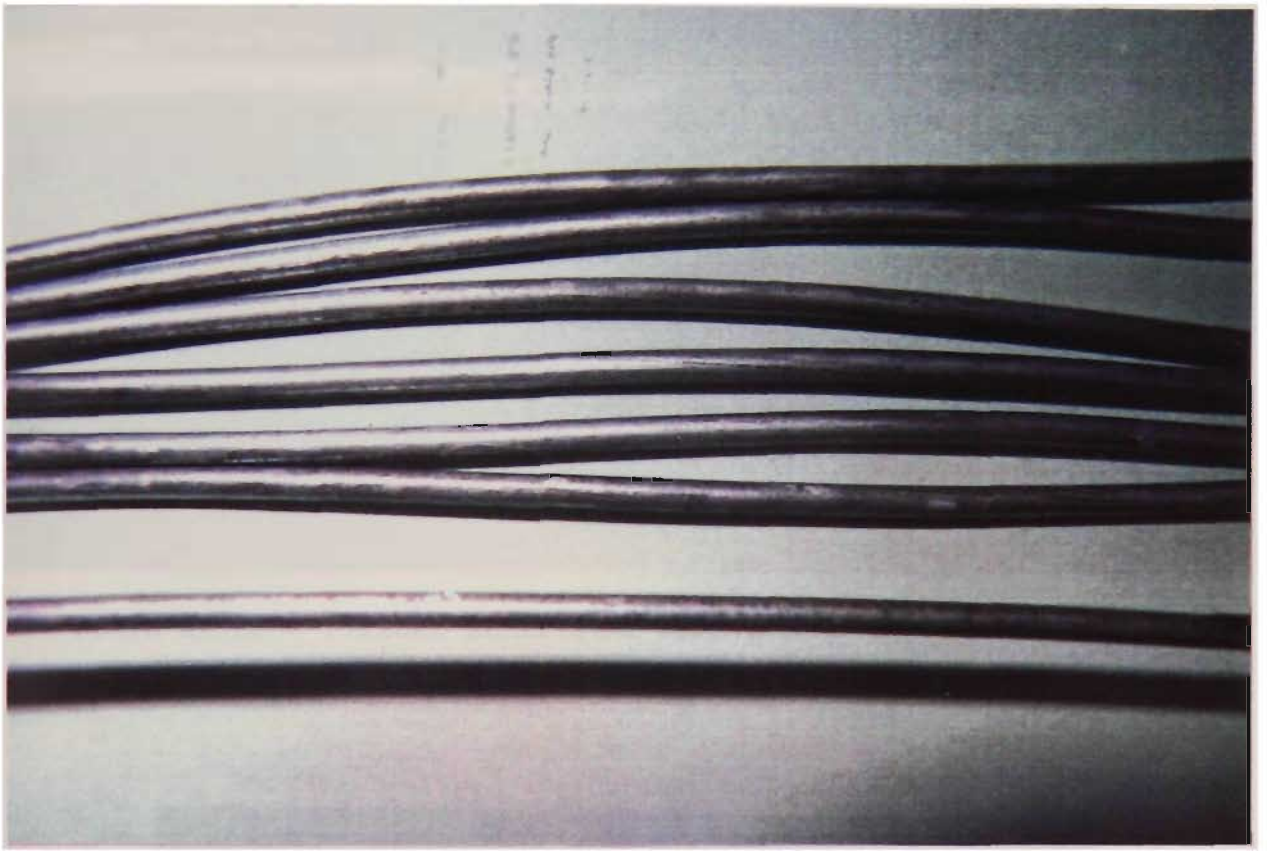

PLATE A3.21 - BELLAMBI TO HEATHCOTE TRANSMISSION LINE
DESTRANDED AND CLEANED 6 WIRE STEEL
LAYER AND STEEL CORE

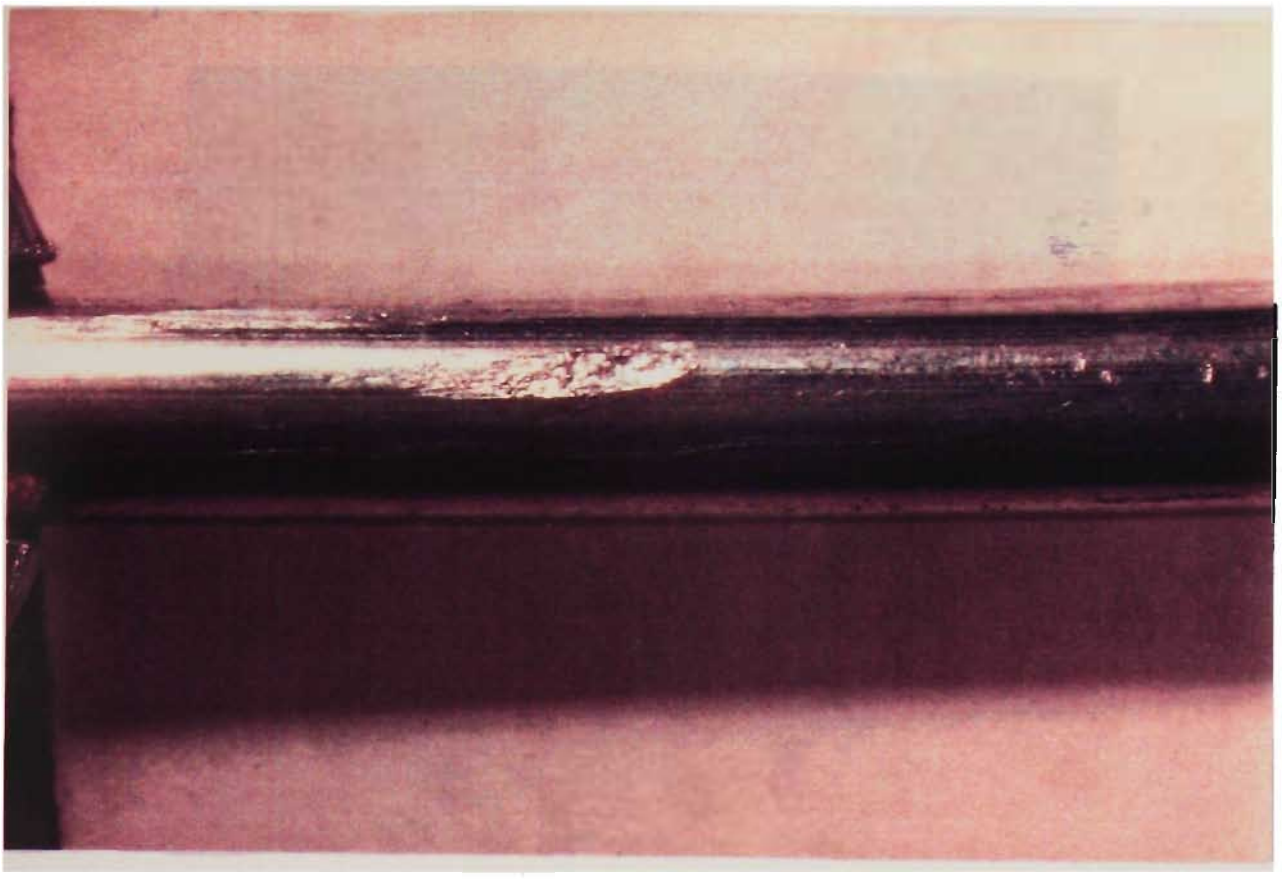

PLATE A3.22 - TYPICAL ELLIPTICAL AREA DAMAGE OF ALUMINIUM STRANDS

PLATE A3.23 - LONGITUDINAL SECTION OF ELLIPTICAL AREA DAMAGE OF ALUMINIUM STRANDS X100

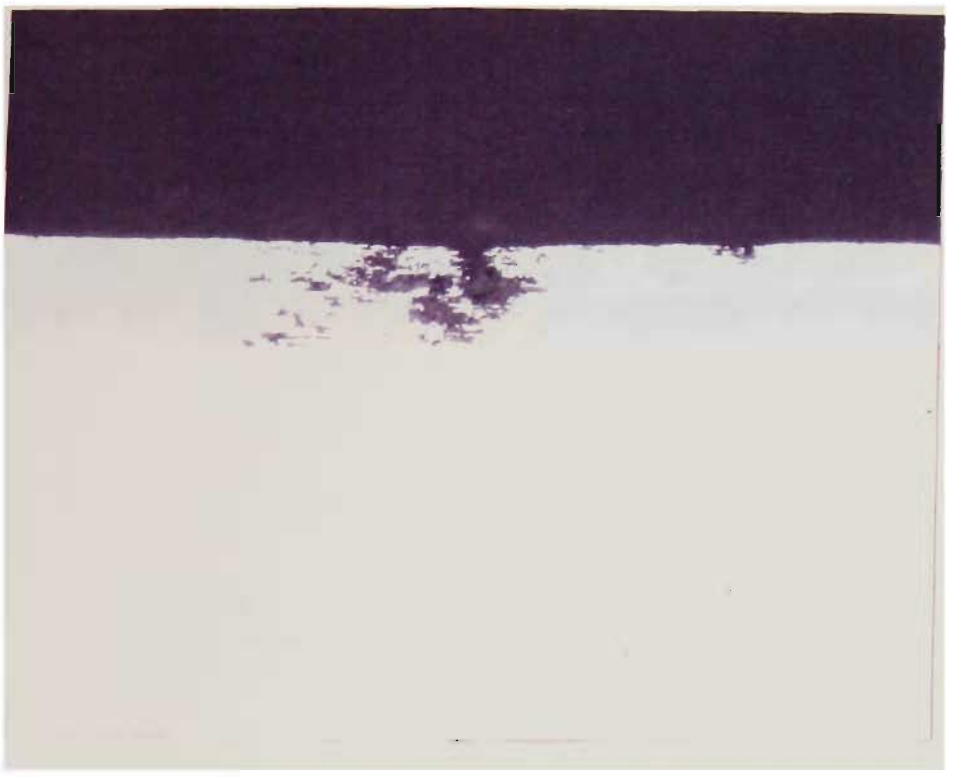

PLATE A3.24 - LONGITUDINAL SECTION OF TYPICAL
OUTER ALUMINIUM LAYER PITTING
X200

PLATE A3.25 - LONGITUDINAL SECTION OF 18 WIRE LAYER
ALUMINIUM PITTING FROM TOMAGO TO TAREE TRANSMISSION LINE
X50

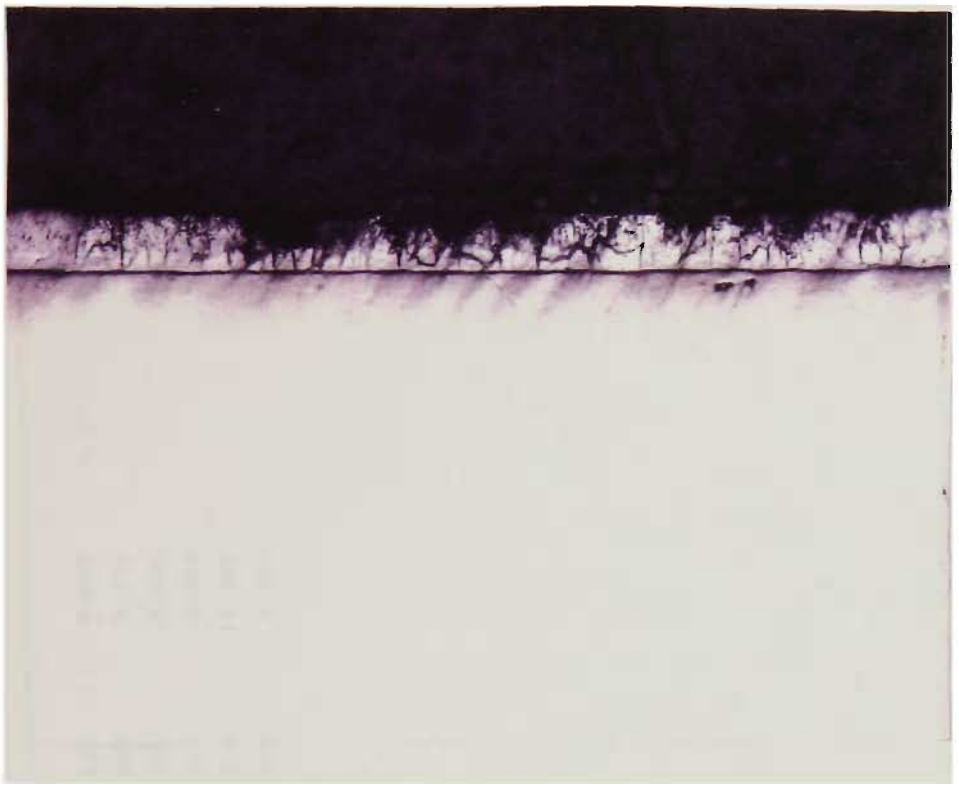

PLATE A3.26 - LOSS OF GALVANIZING FROM STEEL CORE
FROM TOMAGO TO TAREE TRANSMISSION LINE
X200

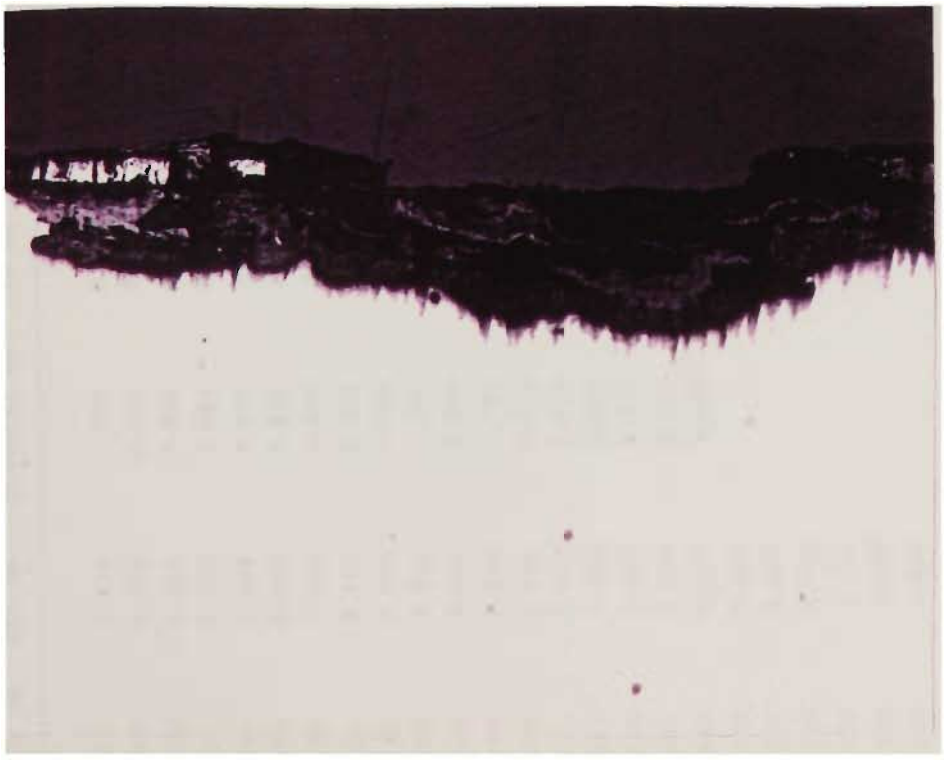

PLATE A3.27 - CORROSION OF STEEL WIRE FROM 6 WIRE LAYER
FROM TOMAGO TO TAREE TRANSMISSION LINE
X100

Strand	24 Wire Layer		18 Wire Layer		12 Wire Layer		6 Wire Layer		Core	
	Diameter mm	CSA mm^2	Diameter mm	CSA mm^2	Diameter mm	CSA mm^2	Diameter mm	CSA mm^2	Diameter mm	CSA mm^2
1	3.535	9.816	3.531	9.796	3.517	9.716	3.543	9.860	3.747	11.028
2	3.547	9.885	3.531	9.796	3.526	9.769	3.527	9.771		
3	3.552	9,913	3.523	9.749	3.538	9,832	3.554	9.921		
4	3.551	9,905	3.501	9.631	3.536	9.824	3.543	9.860		
5	3.554	9.924	3.537	9.828	3.528	9.780	3.578	10.059		
6	3.553	9.916	3.528	9.777	3.527	9.774	3.544	9.869		
7	3.558	9.944	3.535	9.816	3.542	9.855				
8	3.534	9.813	3.537	9,830	3.541	9.852				
9	3.545	9.871	3.536	9.821	3.524	9.755				
10	3.556	9.935	3.551	9.905	3.525	9.763				
11	3.549	9.896	3.528	9.780	3.520	9.735				
12	3.558	9.943	3.522	9.744	3.537	9.830				
13	3.548	9.891	3.533	9.807						
14	3.533	9.805	3.535	9.816						
15	3.553	9.919	3.525	9.756						
16	3.546	9.877	3.541	9.849						
17	3.553	9.916	3.535	9.818						
18	3.556	9.933	3.529	9.782						
19	3.534	9.810								
20	3.547	9.882								
21	3.546	9.880								
22	3.554	9.921								
23	3.549	9.896								
24	3.549	9.894								

TABLE A3.1 - CROSS SECTIONAL AREA AVON TO KEMPS CREEK TRANSMISSION LINE

Strand	24 Wire Layer		18 Wire Layer		12 Wire Layer		6 Wire Layer		Core	
	Diameter mm	CSA mm^2	Diameter mm	CSA mm^2	Diameter mm	CSA mm^2	Diameter mm	CSA mm^2	Diameter mm	CSA mm^2
1	3.574	10.036	3.513	9.699	3.507	9.664	3.548	9.888	3.735	10.961
2	3.564	9.980	3.528	9.777	3.499	9.620	3.532	9.802		
3	3.547	9.882	3.531	9.793	3.518	9.721	3.544	9.869		
4	3.561	9.961	3.526	9.769	3.549	9.894	3.556	9.935		
5	3.562	9.966	3.556	9.933	3.551	9.905	3.557	9.938		
6	3.561	9.963	3.519	9.730	3.542	9.857	3.581	10.076		
7	3.560	9.958	3.536	9.821	3.507	9.661				
8	3.516	9.713	3.532	9.799	3.516	9.710				
9	3.563	9.975	3.526	9.766	3.544	9.869				
10	3.557	9.941	3.557	9.941	3.545	9.871				
11	3.550	9.902	3.521	9.741	3.552	9.913				
12	3.556	9.933	3.542	9.857	3.555	9.927				
13	3.571	10.019	3.504	9.647						
14	3.553	9.916	3.505	9.650						
15	3.574	10.033	3.553	9.916						
16	3.563	9.975	3.506	9.655						
17	3.552	9.913	3.529	9.785						
18	3.572	10.025	3.553	9.916						
19	3.586	10.104								
20	3.579	10.064								
21	3.571	10.017								
22	3.569	10.005								
23	3.562	9.966								
24	3.569	10.008								

TABLE A3.2 - CROSS SECTIONAL AREA DAPTO TO SPRINGHILL TRANSMISSION LINE

Strand	24 Wire Layer		18 Wire Layer		12 Wire Layer		6 Wire Layer		Core	
	Diameter mm	CSA mm^2	Diameter mm	CSA mm^2	Diameter mm	CSA mm^2	Diameter mm	CSA mm^2	Diameter mm	CSA mm^2
1			3.005	7.092	3.001	7.073	2.995	7.045	3.008	7.106
2			3.004	7.087	3.010	7.116	3.000	7.069		
3			3.003	7.083	3.011	7.121	3.004	7.087		
4			3.002	7.078	2.988	7.012	3.017	7.149		
5			3.012	7.125	3.004	7.087	3.009	7.111		
6			3.009	7.111	3.003	7.083	2.998	7.059		
7			3.006	7.097	3.002	7.028				
8			2.997	7.054	3.012	7.125				
9			2.995	7.045	3.006	7.097				
10			3.005	7.092	3.008	7.106				
11			2.993	7.036	3.008	7.106				
12			3.004	7.087	3.006	7.097				
13			2.995	7.045						
14			3.005	7.092						
15			3.014	7.135						
16			3.005	7.092						
17			3.024	7.182						
18			3.009	7.111						
19										
20										
21										
22										
23										
24										

TABLE A3.3 - CROSS SECTIONAL AREA TOMAGO TO TAREE TRANSMISSION LINE

Strand	24 Wire Layer		18 Wire Layer		12 Wire Layer		6 Wire Layer		Core	
	Diameter mm	CSA mm^2	Diameter mm	CSA mm^2	Diameter mm	CSA mm^2	Diameter mm	CSA mm^2	Diameter mm	CSA mm^2
1			3.725	10.898	3.674	10.602	3.687	10.677	3.688	10.682
2			3.712	10.822	3.661	10.527	3.679	10.630		
3			3.689	10.688	3.712	10.822	3.695	10.723		
4			3.723	10.886	3.673	10.596	3.680	10.636		
5			3.716	10.845	3.701	10.758	3.690	10.694		
6			3.720	10.869	3.681	10.642	3.709	10.804		
7			3.687	10.677	3.710	10.810				
8			3.718	10.857	3.715	10.839				
9			3.717	10.851	3.717	10.851				
10			3.733	10.945	3.691	10.700				
11			3.687	10.677	3.690	10.694				
12			3.732	10.939	3.686	10.671				
13			3.724	10.892						
14			3.725	10.898						
15			3.727	10.910						
16			3.726	10.904						
17			3.719	10.863						
18			3.692	10.706						
19										
20										
21										
22										
23										
24										

TABLE A3.4 - CROSS SECTIONAL AREA BELLAMBI TO HEATHCOTE TRANSMISSION LINE

Strand	24 Wire Layer			18 Wire Layer			12 Wire Layer			6 Wire Layer			Core		
	B.L. kN	UTS GPA	Elongation %	B.L. kN	UTS Gpa	Elongation %	B.L. kN	UTS GPa	Elongation %	B.L. kN	UTS GPa	Elongation %	B.L. kN	UTS GPa	Elongation %
1	1.769	0.180	2.0	1.639	0.167	2.0	1.563	0.161	2.0	14.473	1.468	5.9	15.947	1.447	6.0
2	1.748	0.177	2.0	1.685	0.172	2.0	1.603	0.164	1.6	13.408	1.373	6.2			
3	1.801	0.182	2.0	1.552	0.159	2.0	1.625	0.165	1.6	14.946	1.507	5.8			
4	1.727	0.174	2.0	1.637	0.170	1.6	1.599	0.163	1.6	13.906	1.411	5.9			
5	1.680	0.169	2.0	1.633	0.166	1.6	1.598	0.163	1.6	15.029	1.495	5.9			
6	1.729	0.174	1.8	1.672	0.171	1.6	1.620	0.166	1.6	14.282	1.448	6.0			
7	1.763	0.177	1.8	1.582	0.161	1.6	1.675	0.170	2.0						
8	1.746	0.178	1.8	1.572	0.160	2.0	1.670	0.170	1.6						
9	1.732	0.176	2.0	1.604	0.164	2.0	1.627	0.167	2.0						
10	1.694	0.171	2.0	1.664	0.168	2.0	1.604	0.164	1.6						
11	1.772	0.179	1.8	1.636	0.167	1.6	1.667	0.171	2.0						
12	1.742	0.175	1.6	1.598	0.164	2.0	1.622	0.165	2.0						
13	1.754	0.177	1.6	1.414	0.144	2.0									
14	1.718	0.175	1.8	1.659	0.169	2.0									
15	1.682	0.170	1.6	1.666	0.171	1.6									
16	1.646	0.167	2.0	1.616	0.171	1.6									
17	1.689	0.170	1.8	1.688	0.172	1.6									
18	1.747	0.176	1.8	1.678	0.172	1.6									
19	1.720	0.175	1.8												
20	1.715	0.174	2.0												
21	1.770	0.179	1.8												
22	1.730	0.174	1.8												
23	1.720	0.174	1.8												
24	1.732	0.175	1.8												

TABLE A3.5 - MECHANICAL PROPERTIES AVON TO KEMPS CREEK TRANSMISSION LINE

Strand	24 Wire Layer			18 Wire Layer			12 Wire Layer			6 Wire Layer			Core		
	B.L. kN	UTS GPA	Elongation %	B.L. kN	UTS Gpa	Elongation %	B.L. kN	UTS GPa	Elongation %	B.L. kN	UTS GPa	Elongation %	B.L. kN	UTS GPa	Elongation %
1	1.757	0.175	1.8	1.777	0.183	1.6	1.649	0.171	1.4	14.551	1.472	6.4	15.645	1.428	5.8
2	1.830	0.183	1.6	1.763	0.180	1.6	1.799	0.187	1.4	15.063	1.537	5.8			
3	1.704	0.173	1.6	1.582	0.162	1.6	1.736	0.179	1.4	15.342	1.555	6.0			
4	1.754	0.176	1.6	1.610	0.165	1.6	1.678	0.170	1.6	15.161	1.527	5.6			
5	1.888	0.190	1.2	1.851	0.186	1.4	1.747	0.176	1.6	15.479	1.558	6.0			
6	1.779	0.179	1.4	1.738	0.179	1.6	1.693	0.172	1.4	15.093	1.499	6.0			
7	1.829	0.184	1.4	1.749	0.178	1.6	1.609	0.167	1.2						
8	1.693	0.174	1.6	1.774	0.181	1.4	1.721	0.174	1.4						
9	1.722	0.173	1.4	1.584	0.162	1.4	1.721	0.174	1.4						
10	1.804	0.182	1.4	1.765	0.178	1.6	1.620	0.164	1.6						
11	1.786	0.180	1.4	1.572	0.161	1.6	1.693	0.171	1.4						
12	1.680	0.169	1.6	1.678	0.170	1.8	1.660	0.167	1.6						
13	1.774	0.177	1.6	1.725	0.179	1.6									
14	1.639	0.165	1.4	1.698	0.176	1.6									
15	1.768	0.176	1.8	1.825	0.184	1.6									
16	1.615	0.162	1.6	1.659	0.172	1.4									
17	1.726	0.174	1.6	1.720	0.176	1.4									
18	1.685	0.168	1.6	1.715	0.173	1.6									
19	1.678	0.166	1.6												
20	1.792	0.178	1.8												
21	1.799	0.180	1.6												
22	1.776	0.178	1.2												
23	1.692	0.170	1.6												
24	1.722	0.172	1.6												

TABLE A3.6 - MECHANICAL PROPERTIES DAPTO TO SPRINGHILL TRANSMISSION LINE

Strand	24 Wire Layer			18 Wire Layer			12 Wire Layer			6 Wire Layer			Core		
	B.L. kN	UTS GPA	Elongation %	B.L. kN	UTS Gpa	Elongation %	B.L. kN	UTS GPa	Elongation %	B.L. kN	UTS GPa	Elongation %	B.L. kN	UTS GPa	Elongation %
1				1.17	0.165	1.6	1.10	0.156	1.2	9.71	1.378	5.6	9.65	1.358	3.2
2				1.17	0.165	1.6	1.16	0.163	1.4	10.01	1.416	5.8			
3				1.17	0.165	2.0	1.11	0.156	1.8	10.08	1.422	5.6			
4				1.19	0.168	1.8	1.17	0.167	1.4	10.45	1.462	5.4			
5				1.21	0.170	2.0	1.20	0.169	2.0	10.09	1.419	5.8			
6				1.16	0.163	2.0	1.10	0.155	1.0	10.00	1.417	5.6			
7				1.17	0.165	1.8	1.08	0.153	1.6						
8				1.18	0.167	1.6	1.13	0.159	1.8						
9				1.16	0.165	1.8	1.11	0.156	1.6						
10				1.17	0.165	1.8	1.14	0.160	1.4						
11				1.19	0.169	1.8	1.16	0.163	1.6						
12				1.17	0.165	1.6	1.11	0.156	2.0						
13				1.16	0.165	1.8									
14				1.15	0.162	1.6									
15				1.19	0.167	1.8									
16				1.19	0.168	1.8									
17				1.17	0.163	1.8									
18				1.16	0.163	1.6									
19															
20															
21															
22															
23															
24															

TABLE A3.7 - MECHANICAL PROPERTIES TOMAGO TO TAREE TRANSMISSION LINE

Strand	24 Wire Layer			18 Wire Layer			12 Wire Layer			6 Wire Layer			Core		
	B.L. kN	UTS GPA	Elongation %	B.L. kN	UTS Gpa	Elongation %	B.L. kN	UTS GPa	Elongation %	B.L. kN	UTS GPa	Elongation %	B.L. kN	UTS GPa	Elongation %
1				1.62	0.149	-	1.58	0.149	-	15.11	1.415	-	15.27	1.429	-
2				1.65	0.152	-	1.43	0.136	-	15.27	1.436	-			
3				1.58	0.148	-	1.63	0.151	-	15.53	1.448	-			
4				1.68	0.154	-	1.58	0.149	-	15.56	1.463	-			
5				1.59	0.147	-	1.60	0.149	-	15.39	1.439	-			
6				1.75	0.161	-	1.71	0.161	-	15.71	1.454	-			
7				1.62	0.152	-	1.70	0.157	-						
8				1.58	0.146	-	1.56	0.144	-						
9				1.69	0.156	-	1.63	0.150	-						
10				1.58	0.144	-	1.65	0.154	-						
11				1.50	0.140	-	1.62	0.151	-						
12				1.62	0.148	-	1.66	0.156	-						
13				1.83	0.168	-									
14				1.66	0.152	-									
15				1.70	0.156	-									
16				1.77	0.162	-									
17				1.61	0.148	-									
18				1.52	0.142	-									
19															
20															
21															
22															
23															
24															

TABLE A3.8 - MECHANICAL PROPERTIES BELLAMBI TO HEATHCOTE TRANSMISSION LINE

Strand	Resistivity at 20°C μΩm		
	24 Wire Layer	18 Wire Layer	12 Wire Layer
1	0.0280	0.0279	0.0278
2	0.0280	0.0278	0.0278
3	0.0280	0.0278	0.0279
4	0.0280	0.0277	0.0278
5	0.0279	0.0278	0.0279
6	0.0280	0.0279	0.0278
7	0.0279	0.0277	0.0279
8	0.0280	0.0278	0.0279
9	0.0280	0.0279	0.0279
10	0.0278	0.0279	0.0279
11	0.0279	0.0279	0.0280
12	0.0280	0.0278	0.0280
13	0.0280	0.0277	
14	0.0279	0.0278	
15	0.0279	0.0278	
16	0.0278	0.0278	
17	0.0279	0.0279	
18	0.0280	0.0278	
19	0.0279		
20	0.0279		
21	0.0280		
22	0.0280		
23	0.0279		
24	0.0278		

TABLE A3.9 - ELECTRICAL PROPERTIES
AVON TO KEMPS CREEK TRANSMISSION LINE

Strand	Resistivity at 20°C μΩm		
	24 Wire Layer	18 Wire Layer	12 Wire Layer
1	0.0282	0.0280	0.0279
2	0.0282	0.0280	0.0281
3	0.0282	0.0277	0.0281
4	0.0282	0.0278	0.0280
5	0.0284	0.0281	0.0280
6	0.0283	0.0281	0.0279
7	0.0284	0.0280	0.0273
8	0.0281	0.0281	0.0278
9	0.0283	0.0278	0.0280
10	0.0283	0.0278	0.0280
11	0.0283	0.0278	0.0279
12	0.0281	0.0279	0.0278
13	0.0283	0.0281	
14	0.0280	0.0280	
15	0.0283	0.0281	
16	0.0282	0.0279	
17	0.0284	0.0279	
18	0.0283	0.0279	
19	0.0283		
20	0.0285		
21	0.0286		
22	0.0283		
22	0.0282		
24	0.0283		

TABLE A3.10 - ELECTRICAL PROPERTIES
DAPTO TO SPRINGHILL TRANSMISSION LINE

Strand	Resistivity at 20°C μΩm		
	24 Wire Layer	18 Wire Layer	12 Wire Layer
1		0.02739	0.02733
2		0.02732	0.02726
3		0.02740	0.02738
4		0.02736	0.02731
5		0.02752	0.02735
6		0.02735	0.02759
7		0.02742	0.02738
8		0.02742	0.02738
9		0.02735	0.02739
10		0.02735	0.02740
11		0.02747	0.02741
12		0.02739	0.02725
13		0.02759	
14		0.02738	
15		0.02742	
16		0.02737	
17		0.02723	
18		0.02764	
19			
20			
21			
22			
23			
24			

TABLE A3.11 - ELECTRICAL PROPERTIES
TOMAGO TO TAREE TRANSMISSION LINE

Strand	Resistivity at 20°C μΩm		
	24 Wire Layer	18 Wire Layer	12 Wire Layer
1		0.0287	0.0279
2		0.0288	0.0276
3		-	-
4		-	-
5		-	-
6		-	-
7		-	-
8		-	-
9		-	-
10		-	-
11		-	-
12		-	-
13		-	
14		-	
15		-	
16		-	
17		-	
18		-	
19			
20			
21			
22			
23			
24			

TABLE A3.12 - ELECTRICAL PROPERTIES
BELLAMBI TO HEATHCOTE TRANSMISSION LINE

Strand	Zinc Coating Mass $kg.m^{-2}$	
	6 Wire Layer	Core
1	0.359	0.393
2	0.346	
3	0.353	
4	0.382	
5	0.373	
6	0.350	

TABLE A3.13 - ZINC COATING MASS
AVON TO KEMPS CREEK
TRANSMISSION LINE

Strand	Zinc Coating Mass $kg.m^{-2}$	
	6 Wire Layer	Core
1	0.457	0.417
2	0.347	
3	0.431	
4	0.368	
5	0.396	
6	0.441	

TABLE A3.14 - ZINC COATING MASS
DAPTO TO SPRINGHILL
TRANSMISSION LINE

Strand	Zinc Coating Mass $kg.m^{-2}$	
	6 Wire Layer	Core
1	0.2297	0.2125
2	0.2450	
3	0.2433	
4	0.2264	
5	0.2321	
6	0.2069	

TABLE A3.15 - ZINC COATING MASS
TOMAGO TO TAREE
TRANSMISSION LINE

Strand	Zinc Coating Mass $kg.m^{-2}$	
	6 Wire Layer	Core
1	0.310	0.330
2	0.250	
3	0.270	
4	0.270	
5	0.280	
6	0.280	

TABLE A3.16 - ZINC COATING MASS
BELLAMBI TO HEATHCOTE
TRANSMISSION LINE

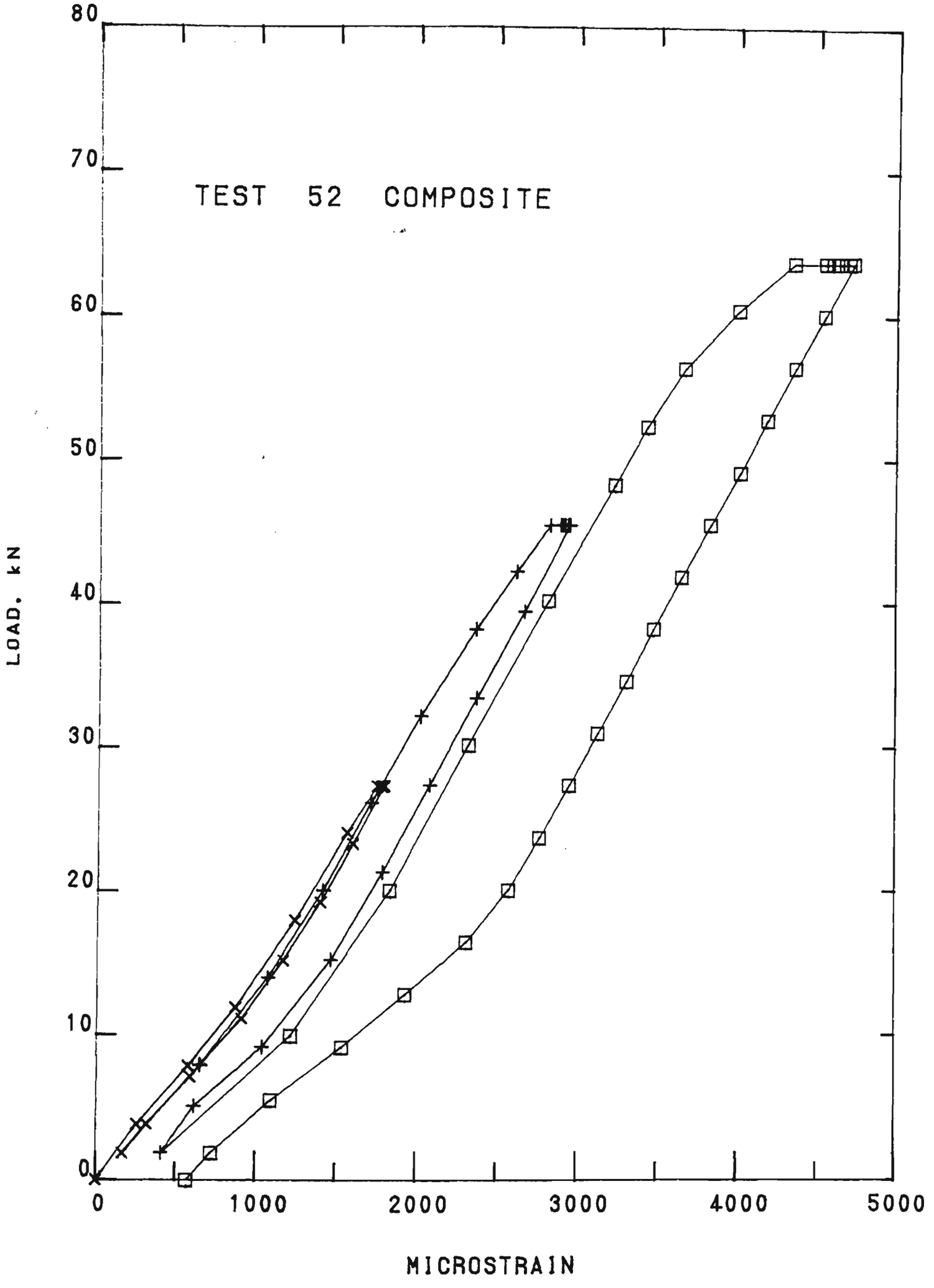

FIGURE A3.1 - STRESS STRAIN TEST
RAW PLOT OF TEST RESULT DATA
TOMAGO TO TAREE TRANSMISSION LINE

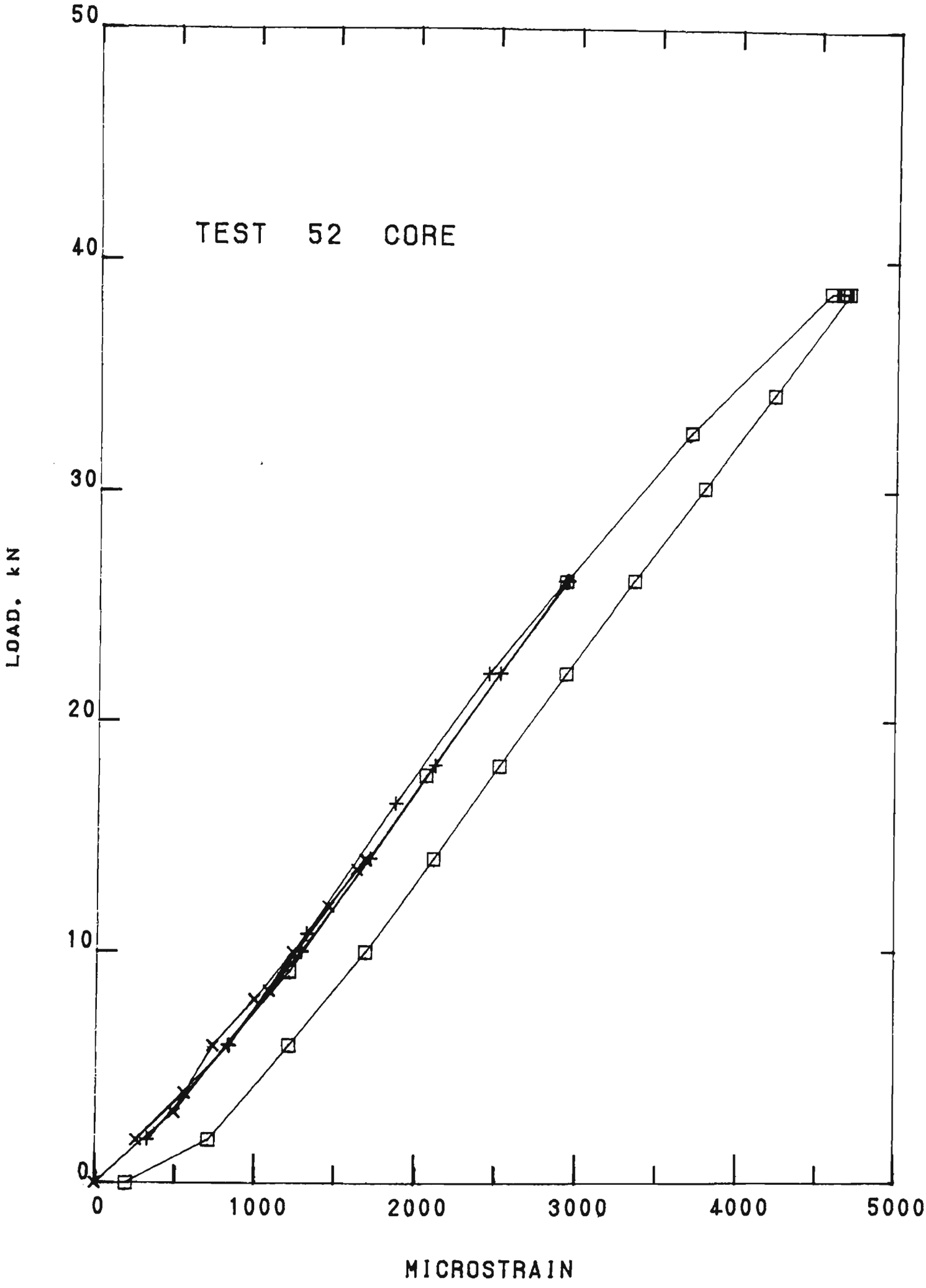

FIGURE A3.2 - STRESS STRAIN TEST
RAW PLOT OF TEST RESULT DATA
TOMAGO TO TAREE TRANSMISSION LINE

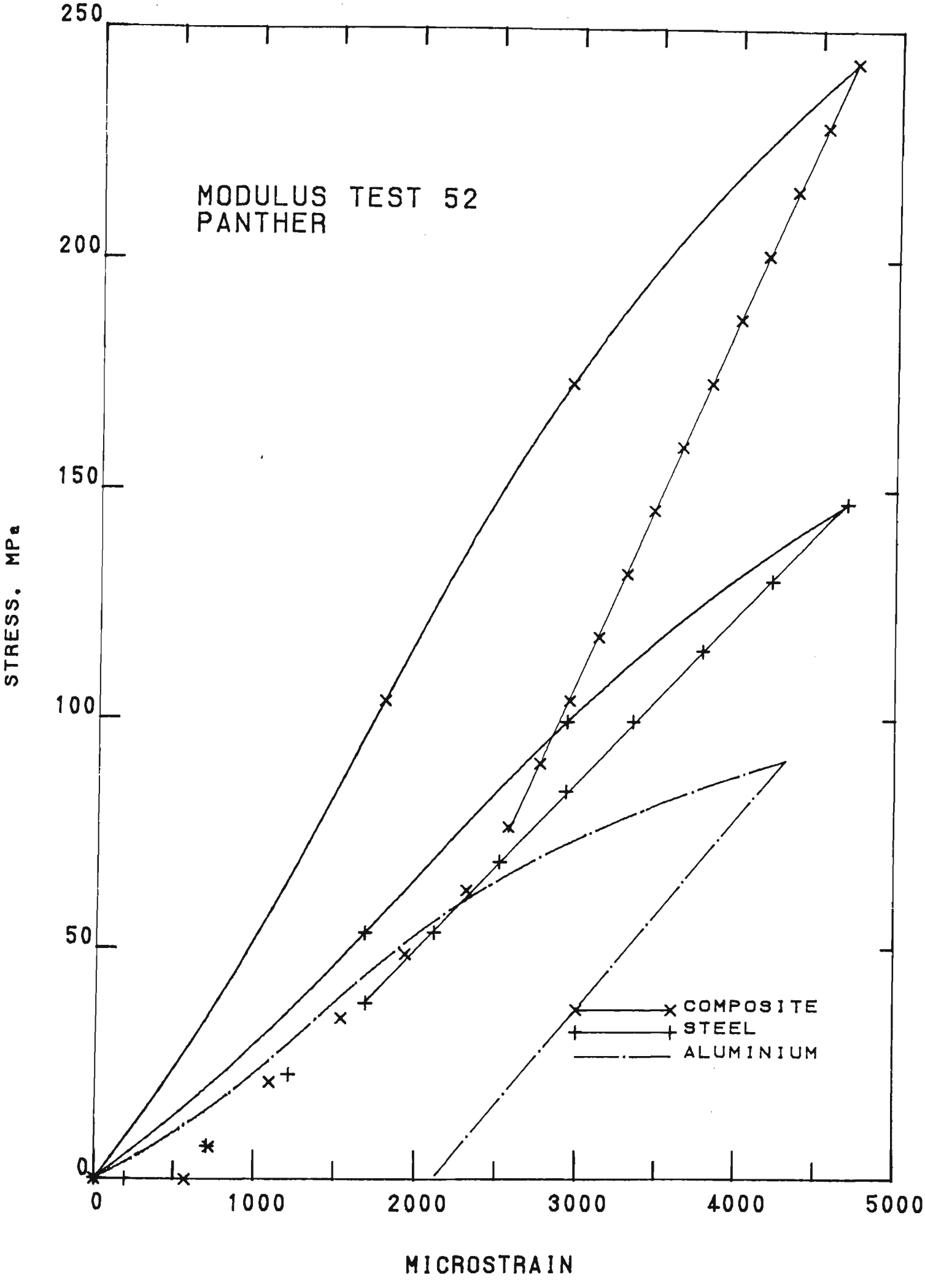

FIGURE A3.3 - STRESS STRAIN TEST
DERIVED TEST RESULTS
TOMAGO TO TAREE TRANSMISSION LINE

Conductor Modulus Data			
Parameter	Equation Constants		Correlation Coefficient
	m	b	
E_{ci}	67.2	-0.135	0.9997
E_{cf}	77.9	-0.124	0.9996
nE_{af}	42.9	-	-
mE_{si}	35.4	-8.21×10^{-3}	0.9998
E_{sf}	191	-0.129	0.9999

m = 0.1891
n = 0.8109

Initial Modulus Curve Polynominal Coefficients			
Curve	A1	A2	A3
Composite	0.224×10^{-4}	-0.789×10^{-7}	0.274×10^{-9}
Steel	0.391×10^{-4}	-0.196×10^{-6}	0.998×10^{-9}
Aluminium	0.558×10^{-4}	-0.689×10^{-6}	0.652×10^{-8}

Critical Tension/Stress Point Data	
Tension kN	18.1
μE	2500

TABLE A3.17 - STRESS STRAIN TEST NO. 52 TEST RESULT DATA
TOMAGO TO TAREE TRANSMISSION LINE

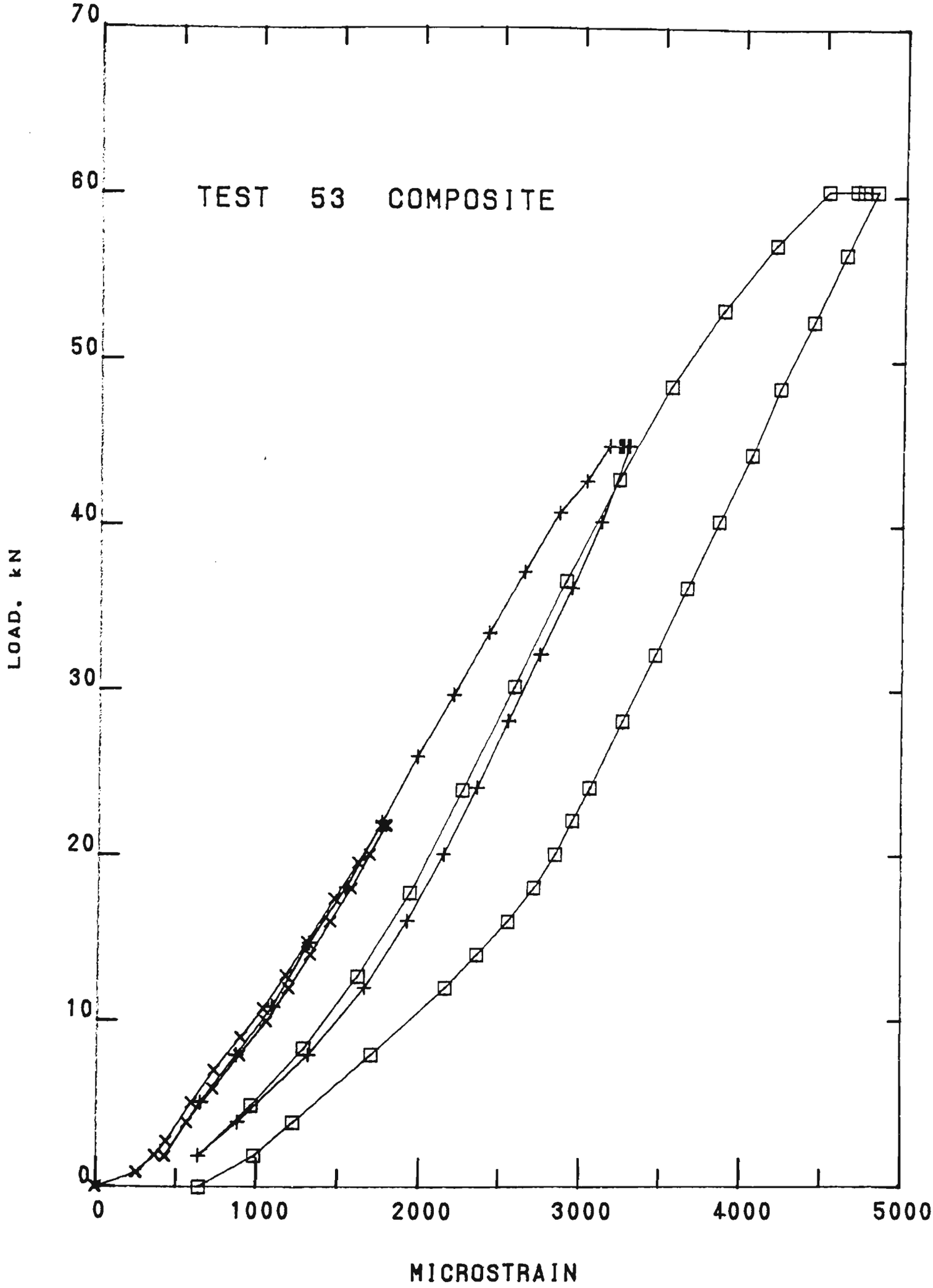

FIGURE A3.4 - STRESS STRAIN TEST
RAW PLOT OF TEST RESULT DATA
TOMAGO TO TAREE TRANSMISSION LINE

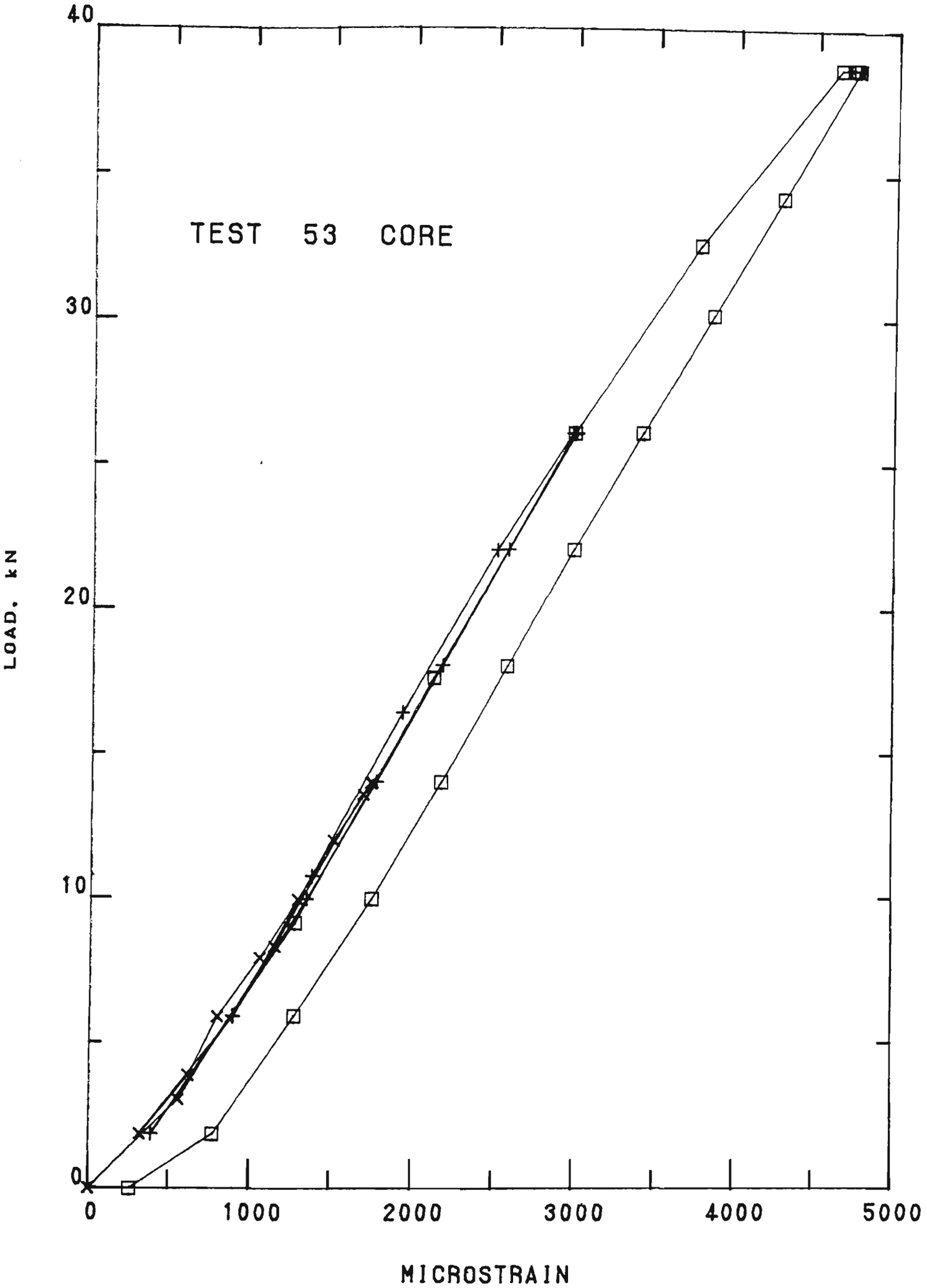

FIGURE A3.5 - STRESS STRAIN TEST
RAW PLOT OF TEST RESULT PLATE
TOMAGO TO TAREE TRANSMISSION LINE

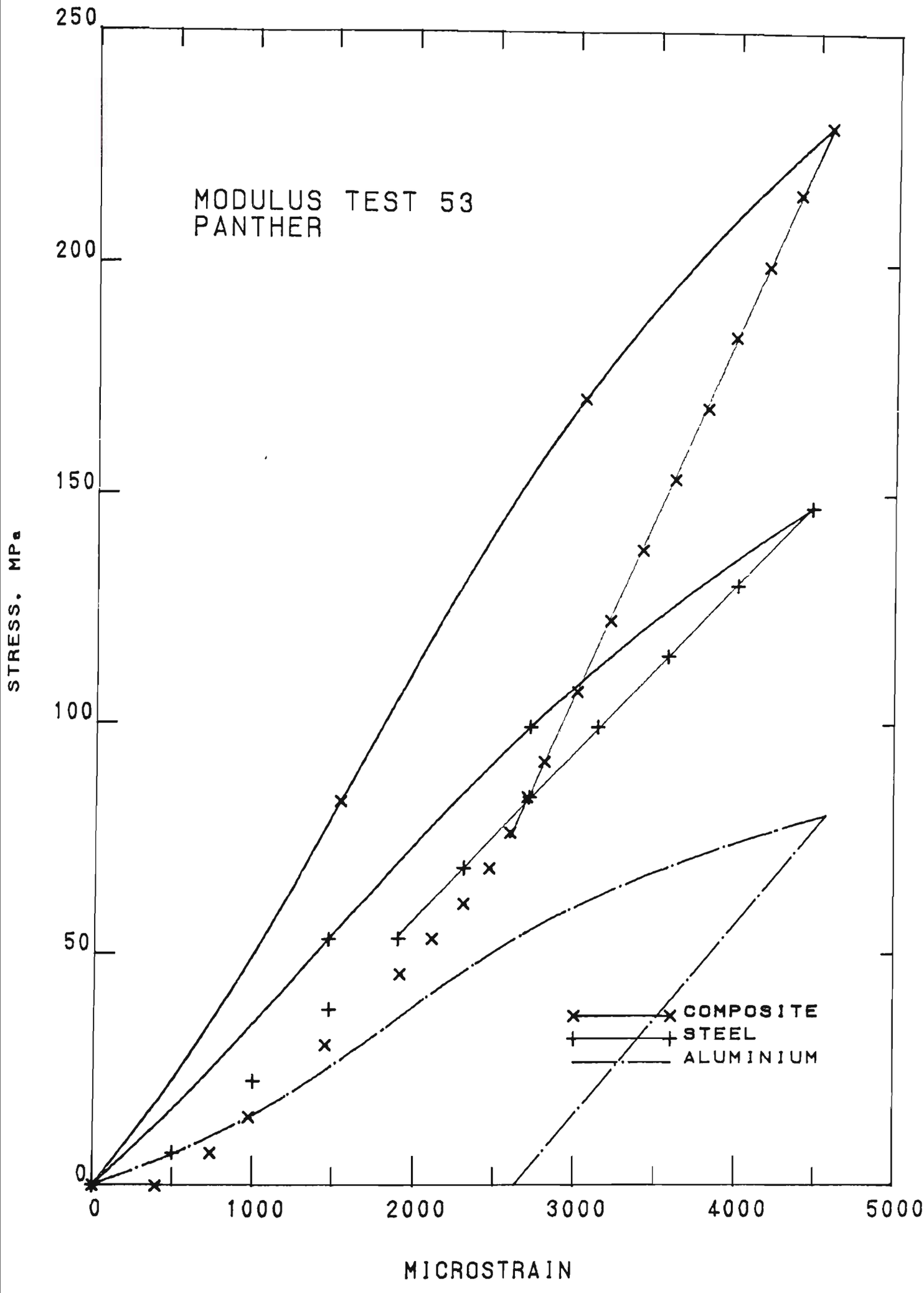

FIGURE A3.6 - STRESS STRAIN TEST
DERIVED TEST RESULT
TOMAGO TO TAREE TRANSMISSION LINE

Conductor Modulus Data			
Parameter	Equation Constants		Correlation Coefficient
	m	b	
E_{ci}	54.25	-1.35×10^{-2}	0.9990
E_{cf}	80.0	-0.147	0.9999
nE_{af}	39.8	-	-
mE_{si}	36.5	-1.00×10^{-2}	0.9999
E_{sf}	191.0	-0.129	0.9999

m = 0.1891
n = 0.8109

Initial Modulus Curve Polynominal Coefficients			
Curve	A1	A2	A3
Composite	0.232×10^{-4}	-0.819×10^{-7}	0.294×10^{-9}
Steel	0.315×10^{-4}	-0.115×10^{-6}	0.727×10^{-9}
Aluminium	0.810×10^{-4}	-0.118×10^{-5}	0.110×10^{-7}

Critical Tension/Stress Point Data	
Tension kN	19.2
μE	2570

TABLE A3.18 - STRESS STRAIN TEST NO. 53 TEST RESULT DATA
TOMAGO TO TAREE TRANSMISSION LINE

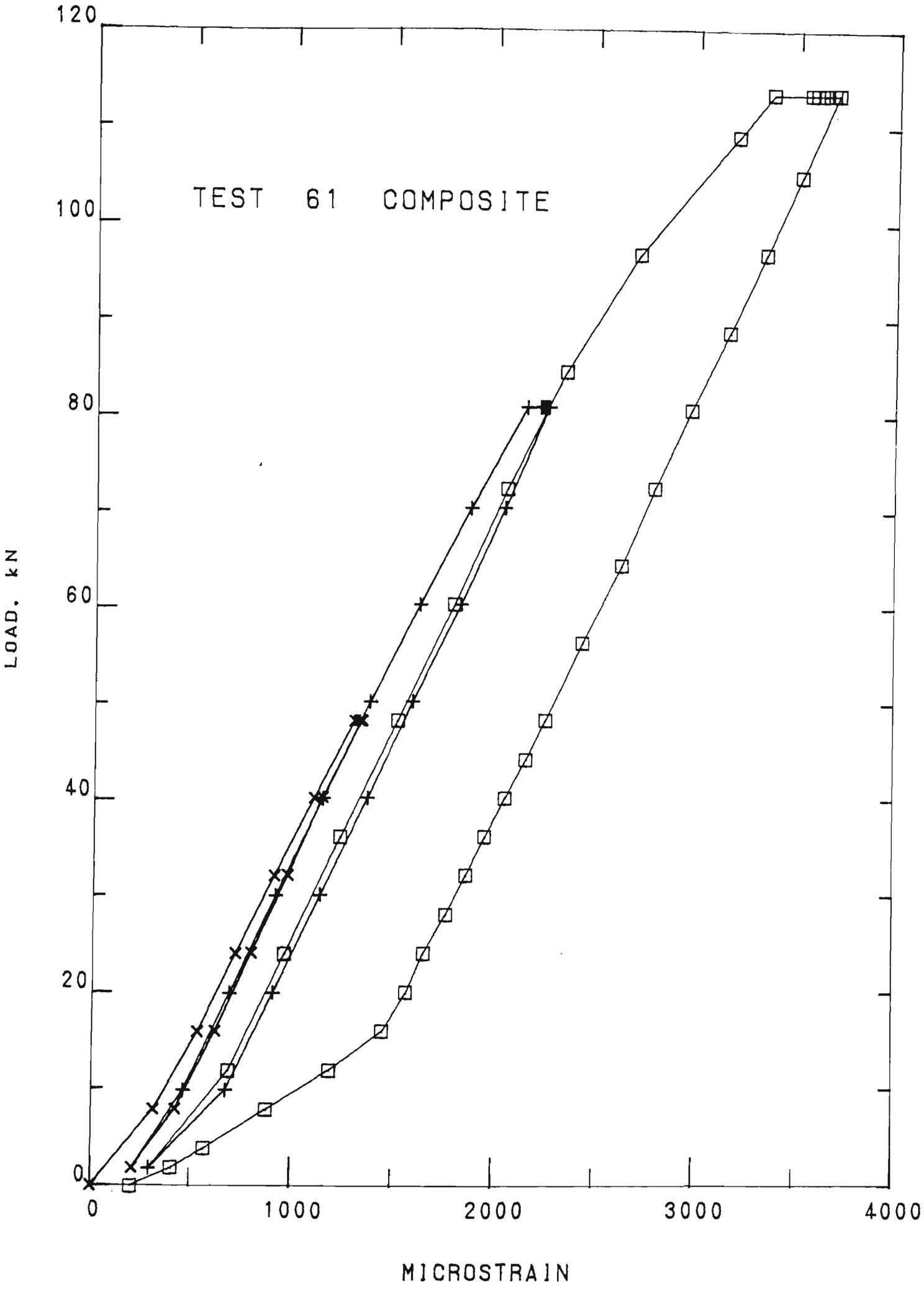

FIGURE A3.7 - STRESS STRAIN TEST
RAW PLOT OF TEST RESULT DATA
DAPTO TO SPRINGHILL TRANSMISSION LINE

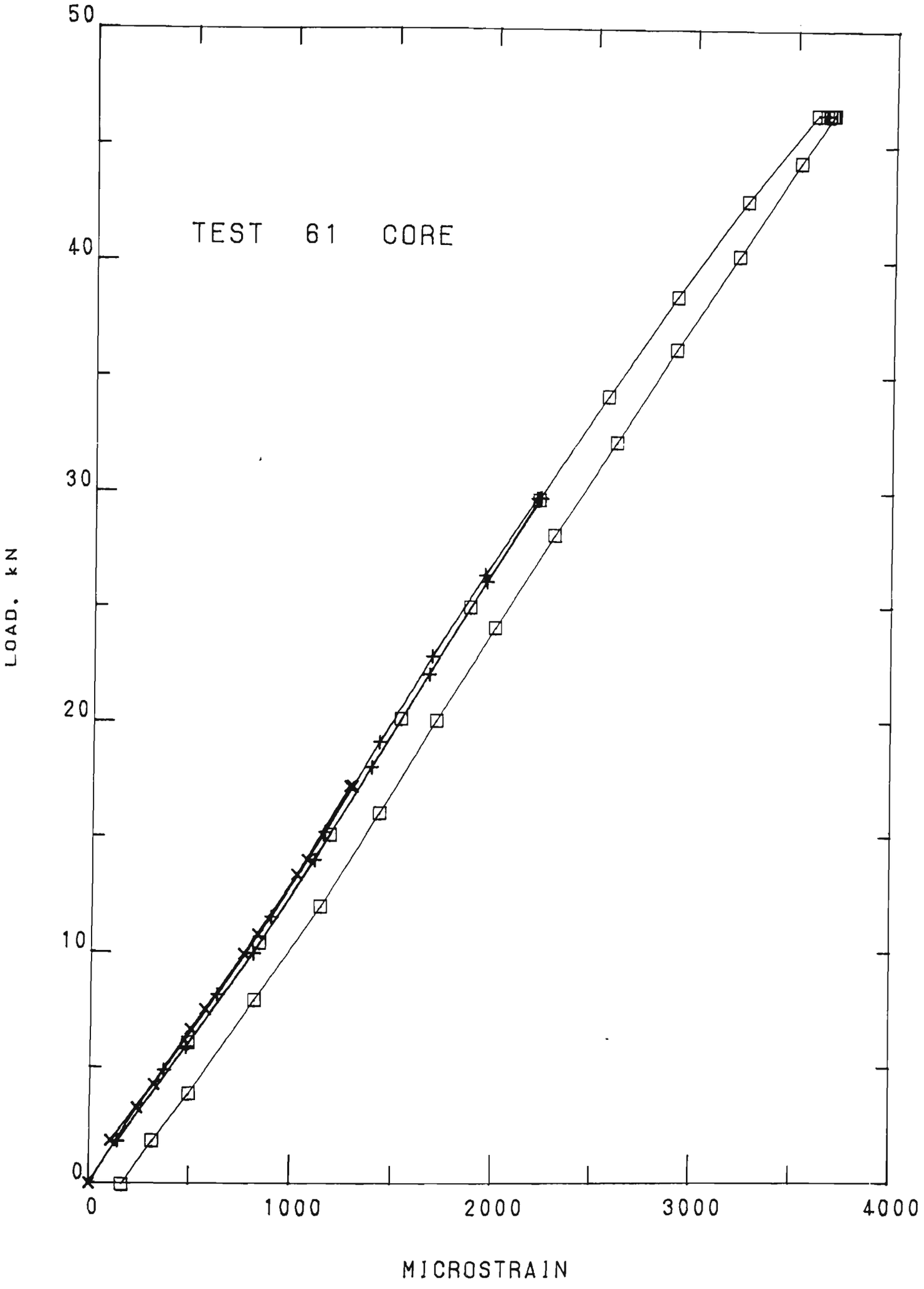

FIGURE A3.8 - STRESS STRAIN TEST
RAW PLOT OF TEST RESULT DATA
DAPTO TO SPRINGHILL TRANSMISSION LINE

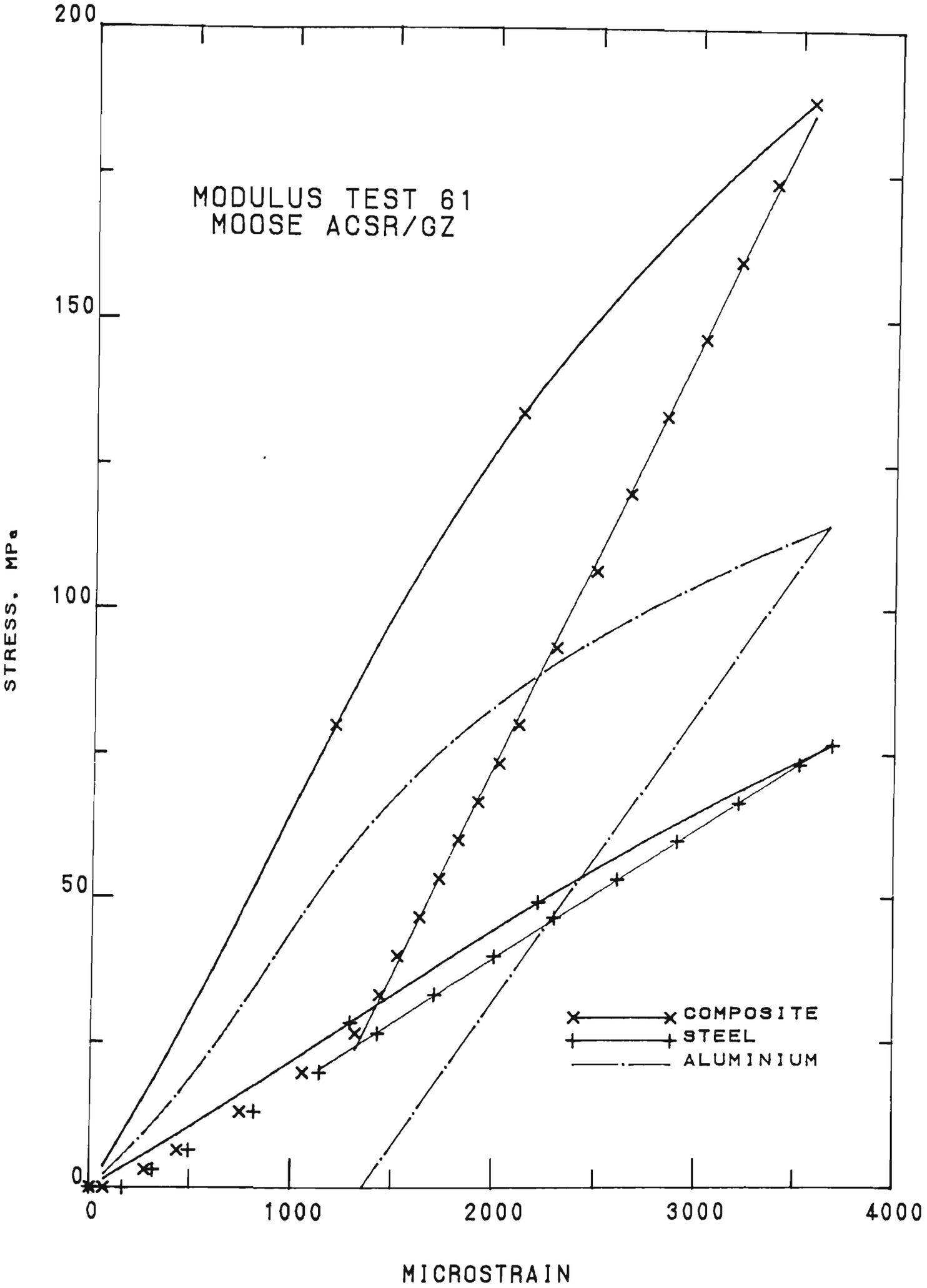

FIGURE A3.9 - STRESS STRAIN TEST
DERIVED TEST RESULT
DAPTO TO SPRINGHILL TRANSMISSION LINE

Conductor Modulus Data			
Parameter	Equation Constants		Correlation Coefficient
	m	b	
E_{ci}	77.9	-1.04×10^{-2}	0.9998
E_{cf}	81.5	-8.00×10^{-12}	0.9997
nE_{af}	51.3	-	-
mE_{si}	24.9	-5.37×10^{-4}	0.9996
E_{sf}	190	-4.18×10^{-2}	0.9999

m = 0.1169
n = 0.8841

Initial Modulus Curve Polynominal Coefficients			
Curve	A1	A2	A3
Composite	0.180×10^{-4}	-0.689×10^{-7}	0.395×10^{-9}
Steel	0.489×10^{-4}	-0.198×10^{-6}	0.244×10^{-8}
Aluminium	0.317×10^{-4}	-0.345×10^{-6}	0.302×10^{-8}

Critical Tension/Stress Point Data	
Tension kN	15.4
μE	1480

TABLE A3.19 - STRESS STRAIN TEST NO. 61 TEST RESULT DATA
DAPTO TO SPRINGHILL TRANSMISSION LINE

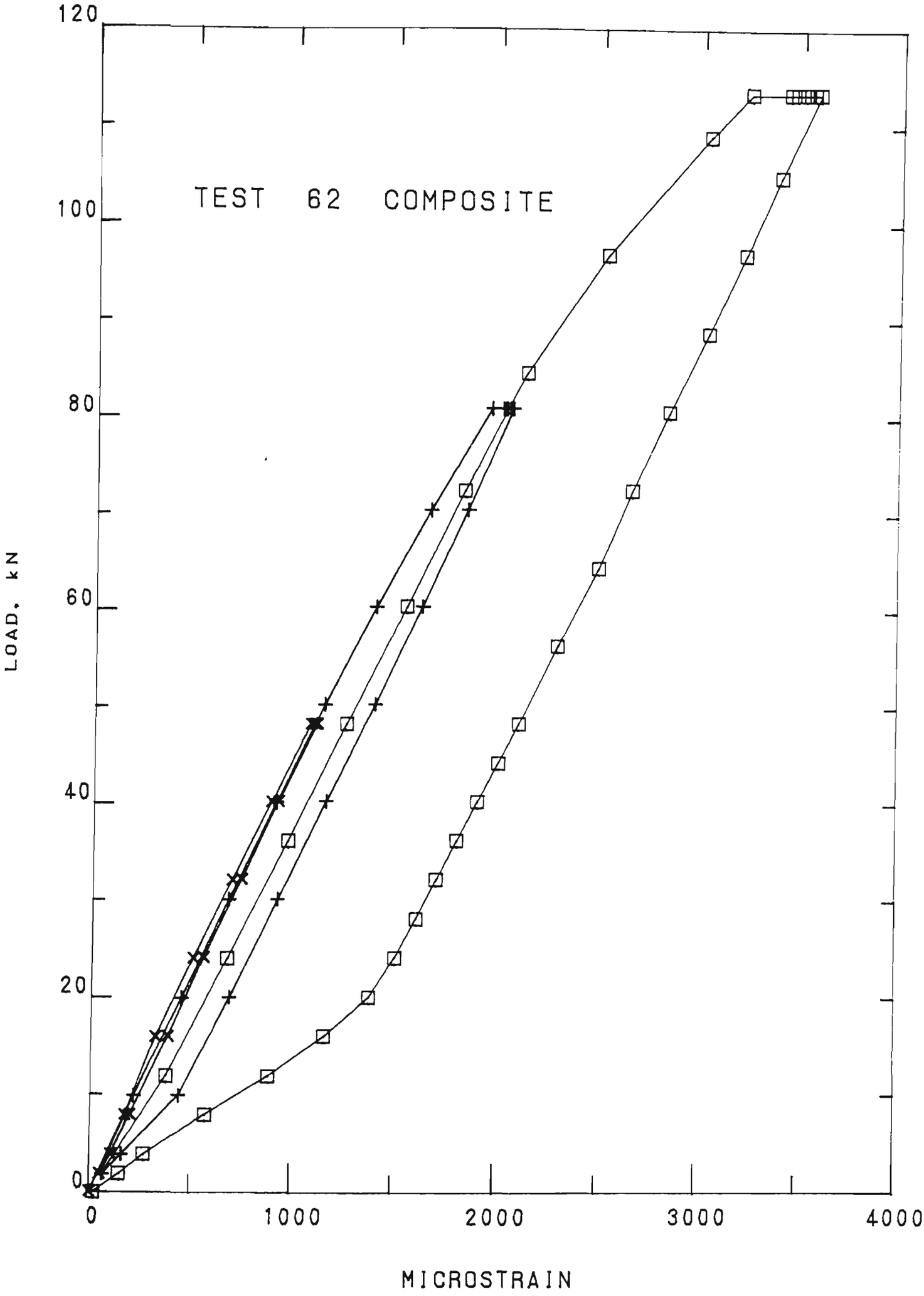

FIGURE A3.10 - STRESS STRAIN TEST
RAW PLOT OF TEST RESULT DATA
AVON TO KEMPS CREEK TRANSMISSION LINE

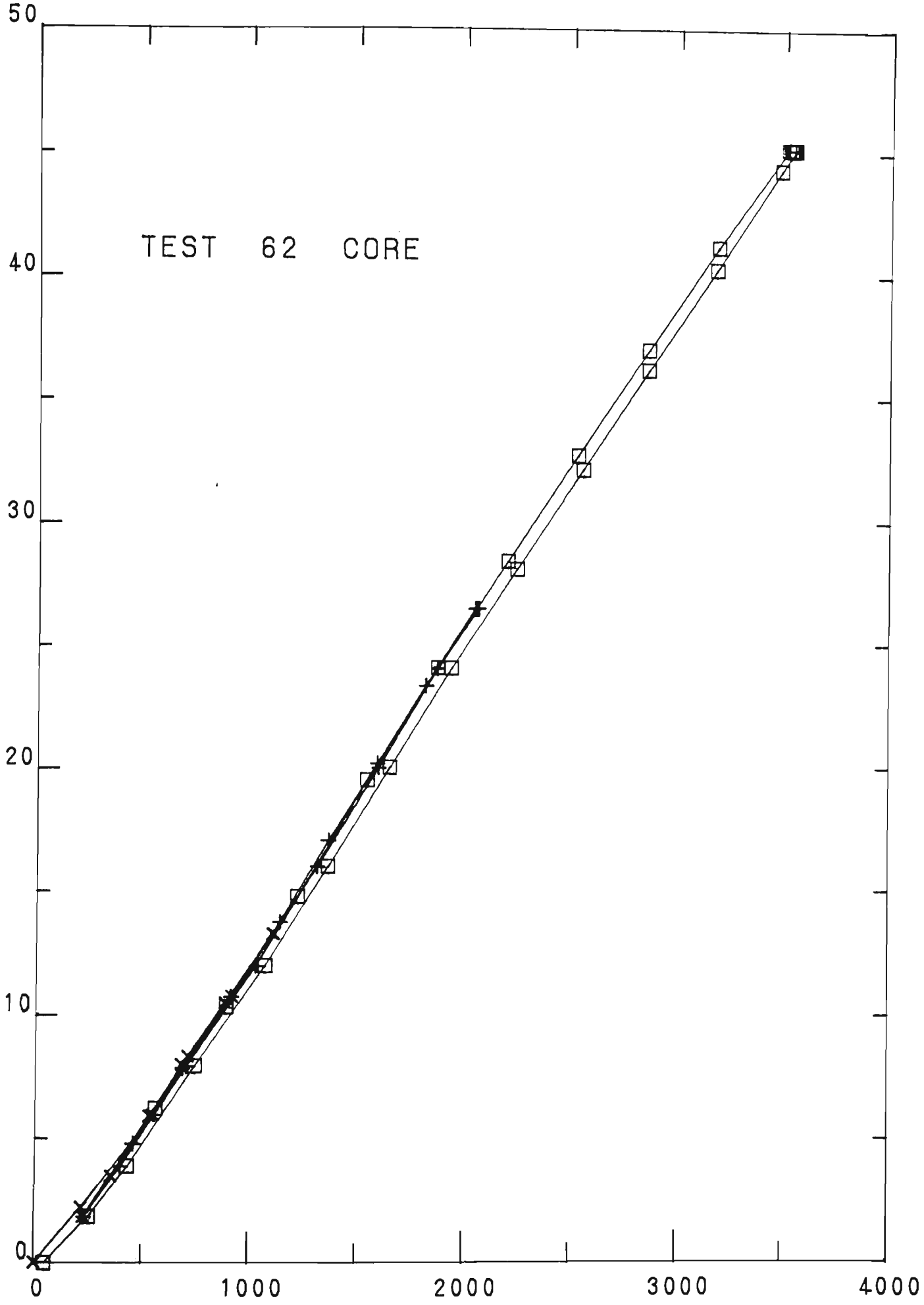

FIGURE A3.11 - STRESS STRAIN TEST
RAW PLOT OF TEST RESULT DATA
AVON TO KEMPS CREEK TRANSMISSION LINE

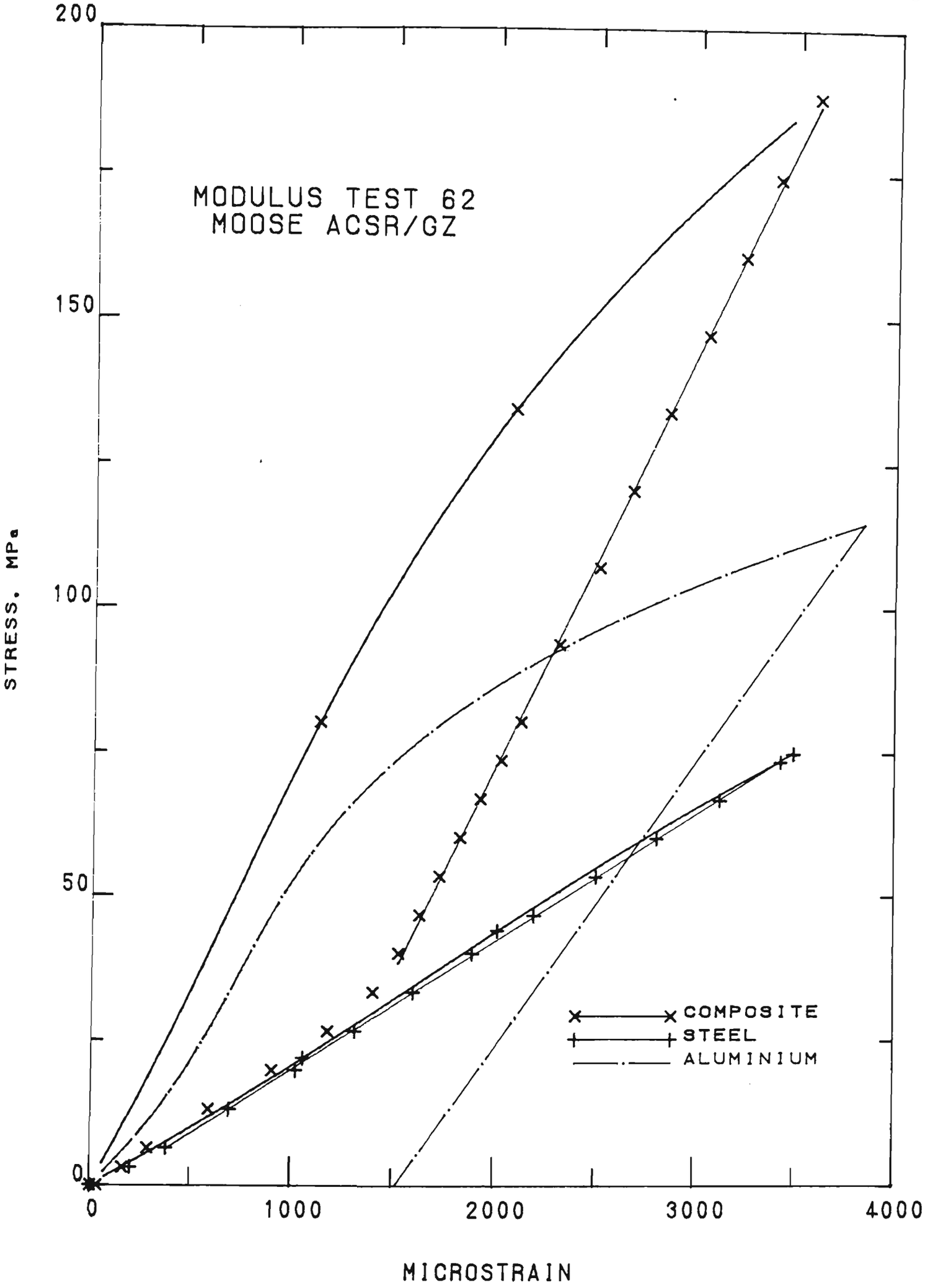

FIGURE A3.12 - STRESS STRAIN TEST
DERIVED TEST RESULT
AVON TO KEMPS CREEK TRANSMISSION LINE

Conductor Modulus Data			
Parameter	Equation Constants m	b	Correlation Coefficient
E_{ci}	84.2	1.11×10^{-3}	0.9992
E_{cf}	81.0	-7.96×10^{-2}	0.9998
nE_{af}	52.1	-	-
mE_{si}	23.7	-1.21×10^{-3}	0.9994
E_{sf}	190	1.81×10^{-2}	0.9999

m = 0.1166
n = 0.8834

Initial Modulus Curve Polynominal Coefficients			
Curve	A1	A2	A3
Composite	0.161×10^{-4}	-0.564×10^{-7}	0.384×10^{-9}
Steel	0.524×10^{-4}	-0.265×10^{-6}	0.250×10^{-8}
Aluminium	0.302×10^{-6}	-0.420×10^{-6}	0.390×10^{-8}

Critical Tension/Stress Point Data	
Tension kN	19.6
μE	1430

TABLE A3.20 - STRESS STRAIN TEST NO. 62
TEST RESULT DATA
AVON TO KEMPS CREEK
TRANSMISSION LINE

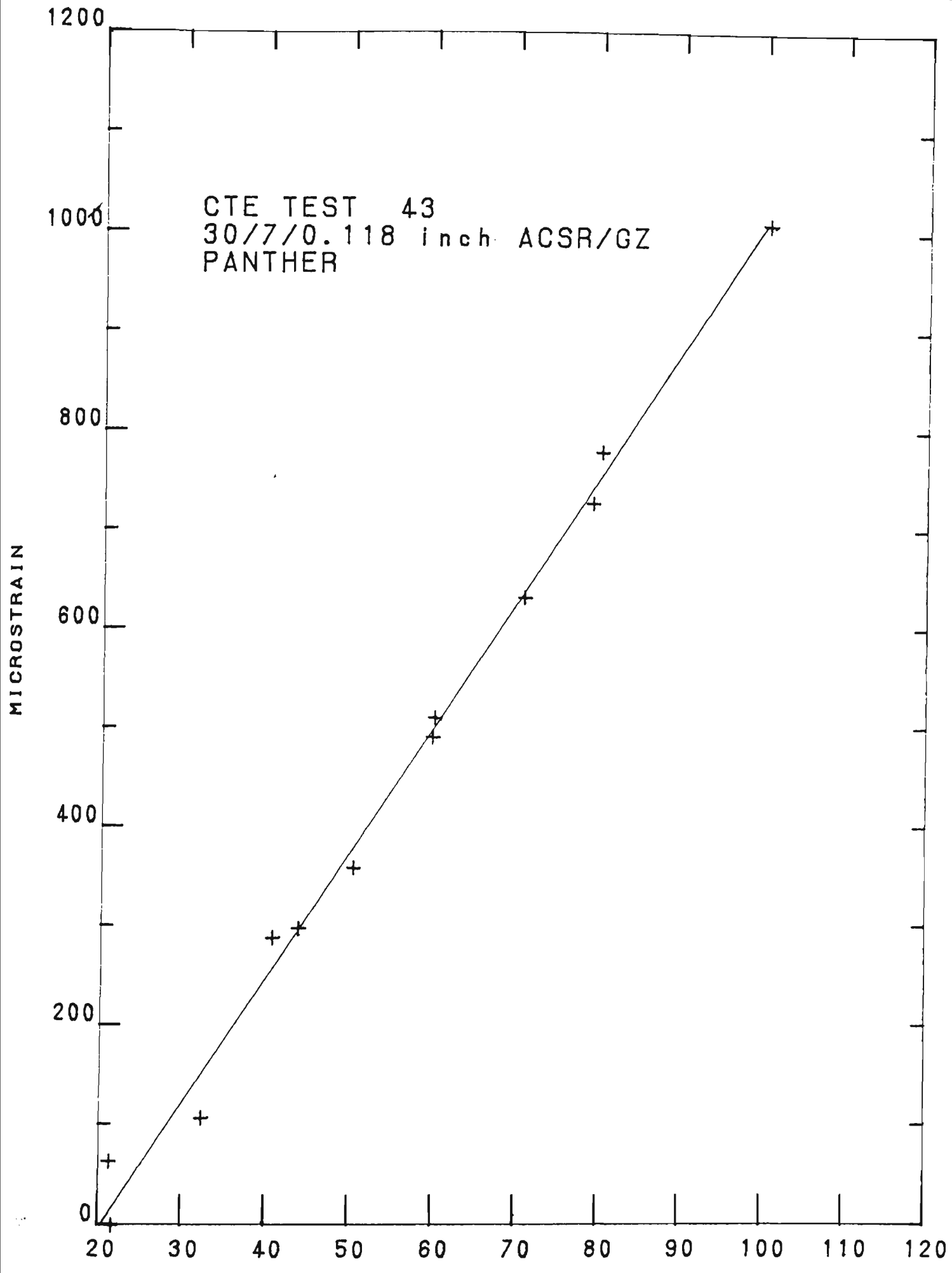

FIGURE A3.13 - COEFFICIENT OF LINEAR EXPANSION TEST
RAW PLOT AND LINEAR REGRESSION TEST RESULTS
TOMAGO TO TAREE TRANSMISSION LINE

Parameter	Data
Test Load	
kN	18.0
% CBL	20
Coefficient of Linear Expansion	12.58×10^{-6} /°C
Correlation Coefficient	0.9965

TABLE A3.21 - COEFFICIENT OF LINEAR EXPANSION
TEST NO. 43 TEST RESULT DATA
TOMAGO TO TAREE TRANSMISSION LINE

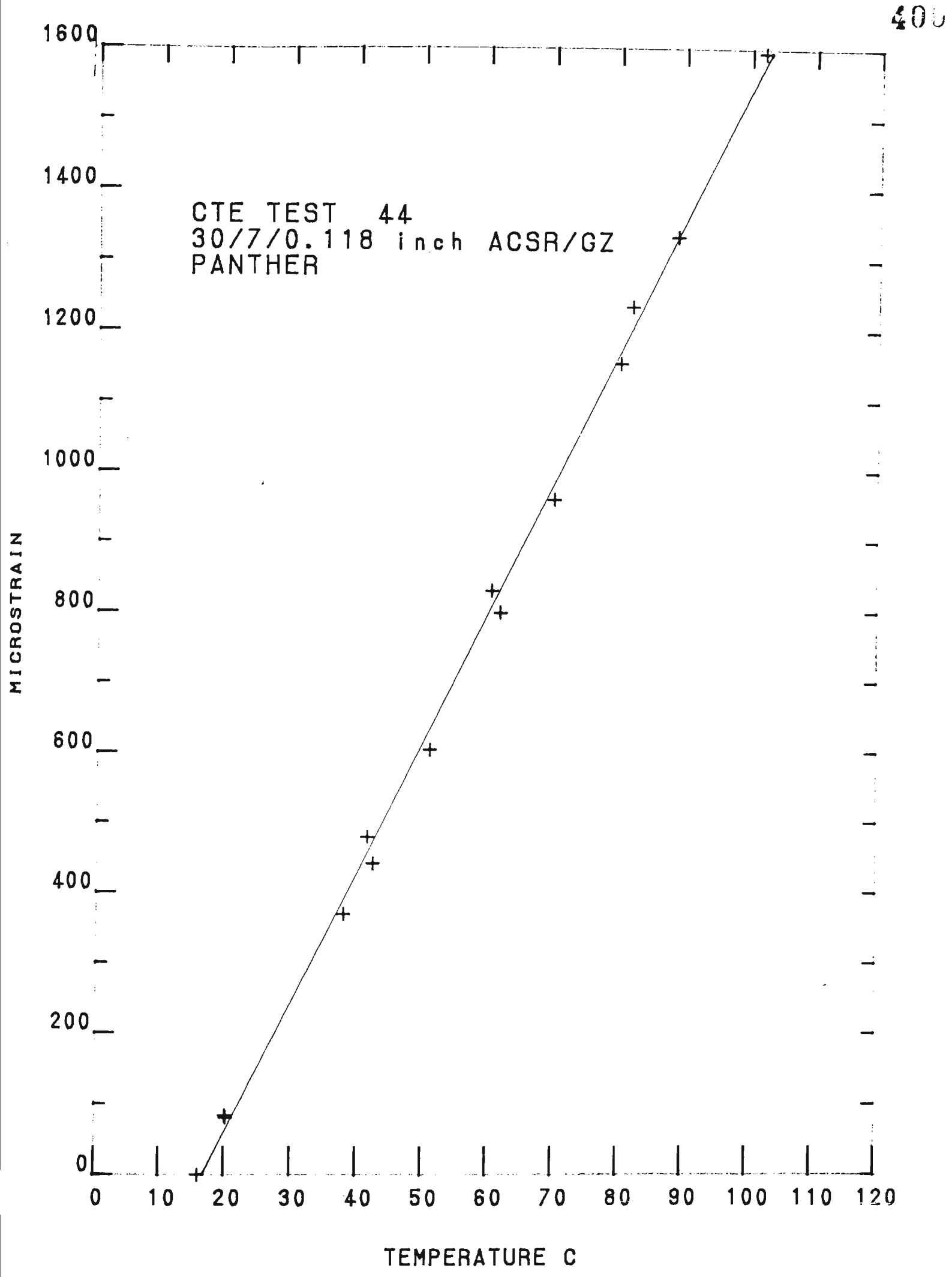

FIGURE A3.14 - COEFFICIENT OF LINEAR EXPANSION TEST
RAW PLOT AND LINEAR REGRESSION TEST RESULTS
TOMAGO TO TAREE TRANSMISSION LINE

Parameter	Data
Test Load	
kN	36.0
% CBL	40
Coefficient of Linear Expansion	18.45×10^{-6} /°C
Correlation Coefficient	0.9989

TABLE A3.22 - COEFFICIENT OF LINEAR EXPANSION
TEST NO. 44 TEST RESULT DATA
TOMAGO TO TAREE TRANSMISSION LINE

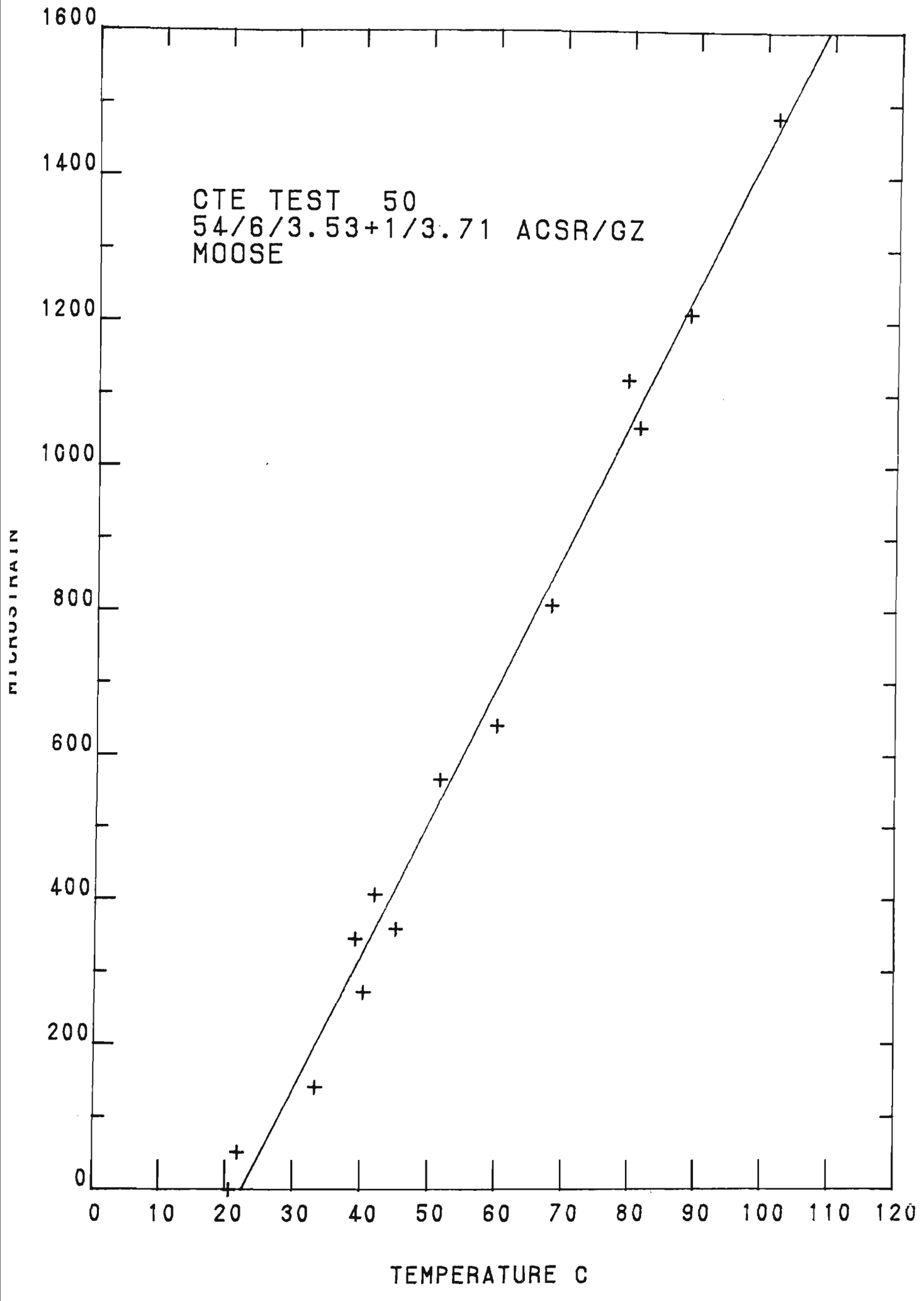

FIGURE A3.15 - COEFFICIENT OF LINEAR EXPANSION TEST
RAW PLOT AND LINEAR REGRESSION TEST RESULTS
DAPTO TO SPRINGHILL TRANSMISSION LINE

Parameter	Data
Test Load	
kN	31.9
% CBL	20
Coefficient of Linear Expansion	18.27×10^{-6} /°C
Correlation Coefficient	0.9946

TABLE A3.23 - COEFFICIENT OF LINEAR EXPANSION
TEST NO. 50 TEST RESULT DATA
DAPTO TO SPRINGHILL TRANSMISSION LINE

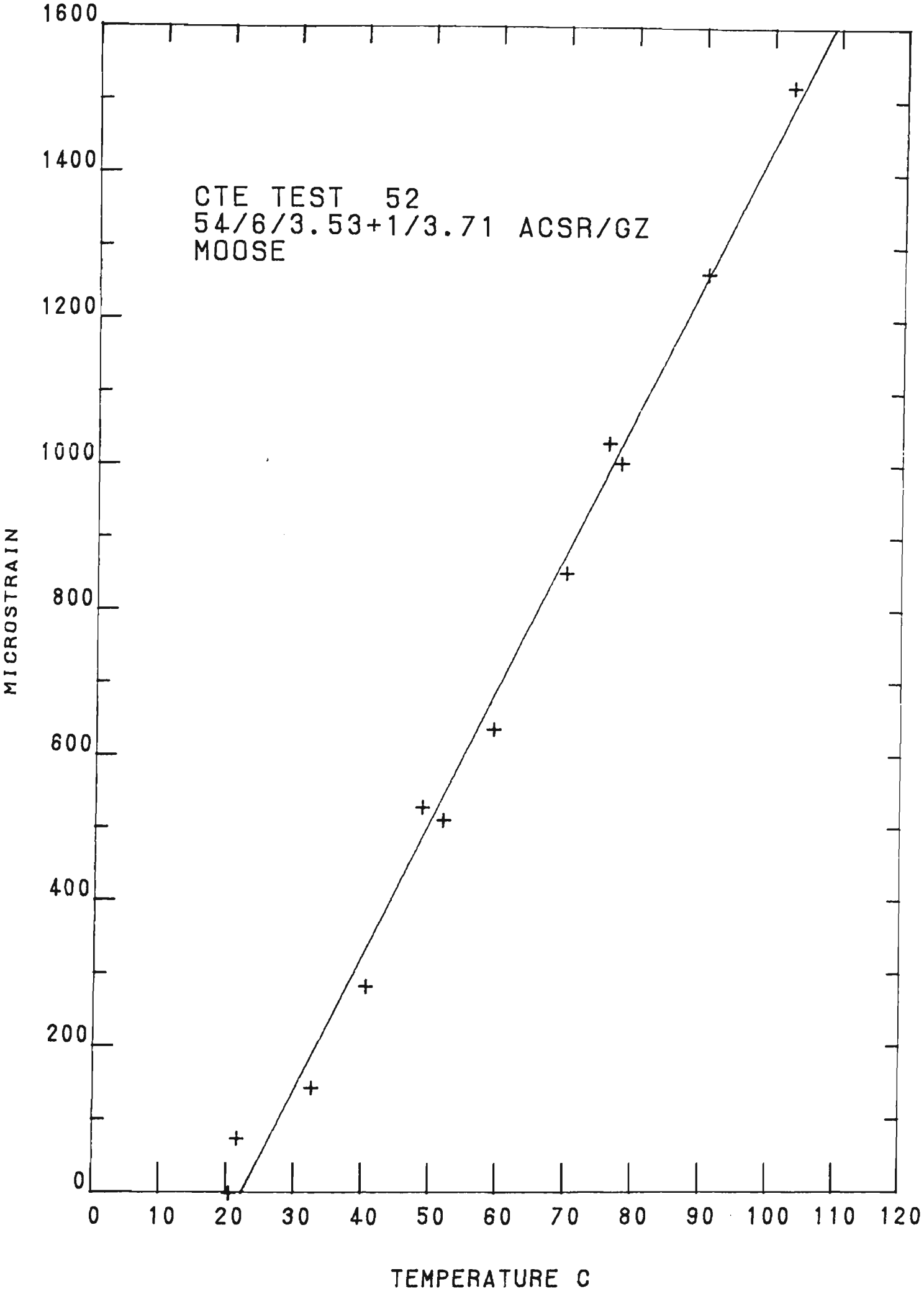

FIGURE A3.16 - COEFFICIENT OF LINEAR EXPANSION TEST
RAW PLOT AND LINEAR REGRESSION TEST RESULT
AVON TO KEMPS CREEK TRANSMISSION LINE

Parameter	Data
Test Load	
kN	31.9
% CBL	20
Coefficient of Linear Expansion	18.31×10^{-6} /°C
Correlation Coefficient	0.9957

TABLE A3.24 - COEFFICIENT OF LINEAR EXPANSION
TEST NO. 52 TEST RESULT DATA
AVON TO KEMPS CREEK TRANSMISSION LINE

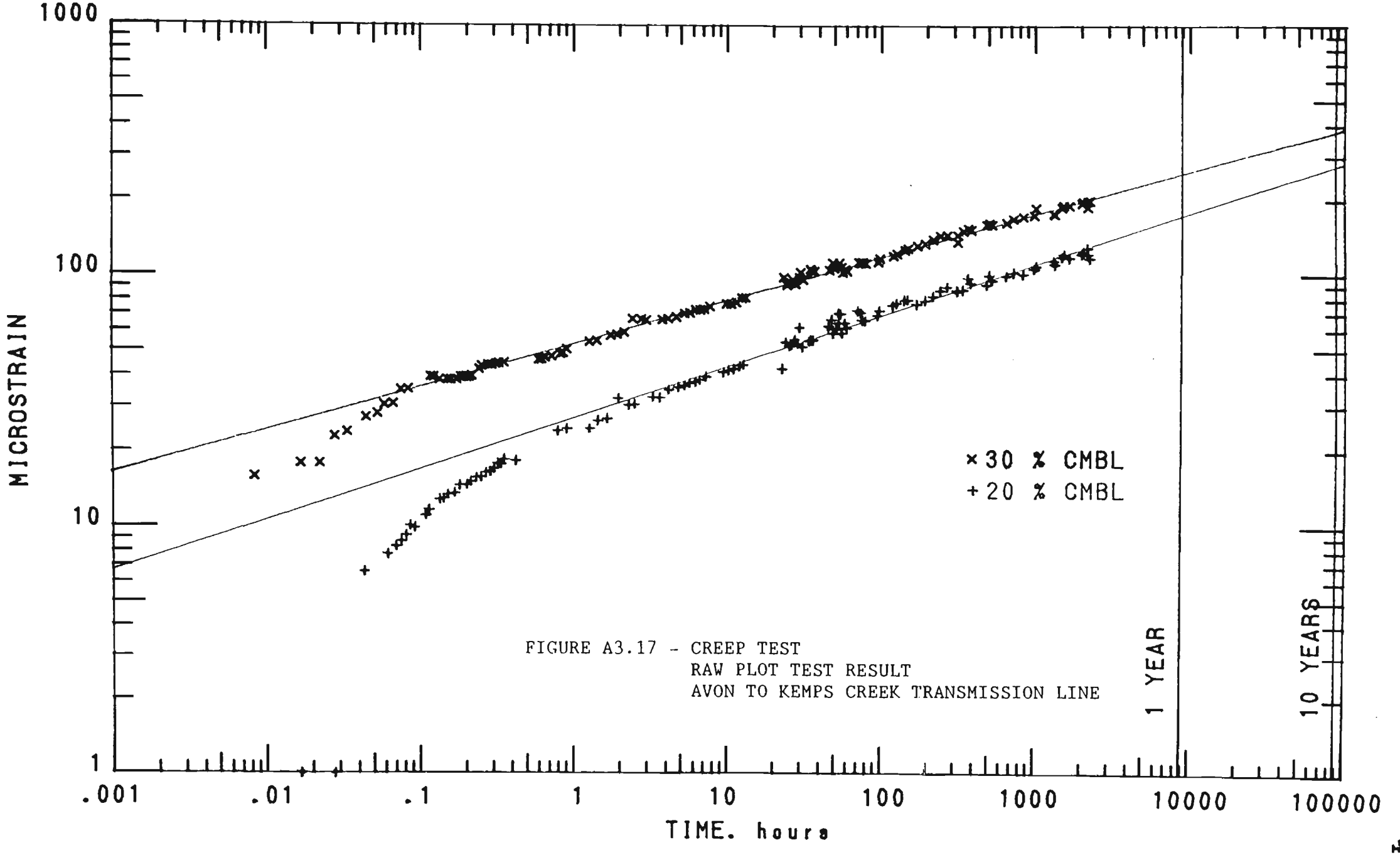

FIGURE A3.17 - CREEP TEST
RAW PLOT TEST RESULT
AVON TO KEMPS CREEK TRANSMISSION LINE

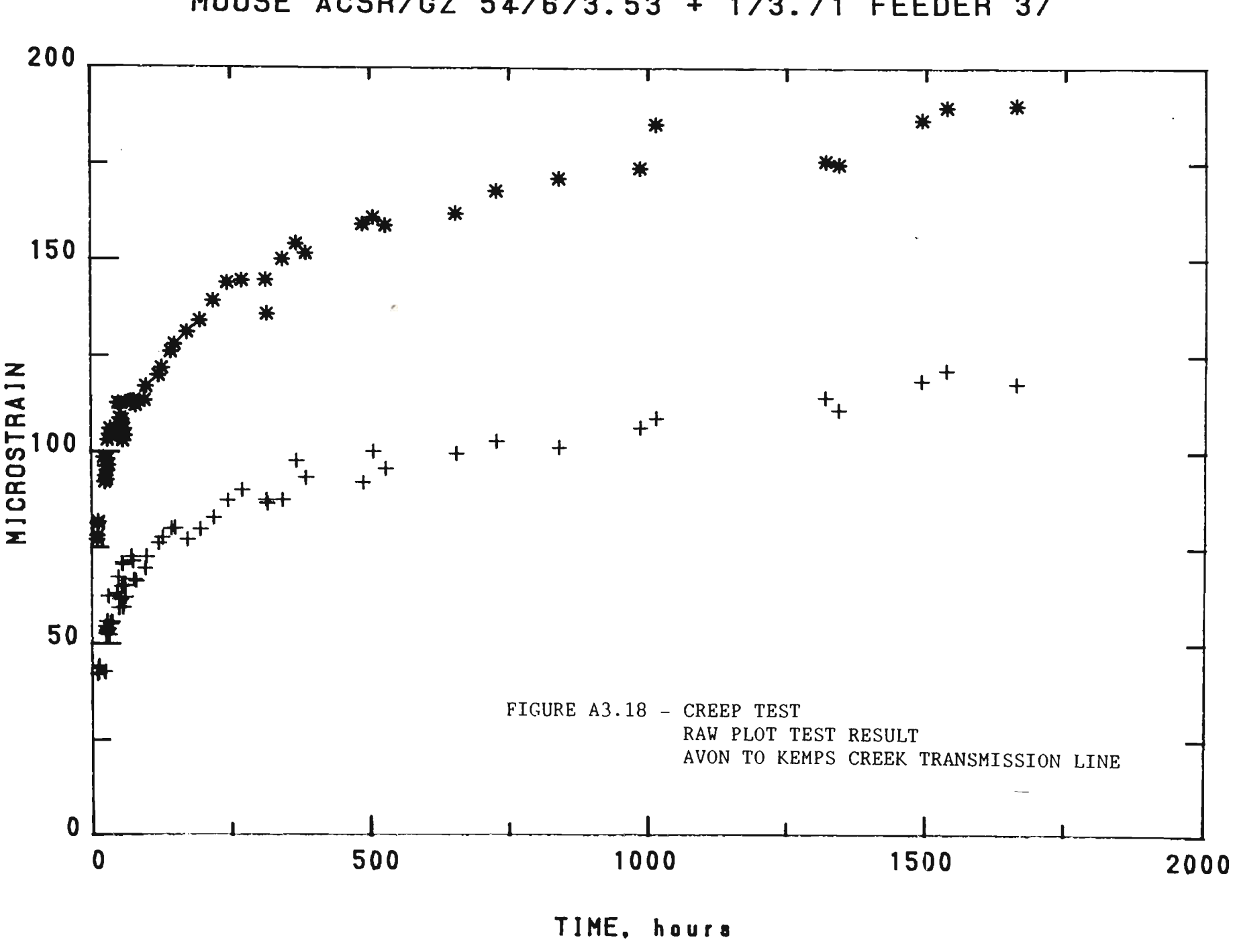

FIGURE A3.18 - CREEP TEST
RAW PLOT TEST RESULT
AVON TO KEMPS CREEK TRANSMISSION LINE

SINGLE REGRESSION EXPODENTIAL EQUATION		
Load		
Stress	53.38 MPa	80.06 MPa
% CBL	20	30
Equation Coefficients		
A_1	164×10^{-6}	249×10^{-6}
n	0.1880	0.1635
Correlation Coefficient	0.9805	0.9922
Correlation Coefficient from 500 hrs	0.9507	0.9452

SINGLE REGRESSION LINEAR EQUATION FROM 500 HRS		
Equation Coefficients		
a	90.4	149
b	16.7×10^{-3}	22.7×10^{-3}
Correlation Coefficient	0.9629	0.9774

MULTIPLE REGRESSION EXPODENTIAL EQUATION	
Equation Coefficients	
A_2	1.066×10^{-6}
n_1	0.1759
n_2	1.255
Correlation Coefficient	0.9914

TABLE A3.25 - CONDUCTOR CREEP TEST RESULT DATA
AVON TO KEMPS CREEK TRANSMISSION LINE

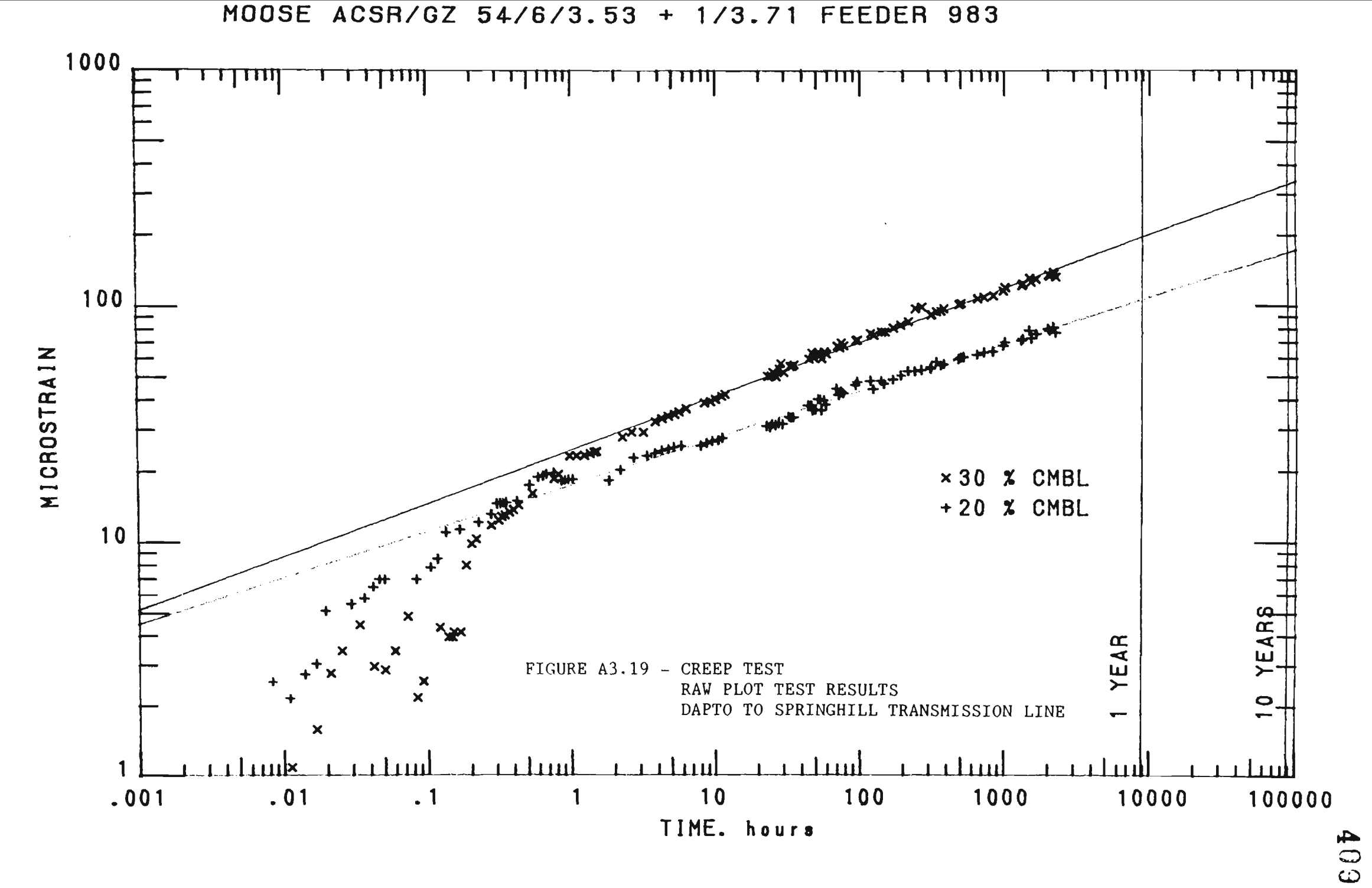

FIGURE A3.19 - CREEP TEST
RAW PLOT TEST RESULTS
DAPTO TO SPRINGHILL TRANSMISSION LINE

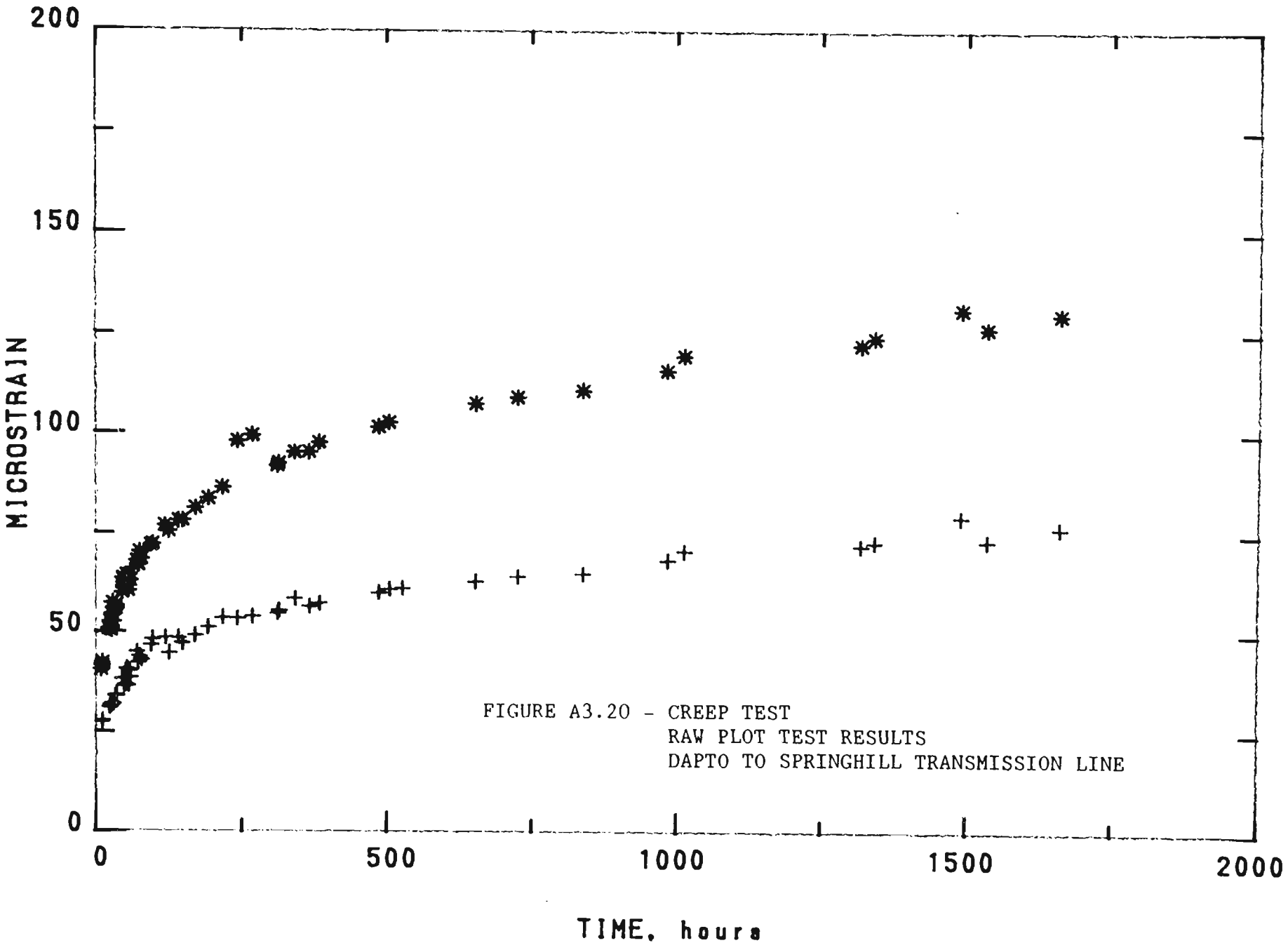

FIGURE A3.20 - CREEP TEST
RAW PLOT TEST RESULTS
DAPTO TO SPRINGHILL TRANSMISSION LINE

SINGLE REGRESSION EXPODENTIAL EQUATION		
Load		
Stress	53.38 MPa	80.06 MPa
% CBL	20	30
Equation Coefficients		
A_1	99.3×10^{-6}	188×10^{-6}
n	0.2028	0.2150
Correlation Coefficient	0.9909	0.9948
Correlation Coefficient from 500 hrs	0.9750	0.9859

SINGLE REGRESSION LINEAR EQUATION FROM 500 HRS		
Equation Coefficients		
a	55.25	96.98
b	12.69×10^{-2}	18.37×10^{-3}
Correlation Coefficient	0.9764	0.9895

MULTIPLE REGRESSION EXPODENTIAL EQUATION	
Equation Coefficients	
A_2	0.8102×10^{-6}
n_1	0.2089
n_2	1.237
Correlation Coefficient	0.9955

TABLE A3.26 - CONDUCTOR CREEP TEST RESULT DATA
DAPTO TO SPRINGHILL TRANSMISSION LINE

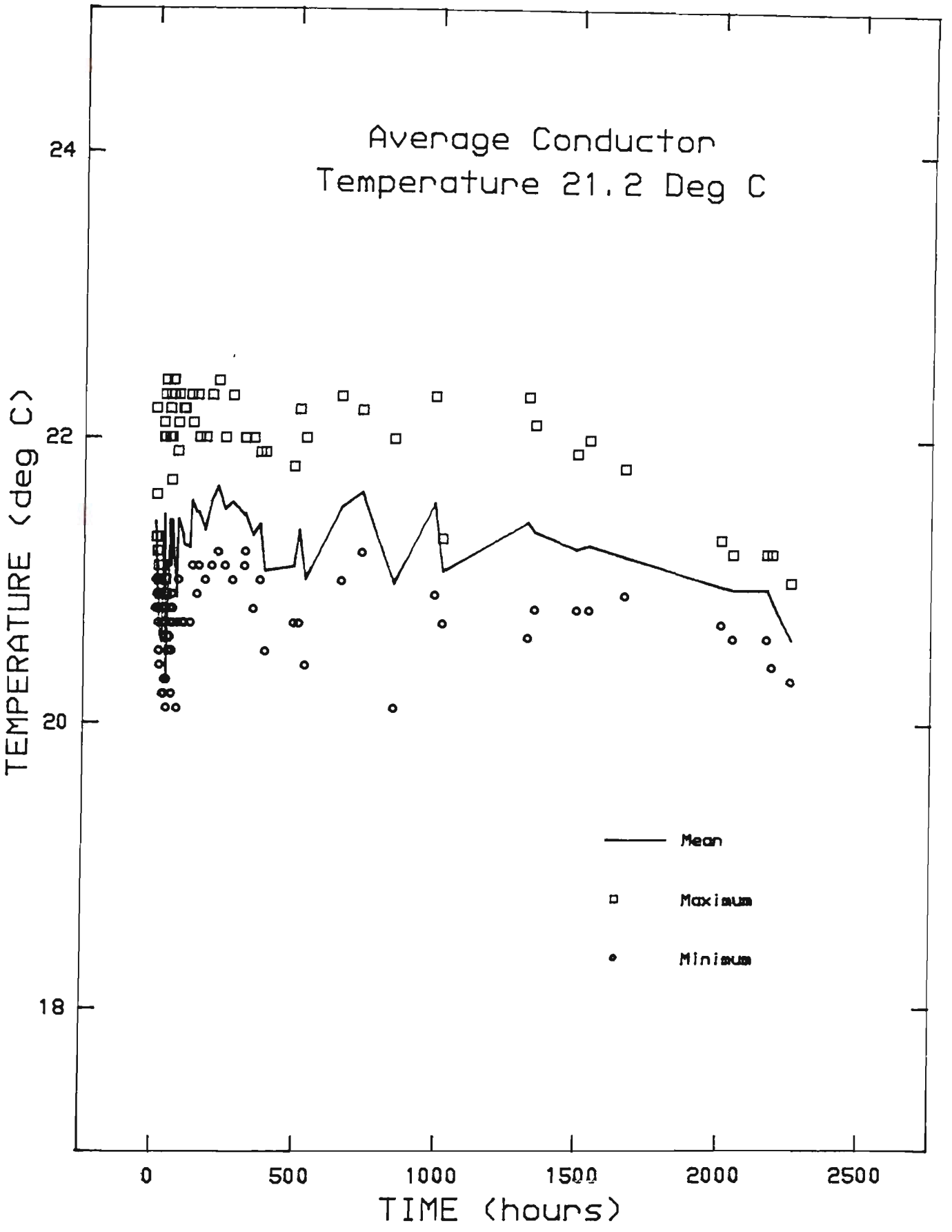

FIGURE A3.21 CONDUCTOR CREEP TEST
TEMPERATURE VARIATION

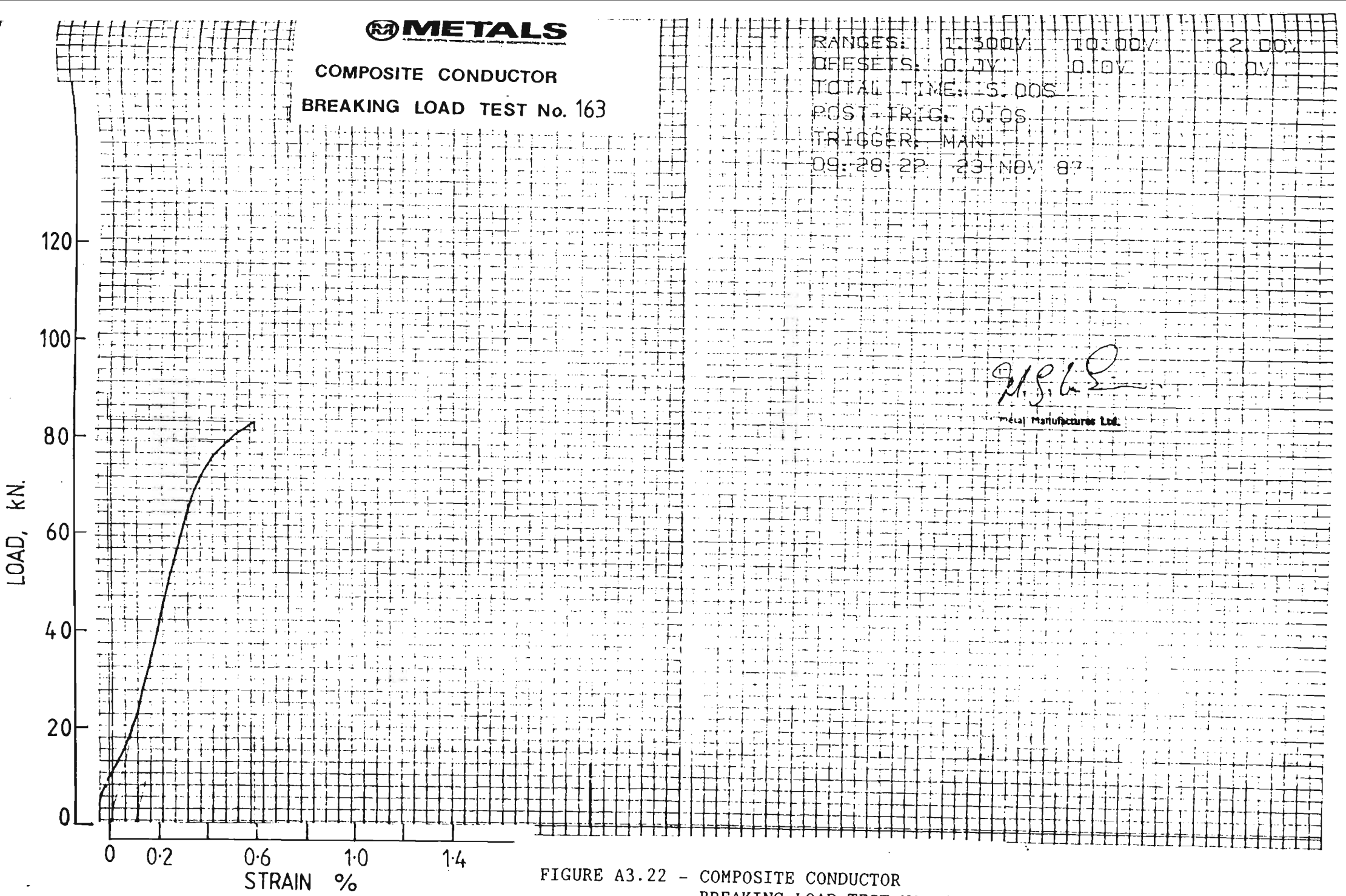

FIGURE A3.22 - COMPOSITE CONDUCTOR
BREAKING LOAD TEST NO. 163

Stress Strain Test Results	
Parameter	Data
Load at 0.1% Strain	79.5 kN
Load at 1.0% Strain	-
Composite Load at Failure	82.4 kN
Total Strain	0.61%
Plastic Strain	0.19%
Steel Load at Failure	-

Description of Failure: Epoxy termination failure.

TABLE A3.27 - BREAKING LOAD TEST NO. 163
TEST RESULT DATA
TOMAGO TO TAREE TRANSMISSION LINE

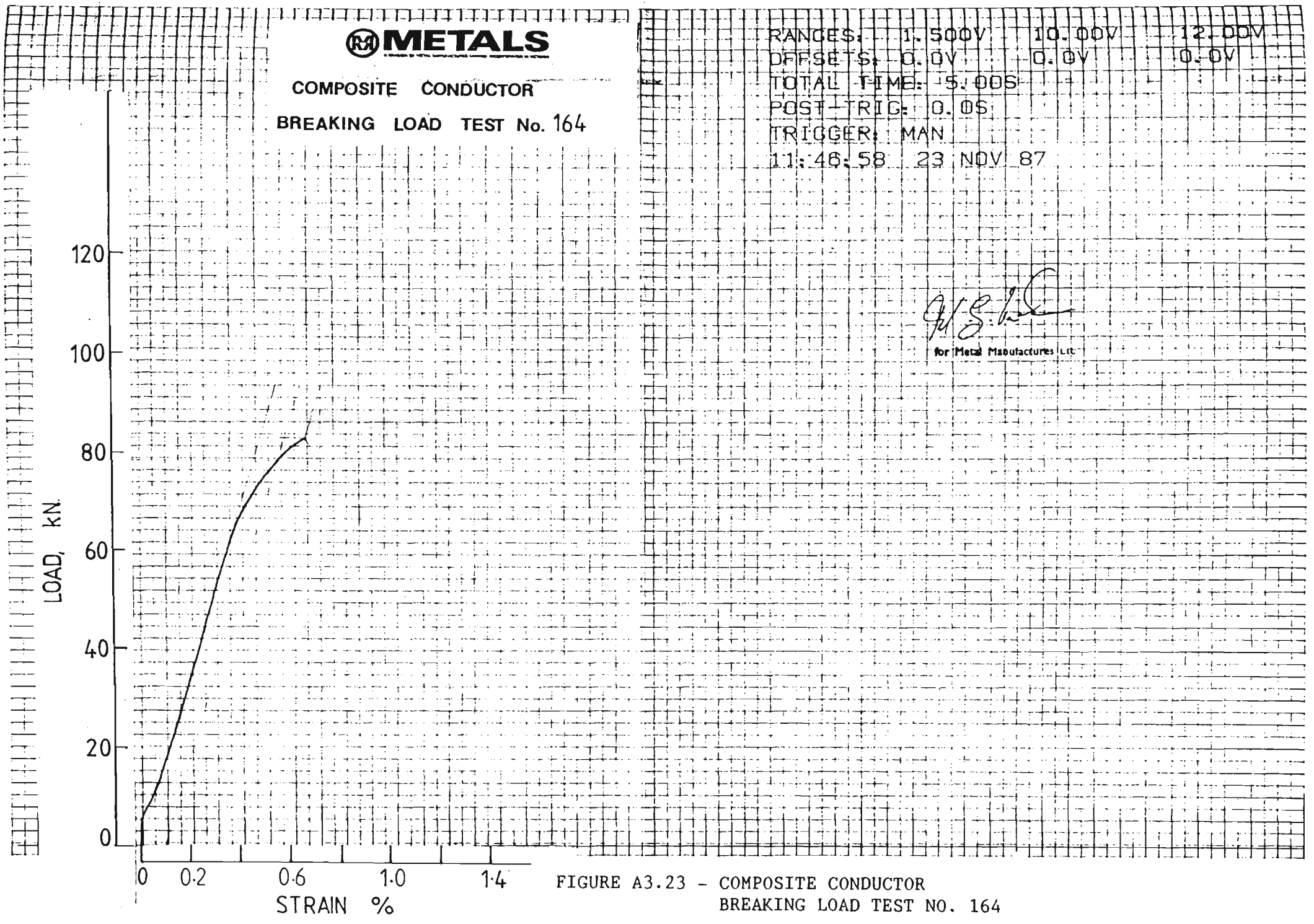

FIGURE A3.23 - COMPOSITE CONDUCTOR
BREAKING LOAD TEST NO. 164

Stress Strain Test Results	
Parameter	Data
Load at 0.1% Strain	78.5 kN
Load at 1.0% Strain	-
Composite Load at Failure	83.3 kN
Total Strain	0.67%
Plastic Strain	0.20%
Steel Load at Failure	-

Description of Failure: Epoxy termination failure.

TABLE A3.28 - BREAKING LOAD TEST NO. 164
TEST RESULT DATA
TOMAGO TO TAREE TRANSMISSION LINE

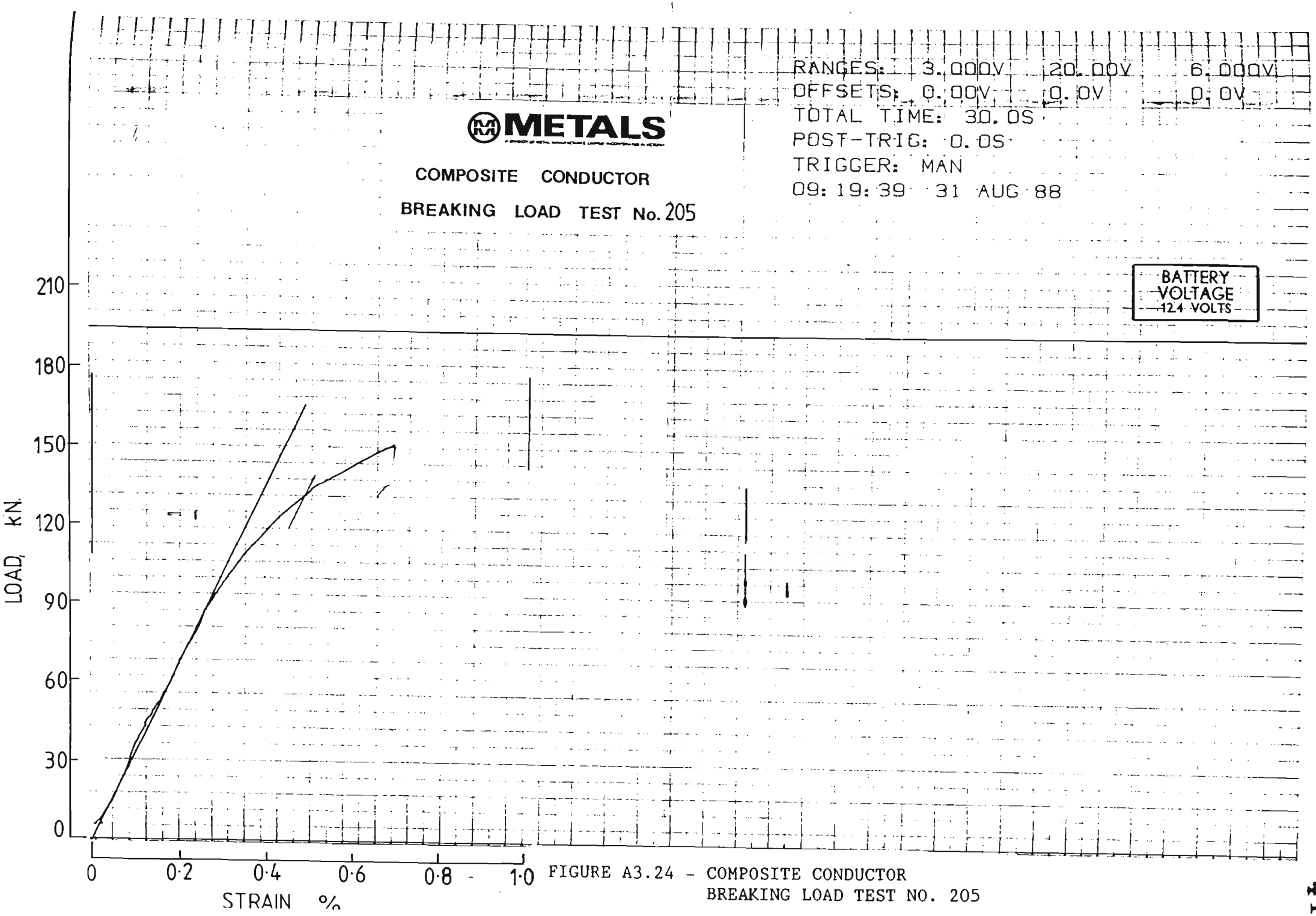

FIGURE A3.24 – COMPOSITE CONDUCTOR BREAKING LOAD TEST NO. 205

Stress Strain Test Results	
Parameter	Data
Load at 0.1% Strain	133.0 kN
Load at 1.0% Strain	-
Composite Load at Failure	153.11 kN
Total Strain	0.69%
Plastic Strain	0.25%
Steel Load at Failure	150.5 kN

Description of Failure: Ten aluminium outer layer wires initially failed at the termination entrance. Remainding aluminium wires failed at or near the termination. The steel core slipped 3 mm from the compression sleeve at some time during the test and ultimately failed. All wires experienced ductile fracture.

TABLE A3.29 - BREAKING LOAD TEST NO. 205
TEST RESULT DATA
AVON TO KEMPS CREEK TRANSMISSION LINE

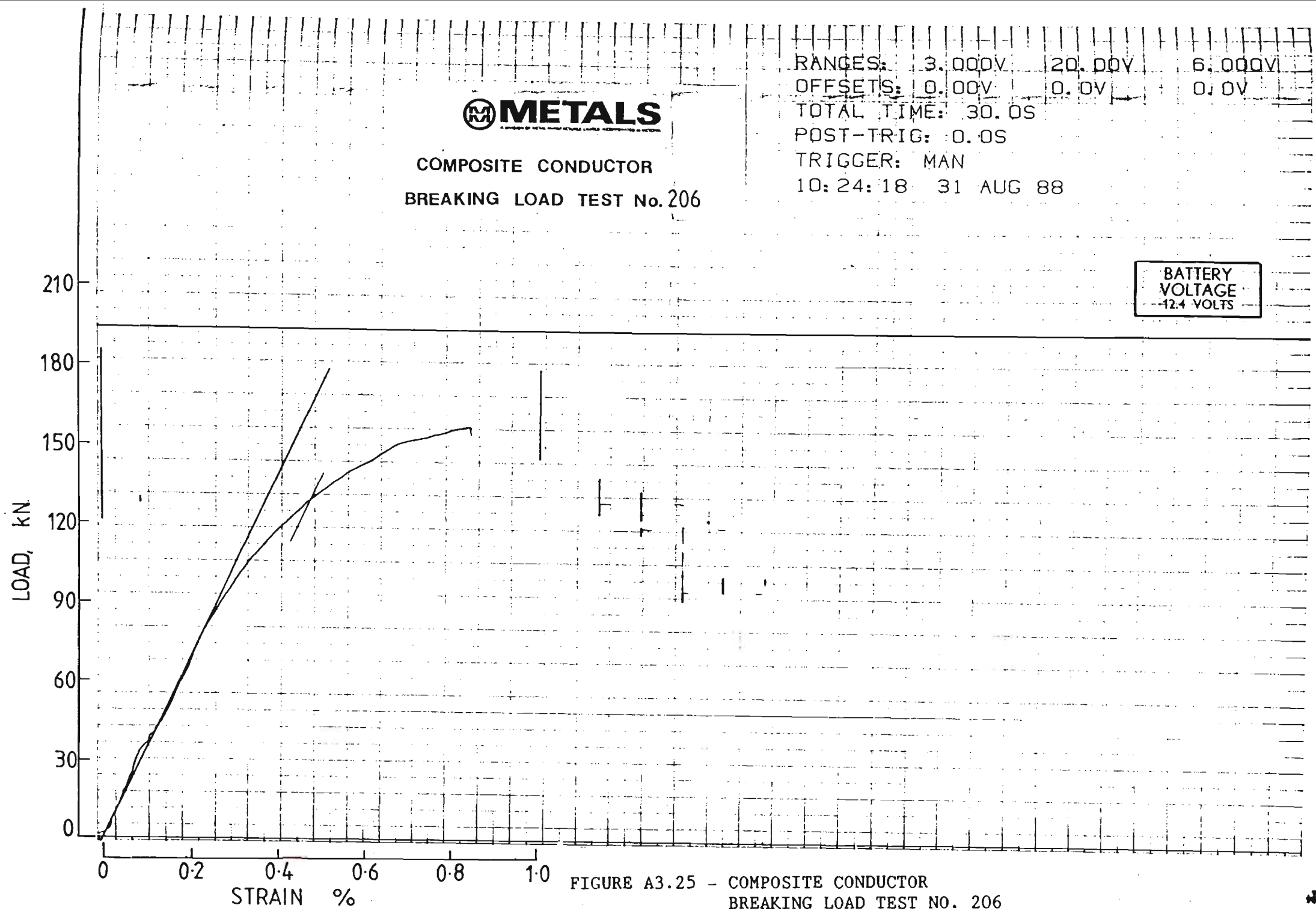

FIGURE A3.25 - COMPOSITE CONDUCTOR
BREAKING LOAD TEST NO. 206

Stress Strain Test Results	
Parameter	Data
Load at 0.1% Strain	130.4 kN
Load at 1.0% Strain	-
Composite Load at Failure	158.9 kN
Total Strain	0.85%
Plastic Strain	0.39%
Steel Load at Failure	139.1 kN

Description of Failure: Seven aluminium outer layer wires initially failed at the termination entrance. Remainding aluminium wires failed at or near the termination. The steel core slipped 2.5 mm during the steel breaking load test. All wires experienced ductile fractures.

TABLE A3.30 - BREAKING LOAD TEST NO. 206
TEST RESULT DATA
AVON TO KEMPS CREEKTRANSMISSION LINE

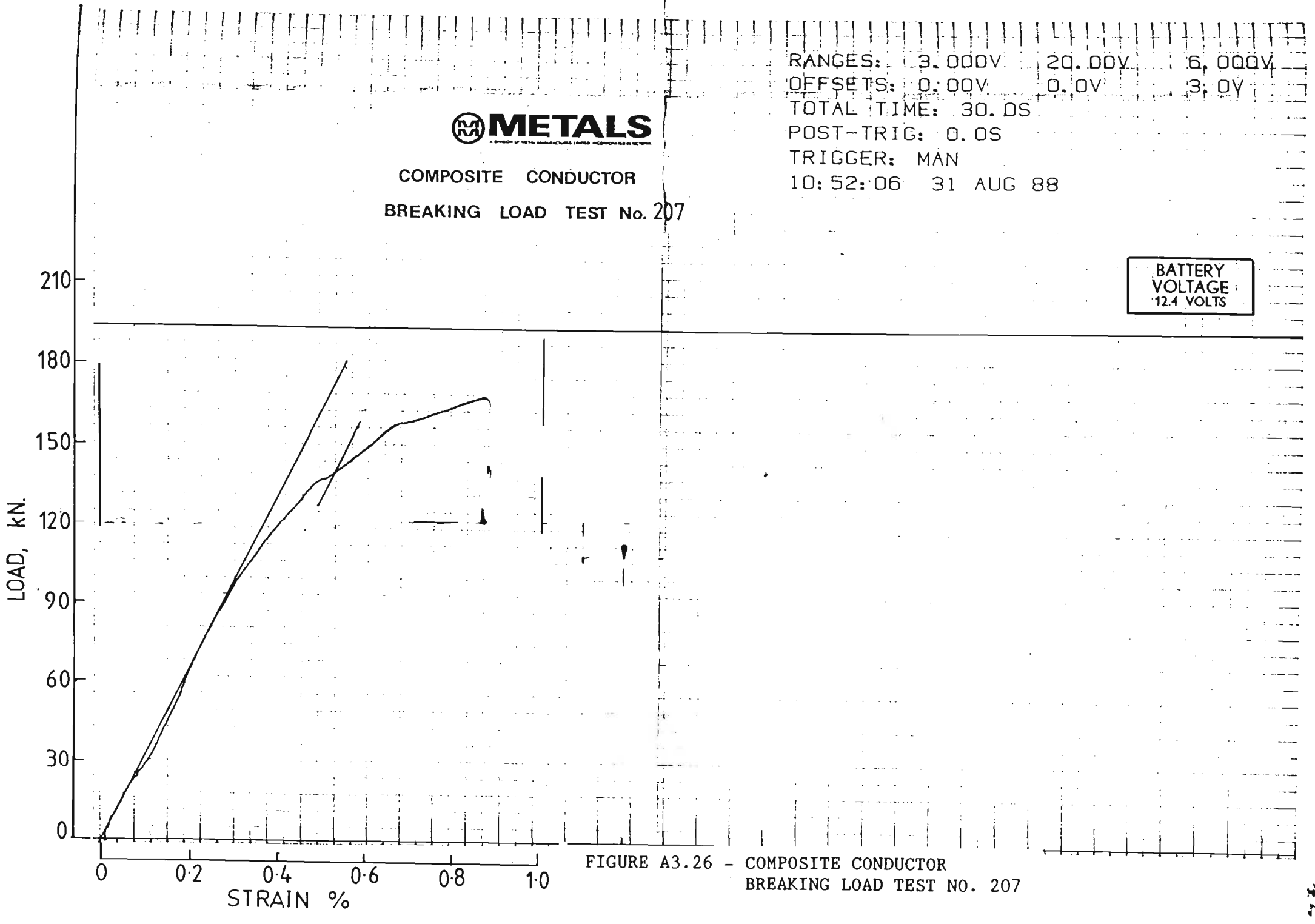

FIGURE A3.26 - COMPOSITE CONDUCTOR BREAKING LOAD TEST NO. 207

Stress Strain Test Results	
Parameter	Data
Load at 0.1% Strain	141.0 kN
Load at 1.0% Strain	-
Composite Load at Failure	170.4 kN
Total Strain	0.88%
Plastic Strain	0.36%
Steel Load at Failure	140.3 kN

Description of Failure: Twenty four aluminium outer layer wires initially failed at termination entrance. Remainder aluminium wires failed at or near the termination. All wires experience ductile fracture.

TABLE A3.31 - BREAKING LOAD TEST NO. 207
TEST RESULT DATA
DAPTO TO SPRINGHILL TRANSMISSION LINE

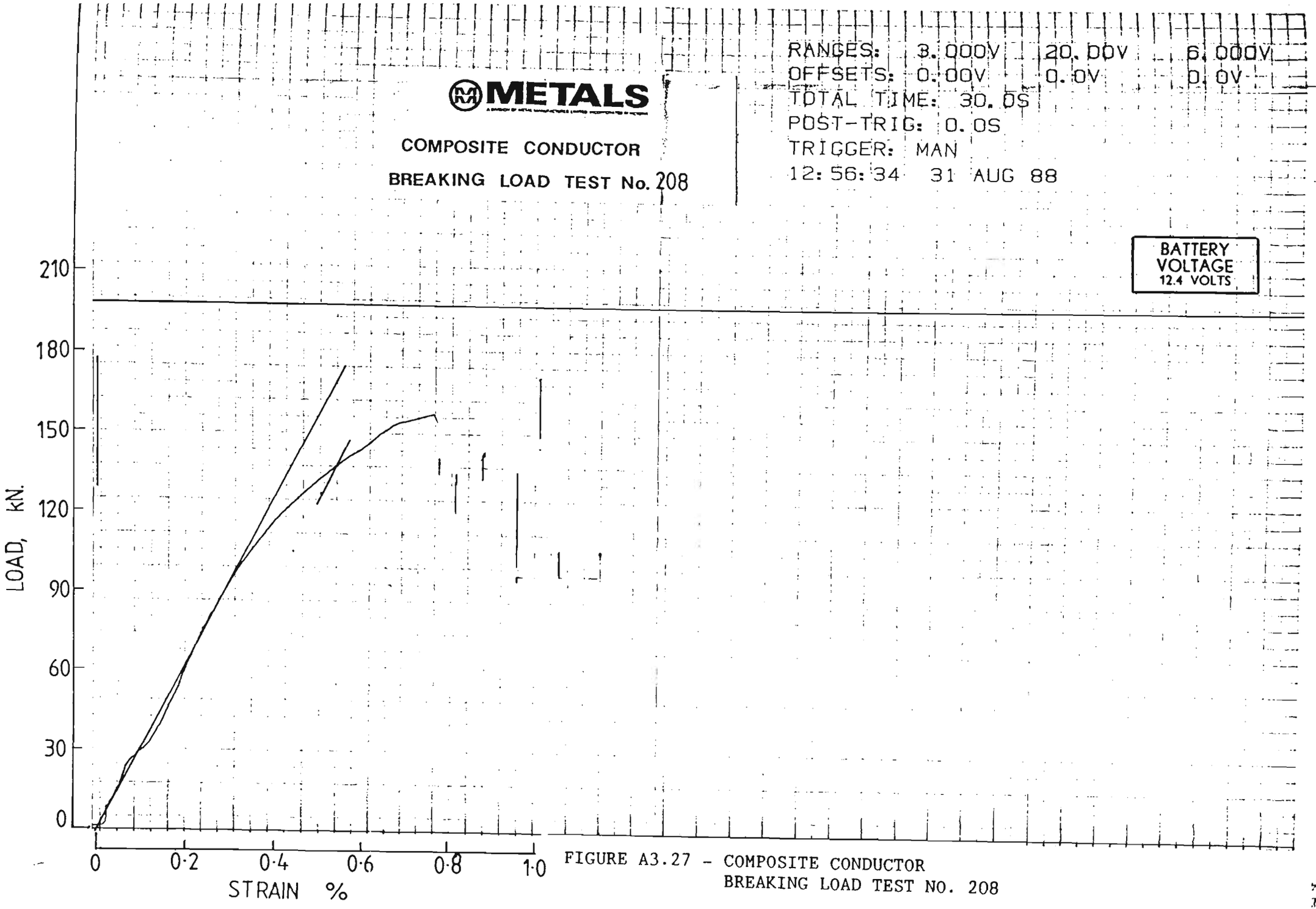

FIGURE A3.27 - COMPOSITE CONDUCTOR BREAKING LOAD TEST NO. 208

Stress Strain Test Results	
Parameter	Data
Load at 0.1% Strain	139.4 kN
Load at 1.0% Strain	-
Composite Load at Failure	159.5 kN
Total Strain	0.76%
Plastic Strain	0.26%
Steel Load at Failure	144.2 kN

Description of Failure: Twenty Four aluminium outer layer wires initially failed at termination entrance. Remainder aluminium wires failed at or near the termination. All wires experience ductile fracture.

TABLE A3.32 - BREAKING LOAD TEST NO. 208
TEST RESULT DATA
DAPTO TO SPRINGHILL TRANSMISSION LINE

Wire Layer	Lay Length
24	10.82
18	14.79
12	16.22
6	24.31

TABLE A3.33 - LAY LENGTH
DAPTO TO SPRINGHILL
TRANSMISSION LINE

Wire Layer	Lay Length
24	10.84
18	14.56
12	16.75
6	25.83

TABLE A3.34 - LAY LENGTH
AVON TO KEMPS CREEK
TRANSMISSION LINE

Parameter	Data
Tar. Drop Point ^{o}C	74
Tar. Mass gm^{-1}	37.0

TABLE A3.35 - CHEMICAL TEST
TEST RESULT DATA
TOMAGO TO TAREE
TRANSMISSION LINE

Parameter	Data
Tar. Drop Point ^{o}C	70
Tar. Mass gm^{-1}	36.8

TABLE A3.36 - CHEMICAL TEST
TEST RESULT DATA
BELLAMBI TO HEATHCOTE
TRANSMISSION LINE

APPENDIX FOUR

CONDUCTOR FATIGUE TEST RESULTS

The conductor fatigue test results that constitute this appendix are in the following order for each fatigue test:

1. Test data sheet,
2. Test frequency spectrum,
3. Test log record,
4. Wire and/or conductor failure report.

Regarding the frequency spectrums the calibration is 1 division equals 2.01 Hz.

CONDUCTOR FATIGUE TEST No. NEP/1

Conductor Details

Code name: NEPTUNE
Material: AAC
CBL = 24.7 kN
Area, A = 157.6 mm^2

Test Conditions

Mass, M = 872 kg

$$\text{Load, } T = \frac{M * 9.81}{1000} = 8.554 \text{ kN}$$

$$\%CBL = \frac{T}{CBL} = \frac{8.554}{24.7} = 34.6\ \%$$

Preconditioning Creep

Duration 3 hrs

V-Scope Details

a = 92.5 mm
b = 9 mm
x = 33.12 mm at 89 mm from termination

$$Y_{p-p} = \frac{x.b}{a} = \frac{33.12 * 9}{92.5} = 3.222 \text{ mm}$$

$$Y_p = \frac{Y_{p-p}}{2} = \frac{3.222}{2} = 1.611 \text{ mm}$$

Loop Details

Length, l = 3130 mm
Deflection$_{max}$, Y_{max} = 54 mm

Frequency Details

Spectrum Analysis No. Not Available
Fundamental Frequency, F = 23.0 Hz
2nd Harmonic - Hz
3rd Harmonic - Hz

Frequency per hour n = F * 3600
= 82,800

Stress Details

$$\text{Static, } \sigma = \frac{T}{A} = \frac{8.554\,k}{157.6} = 54.3 \text{ MPa}$$

Dynamic (from program DSTRAIN.BAS)
Flexural Rigidity = 7.07 Nm^2
Stiffness = 28 mm
Strain = 7515 mm/km
Stress = 511 MPa

TABLE A4.1 CONDUCTOR FATIGUE TEST DATA
TEST NO. NEP/1

CONDUCTOR FATIGUE TEST No. NEP/1 Page No. 1/1.

Started Fatigue Test		Ceased Fatigue Test	Duration, d decimal time	No. of cycles	ΣN Mcycles	Reason for Stoppage	
261088	0820	1630	8·167	679,200	679,200	Overnight	shutdown
271088	0830	1545	7·250	600,300	1,276,500	"	"
281088	0830	1330	5·00	414,000	1,690,500	"	"
311088	0808	1625	8·283	685,800	2,379,300	"	"
011188	0749	1630	8·683	718,980	3,098,280	"	"
021188	0740	1600	8·333	690,000	3,788,280	"	"
031188	0753	13·07	5·233	433,320	4,221,600	Conductor	Failure

TABLE A4.2 CONDUCTOR FATIGUE TEST LOG
TEST NO. NEP/1

DATE OF TEST 261088 - 031188

TEST NUMBER NEP/1

TOP

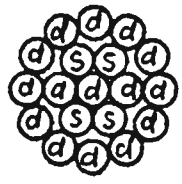

BOTTOM

(s) Shear Breaks

(d) Ductile Breaks

Failure Location Conductor clamp entrance

Failure Description Conductor wires failed simultaneously probably due to one or two fatigue breaks and then instantaneously overloading remaining wires.

Number of cycles to failure 4.22×10^6

CONDUCTOR TESTED NEPTUNE AAC 19/3.25 mm.

FIGURE A4.1 CONDUCTOR FATIGUE TEST
TEST RESULTS TEST NO. NEP/1

CONDUCTOR FATIGUE TEST No. NEP/2

Conductor Details

Code name: NEPTUNE
Material: AAC
CBL = 24·7 kN
Area, A = 157·6 mm²

Test Conditions

Mass, M = 872 kg

$$\text{Load, } T = \frac{M * 9.81}{1000} = 8{\cdot}554 \text{ kN}$$

$$\%CBL = \frac{T}{CBL} = \frac{8{\cdot}554}{24{\cdot}7} = 34{\cdot}6\ \%$$

Preconditioning Creep

Duration 3 hrs

V-Scope Details

a = 92·5 mm
b = 9 mm
x = 33·12 mm at 89 mm from termination

$$Y_{p-p} = \frac{x.b}{a} = \frac{33{\cdot}12 * 9}{92{\cdot}5} = 3{\cdot}222 \text{ mm}$$

$$Y_p = \frac{Y_{p-p}}{2} = \frac{3{\cdot}222}{2} = 1{\cdot}611 \text{ mm}$$

Loop Details

Length, l = Not Recorded mm
Deflection$_{max}$, Y_{max} = Not Recorded mm

Frequency Details

Spectrum Analysis No. Not Available
Fundamental Frequency, F = 24·2 Hz
2nd Harmonic - Hz
3rd Harmonic - Hz

Frequency per hour n = F * 3600
= 87,120

Stress Details

$$\text{Static, } \sigma = \frac{T}{A} = \frac{8{\cdot}554\,k}{157{\cdot}6} = 54{\cdot}3 \text{ MPa}$$

Dynamic (from program DSTRAIN.BAS)
Flexural Rigidity = 7·07 Nm²
Stiffness = 28 mm
Strain = 7515 mm/km
Stress = 511 MPa

TABLE A4.3 CONDUCTOR FATIGUE TEST DATA
TEST NO. NEP/2

CONDUCTOR FATIGUE TEST No. NEP/2 Page No. 1/1

Started Fatigue Test		Ceased Fatigue Test	Duration, d decimal time	No. of cycles	ΣN Mcycles	Reason for Stoppage
081188	1425	1630	2·083	181,500	181,500	Overnight Shutdown
091188	0822	1625	8·05	701,316	882,816	" "
101188	0810	1622	8·20	714,384	1,597,200	" "
111188	0630	1610	9·667	842,160	2,439,360	" "
141188	0805	1630	8·417	733,260	3,172,620	Strand Failure

TABLE A4.4 CONDUCTOR FATIGUE TEST LOG
TEST NO. NEP/2

DATE OF TEST 081188 - 141188

TEST NUMBER NEP/2

TOP

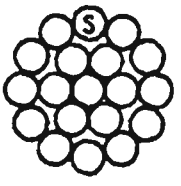

BOTTOM

(S) Shear Breaks

(d) Ductile Breaks

Failure Location Conductor Termination 2mm inside test length

Failure Description Single wire failure

Number of cycles to failure 3.17×10^6

CONDUCTOR TESTED NEPTUNE 19/3.25 AAC.

FIGURE A4.2 CONDUCTOR FATIGUE TEST
TEST RESULTS TEST NO. NEP/2

CONDUCTOR FATIGUE TEST No. NEP/3

Conductor Details

Code name: NEPTUNE
Material: AAC.
CBL = 24.7 kN
Area, A = 157.6 mm^2

Test Conditions

Mass, M = 872 kg

$$\text{Load, } T = \frac{M * 9.81}{1000} = 8.554 \text{ kN}$$

$$\%CBL = \frac{T}{CBL} = \frac{8.554}{24.7} = 34.6\ \%$$

Preconditioning Creep

Duration 24 hrs

V-Scope Details

a = 92.5 mm
b = 9 mm
x = 33.12 mm at 89 mm from termination

$$Y_{p-p} = \frac{x.b}{a} = \frac{33.12 \times 9}{92.5} = 3.222 \text{ mm}$$

$$Y_p = \frac{Y_{p-p}}{2} = \frac{3.222}{2} = 1.611 \text{ mm}$$

Loop Details

Length, l = 3130 mm
Deflection$_{max}$, Y_{max} = 54 mm

Frequency Details

Spectrum Analysis No. SPEC/3
Fundamental Frequency, F = 23.2 Hz
2nd Harmonic 46.4 Hz
3rd Harmonic 69.6 Hz

Frequency per hour $n = F * 3600$
= 83,520

Stress Details

$$\text{Static, } \sigma = \frac{T}{A} = \frac{8.554\ k}{157.6} = 54.3 \text{ MPa}$$

Dynamic (from program DSTRAIN.BAS)
Flexural Rigidity = 7.07 Nm^2
Stiffness = 28 mm
Strain = 7515 mm/km
Stress = 511 MPa

TABLE A4.5 CONDUCTOR FATIGUE TEST DATA
TEST NO. NEP/3

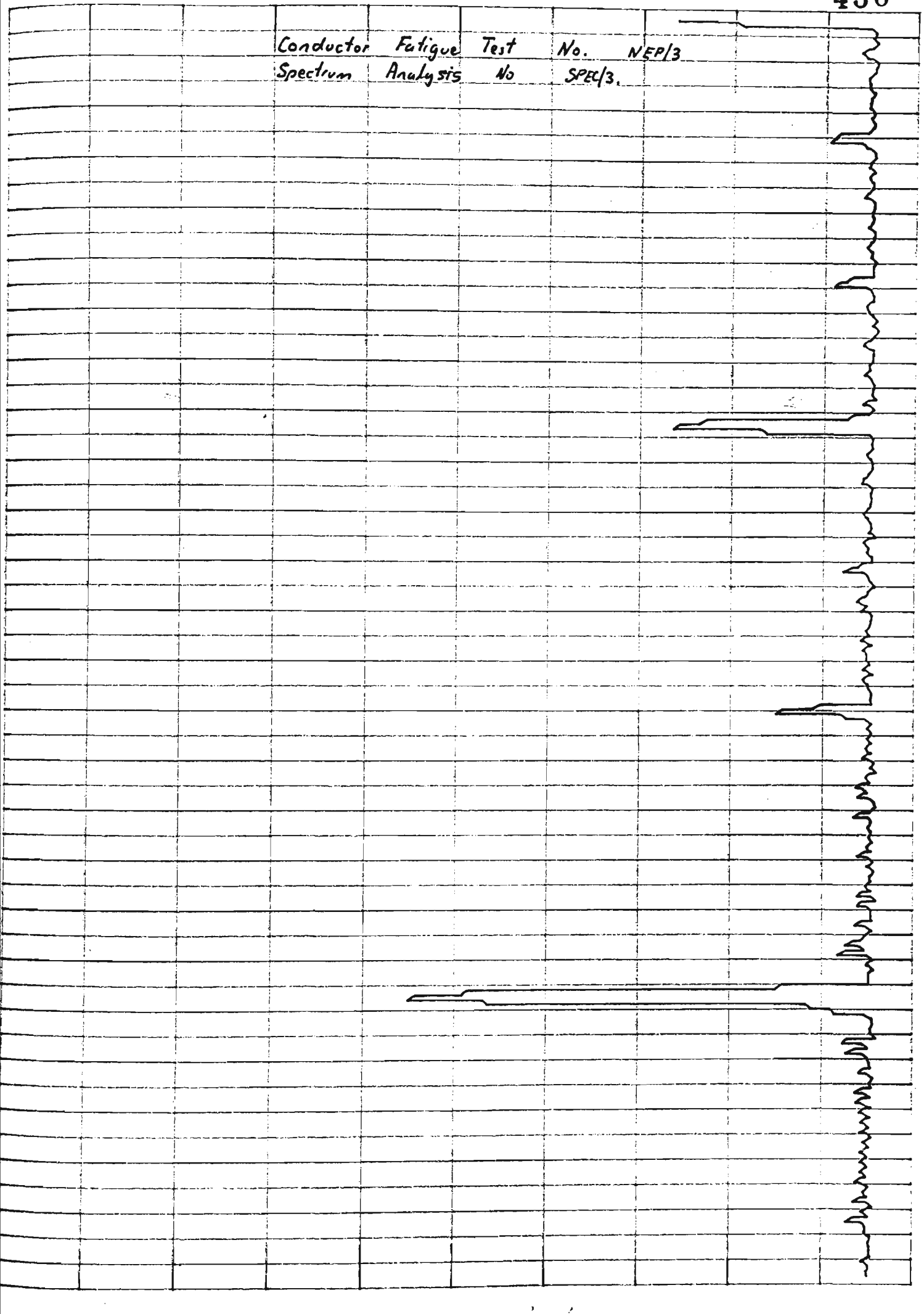

FIGURE A4.3 CONDUCTOR FATIGUE TEST
SPECTRUM ANALYSIS TEST NO. NEP/3

CONDUCTOR FATIGUE TEST No. NEP/3 Page No. 1/1.

Started Fatigue Test	Ceased Fatigue Test	Duration, d decimal time	No. of cycles	ΣN Mcycles	Reason for Stoppage
040189 1227	1551	3·40	283,968	283,968	Overnight shutdown
050189 0803	1123	3·333	278,400	562,368	Drive shaft failure
100189 1535	1628	0·883	73,776	636,144	Overnight shutdown
110189 1113	1158	0·750	62,640	698,784	Motor fuse failure
110189 1410	Could not establish standing wave and as a result of excessive deflection amplitude the conductor wires exceeded the plastic limit and both the north and south conductors failed.				

TABLE A4.6 CONDUCTOR FATIGUE TEST LOG
TEST NO. NEP/3

DATE OF TEST 040189 - 110189

TEST NUMBER NEP/3.

TOP

BOTTOM

(s) Shear Breaks

(d) Ductile Breaks

Failure Location Conductor termination.

Failure Description Instantaneous wire failure.

Number of cycles to failure Invalid test result.

CONDUCTOR TESTED NEPTUNE AAC 19/3.25mm

FIGURE A4.4 CONDUCTOR FATIGUE TEST
TEST RESULTS TEST NO. NEP/3

CONDUCTOR FATIGUE TEST No. NEP/4

Conductor Details

Code name: NEPTUNE
Material: AAC
CBL = 24.7 kN
Area, A = 157.6 mm^2

Test Conditions

Mass, M = 872 kg

$$\text{Load, } T = \frac{M * 9.81}{1000} = 8.554 \text{ kN}$$

$$\%CBL = \frac{T}{CBL} = \frac{8.554}{24.7} = 34.6 \%$$

Preconditioning Creep

Duration 3 hrs

V-Scope Details

a = 92.5 mm
b = 9 mm
x = 7.4 mm at 89 mm from termination

$$Y_{p-p} = \frac{x.b}{a} = \frac{7.4 \times 9}{92.5} = 0.720 \text{ mm}$$

$$Y_p = \frac{Y_{p-p}}{2} = \frac{0.720}{2} = 0.360 \text{ mm}$$

Loop Details

Length, l = 2415 mm
Deflection$_{max}$, Y_{max} = 25 mm

Frequency Details

Spectrum Analysis No. SPEC/4
Fundamental Frequency, F = 30.0 Hz
2nd Harmonic 60.0 Hz
3rd Harmonic 90.0 Hz

Frequency per hour n = F * 3600
= 108,000

Stress Details

$$\text{Static, } \sigma = \frac{T}{A} = \frac{8.554\ k}{157.6} = 54.3 \text{ MPa}$$

Dynamic (from program DSTRAIN.BAS)
Flexural Rigidity = 7.07 Nm^2
Stiffness = 28 mm
Strain = 1680 mm/km
Stress = 114.2 MPa

TABLE A4.7 CONDUCTOR FATIGUE TEST DATA
TEST NO. NEP/4

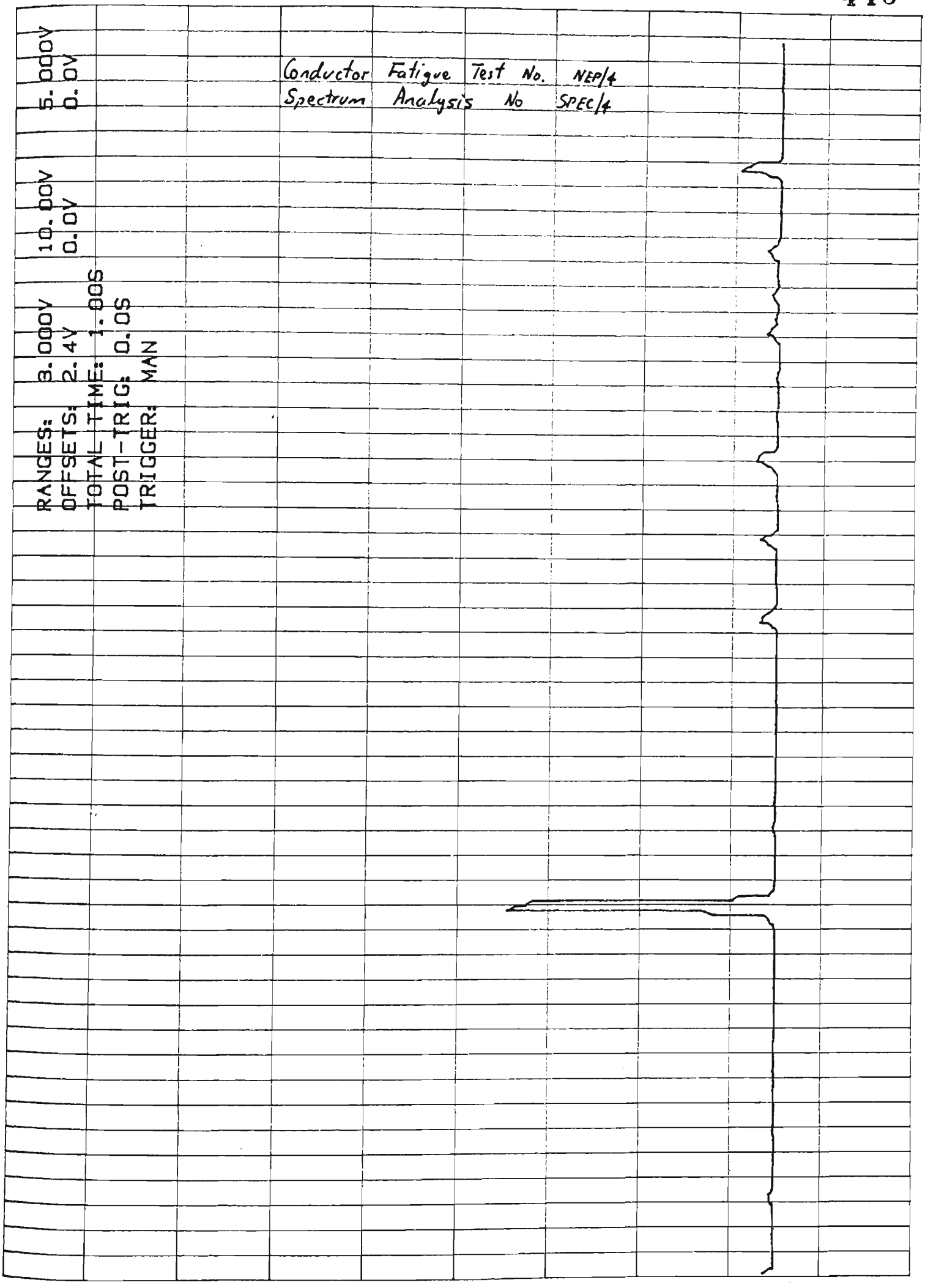

FIGURE A4.5 CONDUCTOR FATIGUE TEST
SPECTRUM ANALYSIS TEST NO. NEP/5

CONDUCTOR FATIGUE TEST No. NEP/4 Page No. 1/2

Started Fatigue Test		Ceased Fatigue Test	Duration, d decimal time	No. of cycles	ΣN Mcycles	Reason for Stoppage
170189	1050	1550	5·000	540,000	540,000.	Overnight Shutdown
180189	0813	1550	7·617	822,600	1,362,600	" "
190189	0747	1600	8·2167	887,400	2,250,000	" "
200189	0809	0835	0·433	46,800	2,296,000	Push rod fatigued
200189	1341	1619	2·633	284,400	2,581,200	Overnight shutdown
230189	0901	0922				
"	0932	1022				Repeated shutdowns
"	1027	1041				because of failure of
"	1125	1200				motor speed controller.
"	1349	1422				
"	1447	1557	4·2167	455400	3,036,000	Overnight shutdown
240189	0753	0908				Repeated shutdowns
"	0912	0948				because of failure of motor speed controller
"	1517	2110	7·73	835,200	3,871,800	Cam shaft fatigued.
010289	1021	1538	5·283	570,600	4,442,400	Overnight Shutdown
020289	0800	1624	8·400	907,200	5,349,600	" "
030289	0804	0940	1·600	172,800	5,522,400	Drive shaft fatigued
070289	0911	1615	7·040	760,320	6,282,720	Overnight Shutdown
080289	0810	1219	4·15	448,200	6,730,920	Maintenance
"	1229	1628	3·983	430,200	7,161,120	Overnight Shutdown
090289	0818	1619	8·017	865,800	8,026,920.	" "

TABLE A4.8 CONDUCTOR FATIGUE TEST LOG
TEST NO. NEP/4 SHEET 1

CONDUCTOR FATIGUE TEST No. NEP/4 Page No. 2/2

Started Fatigue Test		Ceased Fatigue Test	Duration, d decimal time	No. of cycles	ΣN Mcycles	Reason for Stoppage
100289	0827	1648	8·35	901,800	8,928,720	Overnight Shutdown
130289	0856	1629	7·55	815,400	9,744,120	" "
140289	0819	1635	8·267	892,800	10,636,920	Ceased test at 10^7 cycles.

TABLE A4.9 CONDUCTOR FATIGUE TEST LOG
TEST NO. NEP/4 SHEET 2

DATE OF TEST 170189 - 140289

TEST NUMBER NEP/4.

TOP

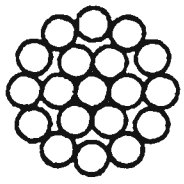

BOTTOM

(S) Shear Breaks

(d) Ductile Breaks

Failure Location No Failures

Failure Description No Failures

Number of cycles to failure 10.36×10^6

CONDUCTOR TESTED NEPTUNE AAC 19/3.25

FIGURE A4.6 CONDUCTOR FATIGUE TEST
TEST RESULTS TEST NO. NEP/4

CONDUCTOR FATIGUE TEST No. NEP/5

Conductor Details

Code name: NEPTUNE
Material: AAC
CBL = 24.7 kN
Area, A = 157.6 mm^2

Test Conditions

Mass, M = 872 kg

$$\text{Load, } T = \frac{M * 9.81}{1000} = 8.554 \text{ kN}$$

$$\%CBL = \frac{T}{CBL} = \frac{8.554}{24.7} = 34.6\ \%$$

Preconditioning Creep

Duration 18 hrs

V-Scope Details

a = 92.5 mm
b = 9 mm
x = 16.44 mm at 89 mm from termination

$$Y_{p-p} = \frac{x.b}{a} = \frac{16.4 \times 9}{92.5} = 1.60 \text{ mm}$$

$$Y_p = \frac{Y_{p-p}}{2} = \frac{1.60}{2} = 0.80 \text{ mm}$$

Loop Details

Length, l = 2595 mm
$Deflection_{max}$, Y_{max} = 45 mm

Frequency Details

Spectrum Analysis No. SPEC/5
Fundamental Frequency, F = 28.0 Hz
2nd Harmonic 56.0 Hz
3rd Harmonic 84.0 Hz

Frequency per hour n = F * 3600
= 100,800

Stress Details

$$\text{Static, } \sigma = \frac{T}{A} = \frac{8,554k}{157.6} = 54.3 \text{ MPa}$$

Dynamic (from program DSTRAIN.BAS)
Flexural Rigidity = 7.07 Nm^2
Stiffness = 29 mm
Strain = 3653 mm/km
Stress = 240.4 MPa

TABLE A4.10 CONDUCTOR FATIGUE TEST DATA
TEST NO. NEP/5

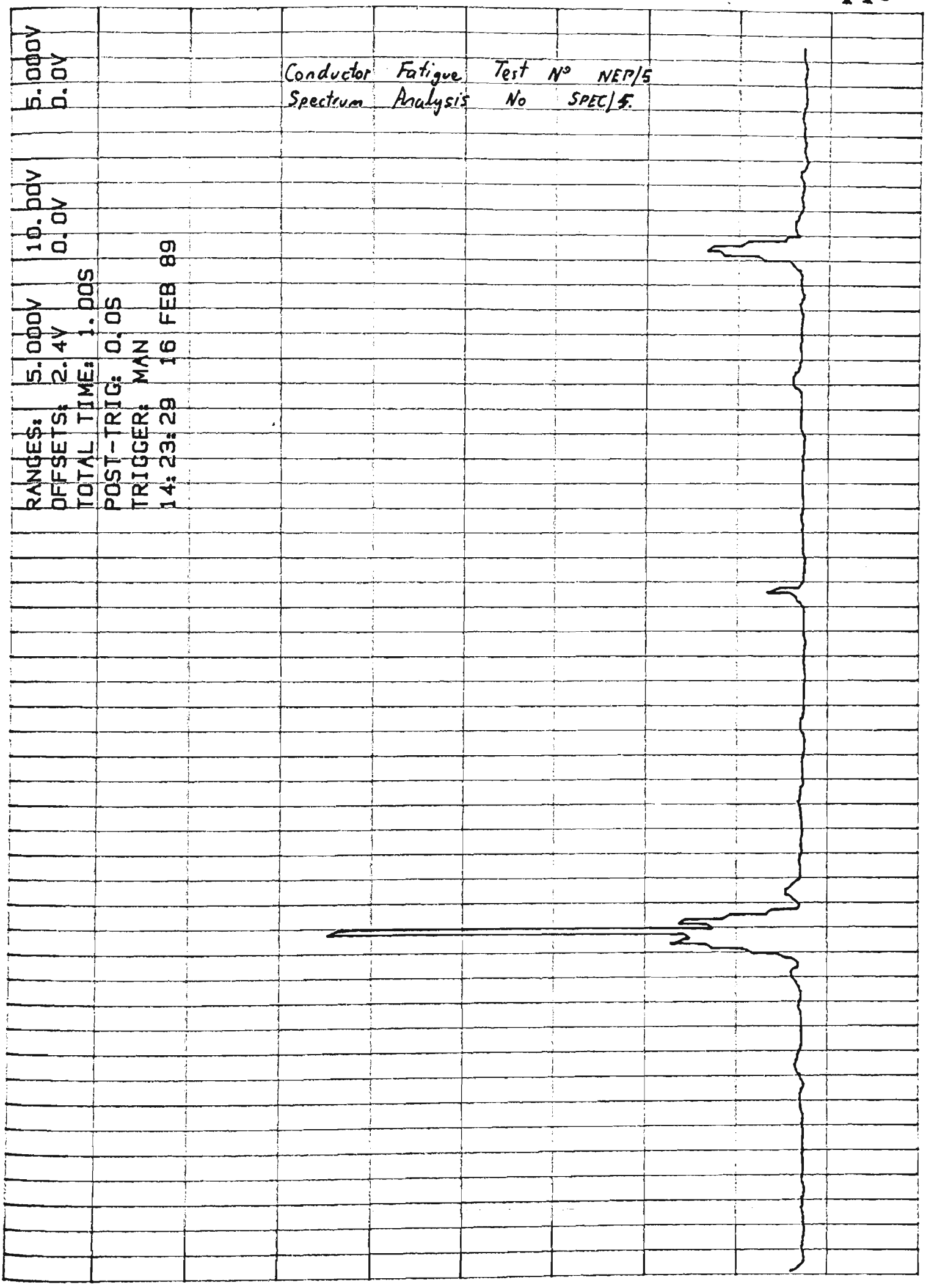

FIGURE A4.7 CONDUCTOR FATIGUE TEST
SPECTRUM ANALYSIS TEST NO. NEP/5

CONDUCTOR FATIGUE TEST No. NEP/5 Page No. 1/1

Started Fatigue Test		Ceased Fatigue Test	Duration, d decimal time	No. of cycles	ΣN Mcycles	Reason for Stoppage
160289	1420	1640	2·33	336,000	336,000	Overnight Shutdown.
200289	0730	1610	8·667	873,634	1,209,634.	" "
210289	0730	1625	8·917	898,834	2,108 468	" "
220289	0730	1645	9·250	932,400	3,040,868	" "
230289	0715	1645	9·500	957600	3,998,468	" "
240289	0720	1640	9·200	940,800	4,939,268	" "
270289	0720	1640	9·333	940,800.	5,880,068	" "
280289	0735	1645	9·285	935,947	6,816,015	" "
010289	0730	1630	9·000.	907,200	7,723,215	" "
020289	0730	2400.	16·500	1,663,200	9,386,415	Continued test overnight
020289	2400	0840	8·667	873,600	10,260015	Ceased test at 10^7 cycles.

TABLE A4.11 CONDUCTOR FATIGUE TEST LOG
TEST NO. NEP/5

DATE OF TEST 160289 - 020289

TEST NUMBER NEP/5

TOP

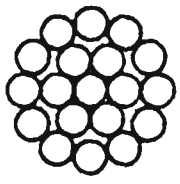

BOTTOM

(s) Shear Breaks

(d) Ductile Breaks

Failure Location No Failures

Failure Description No Failures

Number of cycles to failure 10.3×10^6

CONDUCTOR TESTED NEPTUNE AAC 19/3.25

FIGURE A4.8 CONDUCTOR FATIGUE TEST
TEST RESULTS TEST NO. NEP/5

CONDUCTOR FATIGUE TEST No. NEP/6

Conductor Details

Code name: NEPTUNE
Material: AAC
CBL = 24·6 kN
Area, A = 157·6 mm²

Test Conditions

Mass, M = 872 kg

$$\text{Load, } T = \frac{M * 9.81}{1000} = 8{\cdot}554 \text{ kN}$$

$$\%CBL = \frac{T}{CBL} = \frac{8{\cdot}554}{24{\cdot}6} = 34{\cdot}6\ \%$$

Preconditioning Creep

Duration _____ hrs

V-Scope Details

a = 92·5 mm
b = 9 mm
x = 26 mm at 89 mm from termination

$$Y_{p-p} = \frac{x.b}{a} = \frac{26 * 9}{92{\cdot}5} = 2{\cdot}53 \text{ mm}$$

$$Y_p = \frac{Y_{p-p}}{2} = \frac{2{\cdot}53}{2} = 1{\cdot}265 \text{ mm}$$

Loop Details

Length, l = Not Recorded mm
Deflection$_{max}$, Y_{max} = Not Recorded mm

Frequency Details

Spectrum Analysis No. SPEC/6
Fundamental Frequency, F = 30·8 Hz
2nd Harmonic 61·6 Hz
3rd Harmonic 92·4 Hz

Frequency per hour n = F * 3600
= 110,880

Stress Details

$$\text{Static, } \sigma = \frac{T}{A} = \frac{8{\cdot}554\ k}{157{\cdot}6} = 54{\cdot}28 \text{ MPa}$$

Dynamic (from program DSTRAIN.BAS)
Flexural Rigidity = 7·07 Nm²
Stiffness = 29 mm
Strain = 5777 mm/km
Stress = 392·8 MPa

TABLE A4.12 CONDUCTOR FATIGUE TEST DATA
TEST NO. NEP/6

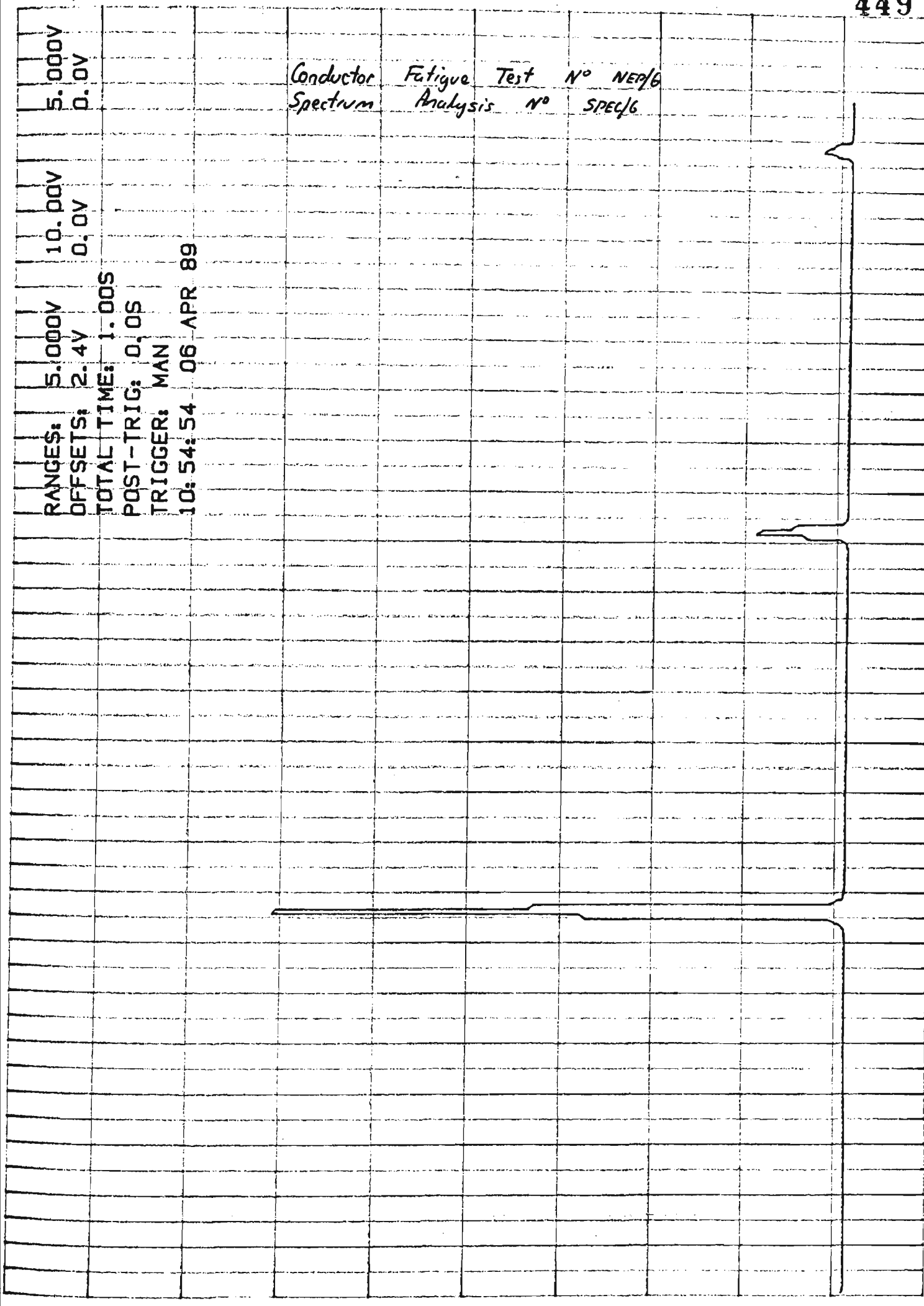

FIGURE A4.9 CONDUCTOR FATIGUE TEST
SPECTRUM ANALYSIS TEST NO. NEP/6

CONDUCTOR FATIGUE TEST No. NEP/6 Page No. 1/1.

Started Fatigue Test		Ceased Fatigue Test	Duration, d decimal time	No. of cycles	ΣN Mcycles	Reason for Stoppage
060489	1045	5.30.	6.75	748,440	748,440.	Overnight Shutdown.
070489	815	4.45	8.50	942480	1690920	" "
100489	820.	2400.	15.667	1737,120	3428040.	-
110489	0000	2400	24.00	2661,120	6,089,160	-.
120489	0000.	0537	5.617	622,776	6,711936	Wire failure.

TABLE A4.13 CONDUCTOR FATIGUE TEST LOG
TEST NO. NEP/6

DATE OF TEST 060489 - 120489

TEST NUMBER NEP/6

TOP

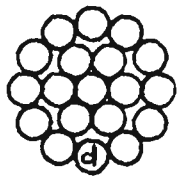

BOTTOM

⑤ Shear Breaks

ⓓ Ductile Breaks

Failure Location Conductor termination

Failure Description Single wire failure.

Number of cycles to failure 6.71×10^6.

CONDUCTOR TESTED NEPTUNE AAC 19/3.25

FIGURE A4.10 CONDUCTOR FATIGUE TEST
TEST RESULTS TEST NO. NEP/6